'BETTER THAN PUREX': TOWARDS THE SUSTAINABLE RECOVERY OF URANIUM FROM SPENT NUCLEAR FUEL

Adam Canner

A thesis submitted in partial fulfilment of the requirements for the degree of
Doctor of Philosophy

The University of Sheffield
Faculty of Engineering
Department of Chemical and Biological Engineering

Original submitted on 5th September 2020.

Corrected version submitted on 4th May 2021.

[This page is left intentionally blank]

Abstract

A sustainable fully-closed nuclear fuel cycle is required in order to fully utilise the limited amount of uranium fuel on Earth. The current process used for the recycling of nuclear fuel, PUREX, can suffer from undesired extraction, poor phase-control, and secondary waste issues due to the use of the solvating extractant tri-*n*-butyl phosphate (TBP) rendering reprocessing economically unfavourable. The work in this thesis looks to replace the TBP solvent with novel monoamide-based alternatives using *N,N*-dihexyl octanamide (DHOA) to reduce or eliminate phosphorous in reprocessing flowsheets to reduce waste and required process steps. Novel ligand mixtures of monoamide with a 'secondary' ligand are studied to offset the reported low uranium loading of standard monoamide solvents by either a phase modifying effect or through the production of a more hydrophobic dual-ligand complex. Tested secondary ligands are diamides, diglycolamides, phosphates and phosphine oxides. Initial spectroscopic tests indicate that monoamide-diamide mixtures do not form a sufficient amount of a dual-ligand complex, but monoamide-diglycolamide solvents likely form two types of dual-ligand complexes. Monoamide-phosphate and monoamide-phosphine oxide solvents were largely inconclusive. Solvent extraction tests showed that monoamide-phosphine oxide solvents are unlikely to form mixed-ligand complexes, but Jobs plots indicate that DHOA-TBP and DHOA-TODGA (*N,N,N',N'*-tetraoctyl diglycolamide) solvents do form enhanced extraction systems over standard DHOA or TBP solvents. Case study solvents of 20 mol% DHOA – 80 mol% and 80 mol% DHOA – 20 mol% TODGA were further studied. These case study solvents were found to be comparable with PUREX solvents within the operating acidity range of PUREX (4-6 M nitric acid) and were more stable solvents than their single-ligand counterparts. Experimental extraction mechanism analysis and scenario modelling with slope analysis revealed that DHOA-TBP solvents are likely enhanced via a solvent phase modifying effect by the presence of both ligands, whereas the DHOA-TODGA solvents are likely enhanced through the formation of a ternary complex as predicted from earlier fundamental spectroscopic studies. Metal loading models used to predict solvent performance and contact stages for a specified mass transfer fit well except at high metal loadings where nitric acid extraction effects interfere with the model assumptions. Main future work for this thesis includes an assessment of competitive extraction (which have been completed pending analysis) and more robust metal uptake models.

Acknowledgements

The work contained within this thesis would not have been possible without a great number of people and things that have kept me going in the most difficult times. I first want to thank my wonderful partner Emma for her continual, invaluable support even as she was going through her own PhD process. You have made this whole experience much more bearable. I particularly want to thank you for your patience and understanding during the pre-caffeinated stages of our days where I may potentially have been more effort than I was worth. On a similar (and *almost* equally as important) note, I would like to thank DeLonghi for their excellent espresso machine that has produced an embarrassing volume of coffee in my vain attempt to appear as a morning person. I would like to thank my Mum, Dad, and brothers Jake, Lewis, and Tom for providing a stressless space away from work when needed and for allowing me to vent when aspects got too much. I would like to thank Pirate Studios for their excellent practice rooms and drum kits that allowed me to hit some skins when my neighbours did not. It would also be rude not to acknowledge the hard efforts of the staff at the Red Deer, Wetherspoons, the Washington, Interval, Thornbridge, and Brewdog both before and after the COVID-19 outbreak for a wide selection of excellent beers and relaxing atmospheres. After the outbreak of COVID-19, I would like to thank Valve and Sony for taking some of the money I would have spent on alcohol and providing great video games to get me through those demanding times.

In terms of help with the actual work contained in this thesis, I would first like the thank the Separation and NUclear Chemical Engineering Research group (SNUCER) for continual support and helpful discussions. In particular, I want to thank Dr Mark Ogden for his supervision, James Bezzina and Alex Riley for the almost excessive number of coffee breaks in between experiments, and Tom Robshaw for the help with chemical analysis. I would like to thank Jasraj Babra and Joe Cowell from Reading University and Frank Lewis from Northumbria University for ligand synthesis that made this work possible. I would also like to thank Sareena Hussain for completing the TOPO work presented in the appendix of this thesis, and the many other master's student tutees who have shaped my PhD experience.

Contents

List of Acronyms and Abbreviations

General

A/O	Aqueous/organic
CF	Concentration factor
CHON	Carbon Hydrogen Oxygen Nitrogen
FP	Fission product
GDF	Geological disposal facility
HLLW	High level liquid waste
HLW	High level waste
IR	Infra-red
LMCT	Ligand-to-metal charge transfer
LOC	Limiting organic content
MODSQUAD	Version of SQUAD
NMR	Nuclear magnetic resonance
REE	Rare earth element
SNF	Spent nuclear fuel
SQUAD	Stability Quotients Using Absorbance Data
SX	Solvent extraction
Thorp	Thermal Oxide Reprocessing plant
TRU	Transuranic
UK	United Kingdom
UV	Ultraviolet

Mathematical

Abs	Absorbance
aq	Aqueous phase
c	Concentration (mol L^{-1} or M)
D	Distribution ratio
E%	Extraction percentage (%)
eq	Equilibrium condition
i	Initial condition
K′	Conditional equilibrium constant
org	Organic phase
SF	Separation factor
V	Volume (L)
x	Mole fraction
X	Aqueous uranium content (g/L)
Y	Organic uranium content (g/L)

Greek Letters

α	DHOA-TBP acid extraction parameter
β	DHOA-TODGA acid extraction parameter
γ	DHOA-TODGA ligand isotherm parameter
δ	DHOA-TOBP ligand isotherm parameter
ε	Molar absorptivity coefficient (L mol^{-1} cm^{-1})

Ligands and Chemicals

CDTA	1,2-cyclohexanediaminetetraacetic
CMPO	*n*-octylphenyl-*N,N*-diisobutyl carbamoyl methyl phosphine oxide
DBAA	*N,N*-dibutyl acetamide
DBBA	*N,N*-dibutyl butanamide
DEAA	*N,N*-diethyl acetamide
DHOA	*N,N*-dihexyl octanamide
DI	deionised water

DMAA	*N,N*-dimethyl acetamide
DMDBTDMA	*N,N'*-dimethyl-*N,N'*-dibutyl-2-tetradecyl-malonamide
DMDOHEMA	*N,N'*-dimethyl, *N,N'*-dioctylhexylethoxy malonamide
DTPA	diethylenetriamine-*N,N,N',N'',N''*-pentaacetic acid
EDC.HCl	*N*-(3-dimethylaminopropyl)-*N'*-ethylcarbodiimide hydrochloride
HDBP	dibutylphosphoric acid
HDEHP	bis-(2-ethylhexyl)phosphoric acid
HDHP	bis-(2-hexyl)phosphoric acid
HEDTA	(2-hydroxyethyl)ethylenediaminetriacetic acid
HEH(EHP)	2-ethylhexylphosphonic acid mono-2-ethylhexyl ester
H_2MBP	monobutylphosphoric acid
H_2MEHP	mono-2-ethylhexylphosphoric acid
HOBt	1-hydroxybenzotriazole hydrate
T2EHDGA	*N,N,N',N'*-tetra(2-ethylhexyl) diglycolamide
TBP	tri-*n*-butyl phosphate
TBU	tetrabutyl urea
TEDGA	*N,N,N',N'*-tetraethyl diglycolamide
TEMA	*N,N,N',N'*-tetraethyl malonamide
TEP	tri-*n*-ethyl phosphate
TMPO	tri-*n*-methyl phosphine oxide
TODGA	*N,N,N',N'*-tetraoctyl diglycolamide
TOPO	tri-*n*-octyl phosphine oxide

Processes and Flowsheets

ALSEP	Actinide-Lanthanide Separation
CCD-PEG	Chlorinated Cobalt Dicarbollide/Polyethylene Glycol process
DIAMEX-SANEX	Diamide Extraction – Selective Actinide Extraction
EXAm	Extraction of Americium process
GANEX	Group Actinide Extraction
NPEX	Neptunium Extraction
PUREX	Plutonium Uranium Reduction Extraction
TALSPEAK	Trivalent Actinide Lanthanide Separation with Phosphorus- Reagent Extraction from Aqueous Komplexes
TALSQuEAK	an advanced TALSPEAK process
THOREX	Thorium Extraction
TRUEX	Transuranic Extraction
TRUSPEAK	An advanced TALSPEAK process
UREX+	Uranium Extraction +

List of Figure Captions

Figure 1.1. Calculated composition (in kg heavy metal) of SNF after 10 year cool of 1 tonne 3.2% enriched UO_2 fuel, 33 MWd/kg U burnup at a mean neutron flux of 3.28 x 10^{18} n m^{-2} s^{-1} in a typical pressurised water reactor *(Choppin, et al., 2002a)*.

Figure 1.2. Overview of the nuclear fuel cycle. Red arrows indicate an open cycle, green arrows indicate a closed cycle and black arrows indicate both. (MOX = mixed oxide fuel, MA = minor actinides, LLFP = long-lived fission products, SLFP = short-lived fission products, HLLW = high level liquid waste, HLW = high level waste).

Figure 1.3. Radiotoxicity of SNF components over time (© *(OECD, 2006)*)

Figure 2.1. A simplified SX process.

Figure 2.2. Chemical structure of tri-n-butyl phosphate (TBP).

Figure B.10. A) Uranyl nitrate extraction with varying nitrate concentrations in different nitric acid concentrations with 0.2 M DHOA and TOPO in n-dodecane with 10wt% 1-decanol at 21±2°C. Initial [uranium] for DHOA and TOPO tests are 596±16 and 551±10 ppm respectively. B) shows the slope analysis plots for the DHOA systems.

Figure B.11. DHOA-TOPO Job plots at 5.7 M nitric acid at 21±2°C. Initial [uranium] = 479±5 ppm. A) depicts the distribution Job plot. B) depicts the organic [uranium] Job plot.

List of Table Captions

List of Scheme Captions

Preface

Over 10 years ago, I learned about the basics of nuclear energy from my high school science teacher which began my passion for nuclear processes. I have carried this passion through my entire higher education; it was here I first learned about the PUREX process for recycling nuclear fuel. The way it was taught, it appeared to be a fantastic orchestra of simple chemistry to solve a very complicated problem. I was fascinated by the treatment of nuclear waste and the PUREX process in particular. Upon further independent study, it became apparent that the classic saying was true: "never judge a process by its summary". Things are never quite as simple as they appear; this is what interested me in studying a PhD in the reprocessing remit in the first place and is a stark lesson I have learned throughout my PhD process. Another lesson I have found to be painfully true over the last 4 years is Hofstadter's Law: "it always takes longer than you expect, even when you take into account Hofstadter's Law". Nevertheless, through force of will, the support of great people, and many (*many*) 14 hour days in the lab, the work for this thesis was completed.

It took me around 4 months in total to write the contents of this thesis. It is the product of my vast research of the literature, extensive time spent experimenting, and my continual improvement of scientific writing. Probably the most difficult part of the process was condensing the large amount of reprocessing literature down into a relevant and concise literature review, but it was all worth it to see the whole document come together at the end.

Before going into the thesis proper, I wanted to give a quick note on the structure. It is common to have an experimental chapter separate to the rest of the work. However, given the variety of the methods used and the sequential nature of the tests I have conducted for this book, I decided that it would be clearer to the reader to have the relevant experimental section in the necessary chapters. It is my hope that the readers of this thesis agree with this perspective.

Declaration

I, the author, confirm that the Thesis is my own work. I am aware of the University's Guidance on the Use of Unfair Means (www.sheffield.ac.uk/ssid/unfair-means). This work has not been previously been presented for an award at this, or any other, university.

Some data and discussions presented in Chapter 3 are also published in:

- Canner, A. J. et al., 2020. Specrophotometric analysis of ternary uranyl systems to replace tri-n-butyl phosphate (TBP) in used fuel reprocessing. *J Sol Chem,* 49(1), pp. 52-67.

[This page is left intentionally blank]

CHAPTER 1   Introduction and Hypotheses

This introductory chapter outlines the background and context for the research contained within this thesis starting with the need for nuclear power, the need for a closed nuclear fuel cycle, and an assessment of the benefits and issues of a closed nuclear fuel cycle. The need to redesign reprocessing flowsheets is identified, the idea of a monoamide reprocessing flowsheet is introduced, and issues with this flowsheet are discussed. Following this, the research hypothesis and sub-hypotheses are stated.

1.1   Background

1.1.1   Nuclear Energy in Context

Nuclear power is a safe form of energy generation (Markandya & Wilkinson, 2013) that is capable of providing a large and reliable baseline power supply with very low CO_2 emissions; aside from hydroelectric power, nuclear energy is the only 'green' energy source that can provide a large and consistent supply of power without requiring sizable energy storage capacities. Nuclear power plants have a high power density along with one of the smallest carbon footprints for power stations (Allen, 2011). The low operating costs make them a cost effective option despite the high initial capital costs. As such, nuclear power is a vital technology as developed countries move to reduce carbon emissions and rely less on fossil fuel energy sources. In 2017, nuclear power produced just over 21% of the UK's domestic electricity generation (World Nuclear Association, 2020a). The 15 nuclear reactors responsible for generating this fifth of the UK's power are reaching the end of their operable lives, but the construction two new pressurised water reactors at Hinkley Point C mean nuclear power will remain in the UK's energy portfolio.

Nuclear reactors are generally powered by uranium fuel pellets held in a cladding material to form long pins. In most operated reactor designs, these fuel pellets are enriched in the fissile ^{235}U isotope. The ^{235}U is split with thermal neutrons to produce fission products (FPs), neutrons and a large amount of energy (~203 MeV per fission). This energy mostly manifests itself in the kinetic energy of the FPs which in turn decays to thermal energy in the fuel pins. This energy transfers to the surrounding coolant (usually light or heavy water in Gen III reactors) which goes on to generate steam to turn a turbine.

When uranium splits, it rarely forms two symmetrical fragments; rather, it will produce a 'light' and a 'heavy' fragment according to probabilistic model based on nuclear stability described by the nuclear shell model (Loveland, et al., 2006). As such, a spectrum of elements is present in used nuclear fuel as shown in Figure 1.1. A build-up of neutron-absorbing nuclei, particularly lanthanides, ultimately renders the fuel inefficient to use as thermal neutrons can no longer go on to induce nuclear fission in a critical nuclear reaction. Table 1.1 shows this in terms of the neutron absorption cross-sections of some lanthanide and actinide cations present in a typical used ^{235}U enriched nuclear fuel. It is at this point that the fuel is considered spent nuclear fuel (SNF). Despite SNF being unusable in nuclear reactors, roughly 96% is still uranium on a heavy metal basis (depending on reactor model, initial fuel composition, burnup, and other reactor operation factors). Not all this uranium is ^{235}U, but generally a third of ^{235}U initially in fresh fuel is present in SNF (IAEA, 2011). Recovery of this unused fuel, as well as fissile ^{239}Pu generated by fast neutron absorption of ^{238}U, is a potential source for fresh nuclear fuel. However, removal of the high neutron absorbing elements is critical for uranium or plutonium recycling for fresh fuel.

1	2	3	4	5	6	7	8	9	10	11	12	13	14	15	16	17	18
H 6×10^{-5}																	He
Li	Be											B	C	N	O	F	Ne
Na	Mg											Al	Si	P	S	Cl	Ar
K	Ca	Sc	Ti	V	Cr	Mn	Fe	Co	Ni	Cu	Zn 4×10^{-11}	Ga 9×10^{-10}	Ge 7×10^{-4}	As 2×10^{-4}	Se 0.056	Br 0.022	Kr 0.36
Rb 0.35	Sr 0.77	Y 0.46	Zr 3.62	Nb 4×10^{-6}	Mo 3.35	Tc 0.77	Ru 2.18	Rh 0.47	Pd 1.37	Ag 0.076	Cd 0.13	In 0.003	Sn 0.096	Sb 0.020	Te 0.48	I 0.24	Xe 5.33
Cs 2.38	Ba 1.73	*	Hf	Ta	W	Re	Os	Ir	Pt	Au	Hg	Tl	Pb	Bi	Po	At	Rn
Fr	Ra	**	Rf	Db	Sg	Bh	Hs	Mt	Ds	Rg							

	La	Ce	Pr	Nd	Pm	Sm	Eu	Gd	Tb	Dy	Ho	Er	Tm	Yb	Lu
* Lanthanides	1.22	2.37	1.12	4.03	0.011	0.86	0.13	0.12	0.003	0.001	0.001	5×10^{-5}	8×10^{-8}		
** Actinides	Ac 7×10^{-11}	Th 8×10^{-6}	Pa 4×10^{-7}	U 956	Np 0.45	Pu 8.69	Am 0.58	Cm 0.13	Bk 4×10^{-14}	Cf 1×10^{-18}	Es	Fm	Md	No	Lr

Figure 1.1. *Calculated composition (in kg heavy metal) of SNF after 10 year cool of 1 tonne 3.2% enriched UO$_2$ fuel, 33 MWd/kg U burnup at a mean neutron flux of 3.28 x 10^{18} n m^{-2} s^{-1} in a typical pressurised water reactor (Choppin, et al., 2002a).*

1.1.2 Nuclear Fuel Cycle Options

Since SNF still contains a high proportion of enriched uranium (albeit less enriched than fresh fuel), there are currently several feasible ways to operate a nuclear fuel cycle (Figure 1.2):

- The 'open cycle' which involves using nuclear fuel once and disposing of it in a geological disposal facility (GDF) after waste encapsulation in a suitable waste form. Canada, Finland, Spain, Sweden, and the USA currently adopt this policy (World Nuclear Association, 2020b).

- The 'partially closed cycle' in which fissile material is recovered before the remaining waste is disposed of in a GDF after encapsulation in a suitable waste form (Regalbuto, 2001a). China, France, India, Japan, Russia, Switzerland, and the UK currently adopt this policy.

- The 'closed cycle' in which both fissile (isotopes that undergo fission through absorption of 'slow' thermal neutrons) and fissionable (isotopes that undergo fission through absorption of both 'slow' thermal and 'fast' neutrons) material are recovered before the remaining waste is disposed of in a GDF after encapsulation in a suitable waste form. No country currently adheres to this policy as fast reactors for transmutation of transuranics (TRUs) are still in development.

Table 1.1 *Total neutron absorption cross-sections for some lanthanides and actinides from SNF as detailed in Figure 1.1 [* average σ_{abs} taken from (NIST, 2020)]*

Element	kg/tonne U	moles	Atoms	Average σ_{abs}* (barns)	$\sum\sigma_{abs}$ (barns)
Nd	4.03	27.94	2.40×10^{19}	50.5	1.21×10^{21}
Sm	0.860	5.72	4.91×10^{18}	5922	2.91×10^{22}
Eu	0.130	0.855	7.35×10^{17}	4530	3.33×10^{21}
Gd	0.120	0.763	6.56×10^{17}	49700	3.26×10^{22}
Total	**10.33**		**6.37×10^{19}**		**6.64×10^{22}**
U	956	4012	3.45×10^{21}	7.57	3.11×10^{22}
Pu	8.69	35.605	3.06×10^{19}	1017	2.61×10^{22}
Am	0.580	2.386	2.05×10^{18}	75.3	1.54×10^{20}
Cm	0.013	0.053	4.52×10^{16}	16.2	7.32×10^{17}
Total	**965.28**		**3.48×10^{21}**		**5.74×10^{22}**
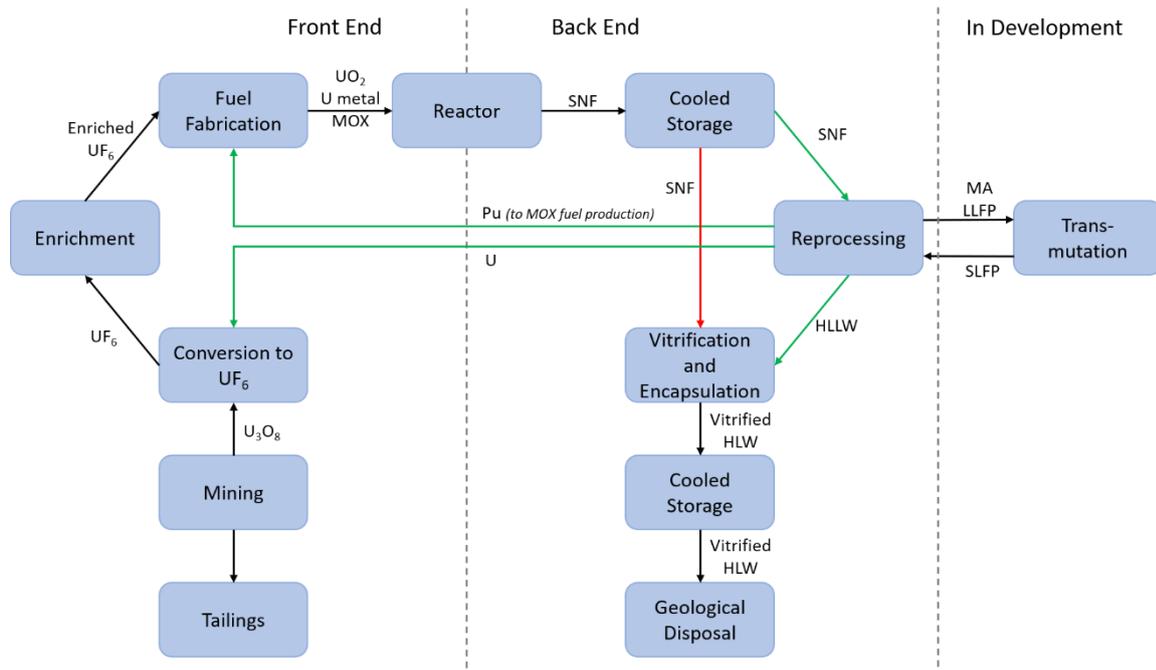
Figure 1.2. *Overview of the nuclear fuel cycle. Red arrows indicate an open cycle, green arrows indicate a closed cycle and black arrows indicate both. (MOX = mixed oxide fuel, MA = minor actinides, LLFP = long-lived fission products, SLFP = short-lived fission products, HLLW = high level liquid waste, HLW = high level waste).*

1.1.3   Benefits of a Closed Nuclear Fuel Cycle

The main benefits of a partial or fully closed nuclear fuel cycle is the increased use of finite global uranium reserves due to uranium recycling. The recovery of fissile elements like ^{235}U and ^{239}Pu allow for the production of fresh uranium or mixed oxide (MOX) fuels from what would otherwise be disposed of. Burning ^{239}Pu as a fuel source in MOX fuels is also reduces proliferation risks as it effectively allows for the safe disposal of this weaponizable isotope. Recovery and usage of unused uranium and plutonium as fresh fuel would gain 25-30% more energy from the original uranium fuel (World Nuclear Association, 2020c). In terms of mass, eight fuel assemblies (*ca.* 7.5 tonnes of fuel) can be reprocessed into a MOX fuel assembly, two-thirds of an enriched ^{235}U assembly, and ~3 tonnes of depleted uranium with the remaining mass being treated as HLW. Further recovery of americium from this HLW may also be desirable for the production of fuel for fast reactors; this is transmuted to plutonium which can again be used to produce MOX fuel for more conventional reactors. However, americium-fuelled fast reactors are still an area of research and are not adopted industrially at present (Gulevich, et al., 2020).

Another benefit of closing the nuclear fuel cycle is the reduction in volume, radiotoxicity, and heat load of the nuclear waste. As the majority of SNF is uranium, the recovery of this metal in a closed fuel cycle would vastly reduce the volume of waste that would be required to be held in a GDF to roughly one-fifth of the original volume. This either results in lower storage-associated costs, or the storage of more reprocessed nuclear waste. At present, roughly 400,000 tonnes of SNF equating to roughly 36,000 m^3 has been removed from nuclear reactors around the world, all of which will need to be disposed of at some point in time (World Nuclear Association, 2020d). Reprocessing this can reduce this global volume to around 7,300 m^3 which is significantly more manageable.

Figure 1.3 shows that SNF is highly radioactive when taken out of a nuclear reactor. It would be reasonable to assume that completely disposed nuclear waste should be no more radioactive than the uranium ore was when it was mined. Radioactivity of SNF is dominated by the β and γ emission from FPs (mainly ^{90}Sr and ^{137}Cs) for the first 300-400 years. α decay of the long-lived TRUs (mainly ^{239}Pu) then dictates the radiotoxicity of the waste for roughly 250,000 years, or around 10 ^{239}Pu half-lives, before radioactivity reaches acceptable uranium-ore-like levels (Nash & Nilsson, 2015a).
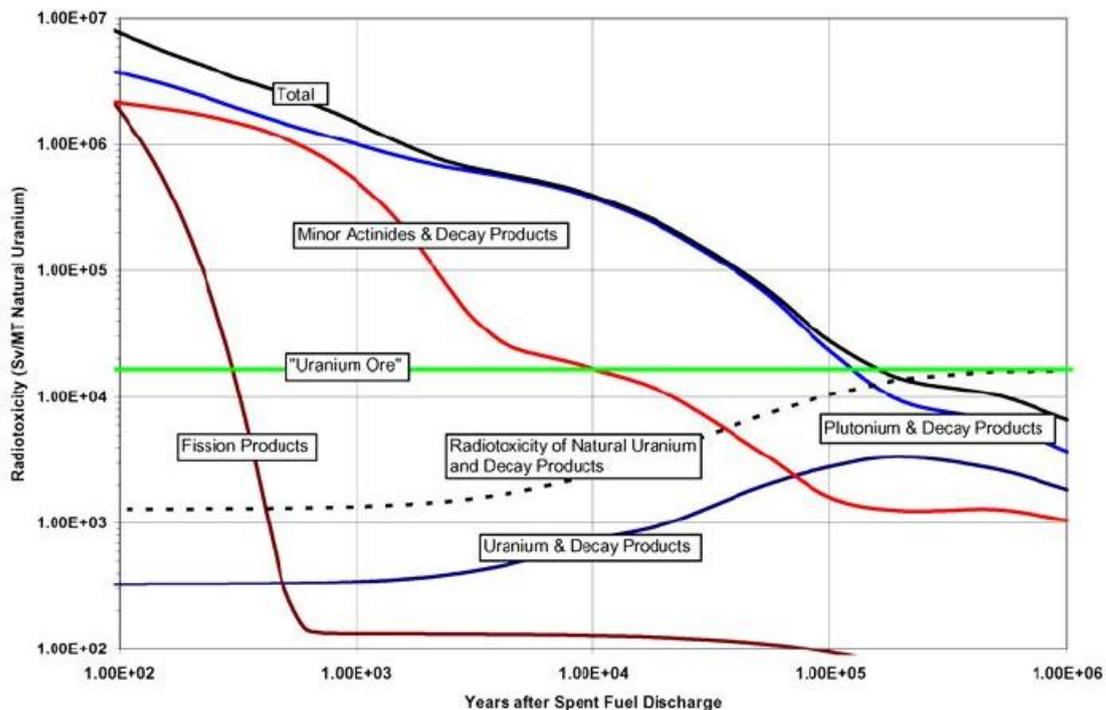
Figure 1.3. *Radiotoxicity of SNF components over time (© (OECD, 2006))*

There is currently no known man-made structure that has lasted 250,000 years, and heat generation by strontium and caesium decay during the first 400 years of storage is also a primary concern for GDF construction and operation. Therefore, the implementation of a closed nuclear fuel cycle to recover ^{239}Pu, caesium, strontium, and the other long-lived TRUs would make the location and/or construction of a GDF substantially simpler due to the reduced radiotoxicity and heat load. Separately recovering americium and curium in reprocessing means that these heavy actinides could be burnt or transmuted in a reactor either to form ^{239}Pu for MOX fuel as previously stated, or to produce smaller fission products that have significantly shorter half-lives which cuts down on waste disposal time requirements (Delpech, et al., 1999). However, transmutation of americium and curium is still in R&D stages. There is also the opportunity to reduce the proliferation risk of ^{239}Pu with a fully closed fuel cycle. Recovering multiple elements in a product stream along with ^{239}Pu (e.g., uranium and/or neptunium) lowers weapons proliferation risk by reducing plutonium purity.

1.1.4   Issues with a Closed Nuclear Fuel Cycle

Current reprocessing flowsheets use the Plutonium Uranium Reduction EXtraction (PUREX, see Section 2.2) process to separate uranium and plutonium from dissolved SNF in nitric acid to produce metal oxides like U_3O_8 for fresh fuel fabrication. The extra processing of the SNF comes at high expense; Bunn, et al. (2005) suggests the Thermal Oxide Reprocessing Plant (Thorp) in Cumbria, UK has a total rough cost of $1800/kg heavy metal including commissioning, decommissioning and refurbishment estimate costs. From February 2011 to March 2020, the U_3O_8 price has steadily decreased from $156/kg to $52.2/kg (Trading Economics, 2020). The reducing value of product means that costs must be cut elsewhere in order for reprocessing to be economically favourable, although it should be noted that the reuse of mined uranium and the decreased volume disposed of in a future GDF need to be taken into account for a more comprehensive assessment of treatment costs.

Reprocessing is extremely complex; desired elements must be separated from a slew of FPs, transmutation and corrosion products while being operated remotely due to the presence of intense ionising radiation which requires large amounts of shielding. As such, it is considered to be one of the most complicated industrial-scale chemical processes (Choppin, et al., 2002b).

Current PUREX processes utilise the organophosphorus extractant tri-*n*-butyl phosphate (TBP) as a hydrophobic ligand to facilitate the extraction of uranium and plutonium from aqueous SNF liquors. The use of TBP utimately leads to large volumes of difficult-to-handle radioactive secondary wastes, as explained in Section 2.2, due to the formation of active phosphate compounds after degraded solvent incineration. The CHON principle is a potential way to eliminate the burden of these secondary wastes. CHON ligands only contain <u>C</u>arbon, <u>H</u>ydrogen, <u>O</u>xygen and <u>N</u>itrogen in their molecular structure. This means the extractants can be completely incinerated to leave no active residue (Musikas, 1987) or other harmful/unwanted products unlike the currently used phosphorus-containing ligands. Waste volume reduction is critical for nuclear waste management; currently, there are no GDFs available to store processed or unprocessed high level waste (HLW), however, the Onkalo GDF site is currently under construction in Finland (Heionen, 2014). If and when a site becomes operational, space will be at a premium and as such the volume reduction or elimination of any waste is a prime concern.

The UK has had reprocessing capability since 1964 using two main reprocessing plants: Thorp and Magnox B205 (Wilkinson, 1987). However, there will soon be no reprocessing capability within the UK due to the closure of Thorp in 2018, the planned closure of Magnox B205 reprocessing plant in 2020 (Leafe, 2017), and no future planned reprocessing capability. In the present economic climate, it can be argued that it is favourable to store spent fuel in interim storage; there is no immediate cost of fuel reprocessing but there is the option to reprocess should it become more economically attractive in the future (Mellinger, et al., 1984). However, this is fundamentally not a long-term option and SNF must be dealt with. Therefore, separations work in this area is required to sustainably recover uranium, plutonium, and other desired elements from SNF rather than waste a valuable resource.

1.1.5 Replacement of TBP in Reprocessing

Many of the issues that arise with reprocessing SNF stem from the use of TBP. The use of this ligand leads to secondary phosphate wastes that are difficult to process, the requirement of extra process steps due to undesired metal extraction, and phase control problems from TBP degradation products; these issues are discussed extensively in Section 2.2 but will be briefly explored here. TBP degrades through radiolysis and acid hydrolysis to produce the degradation products dibutyl phosphoric acid (HDBP),

monobutyl phosphoric acid (H$_2$MBP), and phosphoric acid. These degradation products have a marked effect on plutonium extraction behaviour due to the strong complexing from HDBP or the plutonium precipitant formed with H$_2$MBP. Plutonium losses during stripping are considered excessive even if [HDBP] > 0.001% in the solvent (Irish & Reas, 1957). Therefore, the process requires constant careful controlling. These degradation products also complex with fission products in SNF liquors (mainly zirconium, ruthenium, and molybdenum) which can result in the extraction or co-extraction of metallic impurities. This necessitates several stripping units to ensure the purity of the uranium or plutonium products. Interactions between zirconium and TBP degradation products can also form several different phases in the solvent extraction process (e.g., sludges, emulsions, and precipitates) which can make the liquid-liquid extraction process difficult to control. The acidic TBP degradation products are removed from the solvent using a dilute carbonate wash to yield a spent solvent waste stream, although there have been many studies that work to improve the performance of degraded solvent clean-up processes (Geier, 1979). Spent solvent is typically incinerated, but due to the presence of phosphorus, this yields a phosphate waste that can be radioactive due to extracted metallic ions. What to do with this phosphate waste remains a challenge due to the thermodynamic nature of phosphates. Taking all of this into account, the reduction or elimination of phosphorus in spent fuel reprocessing will not only reduce the amount of waste produced from the process, but it will make it significantly easier to control if extractants can be found that do not have adverse degradation products.

N,N-dialkyl amides, or monoamides, are a type of extractant that have been extensively studied as suitable TBP replacements. They are adduct-forming ligands like TBP and so are chemically similar. Monoamides adhere to the CHON principle which allows for the reduction of difficult-to-process secondary wastes produced after degraded solvent incineration; spent solvent incineration will produce CO, CO$_2$, and NO$_x$ which can be treated to minimise harmful gaseous emissions. Critically, monoamide degradation products have also been shown to have minimal interactions with uranium, plutonium, and most fission products with the slight exception for ruthenium (see Section 2.3). This means that a processing flowsheet with these extractants will be significantly easier to control. Monoamides have also been shown to be much more selective for uranium and plutonium than TBP (Manchanda & Pathak,

2004); (Kulkarni, et al., 2006) which should allow for the reduction in the number of process units required for reprocessing. These benefits should reduce the complexity and economic burden of reprocessing.

N,N-dihexyl octanamide (DHOA) has been identified as one of the most promising monoamides for a TBP replacement, but there are two main issues with DHOA solvents that impede their adoption by industry:

- their overall lower capacity of uranium compared with TBP (Manchanda, et al., 2001); (Manchanda & Pathak, 2004).
- the higher viscosity of DHOA solvents that lead to longer phase separation times (Pathak, et al., 2009); (Parikh, et al., 2009).

The lower solvent capacities have generally been attributed to the poorer solubility of uranyl-nitrate-monoamide complex in aliphatic organic solvents, e.g. *n*-dodecane (Musikas, 1987). Two ways to enhance the solubility of these complexes in aliphatic diluents would be to:

- modify the organic phase with a suitable phase modifier to increase the diluent polarity.
- introduce a second adduct-forming ligand that can form 'ternary' complexes with uranyl-nitrate-monoamide species to increase the hydrophobicity of the extracted complex.

Both of these methods are of interest, but ternary complexes are the main focus for this thesis. Note that a 'ternary' complex in this case indicates a complex with a uranium metal centre and two different lipophilic extractants; this term is used throughout this thesis. Production of a ternary complex requires the non-monoamide ligand to either leave enough space around the metal centre for monoamide complexation or allow for substitution of the non-monoamide ligand by a monoamide. The addition of a second ligand may also have phase modifying effects which may benefit uranium extraction.

The work presented in this thesis is a first step towards determining a viable monoamide solvent for SNF reprocessing. Following a comprehensive literature review, the existence of ternary monoamide complexes with the selected 'second ligand' candidates are assessed spectrophotometrically. Second

ligand candidates are diamides, diglycolamides, phosphates and phosphine oxides; reasonings for these choices are outlined later in Section 2.3. Successful systems are taken forward to solvent extraction tests with uranyl nitrate and compared against conventional solvents.

1.2   Research Hypotheses

The work contained within this thesis is toward testing the following research hypothesis:

"The addition of amide-based or organophosphorus adduct-forming ligands to monoamide solvents will enhance the uranium recovery of these solvents and allow for the reduction or elimination of phosphorus from reprocessing flowsheets"

This hypothesis has been separated into the following sub-hypotheses which concern the distinct ligand systems investigated within this thesis:

1. Diamides can form ternary complexes with uranyl nitrate and monoamides which enhances uranium recovery with a monoamide solvent during solvent extraction.

2. Diglycolamides can form ternary complexes with uranyl nitrate and monoamides which enhances uranium recovery with a monoamide solvent during solvent extraction.

3. Phosphates can form ternary complexes with uranyl nitrate and monoamides which enhances uranium recovery with a monoamide solvent during solvent extraction.

4. Phosphates can modify a monoamide solvent to increase uranyl-nitrate-monoamide solubility which enhances uranium recovery with a monoamide solvent during solvent extraction.

5. Phosphine oxides can form ternary complexes with uranyl nitrate and monoamides which enhances uranium recovery with a monoamide solvent during solvent extraction.

These sub-hypotheses are based on findings from the literature review presented in Chapter 2 and are tested throughout experimental Chapters 3, 4 and 5. Chapter 3 assesses whether these ternary complex systems are formed using spectrophotometric analysis techniques. Promising systems are then taken forward to solvent extraction tests presented in Chapter 4 to confirm synergistic effects and determine likely extraction mechanisms. Suitable solvents are then taken forward to further solvent extraction tests in Chapter 5 to further explore extraction mechanisms and determine effectiveness compared with

standard solvents. Systems that are unsuccessful at any point in this process are disregarded and the relevant sub-hypothesis is considered incorrect. In order to test the hypothesis, the aims and objectives of each chapter are presented in each respective introductory section.

CHAPTER 2 Literature Review

2.1 Introduction

Presented in this chapter is the literature review that forms the knowledge basis for the work completed in this thesis. This chapter is split up into three main sections. The first section describes the <u>P</u>lutonium <u>UR</u>anium <u>R</u>eduction <u>EX</u>traction (PUREX) reprocessing flowsheet and outlines the limitations relevant to this thesis. The second section is review of the research into the use of monoamides as a tri-*n*-butyl phosphate (TBP) replacement in reprocessing operations which identifies the benefits and current limitations of using monoamide ligands. The third section is an assessment of more modern and advanced reprocessing flowsheets that aim to improve or extend upon PUREX to identify how monoamide reprocessing can be utilised effectively in current advanced reprocessing applications. This chapter is concluded with a summary of the key points of the review.

2.2 PUREX

PUREX was developed and implemented in the 1950s for defence purposes in the United States to produce weapons-grade plutonium; today, it remains the globally accepted process for the reprocessing of spent fuel (Nash & Nilsson, 2015b). It is a solvent extraction (SX) process that relies upon TBP to extract uranium and plutonium from spent fuel liquors. Briefly, in the first extraction step, the target uranium and plutonium metals are separated from all other metallic contaminant species. After this, the uranium and plutonium are separated from each other. This section will detail the theory behind SX, PUREX operation, and the relevant issues with this process.

2.2.1 Solvent Extraction

For any separation to take place, there must be a difference in physical or chemical properties that can feasibly be exploited. SX (Figure. 2.1) is a very common process for nuclear reprocessing flowsheets that exploits the polarity of the different solutes; it involves the removal of a desired solute from a solvent, e.g. water, by using a second immiscible solvent, e.g. *n*-dodecane, for which the target solute has a higher affinity. One phase is aqueous (hydrophilic) and supports polar/charged solutes, whereas the other phase is organic (lipophilic) and supports neutral species. Upon agitation of the two appropriate solvent phases, the desired solute would preferentially transfer from its initial phase to the

other whereas the contaminants would remain in the initial phase. The two phases can be separated through gravitational settling or application of centrifugal force. This separates the target from the other solutes in the initial solution; this can be carried out over a number of contact stages to improve recovery.
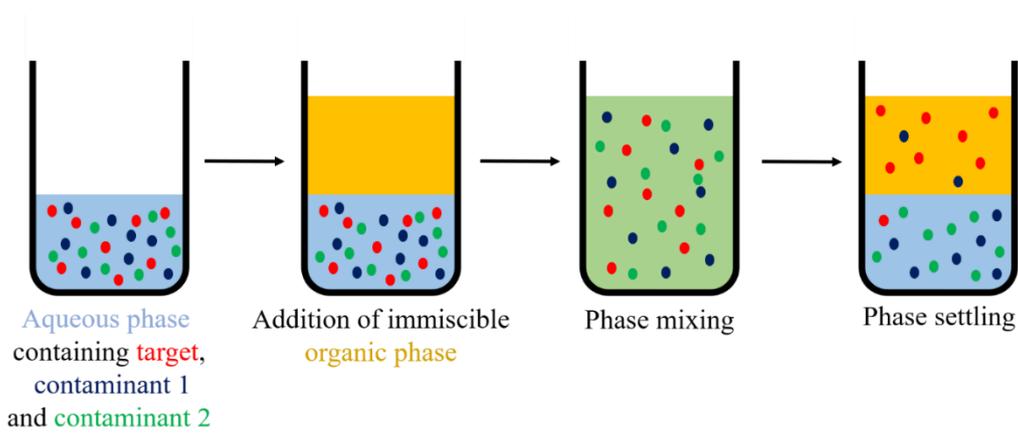
Figure 2.1. *A simplified SX process.*

In reprocessing, target solute transfer between the phases is aided by selective ligands in the organic phase that form complexes with target solutes to improve their recovery. This is done because the low dielectric constant of organic solvents demands that cation and anion species are brought together as electroneutral species. As such, extraction kinetics are governed by three main stages: i) charge neutralisation and complexation of the metal centre, ii) dehydration of the complex, and iii) solubisation into the organic phase.

In general, there are five types of SX systems employed for actinide separations, i.e. uranium and plutonium separations in PUREX [Eq 2.1 – 2.5, (Nash, et al., 2010a)]. Note it is convention to denote organic phase molecular species and concentrations with a bar:

Liquid cation exchangers:

$$M^{m+} + \overline{mHL} \rightleftharpoons \overline{ML_m} + mH^+ \tag{Eq 2.1}$$

Micellar extractants:

$$M^{m+} + \overline{(HL)_n} \rightleftharpoons \overline{MH_{n-m}L_n} + mH^+ \tag{Eq 2.2}$$

Solvating extractants:

$$M^{m+} + \left(\frac{m}{x}\right) X^{x-} + \overline{nS} \rightleftharpoons \overline{MX_{(m/x)}S_n} \tag{Eq 2.3}$$

Ion pair forming extractants:

$$M^{m+} + \left(\frac{m}{x}\right)X^{x-} + \overline{A^{x+}X^{x-}} \rightleftharpoons \overline{MX_{1+(m/x)}A}$$ (Eq 2.4)
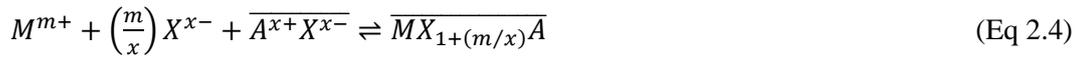
Synergistic extractants:

$$M^{m+} + \overline{mHL} + \overline{nS} \rightleftharpoons \overline{ML_mS_n} + mH^+$$ (Eq 2.5)

where M is a metal cation with charge m, L is a cation-exchanging ligand and H is a proton to act as a model cation in these systems as this is generally the case. S is a solvating ligand, X is an anion of charge x, and n is a stoichiometric coefficient for the relevant species. Liquid cation exchangers and micellar extractants operate by exchanging a number of monovalent cations, e.g., H$^+$, equal to the formal charge of the target metal ion. As such, they operate best at low transferred cation concentration, e.g., low [H$^+$] (in the order of 0.1 M / pH 1 in these systems). The metal should be recoverable back into the more manageable aqueous phase by contacting the metal-loaded organic phase with concentrated [cation], e.g., high [H$^+$] (in the order of 5 M in these systems). Solvating and ion pair forming extractants operate through charge neutralisation of the target species, generally with mineral acid anions. As such, high acid concentration favours metal extraction, and the metal can be recovered through contact with low acid concentration, i.e. low mineral acid anion concentration. Classic synergistic systems utilise solvating ligands along with an ion exchanger within the same phase to facilitate the mass transfer mechanism and so favour low acidity during extraction, like Equation 2.1 and 2.2 (Ogden, et al., 2011).

Separation processes can be characterised by distribution ratios (D, Equation 2.6) and separation factors (SF, Equation 2.7). Fundamentally, D is a mole ratio of the outlet phases with respect to a specific element, M, to describe how well that element has been partitioned between the phases. It is defined as:

$$D_M = \frac{\overline{[M]}}{[M]_{aq}}\frac{V_{aq}}{V_{org}} \rightarrow if\ V_{aq} = V_{org} \rightarrow D_M = \frac{\overline{[M]}}{[M]_{aq}}$$ (Eq 2.6)

where $\overline{[M]}$ and $[M]_{aq}$ are the metal concentrations in the organic and aqueous phases, respectively, and V_{org} and V_{aq} are the volumes of the organic and aqueous phases, respectively. A common simplification comes from the equalisation of phase volumes, as seen in Equation 2.6, reducing the distribution factor to a ratio of outlet phase metal concentrations.

Separation factors (Equation 2.7) are ratios of two different distribution factors to describe how effectively one element is separated from another:

$$SF = \frac{D_M}{D_N} \qquad \text{(Eq 2.7)}$$

where D_M and D_N are distribution coefficients of species M and N respectively.

2.2.2   General PUREX Operation and TBP Chemistry

Ultimately, PUREX aims to extract and separate uranium and plutonium targets from other spent nuclear fuel constituents dissolved in concentrated nitric acid. It achieves this by exploiting the unusual redox behaviour of plutonium, previously observed in the 1940's bismuth phosphate process (Nash, et al., 2010c), and the selective phosphoryl chemistry of the organophosphorus compound TBP (Figure 2.2). Organophosphorus compounds (Figure 2.3) interact with cations through the phosphoryl bond (P=O) to form neutral adducts; they are solvating extractants and follow the extraction mechanism described in Equation 2.3. Due to the strong electronegativity of the oxygen, phosphine oxide compounds interact strongly with many cations of various charges; as such, they have low selectivity.
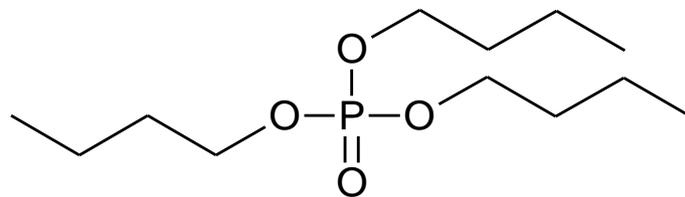
Figure 2.2. *Chemical structure of tri-n-butyl phosphate (TBP).*
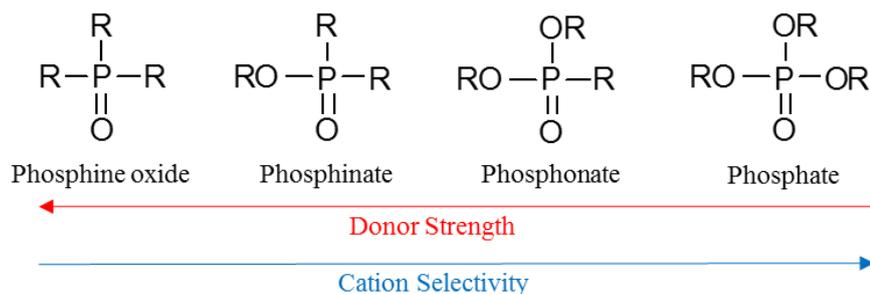
Figure 2.3 *General selectivity and donor strength of organophosphorus species.*

The phosphoryl bond in phosphates is much weaker owing to the conjugation from the other oxygen atoms around the phosphorus. This significantly increases the phosphates selectivity; as a result, it strongly prefers to form complexes with M^{4+} and MO_2^{2+} ions (Herbst, et al., 2001a). This makes phosphates ideal for extracting uranium(VI) and plutonium(IV) from aqueous solutions. Hence, the PUREX solvent is typically 30% TBP in aliphatic (straight-chained) hydrocarbon diluent as this balances the required extraction efficiencies with adequate process conditions (organic phase density, viscosity, etc.).

PUREX pre-treatment is displayed in Figure 2.4. Spent nuclear fuel (SNF) is dissolved in concentrated nitric acid (~10 M) and clarified to remove insoluble material and other solids. Dissolution off-gases are treated to remove iodine, krypton, and xenon before release to the atmosphere. Uranium largely exists in the hexavalent state, uranium(VI), in aqueous solutions below ~ pH 2. Plutonium is more complicated; it can exist in many oxidation states, as many as four at the same time in aqueous solutions (Clark, 2000). Its most stable aqueous oxidation state is generally plutonium(III), but this needs to be carefully controlled through PUREX operations with suitable redox reagents to avoid undesirable partitioning.
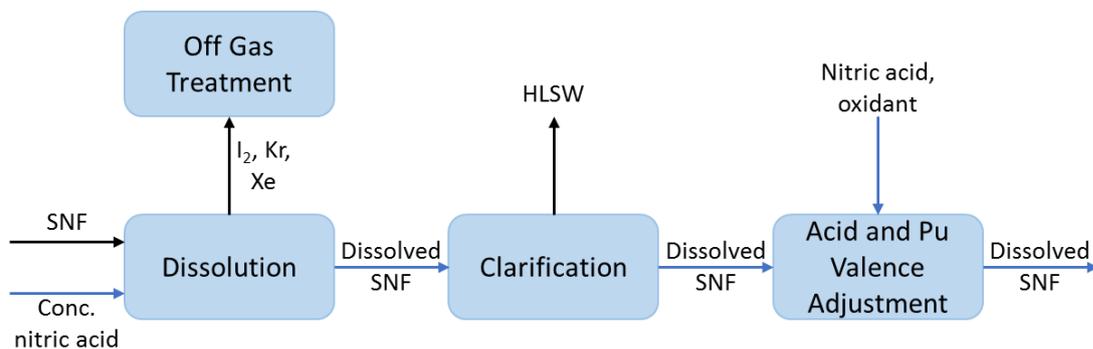
Figure 2.4. *PUREX chemical pre-treatment. HLSW = high level solid waste.*

The PUREX process is displayed in Figure 2.5. Following the PUREX pre-treatment, acid concentration is reduced to 2-4 M and a Pu oxidant, such as H_2O_2 or HNO_2 (Nash, et al., 2010b), is added to increase the amount of plutonium(IV) in solution. In the 'Primary U/Pu Extraction' step of Figure 2.5, TBP

forms metal-ligand complexes with UO_2^{2+} and Pu^{4+} corresponding to the following solvating equilibria (Equation 2.8, 2.9) to solubilise the uranium and plutonium targets into the organic phase:

$$UO_2^{2+} + 2\,NO_3^- + \overline{2\,TBP} \rightleftharpoons \overline{UO_2(NO_3)_2(TBP)_2}$$ (Eq. 2.8)

$$Pu^{4+} + 4\,NO_3^- + \overline{2\,TBP} \rightleftharpoons \overline{Pu(NO_3)_4(TBP)_2}$$ (Eq. 2.9)
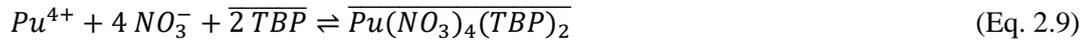
Adduct formation by TBP requires complexation of neutral metallic species. As such, charge neutralisation by NO_3^- forms a neutral species with which TBP can solvate. TBP-metal complexation occurs at the aqueous-organic phase interface where complexed cations are solvated into the organic phase. With consideration of distribution factors (Equation 2.6) and the above ideal equilibria, it can be shown that the distribution of UO_2^{2+} and Pu^{4+} directly correlate to nitrate and TBP concentrations with the following relationships:

$$D_{UO_2^{2+}} = K_{ex}[NO_3]_{eq}^2 \overline{[TBP]_{eq}^2}$$ (Eq 2.10)

$$D_{Pu^{4+}} = K_{ex}[NO_3]_{eq}^4 \overline{[TBP]_{eq}^2}$$ (Eq 2.11)

where K_{ex} is an extraction equilibrium constant. Equations 2.10 and 2.11 show that extraction of uranium and plutonium are heavily dependent on the nitrate/nitric acid concentration. Therefore, either decreasing nitric acid concentration or changing the cation oxidation state will drive the distribution ratio of uranium and plutonium nitrates down and push them back into the aqueous phase; these phenomena form the basis of their partitioning. In the 'U/Pu Partition' step of Figure 2.5, the uranium- and plutonium-loaded organic phase is contacted with concentrated nitric and a plutonium reductant (such as ferrous sulfamate, hydroxylamine nitrate or quadrivalent uranium) to reduce plutonium to its trivalent state (Nash, et al., 2010c); (Phillips, 1992). Trivalent cations have vastly lower solubility in the organic phase due to selective TBP complexation. As a result, plutonium(III) is solubilised into the aqueous phase at the phase interface. It should be noted that it is desirable to have aqueous product streams as these are easier to manage during the downstream purification steps of the uranium and plutonium products.
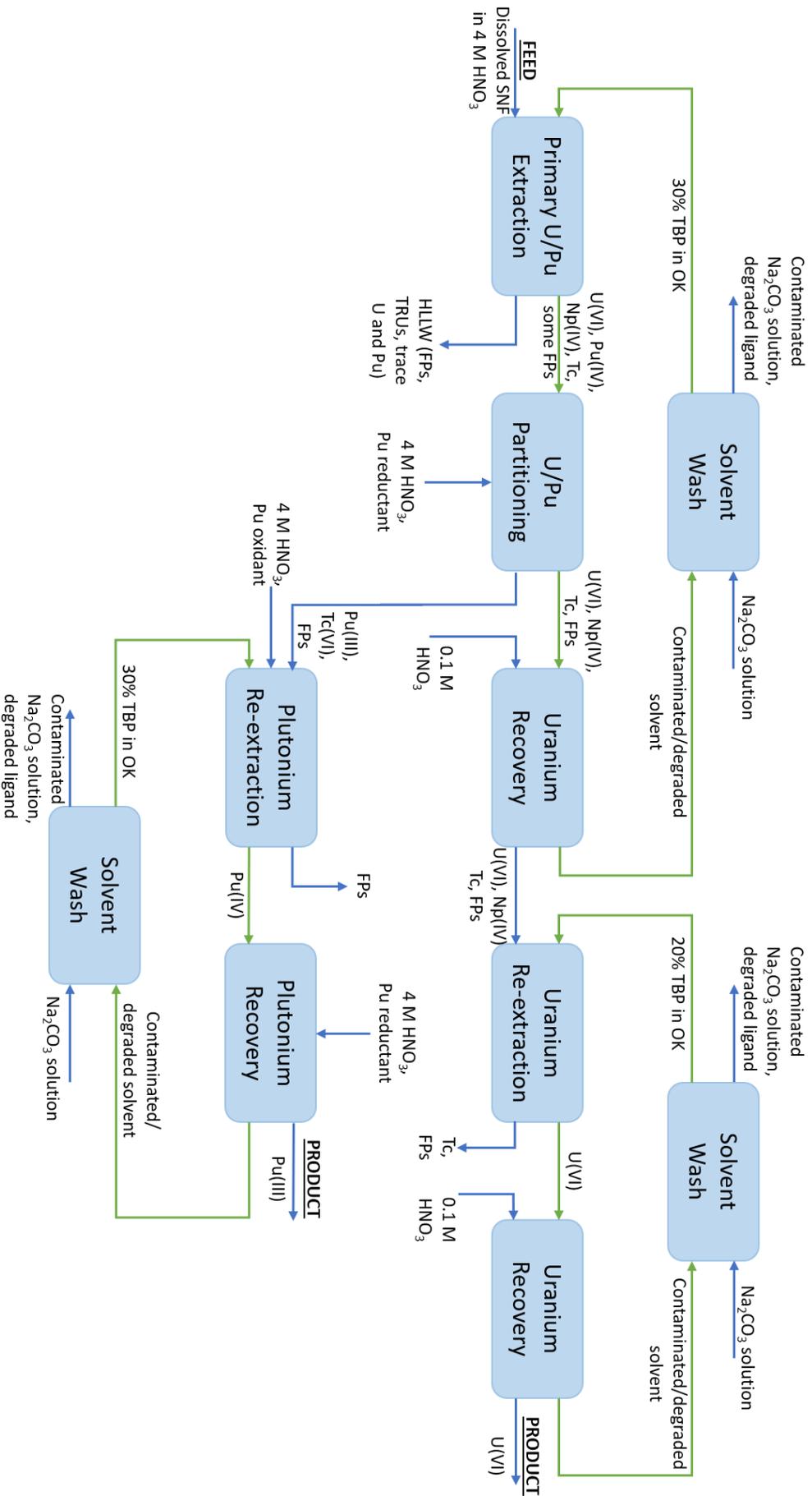
Figure 2.5. *A simplified PUREX process. Blue arrows show aqueous flows. Green arrows show organic flows. [Adapted from (Philips, 1992) & (Nash, et al., 2010b)].*

Following another phase separation, dilute nitric acid contact with the uranium-loaded organic in the 'Uranium Recovery' step in Figure 2.5 reduces uranium(VI) nitrate solubility in the organic phase, as per the distribution equilibria in Equation 2.10. Therefore, uranium(VI) solubilises into the aqueous phase at the phase interface to leave behind the unloaded solvent. The solvent must be decontaminated post-contact as residual radionuclides remain in the organic phase; this is typically achieved with a sodium carbonate wash (Reif, 1988). This carbonate wash also removes the acidic organic degradation products discussed later in this chapter.

2.2.3   Challenges with PUREX - Radiolysis and Hydrolysis

This section covers the effects of radiolysis and acid hydrolysis in PUREX operations. Radiolysis is defined as the breaking up / degradation of compounds as a direct result of interaction with ionising radiation (mainly α, β, and γ radiation). Acid hydrolysis is defined as the breakage of chemical bonds induced by H^+ ions. In both cases, the resultant products are generally termed as 'degradation products'.

The intense ionising radiation field and acidity inherent in PUREX results in the formation of various degradation products. All system components are affected by this, including diluents, ligands, and the process equipment units themselves. For process efficiency and economics, there is a need to recycle used solvent; however, its recyclability is limited by degradation. Generally, the resultant effects of degraded solution components are poorer mass transfer/solute separation, poorer phase separation and the creation of additional phases. Without solvent clean-up to remove the degradation products, the process quickly becomes difficult to operate. Because of the complexity of degradation effects within PUREX, the following discussions have been separated into the major constituents to gradually build a picture. First, only diluents are considered (kerosene/*n*-dodecane and water). Next, the effects on nitric acid are discussed. Finally, and most importantly, the effects on TBP are reviewed.

Alkane diluents with low dielectric constants are preferred to reduce potential undesired cation extraction and to aid phase separation/minimise organic solubility in the aqueous phase. Odourless kerosene (a mixture of high boiling point aliphatic hydrocarbons) or *n*-dodecane are typical choices which give the necessary organic phase density and viscosity to result in adequate phase separation

kinetics (Wojnárovits, 2011). Radiolysis of these diluents does still occur to produce various alkane radicals, alkenes or even peroxy radicals in the presence of oxygen (Neta, et al., 1990). Radiolysis of water produces hydroxyl radicals, hydrogen atoms (radicals) and hydrogen peroxide (Buxton & Greenstock, 1988); (Mincher, et al., 2009a). In both aqueous and organic radiolysis cases, solvated electrons are produced which can chemically reduce components of the system. This demonstrates that the system quickly becomes complicated even without the consideration of acids, ligands and complexes, and there is no further way to mitigate this problem within a spent fuel SX process.

The nitric acid in the PUREX aqueous phase is also susceptible to radiolysis; this produces nitrite and hydroxyl radicals. The nitrite radicals are particularly problematic as they can react with alkanes to form nitrous acid (which acts as a redox reagent for various aqueous species like plutonium and neptunium (Burger & Money, 1959)) or with hydrocarbon radicals to produce nitro or nitrite molecules. These can further react with solution components to produce nitroso molecules, carboxylic acids and even alcohols (Smith, et al., 1997) which may go on to support third phase formations. Third phases are caused by the splitting of the organic phase when metal, acid or other polar component concentrations in the organic are too high and increases the polarity of organic phase above a certain point. This results in two organic phases; one is a more polar, heavier, metal-solvate rich phase, and the other is a less polar, lighter, diluent-rich phase. Third phases should be avoided as the concentration of fissile isotopes in a metal-rich third phase could potentially lead to a sustained, critical nuclear fission reaction in separation systems.

Diluents are not the only system components prone to degradation; TBP degradation products result in large complications in reprocessing from poor phase control to undesired metal extraction. A degradation route is presented in Figure 2.6. The main TBP radiolysis products are dibutylphosphoric acid (HDBP), methane and hydrogen, but monobutylphosphoric acid (H_2MBP) and phosphoric acid (H_3PO_4) are also produced in much lower concentrations assuming regular solvent clean-up with caustic solutions. HDBP is a complexing agent; it forms complexes with zirconium that readily co-extract molybdenum, iron, rare earth elements (REEs), and transuranic (TRU) elements into the degraded PUREX organic phase (Zilberman, et al., 2003).
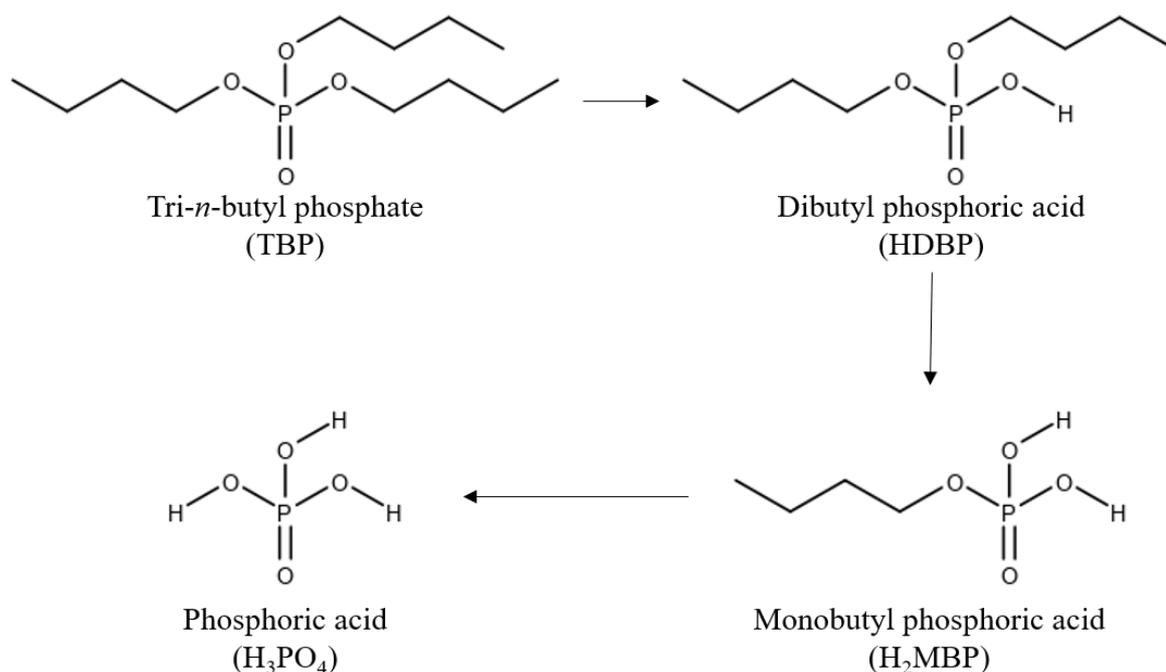
Figure 2.6. *Radiolysis/hydrolysis degradation route for TBP.*

While HDBP is by far the dominating TBP degradation product, the effects of H_2MBP and H_3PO_4 are still significant. Complexes of zirconium with H_3PO_4 are known to precipitate; these precipitates form water-organic emulsions at increased pH like that used in the sodium carbonate solvent clean-up units which complicate phase separation and process operation. The emulsions are stabilised by Zr-H_2MBP complexes (Sugai, et al., 1992). The general term for such precipitation-stabilised emulsion is interfacial 'crud' (Sugai, 1992). The continual removal of crud (and replacement of lost TBP and diluent) returns the process back to normal operation; however, the removed crud is difficult to dispose of and remains a left-over legacy waste. It can be highly radioactive due to coextracted TRUs and chemically unreactive due to the thermodynamic nature of phosphate precipitates (Mincher, et al., 2009a). Final solvent disposal involves incineration (Todd, et al., 2000) which leaves behind radioactive, inorganic phosphate residue as a secondary waste.

While both radiolysis and hydrolysis mechanisms degrade TBP, it has been shown that direct nitric acid hydrolysis rates for TBP are small or negligible; Egorov, et al. (2005) detected no hydrolysis of TBP to HDBP in 1.5-3 M HNO_3 at 40°C over 100 hours. At 95°C, the rate constant of TBP hydrolysis was found to be 0.015 h^{-1}. There are a number of suggested TBP radiolysis mechanisms to form HDBP. The

21

most notable are the reactions of TBP with radiolytically produced hydrogen or hydroxyl radicals to form a TBP carbon-centred radical which then either decays to HDBP (Burr, 1958), or undergoes hydrolysis to produce HDBP (Von Sonntag, et al., 1972). This mechanism would repeat on successive butyl groups of TBP to produce HDBP, H_2MBP and H_3PO_4. The removal of butyl groups alters the phosphoryl bond strength, and as such, the process chemistry changes as radiolysis goes on without solvent clean-up.

2.2.4   Challenges with PUREX - Problematic Elements

This section concerns the contaminants in PUREX operations that are extracted or co-extracted alongside the uranium and plutonium targets in an ideal PUREX process (i.e. assuming no degradation effects). Note that a co-extracted metal is defined as a metal that is extracted by a previously generated metal-ligand complex. The main contaminants discussed are neptunium, zirconium, ruthenium, and technetium; these elements will be discussed in turn. Capturing these contaminants ultimately reduces the purity of the product streams which will affect downstream fuel fabrication processes. Therefore, the extraction of these contaminants either must be avoided or should be stripped from the organic phase before continuing with PUREX operations.

Neptunium redox behaviour makes it similar to both uranium and plutonium; it can exist in oxidation states between +3 and +7. Neptunium(V) is the most stable oxidation state in aqueous solution (Yoshida, et al., 2010) but neptunium(VI) in the form NpO_2^{2+} also exists within oxidative reprocessing conditions (Guillaume, et al., 1984). Neptunium(IV) is common under reducing environments, such as the plutonium chemical reduction step of PUREX or where there are high nitrous acid concentrations. As such, two groups of neptunium oxidation states exist in reprocessing solutions under the oxidative or reductive conditions, either neptunium(V) and (VI), or neptunium(IV) and (V), respectively. This allows some neptunium to follow uranium(VI) extraction mechanisms through the primary extraction step in oxidising environments. During plutonium reduction, neptunium(V) would follow plutonium(III) into the aqueous phase, but reduced neptunium(IV) would remain extractable by TBP and allow it to follow uranium(VI). The vast majority of neptunium decontamination occurs within the uranium purification stage whereby heating at low acidity oxidises neptunium(IV) to the inextractable

neptunium(V). While avoiding neptunium recovery is good for standard PUREX processes for suitable product purity, it should be noted that neptunium decontamination is not always desired. Nowadays, with the aforementioned efforts to reduce the radiotoxicity and heat load of nuclear waste forms, there are some advanced flowsheets that are designed to completely recover neptunium with either plutonium or uranium-plutonium product streams in order to be incorporated into fuel (Taylor, et al., 2013); (Herbst, et al., 2011b). This requires either the complete extraction of neptunium within the first 'U-Pu extraction' step, or further processing on the PUREX raffinate. These flowsheets are discussed further in Section 2.4.

Zirconium and, to some extent, ruthenium (in the form $RuNO^{3+}$) are problematic elements in PUREX because they are both extractable by TBP within the 'Primary U-Pu Extraction' step of PUREX. Ignoring the effect of Zr-HDBP/H_2MBP/H_3PO_4 complexes on process operation, both zirconium and ruthenium can be stripped from the organic phase by using nitric acid strip units. Strip units are units that are designed to remove contaminants from the organic phase. As zirconium is extracted at high nitric concentrations (Alcock, et al., 1957), low nitric concentrations push the extraction equilibria the opposite way. On the other hand, ruthenium is stripped at high nitric acid concentrations (Herbst, et al., 2011c). This means that two nitric acid strip units are required before the U-Pu partitioning stage. It should be noted that an oxalic acid strip also works for zirconium which is seen in more recent flowsheets (see Section 2.4); this is likely to avoid uranium stripping by dilute nitric acid.

Technetium is a problematic element in PUREX, but it behaves differently to the other considered metals. In acidic and oxidising reprocessing conditions, technetium exists as pertechnetate anions (TcO_4^-) which form co-extractable complexes with metal-TBP species according to the following equilibria (Herbst, et al., 2011d):

$$UO_2(NO_3)_2 \cdot 2TBP + TcO_4^- \rightleftharpoons UO_2NO_3(TcO_4) \cdot 2TBP + NO_3^- \qquad \text{(Eq 2.12)}$$

$$M(NO_3)_4 \cdot 2TBP + TcO_4^- \rightleftharpoons M(NO_3)_3(TcO_4) \cdot 2TBP + NO_3^- \qquad \text{(Eq 2.13)}$$
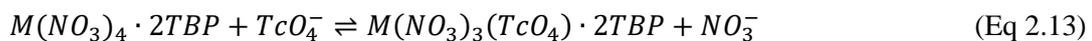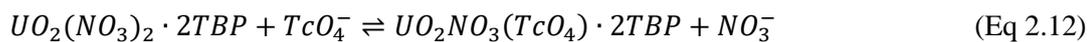
where M in Equation 2.13 is a quadrivalent cation, such as zirconium(IV) or plutonium(IV). In both cases, a cationic nitrate ligand is substituted by a pertechnetate. While both extractable complexes

shown in Equations 2.12 and 2.13 are known to occur within reprocessing solutions, technetium extraction is largely dominated by technetium-zirconium co-extractable complexes. During initial experimental trials at the Thermal Oxide Reprocessing Plant in the UK, roughly one third of technetium was found to be extractable at the U-Pu extraction step (Garraway, 1984). During fully active SNF trials, it was discovered that technetium completely extracts into the organic phase during the U-Pu extraction step by forming extractable TBP-complexes with zirconium. Then, at the U/Pu partition, it is reduced by U(IV) (a plutonium reductant) to technetium(VI) and follows plutonium(III) to the plutonium cycle of the flowsheet. This indicates that initial tests for problematic element distribution may not represent the proper system at all should the test conditions change. Technetium also reacts with hydrazine which is a redox stabiliser used in the U/Pu partition. This means that the amount of hydrazine must be varied given the amount of technetium in the system (Phillips, 1992). Both these issues are somewhat resolved by employing a concentrated nitric acid strip prior to the U-Pu partition to remove the extracted technetium. This resolution coincides with ruthenium stripping. This is followed by dilute nitric acid stripping to remove zirconium bound by TBP.

2.2.5 PUREX Review Conclusion

PUREX is a SX process that uses TBP as an extracting ligand to separate uranium(VI) and plutonium(IV) from dissolved SNF in nitric acid. TBP is selective for hexavalent and tetravalent cations; however, there is a considerable amount of undesired extraction (neptunium(IV)/ neptunium(VI), zirconium(IV), $RuNO^{3+}$) and coextraction (technetium(VII)) that occurs under normal operation. Acid hydrolysis and radiolysis degrade TBP into acidic HDBP, H_2MBP and phosphoric acid which generate a myriad of extraction and phase complication issues. Most notably, HDBP readily extracts zirconium which then coextracts molybdenum, iron, REEs and TRUs. Zirconium also forms stable emulsions with H_2MBP and phosphoric acid. Degradation products are usually washed with a carbonate strip of degraded organic. Completely degraded organic is incinerated which generates an active phosphate ash which is difficult and expensive to process. As a result, replacement of TBP with an incinerable alternative could reduce secondary wastes and reduce reprocessing costs.

2.3 Monoamide Applications to Reprocessing

This section discusses how *N,N*-dialkyl amides, termed monoamides herein, have been researched as potential TBP replacements in reprocessing. First, a brief history of how research has led to modern advancements is presented to identify 'dead ends' as well as gaps in the literature. Following this, important studies are discussed and categorised by monoamide testing in different scenarios (e.g. acid extraction performance, uranyl loading performance, etc.) and compared with TBP where possible.

2.3.1 Brief History of Monoamide Research

Section 2.2 demonstrates that there is a requirement to replace TBP in order to make reprocessing more sustainable and economical; this has prompted significant work into the development of new ligands that are comparable with TBP without the use of phosphoryl donors. In particular, ligands adhering to the CHON principle are of interest; these are organic complexants that only incorporate Carbon, Hydrogen, Oxygen and Nitrogen in their molecular structure. Avoiding the incorporation of phosphorus in the ligand structure avoids complications like phosphate precipitation and allows the spent/degraded organic phase to be combusted without leaving residue (Musikas, 1987) which will reduce the legacy waste produced from reprocessing.

Monoamides (Figure 2.7) are a key group of ligands that have been identified as potential TBP replacements for a number of reasons. Firstly, they are CHON ligands. Secondly, they are easy to synthesise with a number of different synthesis routes. The main route is the nucleophilic substitution of an acyl chloride (or anhydride) with a disubstituted amine in the presence of a base; however, other synthesis avenues include the partial hydrolysis of nitriles or the reaction of carboxylic acids and secondary amines in the presence of a dehydrating reagent. Thirdly and most importantly, monoamides are chemically similar to TBP and form similar complexes. The amide carbonyl bond is analogous to the phosphoryl bond of TBP, although the larger electronegativity of the carbon relative to phosphorus results in a weaker donor strength. The nitrogen provides conjugation from its lone pair similarly to TBP's ether oxygens and the amount of stability provided can be tweaked through manipulation of the 'R' side chains. The ionic conjugation form seen in Figure 2.7 is thought to be the structure responsible for cation extraction (Siddall, 1960).
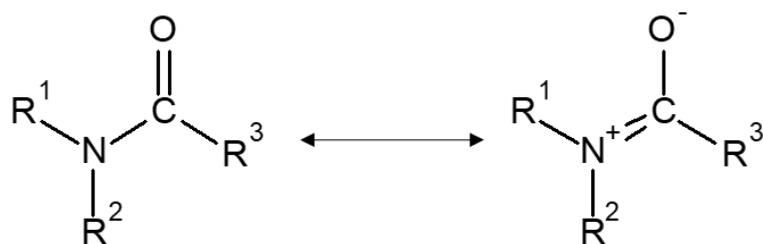
Figure 2.7. *Structure and conjugation form of monoamides*

Much of the recent work towards CHON implementation within PUREX stems from the monoamide work of Siddall (1960). He suggests methyl branching of the carbonyl α-carbon (R^3) increases separation of hexavalent uranium from quadrivalent plutonium, thorium, and zirconium species by factors of between 10^2 and 10^4, but that longer chain branching does little to change this effect. He also suggests a similar lesser effect to branching on the amine side of the of the amide group (R^1 and/or R^2). This difference was attributed to steric hindrance; uranium(VI) ions generally need two amide molecules for extraction whereas neptunium(IV) and thorium(IV) require more than two amide molecules. This is clearly more difficult to achieve when amide molecules are branched and bulky. uranium(VI) extraction generally exceeded that of plutonium(IV) with most of the amides tested at 3 M nitric acid; however, at 6 M nitric acid, uranium(VI) extraction remains largely unchanged or decreases, whereas most monoamides show enhanced plutonium(IV) extraction.

Following from this study, (Dukes & Siddall, 1966) believed tetrabutyl urea (TBU, Figure 2.8) would act as a 'super amide' extractant due to the higher abundancy of free electrons from two N^+/O^- conjugation forms. It was found that TBU behaved roughly the same as monoamides with the same extraction mechanism for hexavalent uranium, although thorium(IV) and neptunium(IV) extraction mechanisms required fewer ligand molecules. [1]H nuclear magnetic resonance (NMR) and infra-red (IR) analysis of uranyl-TBU complexes suggested bonding with the carbonyl oxygen was consistent with that seen with standard amides. It was argued that availability of electrons was not an issue with TBU, but the carbonyl oxygen has a limit to its electron density which drives the extraction process and determines a molecules extraction strength. Hence, standard monoamides and diamides has become a research focus.
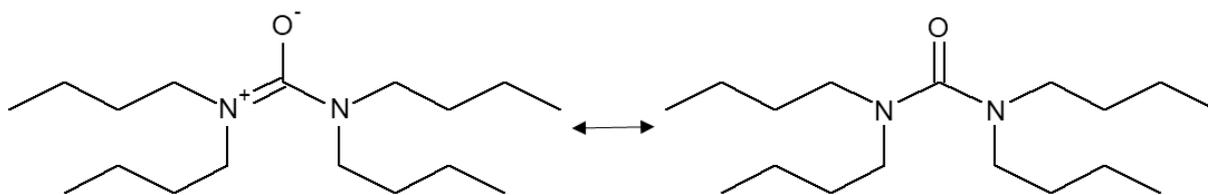
Figure 2.8. *Structure and some conjugation form of TBU*

Musikas (1987) found ethyl substitution on the amine β-position carbon significantly increased complex solubility in aliphatic organic diluent. It was suggested that the amine side of the molecule is more responsible for organic phase solubility although it was noted that the reason for this phenomenon was unknown. Carbonyl-side branching was again observed to separate uranium(VI) from plutonium(IV) and zirconium(IV); this time the β-carbon was substituted rather than the α-carbon in Siddall's tests.

Throughout the early studies of monoamides, two key limitations of their applications were identified: i) poor solubility of the uranyl-nitrate-monoamide complex in an organic phase, and ii) susceptibility to form third phases or micelles under certain conditions (Gasparini & Grossi, 1986); (Musikas, 1987). The former limitation is significant as is directly impacts uranium recovery from reprocessing solutions. The latter limitation is significant as third phases can lead to concentration of fissile isotopes as discussed previously. More modern studies have generally focused changing monoamide structure or solvent systems in order to mitigate the two limitations mentioned above. Two main directions have been taken with monoamide research: i) to improve aliphatic monoamides ability to extract uranium and plutonium in PUREX systems by tweaking ligand structure and process conditions, or ii) to exploit the branched monoamides enhanced separation of hexavalent and quadrivalent cations in uranium and thorium separations for a thorium-based nuclear fuel cycle. The following review will focus on the former because branched monoamides cannot effectively extract plutonium(IV) which is required in PUREX operations.

2.3.2   SX Process Parameters

There are several parameters that must be investigated to determine suitable SX processes; these are outlined in Table 2.1. The following sections go through each of these parameters in turn to review the current state of knowledge within the field of monoamide reprocessing.

Table 2.1 *Parameters that can be explored to determine SX process suitability.*

Parameter(s)	Requirement	Determination methods
Metal-ligand complex speciation	• Provides a picture of what species are in solution • Allows prediction of species behaviour in varying conditions	• Slope analysis (see Section 2.3.2) • Organic saturation • UV-vis spectroscopy
Acid extraction / acid-ligand complex speciation	• Assesses the competitive extraction of acid and allows for the calculation of 'free ligand' for metal extraction – this value is required for quantitative assessment of SX processes	• Acid-base titrations • Slope analysis • IR spectroscopy
Influence of pH and ionic strength	• Assesses solvent behaviour throughout varying acidity and salt conditions • Allows selection of optimal extraction conditions	• Batch SX tests at varying acidity and ionic strength
Loading and stripping	• Determines suitability of solvents for particular extraction conditions • Allows comparability of different solvents in multi-stage processes	• Single-stage equilibrium data with McCabe-Thiele methodology • Multi-stage loading and stripping tests.
Influence of temperature	• Assesses the performance of solvents at elevated temperature	• Batch SX tests with varying temperature
Ligand degradation	• Assesses the performance of solvents under radiolysis or hydrolysis conditions • Identification of key problematic ligand degradation products	• Irradiated SX tests • Gas chromatography
Phase modifiers and synergy	• Assesses whether solvent performance can be enhanced through addition of polar phase modifiers or ligands to aid in complexing reactions	• Batch SX tests with varying ligand concentrations • Jobs plots

2.3.2   Metal Complex Speciation

Complex speciation is important to define as it allows prediction of species behaviour in different conditions. Complexes can be categorised by their level of solvation by an extracting ligand; cations solvated by one ligand are termed 'monosolvate' complexes, and cations solvated by two ligands are termed 'disolvate' complexes, etc. One of the methods to determine complex stoichiometry is via slope analysis; this method is described and discussed fully in Section 4.2.3, but it will be briefly shown here

for the purposes of this review. Say metal cation A^+ is neutralised by anion B^- and solvated by ligand L by the equilibria shown in Equation 2.14:

$$A^+ + B^- + \overline{nL} \rightleftharpoons \overline{AB \cdot nL} \qquad (Eq.\ 2.14)$$

where n is the stoichiometric coefficient of ligand L. Distribution of A is shown in Equation 2.15:

$$D_A = K_{ex}[B^-]_{eq}[\bar{L}]^n_{eq} \qquad (Eq.\ 2.15)$$

By taking the logarithms of Equation 2.15, it can be shown that:

$$\log(D_A) = \log(K_{ex}) + \log([B^-]_{eq}) + n\log([\bar{L}]_{eq}) \qquad (Eq.\ 2.16)$$

Assuming constant ionic strength, $[B^-]$, Equation 2.16 shows that a plot of $\log(D_A)$ against $\log([\bar{L}]_{eq})$ yields a slope of n which tells us the number of solvating ligands required for the extraction process. It should be noted that equilibrium values for concentrations are required for this method to work effectively. It should also be noted that this method is simplistic and non-integer slopes should be taken with caution and discussed qualitatively; in these cases, it is likely that a number of different complex species are formed. As stated before, a more in depth description and discussion of this method can be seen in Section 4.2.3.

Summarised here is the literature on uranium and plutonium complexation with monoamides to identify which species are formed and to discuss what this means in terms of operating a monoamide extraction process. Early studies showed that monoamides form disolvate complexes with uranyl cations through slope analysis (Gasparini & Grossi, 1986); (Prabhu, et al., 1997) and through organic saturation tests (Condamines & Musikas, 1992). The latter study also proposed trisolvate uranyl complexes through outer sphere coordination resulting from a gradient of 2.5 from slope analysis plots. No other supporting data was found for this, but Condamines & Musikas concluded that there are simply random interactions between inner-coordination sphere amides and free amide. In nitric acid concentrations < 4 M, it is generally accepted that uranyl complexes are disolvate and plutonium complexes are trisolvate (Prabhu,

et al., 1993); (Nair, et al., 1994); however, disolvate plutonium species have been reported (Nair, et al., 1996).

Complex speciation is not quite as simple at higher nitric acid concentrations. Under these conditions, the complex structure is seen to change for both uranium(VI) and plutonium(IV) (Musikas, 1987); neutral metal-nitrate compounds which complex with neutral amides become metal-nitrate anions which bond to protonated amides. For example, the complexation at low acidity is:

$$UO_2^{2+} + 2NO_3^- + 2\overline{L} \rightleftharpoons \overline{UO_2(NO_3)_2 \cdot 2L}$$
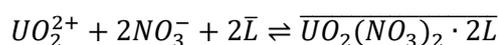
where L is the monoamide ligand, whereas complexation at high acidity becomes:

$$UO_2^{2+} + 3NO_3^- + \overline{HL^+} \rightleftharpoons \overline{(UO_2(NO_3)_3)^- \cdot HL^+}$$
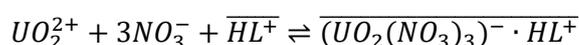
The latter complex is termed an 'ionic species'. Musikas (1987) noted that this phenomenon is not seen with TBP and attributed it to the higher basicity of amides. Further studies have reported this ionic species through slope analysis (Condamines & Musikas, 1992); (Gupta, et al., 2000b); (McCann, et al., 2017), spectroscopy experiments and calculations (Acher, et al., 2016); (Acher, et al., 2017), and determination of the ratio of ligand and metal concentrations in the organic phase at the limiting organic content (LOC) of uranium (Gupta, et al., 2000c). LOC is the point at which the organic phase splits due to high concentration of a component. It is worth noting that while the ionic complex exists, it does not dominate for aliphatic monoamides until acid concentrations above 12 M (Berger, et al., 2020); the exact point will depend on amide structure and solution conditions. However, because this ionic complex is undoubtedly more polar than the standard disolvate, it will result in a drop in recovery at higher nitric acid concentrations. Therefore, high acid concentrations should be avoided in monoamide processes looking to recover uranium and plutonium.

2.3.3 Acid Extraction

Mineral acid extraction by a solvent is an important factor to consider in SX process development as it directly impacts the metal recovery of ligands through competition. Uptake of acid will also change aqueous phase conditions which may have adverse effects on metal recovery; this is why solvents are

generally 'pre-conditioned' with acid before metal extraction steps to ensure aqueous conditions can be controlled. An understanding of the acid-ligand species can help predict acid requirements for pre-conditioning and predict extraction behaviour in changing conditions. An understanding of the 'free ligand' after acid extraction is also vital to slope analyses or loading models which use equilibrium concentration values. Below is a summary of the literature on mineral acid extraction, specifically nitric acid, with monoamide solvents.

Studies of nitric acid extraction with aliphatic monoamides indicate that the same HNO_3 complexes are formed as with TBP, i.e. $(HNO_3)(Amide)_2$, $(HNO_3)(Amide)$ and $(HNO_3)_2(Amide)$ (Condamines & Musikas, 1988). Concentrations of these species depend on acid concentration, but the major species was found to be the monosolvate which is also similar to TBP. Qualitative IR spectra suggest that these complexes are the result of hydrogen bonding from HNO_3 to either the amide carbonyl oxygen or, in the case of the latter complex, to a nitrate N=O oxygen. Other studies only report the existence of the monosolvate acid complex either through slope analysis (Prabhu, et al., 1993) or organic saturation (Gupta, et al., 2000c); (Vidyalakshmi, et al., 2001). Gupta et al. (2000c) included the monoamide *N,N*-dihexyl octanamide (DHOA) in their tests; this is one of the most promising TBP replacements for reasons that will become apparent throughout this section. Overall, it appears that the monosolvate acid species is the major one to consider in a practical sense similar to that of TBP. The similarity to TBP solvents is encouraging as the same processes will be required in a monoamide reprocessing flowsheet which will help the adoption of the process.

As acid extraction with monoamides will partly be associated with the ligand basicity, the ligand structure can play a part in the amount of extracted acid. Increasing the carbonyl-side chain length slightly increases the ligand basicity; this has been shown to increase acid extraction rate constants determined by slope analysis plot intercepts (Prabhu, et al., 1993), although D_{HNO3} does not change significantly (Vidyalakshmi, et al., 2001). Ligands are unlikely to be chosen based on their acid extraction performance, but this trend is important to consider when suitable monoamides are tested.

Third phases form in a monoamide solvents when too much nitric acid is extracted which causes the organic phase to split. Aliphatic monoamide solvents have been shown to split in the range of 4 – 8 M nitric acid (Gupta, et al., 2000c)**;** (Vidyalakshmi, et al., 2001). Within this, the promising ligand DHOA has been shown to split at 8 M nitric acid which demonstrates that this monoamide solvent has a high acid tolerance. This is a critical characteristic due to the highly acidic conditions of current reprocessing flowsheets.

Due to the higher basicity of amides, it could be expected that monoamides extract more acid than TBP. This means that more acid would be required for solvent preparation which may increase operation costs. It also means that the organic phase will have a lower metal capacity as more monoamide will be complexed with acid; this may depend on initial metal concentration and ligand affinity for that metal as acid may get displaced. However, the weaker donor strength of monoamides may offset the increased affinity from the ligand basicity. It is unclear from the current literature which scenario is the case.

2.3.4   Influence of pH and Ionic Strength

Understanding the behaviour of separation systems under different pH and ionic strength conditions allows for the manipulation of desired (and undesired) metal mass transfer. This section looks at the literature surrounding the effects of acidity and ionic strength on metal recovery of monoamides, including that of potential contaminants. Monoamide solvent performance is compared with TBP where possible.

Generally, a positive relationship between acid concentration and uranium extraction is reported by aliphatic monoamides until a certain point (~6-8 M nitric acid depending monoamide side-chains) where acid extraction begins to dominate and aqueous uranium(VI) anion species form (Gasparini & Grossi, 1986); (Condamines & Musikas, 1992); (Nair, et al., 1995); (Gupta, et al., 2000b). Overall, monoamides are shown to have a higher recovery for plutonium(IV) than TBP, but much lower recovery for uranium(VI) (Gasparini & Grossi, 1986); (Pathak, et al., 2010). This reduced loading of uranium has resulted in more efficient uranium stripping as there is less metal to recover. Because of this, more recent studies usually report that monoamides are easily stripped rather than less efficient extractants. While the lower uranium(VI) recovery is not ideal, the similar pH profile shape indicates similar

mechanisms are at work which further indicates similarity between the two reprocessing flowsheets. This is encouraging as a greater degree of similarity between the processes will make process adoption simpler.

It is not only the extractive performance that is important for a solvent; the selectivity for uranium is equally crucial. Monoamides are shown to be much more selective for uranium(VI) and plutonium(IV) than TBP (Gasparini & Grossi, 1986); (Pathak, et al., 2000); (Manchanda, et al., 2001); (Manchanda & Pathak, 2004); (Kulkarni, et al., 2006). Separation factors of uranium(VI) with americium(III), thorium(IV), protactinium(V), zirconium(VI), niobium(V), europium(III), cerium(III) and ruthenium(III) are much higher with monoamide solvents than that with TBP. This means there will be a lower requirement of decontaminating a uranium- and/or plutonium-loaded organic phase from contaminants with monoamide solvents. Note that elements other than those identified as problematic in PUREX are tested here to ensure that other abundant contaminants do not reduce the purity of the product streams. The exception to the selectivity of monoamides is neptunium; neptunium(IV) and (VI) are also extracted strongly by monoamides. However, this may not be such a disadvantage what with the recent moves toward co-recovering neptunium with other product streams in more advanced flowsheets to reduce proliferation risks (see Section 2.4).

A particular study of note for metal competition tested over a range of acidity is published by Kulkarni et al (2006). This study is highlighted because extraction of common problematic fission products is also tested under uranium-loading conditions with DHOA and TBP solvents. This means that potential co-extraction effects have been investigated as well as standard separation factors. The authors found no evidence the zirconium(IV) co-extraction that afflicts TBP solvents and confirm the significantly enhanced selectivity of monoamide solvents. The similarities between the distribution trends for the tested metals in this study further indicate that DHOA and TBP extraction mechanisms are similar.

As discussed previously when considering acid extraction, high loading of acid can lead to third phase formation, or organic phase splitting, and this will occur when aqueous nitric acid concentration exceeds a critical point (depending on the solvent conditions). This also holds true for metal loading; high metal loading leads to third phase formation when the increased polarity of the organic phase exceeding a

threshold boundary. The LOC of uranium(VI) in monoamide solvents decreases with increasing aqueous acidity which is consistent with higher acid uptake at higher acid concentrations (Gupta, et al., 2000c); (Manchanda & Pathak, 2004).

It is not only acidity that can shift recoveries and separation factors. Ionic strength (namely, nitrate concentration) plays a large role in extraction as per the extraction equilibria shown in Equations 2.8 and 2.9. Nitrate is not only present from the use of nitric acid in reprocessing; the addition of nitrite salts to PUREX liquors as a redox reagent also produces nitrate anions (Gupta, et al., 2000c). LOC of uranium(VI) in DHOA solvents has been shown to decrease with increasing nitrate concentrations up to 4 M additional nitrate in 3 M nitric acid. Gupta et al. (2000c) suggest that the increased nitrate favours production of the previously discussed solvated ionic species which results in a more polar organic phase that would be more susceptible to splitting. This indicates that monoamide solvents may have stability issues at the high acidity and ionic strength of PUREX aqueous phases. However, the LOC with DHOA solvents was found to be larger and decreased less than another promising monoamide system which indicates that DHOA is the stronger, more resilient extractant.

2.3.5   Uranium Loading and Stripping

This section reviews the literature concerning the loading and stripping of monoamide solvents. Loading tests look to assess the capacity of a solvent in either a single-stage or multi-stage environment. Stripping tests look to assess how metal can be recovered from an organic phase back into the more easily processable aqueous phase. Together, loading and stripping tests of organic solvents showcases a solvent's applicability to a process under the tested conditions and are both vital to build a coherent process. In the following section, the extraction and recovery efficiencies of monoamide solvents are compared with standard PUREX solvents, as well as metal loading effects on hydrometallurgical parameters that will affect phase separations in a dynamic process.

Usually, system conditions have to be equal or similar to compare loading data. However, this does not appear to be the case with monoamide solvents. Loading isotherms published by Gasparini & Grossi (1986) reveal that doubling the monoamide concentration from 0.5 to 1 M effectively doubles the

loading capacity of the solvent. This indicates that complex speciation remains constant with increasing monoamide concentration. It follows that any ligand concentration can be used in loading tests and a suitable multiplier can be applied to the results for comparability with other studies. This can likely be extended to ligands that follow similar extraction mechanisms, i.e. TBP.

Monoamide solvents have been shown to have a higher loading capacity for plutonium(IV) than TBP solvents, but a lower capacity for uranium(VI). Despite this lower loading of uranium(VI), it has been shown that TBP and DHOA can require the same number of contact stages for quantitative uranium(VI) recovery (Manchanda, et al., 2001); (Manchanda & Pathak, 2004). In these studies, it is shown that DHOA extracts more uranium per stage than TBP which contradicts all previous studies on monoamide/ phosphate uranium(VI) extraction behaviour. This indicates that single stage batch extraction data may not tell the entire story of how a process will operate and highlights the importance of conducting multi-stage extractions to inform process design; the design of these multi-stage extractions themselves should be based upon single-stage batch data.

It has previously been shown that monoamide solvents are very selective for uranium(VI) and plutonium(IV). This carries forward into a uranium-loading environment. Monoamide solvents extract fewer contaminants as uranium-loading of the solvent increases. This is shown in a study by Kulkarni et al. (2006) who demonstrated that zirconium(IV) and ruthenium(III) distribution decreases for both DHOA and TBP systems as uranium loading increases. DHOA consistently extracts much less zirconium(IV) than TBP (by ~1-2 magnitudes). At low uranium loading, DHOA extracts less RuNO(III); however, above ~45% uranium loading, TBP begins to extract less ruthenium(III) and extracts roughly 3 times less ruthenium at high loading conditions. Despite this higher loading of ruthenium(III) at high uranium loading with DHOA, monoamide solvents should still require less purification units due to the lower contamination of all other contaminants; this will cut down on process costs.

High levels of metal loading can lead to changes in the physical characteristic of the solvent, namely density and viscosity. It is important to understand how loading affects the hydrometallurgical

parameters of the extracting solvent as this will directly affect phase separations in a dynamic solvent extraction system which ultimately affects process throughputs. In a study testing hydrometallurgical parameters of 1.1 M DHOA and TBP, it was found that uranium loading linearly increases the density of both DHOA and TBP and that there was marginal difference between the two solvents (Pathak, et al., 2009). Before uranium loading, the phase separation time for DHOA is roughly double that of TBP. Uranium loading has a slight effect of TBP viscosity and the phase separation time almost doubles at 83 g/L organic uranium. The increase in DHOA viscosity is much more pronounced and increases from 2.6 to 7.5 cP. Phase separation time is almost triple that of TBP at ~73 g/L organic uranium. It appears that phase separation time is largely dependent on viscosity. As it is recommended that solvent viscosity be roughly 2 cP for ease of processing (Parikh, et al., 2009), this may be an issue for DHOA application to reprocessing. Solvent viscosity over 2 cP would lead to longer separation times in conventional separations equipment, like mixer-settler batteries and pulsed columns, and will directly reduce process throughputs. Although, this may be less of an issue with the application of centrifugal contactors which is where much of the advanced reprocessing research is currently focused (Kudo, et al., 2017); (Whittaker, et al., 2018).

Loading capacity is an important factor to consider to efficiently extract target metals from a feed stream, but stripping is equally as important as it informs how efficiently a target can be recovered from an extracting solvent. A process with high loading capacity but no stripping capability is of no practical use. Monoamide solvents have been shown to be more efficiently stripped of uranium(VI) than TBP solvents when using dilute nitric acid. In a multi-stage strip test, a pH 1 nitric acid strip saw quantitative recovery of uranium(VI) from a DHOA solvent by stage six at which point the TBP solvent had only 74% recovery and required a further two stages to achieve <97% stripping (Manchanda, et al., 2001); (Manchanda & Pathak, 2004). It should be noted that the phase volume ratios were not equal for this test, but even if they were, DHOA stripping would still have outperformed that of TBP. This, along with the loading discussions, mean that a more consolidated process can be designed using monoamide solvents which will cut down on both capital and operating costs of reprocessing.

The stripping capability for plutonium(IV) is also an important factor to consider for the application of monoamides in PUREX operations. Plutonium(IV) stripping is controlled by redox chemistry in PUREX; by reducing to plutonium(III), the metal is no longer extractable by TBP and so shifts to the aqueous phase. DHOA has been shown to be stripped of plutonium(IV) more efficiently than that of TBP solvents when using a range of non-salt forming reductants over 0.5-4 M nitric acid (Prabhu, et al., 2013). This means that monoamides have superior extraction and stripping of plutonium and, as such, the issue with monoamide application to reprocessing still lies with uranium solubility in the organic phase.

2.3.6   Influence of Temperature

This section reviews the effect of temperature on the performance of monoamide solvents. Understanding solvent behaviour with temperature is important as not all PUREX operations are at standard temperature, e.g., initial dissolution of the fuel to conducted in hot nitric acid (Nash & Nilsson, 2015c). The radioactive decay of dissolved SNF constituents will also raise solution temperatures, so thermal robustness of a solvent is beneficial.

Generally, it is observed that increasing temperature leads to a lower distribution of uranium(VI) and plutonium(IV) with monoamide solvents. Uranium(VI) and plutonium(IV) distributions are shown to decrease to 40% and 46% of its value, respectively, when increasing temperature from 15-45°C (Nair, et al., 1994), but larger monoamides show a greater resistance to this observed decrease (Prabhu, et al., 1993). While DHOA was not tested, this indicates that it will be fairly thermally robust relative to other monoamides.

Despite the decreased metal distribution, total loading capacities of the solvents are seen to increase with increasing temperature. Although some studies show continual increase in capacity with temperature up to 45°C (Manchanda, et al., 2001); (Manchanda & Pathak, 2004), others show that LOC of uranium(VI) increases with temperature until 25°C and then remains constant in 3 M nitric acid (Gupta, et al., 2000c). In 3 M nitric acid and 4 M sodium nitrate, LOC continues to increase with increasing temperature. Gupta et al. suggest that this is due to the previously formed ionic solvate

species dissociating to the disolvate species. It has also been reported that LOC increases with increasing carbonyl-side chain (Vidyalakshmi, et al., 2001); LOC also changed with amine-side chain of the amide, but no trend in this data was observed. Again, this indicates that larger monoamides are more thermally robust which supports the use of the high molecular weight DHOA.

2.3.7   Ligand Degradation and Influence on Extraction

This section reviews the literature surrounding metal recovery with irradiated or degraded monoamide solvents. Due to the intense radiation field and acidity in PUREX processes, an assessment on solvent performance after irradiation or hydrolysis is critical to avoid the phase control and contamination issues presented by degraded TBP in current reprocessing flowsheets. This section first considers the effects of hydrolysis on monoamide solvents, followed by the effect of solvent irradiation. Comparisons are drawn with TBP solvents where possible.

Monoamides are inert towards water, but acids and bases catalyse hydrolysis. Monoamides were found to be roughly as hydrolytically stable as TBP (Gasparini & Grossi, 1986), and main hydrolysis products were the corresponding carboxylic acids and secondary amines which indicates a rupture of the C-N amide bond. The similarity to TBP is encouraging. The monoamide degradation products should also have a far lesser effect on contaminant extraction; this is discussed further below.

Irradiation tests are conducted by dosing a solvent with an amount of ionising radiation. Dose is usually measured in Grays (Gy, or J/kg). Monoamides appear to be slightly more susceptible to radiolysis than TBP (Gasparini & Grossi, 1986), although it was found that DHOA degradation was less than 1% even after a 1 MGy γ-ray dose (Parikh, et al., 2009). Gas chromatography of degraded DHOA identified similar hydrolysis products, i.e. caprylic acid and dihexylamine, as well as dihexylketone; concentrations of these products increased with increasing dose.

One of the major considerations for degraded solvents is its capacity for the target metals. Unlike with TBP solvents, uranium(VI) extraction by monoamide solvents is seen to very gradually decrease with increasing dose but remains constant after roughly 500 kGy (Ruikar, et al., 1995); (Manchanda & Pathak, 2004) which indicates that monoamide solvents are fairly robust to radiolysis in terms of

uranium recovery. This is further supported by another study where a 30% degraded monoamide solvent showed a relatively small decrease in uranium distribution over a 0.5 – 6 M nitric acid range (Gasparini & Grossi, 1986). Plutonium(IV) is more complex; extraction by monoamide solvents is seen to decrease with increasing dose up to 100-400 kGy, after which it sharply increases up until 720-800 kGy before falling steeply (Ruikar, et al., 1995). The gradual distribution increases observed by Ruikar et al. were attributed to synergistic effects of the carboxylic acid and amine degradation products, but the steep distribution decreases were attributed to third phase formation. This highlights that solvent clean-up will still be a necessary step to remove ligand degradation products and allow sufficient control of the process.

Another important consideration for degraded solvents is the effect on contaminant extraction. This is seen to be a large issue in standard PUREX processes and so must be investigated with monoamides to ensure an adequate understanding of process behaviour. Zirconium(IV) is a key contaminant that has similar behaviour to plutonium(IV); extraction with irradiated monoamide solvents is increased up until 720 kGy after which extraction decreases (Ruikar, et al., 1995). It should be noted that even at 720 kGy, zirconium extraction is still low. It is unlikely that this increase in extraction is due to the monoamide degradation products based on the findings of Kulkarni et al. (2006). Kulkarni et al. found that the addition of caprylic acid and *n*-dihexylamine were not seen to affect zirconium extraction at all and increasing degradation product concentration displayed no trend at acidities between 0.5-5 M nitric acid. The same cannot be said for TBP; the presence of HDBP in TBP systems significantly enhanced zirconium extraction and increasing acidity as well as HDBP concentrations exacerbates this.

Other key contaminants, ruthenium(III) and europium(III), were not extracted by the monoamides over the entire dose range tested in Ruikar et al.'s (1995) study (1.84 MGy) which is supported by the findings of some other studies with DHOA (Parikh, et al., 2009); (Pathak, et al., 2010). Both degraded TBP and DHOA solvents see increased retention of metals after nitric acid strips, but DHOA retains much less (1.7 – 17 times less retained plutonium depending on the organic phase treatment). This means that strip units should be less intensive. Carbonate strips are very effective for uranium and

fission product decontamination, so any organic metal retention after nitric acid strips should be dealt with in the caustic solvent wash unit.

A final consideration for degraded solvents is the hydrometallurgical performance. Changes to the hydrometallurgical parameters will change the phase separation time and lessen the control on the process. Degraded monoamide solvents have been shown to become marginally denser, but this had little effect on phase separation times. However, viscosity of a solvent irradiated with 600 kGy is seen to increase by 52% to 3.93 cP (Parikh, et al., 2009); (Pathak, et al., 2010) which may almost double the phase separation time (Pathak, et al., 2009). It is recommended that solvent viscosity should be ~2 cP to allow for easy fluid dispersion and phase setting in extraction columns, so this may be an issue unless extraction processes are reassessed or redesigned.

2.3.8   Phase Modifiers and Synergy

One way to potentially improve the uranium(VI) extraction of monoamides so it can compete with TBP is to use phase modifiers or synergic ligands to enhance metal extraction. Phase modifiers work by altering the polarity of the organic phase to increase the solubility of more polar complexes. Synergic ligands enhance extraction by either being involved in the reaction as a catalyst or being in the complex formation itself to form 'ternary complexes' or 'mixed-ligand complexes' (Figure 2.9). In this thesis, a ternary complex is defined as a complex that has a metal centre with two different solvating ligands (nitrate anion ligands are taken to be part of the metal centre). Not all ligands have synergic interactions in all cases, so careful testing is required to determine suitable mixtures.
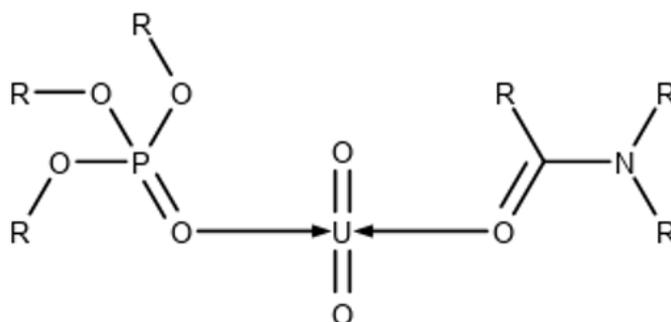
Figure 2.9. *An example of a speculative ternary uranyl complex involving a phosphate and a monoamide. Nitrate anion ligands bound to the uranyl cation have been omitted for clarity.*

Using mixtures of monoamides could be a simple way to enhance target uranium(VI) and plutonium(IV) extraction using a purely CHON solvent. However, it has been found that mixtures of aliphatic and branched monoamides led to antagonistic interactions, i.e. metal recovery decreased in the monoamide mixtures (Condamines & Musikas, 1992); (Nair, et al., 1994). At no point is the metal recovery better than with the aliphatic monoamide alone. These studies determined that ternary complexes with the two types of monoamide were generated with uranium(VI), but not with plutonium(IV) due to steric hinderance from the branched ligands. This means that quantitative separation with these mixtures cannot be accomplished with monoamide mixtures alone; stronger 'second ligand' donors may be required alongside an aliphatic monoamide ligand to enhance recovery.

Synergy is not the only way to improve recovery. Using phase modifiers can help enhance extraction by altering the solvent properties to either support more of the extracted complex or allow operation in previously inoperable conditions. For example, monoamides have been added to diamide solvents to greatly increase the operating acidity range by inhibiting third phase formation (Smith, et al., 1997); although, addition of the monoamide led to reduced recovery of the americium(III) target in that study due to the monoamides lack of affinity for trivalent cations. Similar results were found when using DHOA as a phase modifier for *N,N,N',N'*-tetraoctyl diglycolamide (TODGA). DHOA addition extends the acidity working range of the solvent but caused a slight reduction in americium(III) (Tachimori, et al., 2002) or neodymium(III) (Sasaki, et al., 2005) recovery by TODGA, although, metal recovery was still sufficiently high. DHOA was chosen as a phase modifier due to its high polarity that would increase solvent capacity for metal, and the low extractability for trivalent actinides and lanthanides mean it would not interfere with extraction due to the lack of monoamide affinity for trivalent cations, as well as steric hinderance from the high solvation number of americium(III)-diglycolamide species (Wang, et al., 2017). This means that there is the potential to add polar phase modifiers to monoamide solvents as well to boost the solubility of the uranium(VI)-monoamide complex.

Diamides and diglycolamides (Figure 2.10) have been shown to extract uranium(VI) from nitric media (Nair, et al., 1993); (Mahajan, et al., 1998); (Mowafy & Aly, 2002); (Peng, et al., 2017). They also generally have lower solvation numbers than with trivalent actinides and lanthanides. Theoretically,

mixtures of these ligands with monoamides would enhance uranyl extraction by: i) increasing the polarity of the organic phase which may boost uranyl-monoamide complex solubility, and/or ii) forming ternary complexes with uranyl cations which would have differing hydrophobicity to normal uranyl-monoamide complexes. The former point is supported by Gupta, et al. (2000c) who found that addition of 1-octanol or 1-decanol steadily increases monoamide extraction of uranium(VI). The latter point has not been investigated to the best of the authors knowledge. Raut & Mohapatra (2013) mention that DHOA and TODGA have a synergic effect when extracting metal ions due to the replacement of the leftover inner-sphere water molecules in uranium(VI)-DHOA complexes by TODGA ligands, but any support for this claim could not be found in the literature.
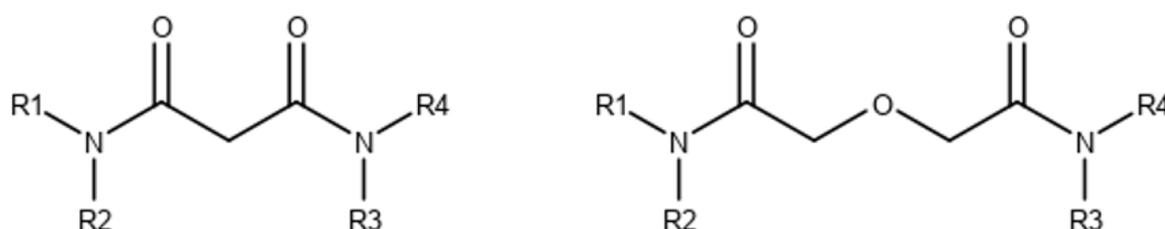
Figure 2.10. *Structure of a diamide (left) and a diglycolamide (right).*

For the work in this thesis, diamides and diglycolamides have been identified as potential 'second ligand' candidates as they are multidentate amide-based ligands that have previously been used to extract uranium; if successful, the use of these mixtures would allow for the elimination of phosphorus in reprocessing flowsheets. The addition of these ligands to monoamide systems may result in an enhanced solvent performance due to their high affinity for uranium; however, uranium selectivity over trivalent lanthanides/actinides may be an issue (Ansari, et al., 2009); (Raut & Mohapatra, 2013); (Wang, et al., 2017). Therefore, it must be shown that these systems form ternary complexes with monoamides to take advantage of the monoamide selectivity rather than rely on a phase modifying effect to boost performance. If there is no mixed interaction between the ligands, it is likely that application of these mixed ligand solvents would result in low separation factors. Diamides have generally been shown to have a solvation number of 2 for uranyl nitrate (Ruikar & Nagar, 1995) which leaves no room around

the metal centre. This means that a diamide molecule would have to be substituted by a monoamide molecule; the likelihood of this happening depends on the stability of the individual complexes. The stability of these uranyl complexes can be assessed using ultraviolet-visible (UV-vis) analysis (Ogden, et al., 2012). Diglycolamides are shown to have multiple solvation numbers with uranyl nitrate depending on extraction conditions (Panja, et al., 2009); (Sasaki, et al., 2013); (Sasaki, et al., 2015); (Liu, et al., 2015); (Peng, et al., 2017); (Ren, et al., 2017); (Boltoeva, et al., 2018) but the monosolvate species would be vulnerable to ternary complex formation.

Phosphoryl donor ligands like phosphates and phosphine oxides have also been identified as potential 'second ligand' candidates; they have high affinity for uranium and are mechanistically similar to monoamides during solvent extraction which may mean they can form exploitable ternary complexes (although selectivity issues may be observed with phosphine oxides). A successful solvent of this type would not eliminate phosphorus in reprocessing flowsheets, but it would reduce it. While a reduction of phosphorus in reprocessing is not as beneficial as eliminating it, it is certainly a step in the right direction. As monoamides are frequently used as phase modifiers, introducing monoamide ligands into a phosphate solvent may even inhibit some of the effects of the degradation products, although this claim would have to be tested experimentally. Both phosphates and phosphine oxides are shown to have solvation numbers of 2 with uranyl nitrate so ligand substitution by a monoamide would be necessary for ternary complex formation; again, production of these ternary complexes will be based on the stability of the individual complex species which can be determined through UV-vis analysis. Although, even if no ternary complex is observed with the addition of a phosphate, there is the potential that a phosphate may have a beneficial phase modifying effect like that seen before with TBP (Modolo, et al., 2007a); (Gujar, et al., 2012). Contaminant extraction issues with TBP are less severe given that it is currently used in the PUREX process anyway.

2.3.9   Monoamide Review Conclusion

Presented above is a comprehensive review of current aliphatic monoamide research in the area of nuclear fuel reprocessing. To summarise, monoamides are solvating extractants that are mechanistically similar to TBP. They are simple to synthesise and can be completely incinerated upon solvent

degradation. Generally, monoamides extract and strip plutonium(IV) far better than TBP but uranium(VI) extraction is poorer. This poorer extraction is attributed to poor organic-phase solubility of the uranyl-nitrate-monoamide complex. Decontamination factors for uranium are far higher with monoamides, except for ruthenium which is either comparable or somewhat poorer depending on extraction conditions. Degradation products tend to be carboxylic acids, disubstituted amines and disubstituted ketones, but these are shown to not affect uranium decontamination factors nearly as much as TBP's degradation products. Mixtures of monoamides are shown to not have synergic effects on uranyl extraction.

More recent monoamide studies have investigated monoamides as phase modifiers for diamide or diglycolamide systems for the extraction of trivalent lanthanides or actinides. Monoamides were generally chosen as they will increase the polarity of the organic phase but will not interfere with the extraction. Diamides and diglycolamides have been shown to extract uranium(VI), so it may be the case that monoamides generate more hydrophobic mixed-ligand uranyl complexes with diamides or diglycolamides. The higher hydrophobicity may enhance uranyl extraction. As monoamides and phosphoryl-donor ligands are mechanistically similar, these may generate exploitable complexes too. To these ends, diamides, diglycolamides, phosphates and phosphine oxides have been selected as 'second ligands' for ternary complex testing with monoamides.

2.4   Current Advanced Nuclear Flowsheets

As the focus of this thesis is to work towards an advanced reprocessing flowsheet which reduces the need for TBP, the major modern flowsheets are discussed below to identify where the novelty for the current work lies. Many processes have been developed to attempt to improve upon PUREX by designing significantly different flowsheets and/or using improved ligands. The flowsheets discussed are DIAMEX-SANEX, GANEX, UREX+ processes, TALSPEAK, ALSEP and EXAm.

2.4.1   DIAMEX-SANEX

The key goal of current <u>DIAM</u>ide <u>EX</u>traction (DIAMEX) processes is to separate the minor actinides from the PUREX raffinate to ultimately reduce the radiotoxicity and amount of decay heat produced

from vitrified high level waste (HLW). Within the scope of the present work, the drawback of DIAMEX processes is already apparent; operation of the PUREX process is required before treatment with DIAMEX. As such, there is no reduction in the production of secondary phosphate wastes, and the process as a whole is subject to the same drawbacks as PUREX. However, the production of further phosphate wastes is eliminated with most DIAMEX systems due to their exclusive use of CHON solvents. Incineration of these would only produce carbon dioxide, NO_x, and water vapour (assuming complete combustion) which can be scrubbed before being released to the atmosphere.

The chemical similarities between lanthanides and minor actinides complicates their separation. Both groups strongly favour the trivalent oxidation state, however, americium(V) and (VI) are exceptions in extremely oxidising conditions. Both actinide and lanthanide groups are relatively similar in size and have similar decreasing cationic radii. Both are considered hard acids and, therefore, prefer to interact with hard electron donors. Their separation relies on the very subtle differences in solution chemistry owing to the different electron configurations of the groups; the 5d, 6d, 7s and 7p orbitals of trivalent actinides have been shown to overlap and interact with certain ligand orbitals (Choppin, 2002) implying increased bond covalency not seen with trivalent 4f elements. Whether this interaction actually results in increased covalent character remains a matter of discussion, with evidence for and against covalency (Kirker & Kaltsoyannis, 2011). Regardless, it is wholly accepted that ligands with 'soft' or 'softer' electron donor atoms, i.e. ligands that have increased covalent character, form the basis of trivalent Ln/An separations through preferential bonding to actinides. This phenomenon has prompted work into the development of nitrogen-containing ligands; nitrogen is considered a hard Lewis base, but is 'less hard' than donors such as oxygen (Ogden, et al., 2011). This is an important point to raise for the current work; flowsheets based on phosphorus extraction chemistry can assume that lanthanide extraction behaviour largely mimics that of the minor actinides. This simplification cannot be made with nitrogen-containing ligands like amides, diamides and diglycolamides, and competitive extraction with systems containing these ligands should be tested for complete characterisation of the system.

The DIAMEX process (Modolo, et al., 2007b) is a process initially proposed as an addition to PUREX reprocessing using diamide-based ligands, shown in Figure 2.10, to remove lanthanides and minor

actinides from the highly acidic PUREX raffinate. (Musikas, 1987) first investigated the use of tetra- and pentaalkyl diamides for the extraction of trivalent 4f and 5f ions. He suggested steric hindrance prevents metal extraction when alkyl chains exceed C_8H_{17} with tetraalkyl diamides, and that alkyl substitution on the central carbon produces a pentaalkyl diamide which increases extraction tenfold. NMR and IR spectroscopy revealed both carbonyl groups were bonded to trivalent lanthanides; this is expected due to the hard acid nature of lanthanides. Trivalent actinide bonding to diamides was not discussed, but it was indicated later in the work that americium(III) also favoured bonding with both carbonyl groups.

From Musikas' work, *N,N'*-dimethyl-*N,N'*-dibutyl-2-tetradecyl-malonamide (DMDBTDMA) became the first reference ligand for the DIAMEX process. Many studies following on from this focused on optimising chemistry and process conditions of DMDBTDMA for Ln(III) and An(III) extraction from PUREX raffinates (Nigond, et al., 1994); (Madic, et al., 1994); (Courson, et al., 1998); (Facchini, et al., 2000) (Berthon, et al., 2001); (Modolo, et al., 2003); (Berthon, et al., 2007); (Modolo, et al., 2007b), as well as drawing comparisons of DIAMEX with a <u>TRU</u> <u>EX</u>traction (TRUEX) solvent (Mahajan, et al., 1998); (Kumbhare, et al., 2002). TRUEX generally uses *n*-octyl(phenyl)-*N,N*-diisobutyl-methylcarbamoyl phosphine oxide (CMPO) and TBP to extract TRUs. Comparison of 1 M DMDBTDMA and the TRUEX solvent (0.2 M CMPO + 1.2 M TBP) revealed that the DIAMEX process had lower, but still relatively high An(III) extraction yield despite high Ln(III) loading. Third phase issues arose in DIAMEX tests with the diamide above 4 M nitric acid. Despite this, it was concluded that DMDBTDMA showed promise as a TRUEX solvent replacement due to the high yields at workable conditions.

Optimisation of diamide structure to improve Ln(III) and An(III) distributions and decrease third phase formation resulted in the suggestion of DMDOHEMA (*N,N'*-dimethyl-*N,N'*-dioctylhexylethoxy malonamide) as a potential DIAMEX solvent. Inactive mixer-settler tests using DMDOHEMA showed it quantitatively eliminated zirconium extraction like DMDBTDMA. DMDOHEMA also improved upon DMDBTDMA's lower selectivity by extracting less molybdenum, iron, and ruthenium (Bisel, et al., 1998). However, ruthenium extraction elimination was only 50% and it was noted that iron and

ruthenium chemistry required more investigation as extraction behaviour did not fit with the expected models. With alkaline solvent treatment, it was shown that DMDOHEMA hydrolysis and radiolysis products do not adversely affect solvent properties (Cames, et al., 2004).

Because DMDOHEMA extracts both Ln(III) and An(III), researchers saw an opportunity to incorporate Selective ActiNide EXtraction (SANEX) aspects into the DIAMEX flowsheet. To separate An(III), an aqueous complexing agent (HEDTA, (2-hydroxyethyl)ethylenediaminetriacetic acid) can be added to pull An(III) into the aqueous phase (Baron, et al., 2006); (Bisel,, et al., 2007); (Hérès, et al., 2008). This mechanism requires a pH above 2; however, at this pH, DMDOHEMA will be incapable of complexing with Ln(III). As such, a lipophilic Brønstead acid is added to retain Ln(III) in the organic phase: either bis-(2-hexyl)phosphoric acid (HDHP), or bis-(2-ethylhexyl)phosphoric acid (HDEHP). This is an example of a classical synergic SX system; Ln(III) complexation with the diamide is facilitated by the lipophilic acid. An example of this flowsheet is seen in Figure 2.11. The main HDEHP degradation product, mono-2-ethylhexylphosphoric acid (H_2MEHP), was not detected after nitric acid and sodium hyroxide solvent washes (Bisel,, et al., 2007), but this does not reveal whether the recovered H_2MEHP was complexed with metal or how it could be disposed of. Degradation of DMDOHEMA and HDEHP, as well as the hydrogenated tetrapropylene diluent evaporation resulted in significant solvent volume reduction. Solvent degradation appeared to have no effect on extraction, however, solvent viscosity increased by 20% which will increase phase separation times. As seen previously, organophosphorus extractants can lead to undesired extraction of zirconium, molybdenum and iron; this requires an additional 'extractant separation' step for DMDOHEMA and HDHP/HDEHP (Hérès, et al., 2008).

It should be noted that significant work into Ln(III)/An(III) separations with bistriazinyl-pyridine, -bipyridine, and -phenanthrolines compounds has been reviewed (Panak & Geist, 2013) and separation processes have been tested (Magnusson, et al., 2009). These ligands are effective but are also large and difficult to synthesise in large quantities. For reprocessing with these ligands to be feasible, large quantities of ligand must be easily producible which may prove challenging with these types of ligand. Simple ligands are not only easier to produce, but also limit the number of potential degradation products in solution that may unnecessarily complicate separation chemistry.
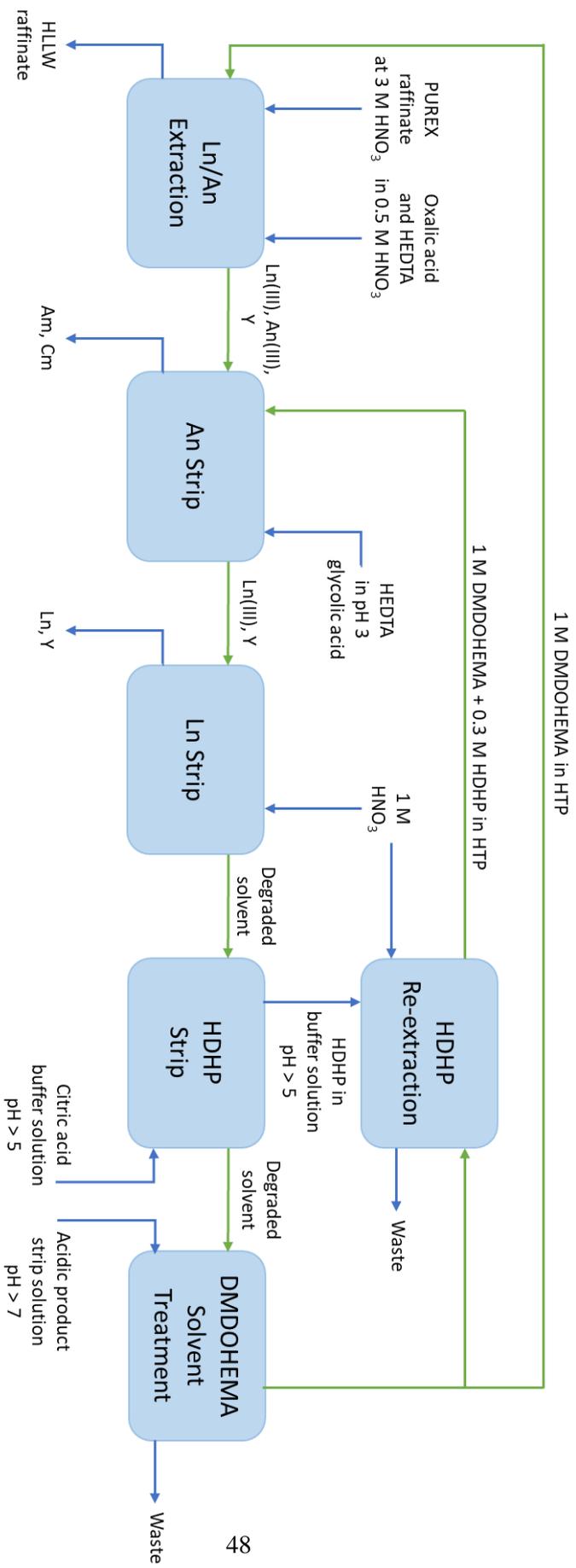
Figure 2.11. *An example of a DMDOHEMA DIAMEX-SANEX process flowsheet. Blue arrows show aqueous flows. Green arrows show organic flows. [Adapted from (Hérès, et al., 2008) and (Serrano-Purroy, et al., 2004)].*

Uranium extraction with DMDOHEMA is much less studied. However, DMDOHEMA has been shown to effectively separate uranium(VI), with distribution values far exceeding that of lanthanides and minor actinides (Mowafy & Aly, 2002). This demonstrates DMDOHEMA could potentially be used in a CHON PUREX process if suitable aqueous holdback reagents for lanthanides and minor actindes can be found.

Diglycolamides for Ln(III)/An(III) separations were researched around the same time as DMDOHEMA (Sasaki & Choppin, 1996); (Sasaki, et al., 2001). It was reported that the diglycolamide TODGA has a higher affinity for Ln and An than DMDOHEMA; this was demonstrated by contacting a mixture of TODGA and TBP with a genuine SNF solution (Magnusson, et al., 2009). Ln(III) and An(III) have very low affinity for TBP, however, the addition of TBP here is reported to improve lanthanide loading into the organic phase as well as reduce third phase formation (Modolo, et al., 2007a). Oxalic acid is added to eliminate zirconium extraction by TBP as with previous studies (Musikas, 1987). It is stated that the TODGA/TBP system is radiolytically stable enough for continued research as an extracting system; however, TBP is expected to still degrade much like in PUREX. It is demonstrated that radiolysis has an insignificant effect on americium(III) and europium(III) extraction up to an absorbed dose of 1 MGy; however, no statement is made as to the amount of TBP degradation products and their effect on phase separation and clean-up (Modolo, et al., 2007a); (Modolo, et al., 2008); (Magnusson, et al., 2009). The incineration of spent solvent remains an issue as well for solvents containing phosphorus.

2.4.2 GANEX

Grouped ActiNide EXtraction (GANEX) is a process developed to handle all TRUs in a single stream. This is done to mitigate plutonium proliferation and to generate a feed for future transmutation processes to reduce long-lived radioisotopes in HLW. It is assumed that uranium is extracted by a branched monoamide prior to TRU separation (Miguirditchian, et al., 2008). This requires a solvent capable of handling multiple oxidation states (III–VI) and high plutonium loading. TODGA/TBP systems looked promising in thorium extraction systems (thorium used as a plutonium-analogue), but even small loading in plutonium extraction tests produced a precipitate that was not soluble in fresh solvent, pure kerosene, water or nitric acid; however, it was soluble in acetohydroxamic acid dissolved in nitric acid

(Brown, et al., 2012). Extensive screening revealed TODGA/DMDOHEMA systems with higher concentrations of diamide produced no stubborn precipitates and formed a third phase at the plutonium loading limit of the organic phase. Low levels of DMDOHEMA (< 0.25 M) resulted in precipitation even at relatively low plutonium concentrations (< 20 g L^{-1} Pu). It was concluded that 0.2 M TODGA + 0.5 M DMDOHEMA extraction from 2 M nitric acid was best for plutonium loading. Back extraction with acetohydroxamic acid recovered plutonium and neptunium while americium and europium remained extracted by the solvent.

In another study, a mixture of 0.2 M TODGA and 0.5 M DMDOHEMA was found to perform well for TRU extraction and the addition of 1,2-cyclohexanediaminetetraacetic acid (CDTA) suppressed zirconium and palladium uptake into the organic phase (Bell, et al., 2012). The change from oxalic acid in the DIAMEX process to CDTA in the GANEX process is due to plutonium oxalate precipitation. However, Np extraction is problematic due to its variable oxidation state; neptunium(IV)/(VI) are readily extractable by GANEX solvent, but neptunium(V) is extracted at much lower rates. That said, it was found that neptunium(V) quickly disproportionated to neptunium(IV) and (VI) in the organic phase, particularly at high acidities, thereby solving the issue. Molybdenum, strontium, iron, technetium, ruthenium and Ln(III)'s are still extractable by GANEX solvent; molybdenum and strontium may be stripped with dilute nitric acid but technetium and ruthenium are problematic. Iron has been seen to accumulate in the organic phase which could cause third phase formations at high iron loading (Taylor, et al., 2016). Stripping of An(III) from Ln(III) is facilitated by the aqueous complexant sulfonated-bistriazinyl pyridine (Wilden, et al., 2015). Ln(III) could then be stripped by a citric acid strip. An example GANEX flowsheet is seen in Figure 2.12.

Uranium extraction with TODGA/TBP systems has also been demonstrated (Brown, et al., 2010). Although the addition of TBP to the system will still generate the same issues observed with PUREX, mixing with CHON ligands will reduce the amount of phosphate waste produced. TBP will aid the recovery of uranium and plutonium, however, TODGA will also increase the recovery of lanthanides and minor actinides. Aqueous holdback reagents may likely be necessary for TODGA to be considered in a CHON PUREX scheme.
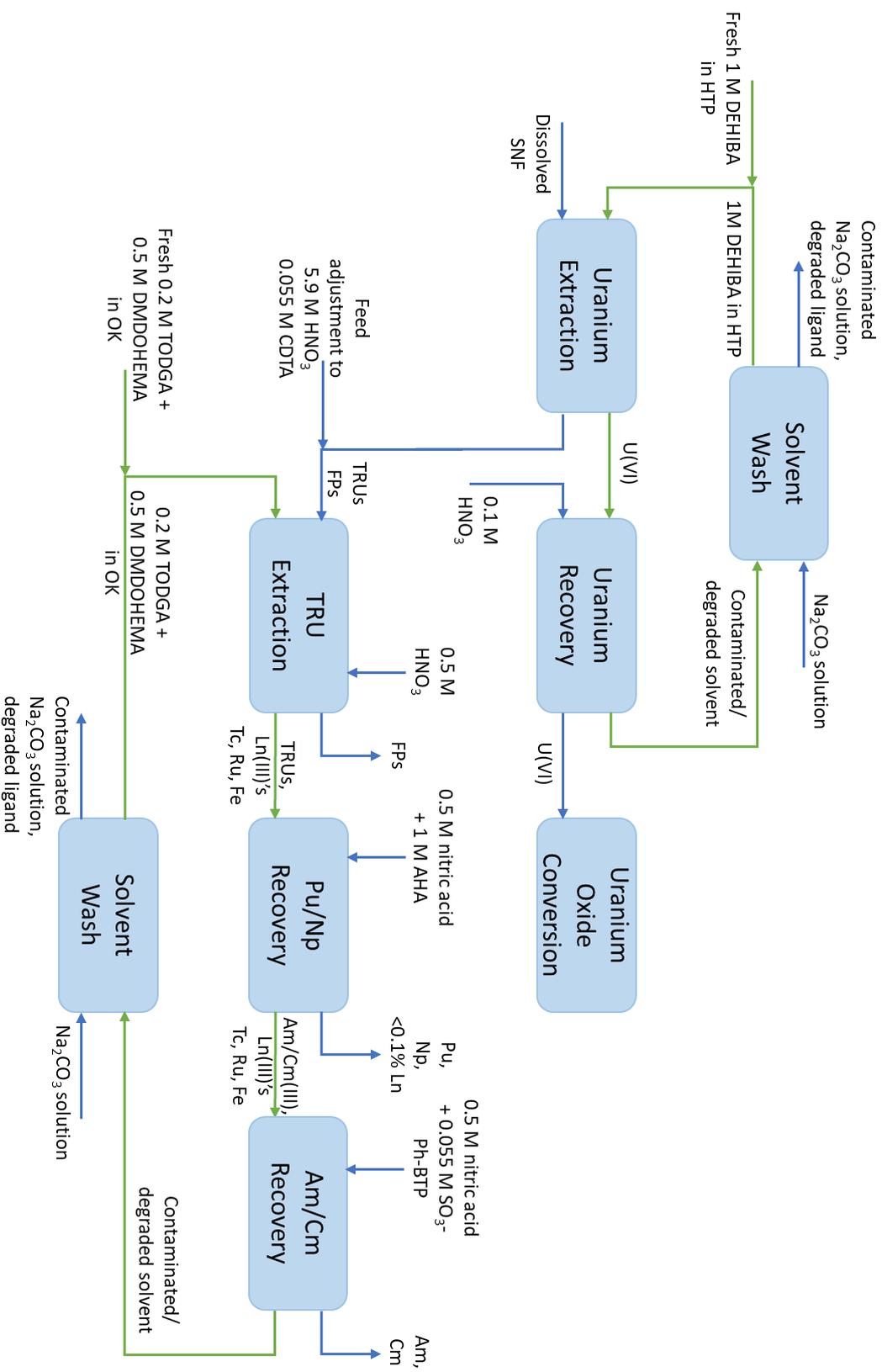
Figure 2.12. *An example of a TODGA/DMDOHEMA GANEX process flowsheet. Blue arrows show aqueous flows. Green arrows show organic flows. [Adapted from (Miguirditchian, et al., 2008) and (Taylor, et al., 2016)]*

51

2.4.3 UREX+

The UREX+ (<u>UR</u>anium <u>EX</u>traction <u>+</u>) process (Figure 2.13-14) is a collective term that comprises of multiple similar flowsheets for the complete reprocessing of nuclear fuel. Each flowsheet is modular in nature whereby the extract or raffinate outputs of one process 'module' is usually an output product stream or an input to the next process module. The choice of flowsheet depends on the desired product streams, which is outlined in Table 2.2. A different number following 'UREX+' indicates a different set of modules, i.e. a set flowsheet. Different iterations denoted by 'a' and 'b' indicate condition changes within a set flowsheet to partition metals differently. The different flowsheets were designed as new separations were desirable, with some separations being easier to design than others. For example, the separation of An(III) from Ln(III) is complicated by their chemical similarities, but the potential disposal of TRU through fast reactor burning or transmutation made this separation desirable.

UREX+ is not necessarily all based on SX; some process modules may include ion exchange, precipitation, or other separation processes (Regalbuto, 2011b). Common to all UREX+ flowsheets are the separation of uranium, technetium, and caesium/strontium from reprocessing liquors. They differ in how they treat the remaining raffinate. Iterations of the same flowsheet (characterised by 'a' and 'b') vary by routing some uranium to exit with TRU or Pu/Np streams in an effort to reduce the plutonium proliferation risk of the process. In reality, it can be argued that this does little to reduce the proliferation risk of the process; it has already been demonstrated in PUREX that plutonium can be separated by careful redox control. As seen in Table 2.2, development of UREX+ flowsheets saw the progressive separation of Pu/Np from Am/Cm/Ln, Am/Cm from Ln, and Am from Cm. UREX+4 completes virtually all separations required for the advanced reprocessing of SNF, aside perhaps the recovery of lanthanides which has been demonstrated in UREX+2.
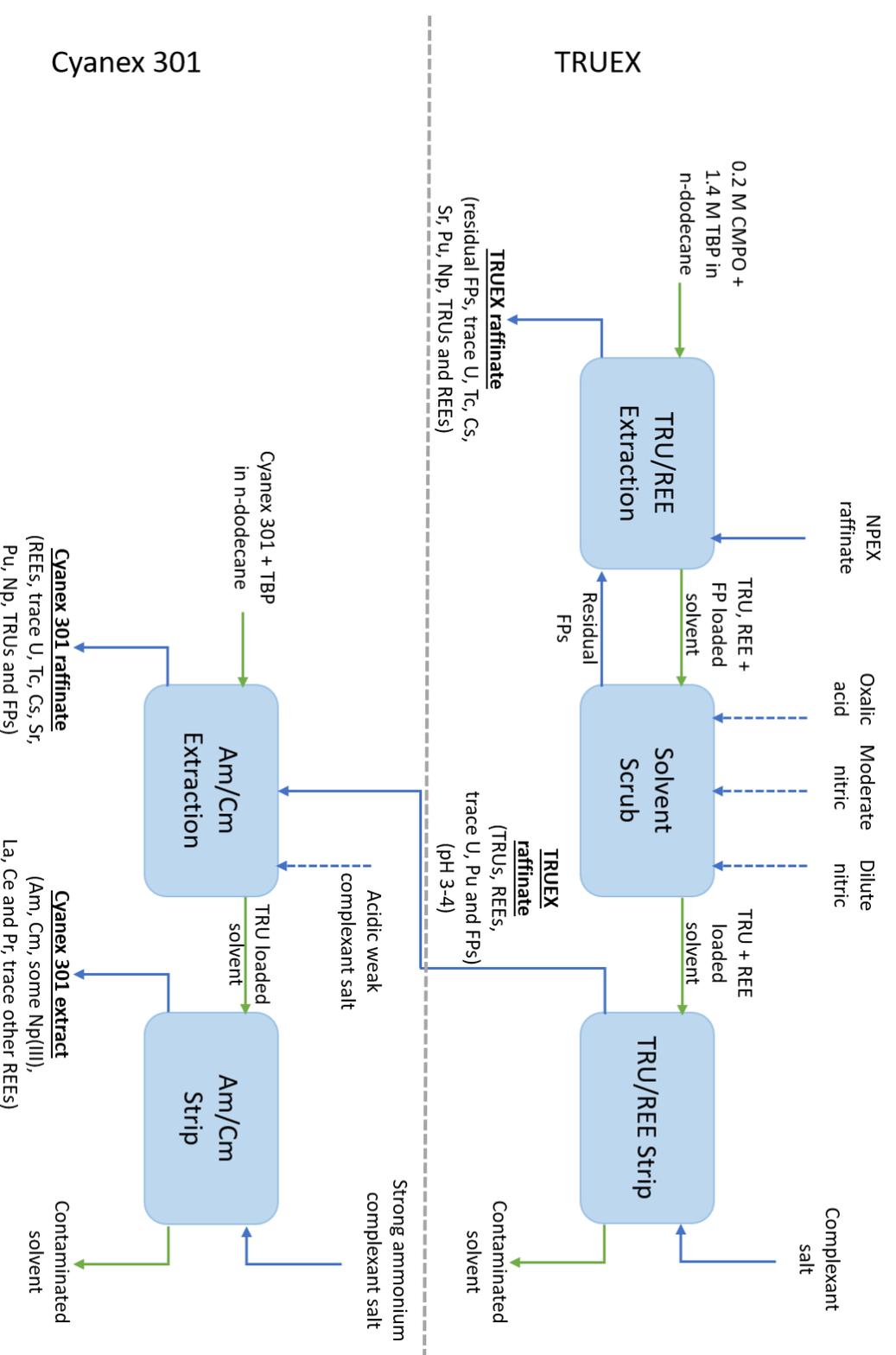
Figure 2.13. *The TRUEX and Cyanex 301 process steps in the UREX+3 process. Note this is the second half of the UREX+3 flowsheet but is presented first to match up with the following Figure 2.14. Blue arrows show aqueous flows. Green arrows show organic flows. [Adapted from (Vandegrift, et al., 2004)].*

53
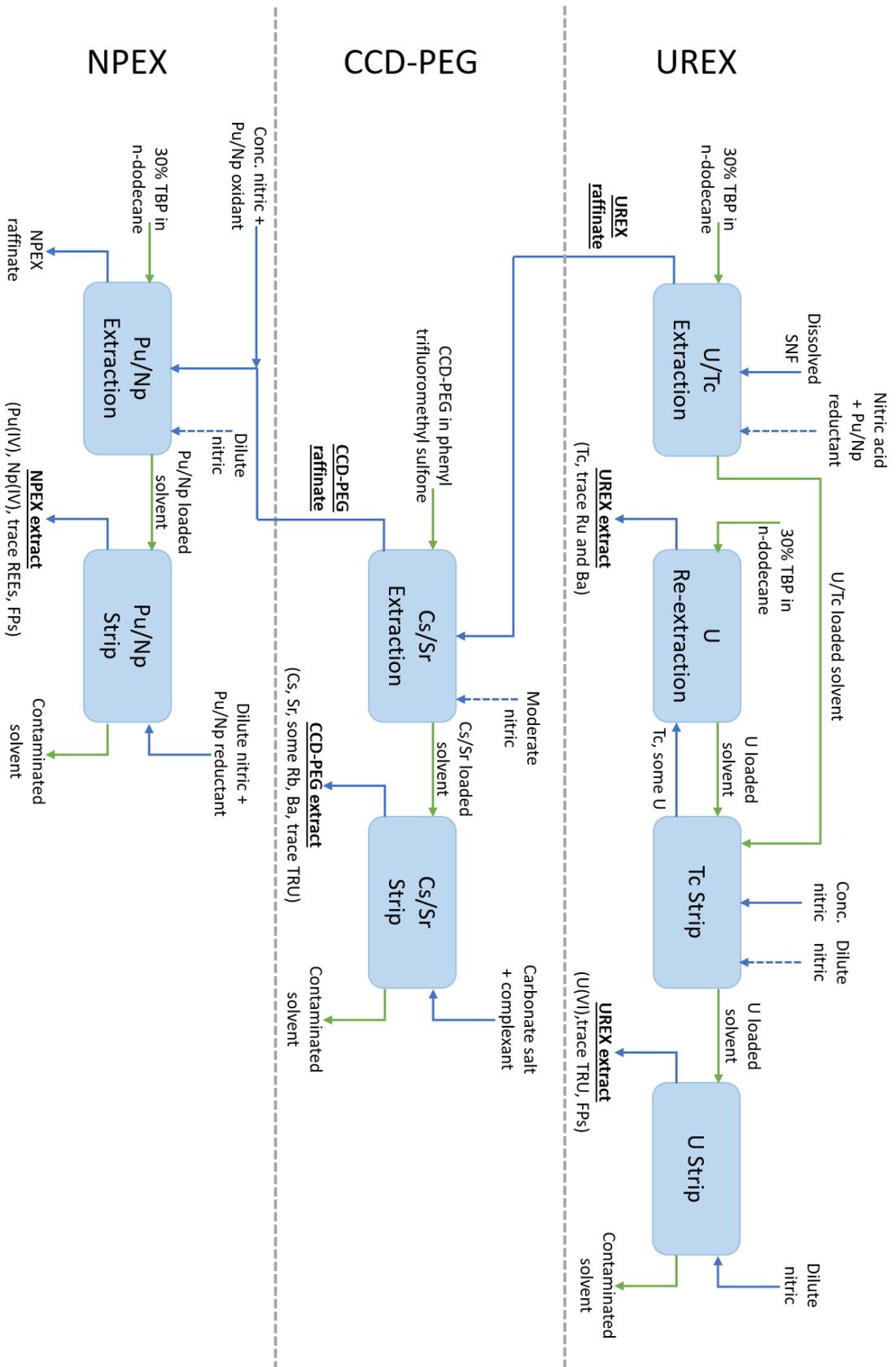
Figure 2.14. *The UREX, CCD-PEG and NPEX process steps in the UREX+3 process. Note this is the first half of the UREX+3 flowsheet but is presented second to match up with the preceding Figure 2.13. Blue arrows show aqueous flows. Green arrows show organic flows.* [*Adapted from (Vandegrift, et al., 2004)*].

54

The relevance of UREX+ to the present work is with its associated issues; primarily the continued reliance on phosphorus-based extraction chemistry. As shown in Figure 2.13-14, the separation of uranium, TRUs and REEs still require the application of TBP and or CMPO in an aliphatic diluent. As such, these processes are subject to the same significant drawbacks as PUREX with regards to radiolysis products and undesired metal extraction. UREX+ processes will also produce the same secondary radioactive phosphate waste produced from the incineration of degraded organic solvent. UREX+ may have the potential to completely reprocess spent fuel, but the production of the same (and probably more) secondary wastes and the number of process units could leave it as uneconomical as PUREX.

The increased number of product streams generated from successive UREX+ flowsheets require an increased number of different process units using either different conditions or reagents to facilitate the required separation. Different reagents used in the different process modules increase the complexity of the solution chemistry; both the original compounds and their degradation products must be considered. Testing of the desired modules '*in situ*' is required to ensure upstream reagents do not affect downstream processes. For example, polyethylene glycol is used in the CCD-PEG module to separate caesium and strontium from the UREX raffinate. Polyethylene glycol is known to have significant aqueous solubility which may affect subsequent extraction modules or required module pre-treatments.

Table 2.2 *Products from different UREX+ processes operating on light water reactor SNF [adapted from* (Regalbuto, 2011c)*].*

Process	Product Stream						
	1	2	3	4	5	6	7
UREX+1	U	Tc	Cs, Sr	TRU, Ln	FPs	-	-
UREX+1a	U	Tc	Cs, Sr	TRU	FPs, Ln	-	-
UREX+1b	U	Tc	Cs, Sr	TRU, U	FPs, Ln	-	-
UREX+2	U	Tc	Cs, Sr	Pu, Np	Am, Cm, Ln	FPs	-
UREX+2a	U	Tc	Cs, Sr	Pu, Np, U	Am, Cm, Ln	FPs	-
UREX+3	U	Tc	Cs, Sr	Pu, Np	Am, Cm	FPs, Ln	-
UREX+3a	U	Tc	Cs, Sr	Pu, Np, U	Am, Cm	FPs, Ln	-
UREX+4	U	Tc	Cs, Sr	Pu, Np	Am	Cm	FPs, Ln
UREX+4a	U	Tc	Cs, Sr	Pu, Np, U	Am	Cm	FPs, Ln

2.4.4 TALSPEAK and Derivatives

The Trivalent Actinide Lanthanide Separation by Phosphorus reagent Extraction from Aqueous Komplexes (TALSPEAK) process looks to separate trivalent lanthanides from actinides in a PUREX raffinate (Nash, 2015). Rather than relying solely on lipophilic extractants, this process uses aqueous complexants to mask actinide extraction by the unselective lipophilic extractant HDEHP (Nilsson & Nash, 2007). Following numerous studies into these kinds of separations, diethylenetriamine-*N,N,N',N'',N''*-pentaacetic acid (DTPA) is used as the masking agent from a concentrated lactic acid buffer in normal TALSPEAK processes (Fuger, 1958); (Weaver & Kappelmann, 1964); (Kappelmann & Weaver, 1966); (Weaver & Kappelmann, 1968). The DTPA is thought to preferentially complex trivalent actinides due to their higher covalent character from the over-extension of the 5f orbitals, so they have higher affinity for softer N donors (Choppin, 2002). This claim is not without opposition and it remains unclear exactly why An(III) are preferentially complexed in these systems (Kirker & Kaltsoyannis, 2011).

TALSPEAK chemistry is very complex. Performance is very sensitive to pH owing to the proton-exchange reaction required to extract the trivalent lanthanides. Extraction of both actinides and lanthanides is seen to increase as acidity increases. As an increase in acidity would supress the HDEHP extraction mechanism, it is thought that acidity affects DTPA complexation more in the pH range tested. Increasing DTPA concentration led to a decrease in trivalent metal extraction due to higher DTPA complexation with all metal cations (Weaver & Kappelmann, 1968); (Kosyakov & Yerin, 1978); (Svantesson, et al., 1979). Radiolysis generates H_2MEHP in the organic phase which in low concentrations will increase distribution ratios and decrease separations factors, but in high concentrations will supress metal extraction (Tachimori & Nakamura, 1979), possibly due to polymerisation of the H_2MEHP and HDEHP molecules (Schulz, 1972).
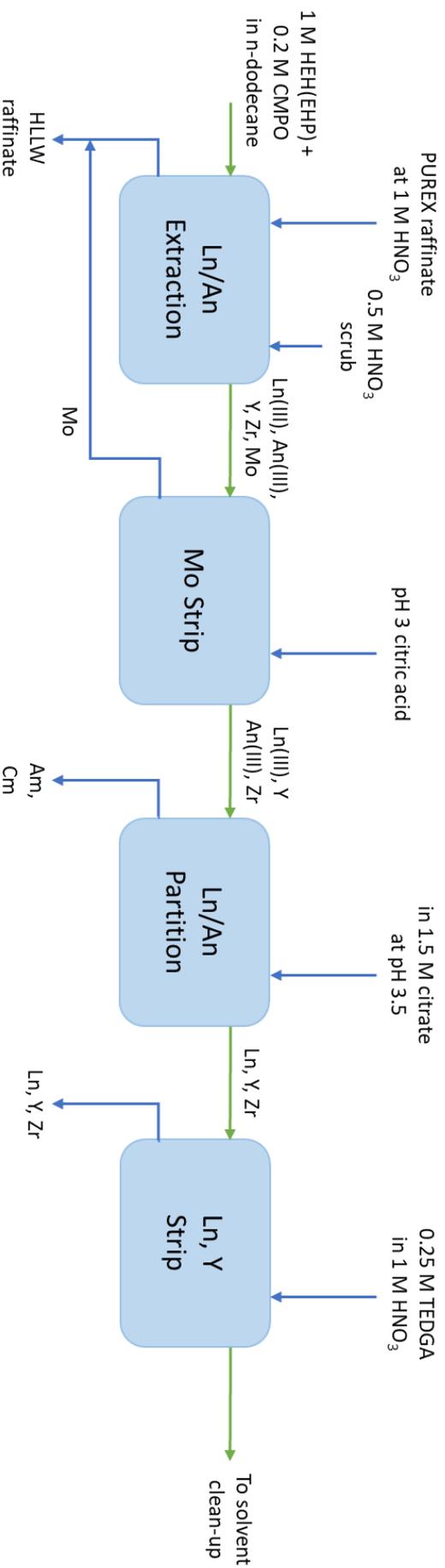
Figure 2.15. *An example TRUSPEAK process. Blue arrows show aqueous flows. Green arrows show organic flows. [Adapted from (Lumetta, et al., 2013) and (Braley, et al., 2013)].*

Some more modern TALSPEAK processes have been developed to improve upon TALSPEAK performance which include Advanced TALSPEAK (or TALSQuEAK) and TRUSPEAK (Figure 2.15). TALSQuEAK aims to reduce the issues with undesired sodium, water, and lactic acid extraction into the organic phase. Lactic acid extraction and competition with HDEHP is thought to exacerbate the steep pH dependence of TALSPEAK. This is done through the replacement of HDEHP with the more basic 2-ethylhexylphosphonic acid mono-2-ethylhexyl ester (HEH(EHP)). It is thought that the increased basicity of the ligand would decrease buffer partitioning and remove acid competition with the extractant. DTPA is replaced by HEDTA like in the DIAMEX-SANEX process. The combination of these ligands suitably flattens the pH dependence in TALKSPEAK operating windows and facilitates more rapid phase separations without the need for higher lactate concentrations (Braley, et al., 2012).

TRUSPEAK aims to consolidate Ln/An separations into a single process to simplify the requirements and improve the economics (Braley, et al., 2013). It was initially thought that a CMPO-HDEHP solvent to extract Ln(III) and An(III) followed by a DTPA strip in citric acid to selectively separate An(III) would be successful, however, initial studies revealed that the lipophilic extractants interact with one another and reduce total free ligand concentrations which led to decreased metal extraction (Lumetta, et al., 2011); (Lumetta, et al., 2012); (Tkac, et al., 2012). Synergism between these ligands also enhanced americium(III) extraction which ultimately reduced separation factors. Similar to TALSQuEAK, current TRUSPEAK processes now use a CMPO-HEH(EHP) solvent to extract Ln(III) and An(III), however, zirconium(IV) is strongly extracted into the organic phase from citrate media, and both zirconium(IV) and molybdenum(VII) are extracted from nitric acid. Molybdenum(VII) can be stripped with a citrate buffer solution, but zirconium(IV) remains extracted and currently leaves the process in the Ln(III) product stream (Lumetta, et al., 2013). As HEH(EHP) is a weaker extractant, a weaker aqueous strippant is required to facilitate adequate separations. To this end, HEDTA is used rather than DTPA similar to TALSQuEAK.

2.4.5 ALSEP

The <u>A</u>ctinide-<u>L</u>anthanide <u>SEP</u>aration (ALSEP) process uses the neutral extractants TODGA and T2EHDGA (*N,N,N',N'*-tetra(2-ethylhexyl) diglycolamide) to extract Ln(III) and An(III) into an organic phase from nitric acid. This is carried out alongside acidic HEH(EHP) to retain Ln(III) in an organic phase while An(III) are stripped into pH 3-4 citrate media by an DTPA (Lumetta, et al., 2014) or HEDTA (Guelis, 2013). This process builds upon TALSPEAK principles, but the use of these neutral extractants allows higher distribution ratios at higher acidities during the initial extraction and decreases the pH sensitivity of the An(III) strip. This process suffers the same undesired zirconium(IV) and molybdenum(VII) extraction as TALSPEAK processes. To mitigate this, molybdenum(VII) is stripped with a citrate buffer prior to An(III) stripping with DTPA in citrate media. TEDGA in dilute nitric acid is used to strip Ln(III) from the loaded organic to leave only zirconium(IV) which can be stripped with oxalic acid. An example ALSEP process can be seen in Figure 2.16.

2.4.6 EXAm

The EXAm process (Figure 2.17) aims to separate americium alone from a PUREX raffinate (Rostaing, et al., 2012). Americium(III) and light Ln(III) in strongly acidic conditions are extracted by DMDOHEMA/HDEHP in hydrogenated tetrapropylene which initially has a $SF_{Am/Cm} \sim 1.6$. This separation is further aided by TEDGA which preferentially complexes with curium(III) and heavy Ln(III) in the aqueous phase. After this separation, americium(III) is stripped using DTPA or HEDTA similar to previous processes. However, palladium remains an issue with a substantial amount flowing through the americium product stream.
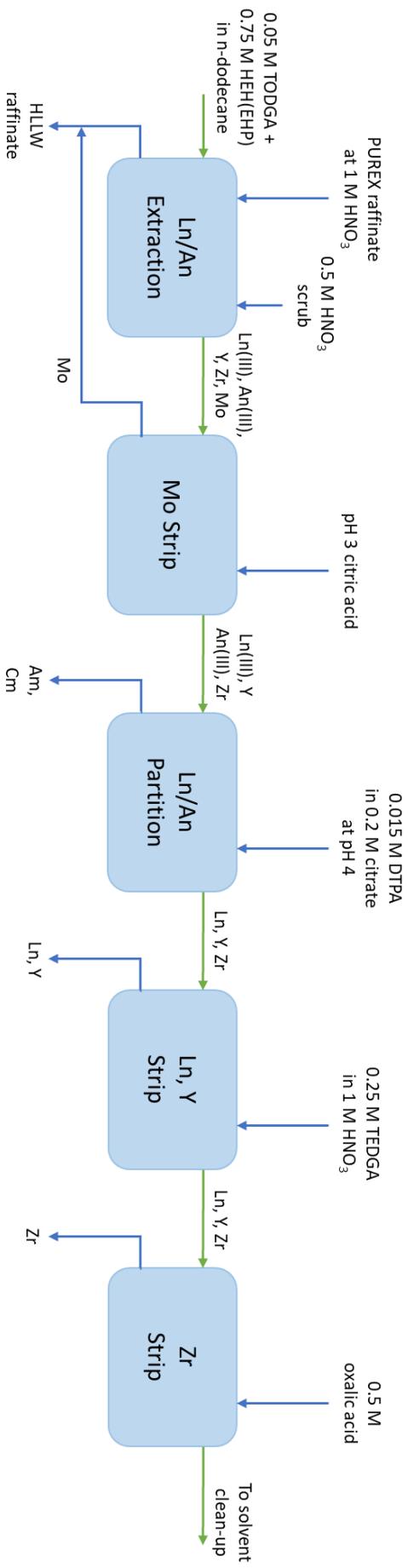
Figure 2.16. *An example ALSEP process. Blue arrows show aqueous flows. Green arrows show organic flows.*
[Adapted from (Lumetta, et al., 2014)]

60

0.6 M DMDOHEMA +
0.3 M HDEHP in HTP

PUREX raffinate
at 5 M HNO$_3$

0.05 M TEDGA
In 5 M HNO$_3$

Am Extraction

HLLW
raffinate

Mo, Ru, most Pd,
0.7% of total Am

Am,
light Ln(III),
Mo, Pd,
Ru, Fe

Mo Strip

pH 3 citric acid

Am,
light Ln(III),
some Pd,
Fe, Zr

Am Strip

0.01 M DTPA
in 0.3 M malonic acid

Am,
Pd

Light Ln(III),
Fe Zr

Ln, Y Strip

0.25 M TEDGA
in 1 M HNO$_3$

Light Ln(III),
Fe, Zr

To solvent
clean-up
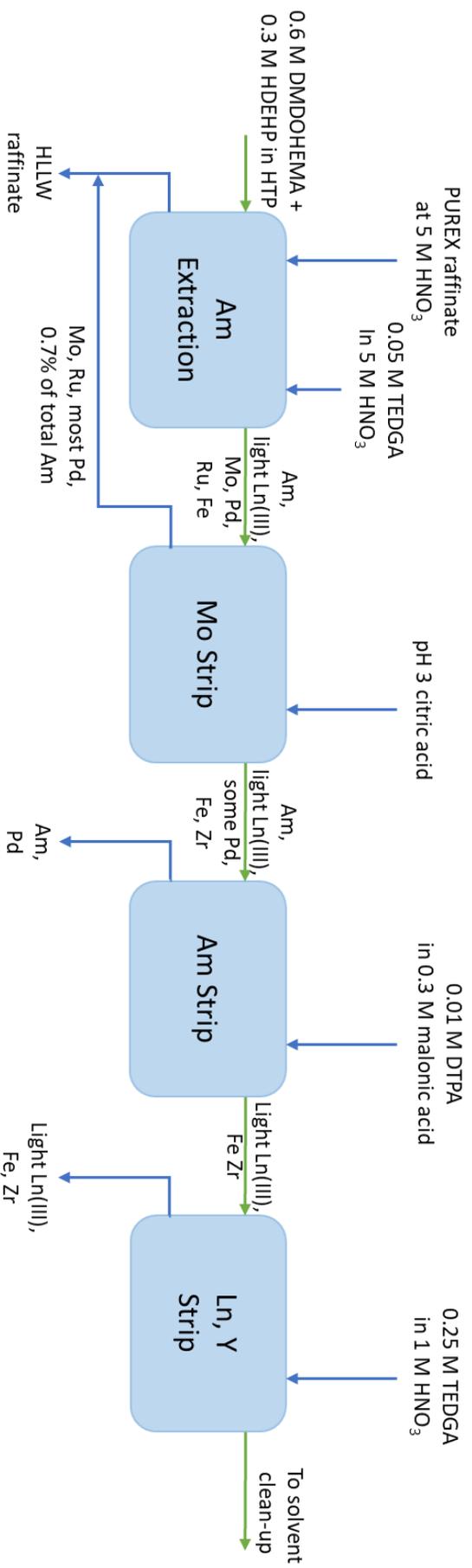
Figure 2.17. *An example EXAm process. Blue arrows show aqueous flows. Green arrows show organic flows. [Adapted from (Vanel, et al., 2012) and (Rostaing, et al., 2012)]*

61

2.4.7 Advanced Flowsheet Review Conclusion

There are a number of advanced reprocessing flowsheets all of which have different aims for the treatment of SNF. DIAMEX-SANEX flowsheets use diamides to extract and ultimately separate An(III) from PUREX raffinate. This requires prior PUREX processing so this flowsheet is subject to the same disadvantages as PUREX. GANEX flowsheets generally extract uranium with branched monoamides and then separate TRUs with diglycolamide/diamide mixtures and aqueous holdback reagents. UREX+ processes provide a fleet of flowsheets that are modular in nature to separate individual problematic components of spent fuel. These flowsheets can be powerful if implemented correctly but are complex to fit together coherently, may present waste management issues, and may require high initial capital costs. Many UREX+ processes also rely on phosphoryl chemistry for adequate separations. Similarly to DIAMEX-SANEX, TALSPEAK processes aim to ultimately separate An(III) from a PUREX raffinate using aqueous complexants, but use lipophilic phosphorus-containing extractants to initially extract Ln(III) and An(III). ALSEP builds upon advanced TALSPEAK processes and uses a diglycolamide/phosphonic acid solvent for the initial separation. EXAm seeks to separate Am from a PUREX raffinate using aqueous complexants to mask Cm and heavy Ln extraction by diamide followed by a selective aqueous complexant strip; however, there is significant Pd contamination of the Am product.

2.5 Literature Review Conclusion

The above literature review details processes for the current and future reprocessing of spent nuclear fuel. Recovery of uranium and plutonium is desirable to increase the lifespan of mined uranium as nuclear fuel. The removal of certain heat-generating or long-lived radioactive products of the fission process is also desirable to ease the burden of nuclear waste disposal in a geological facility. The reprocessing capability in the UK will soon be gone in favour of interim storage due to high costs and process complexity; therefore, research into economically favourable reprocessing is necessary to recover desired elements.

PUREX is the current standard process for reprocessing. SNF dissolved in concentrated nitric acid is contacted with 30% TBP in aliphatic diluent which quantitatively extracts uranium and plutonium.

Plutonium reduction partitions these metals after which the separate uranium and plutonium streams are further purified. Complications of the PUREX process include undesired neptunium, zirconium, and ruthenium extraction by TBP. Zirconium-TBP complexes further extracts all undesired technetium in solution. Additional process steps are required to minimise this undesired extraction. Radiolysis and hydrolysis products of TBP result in undesired zirconium-HDBP complexation which increases the extraction of molybdenum, iron, REEs and TRUs into the organic phase. TBP degradation products cause the formation of interfacial 'crud' – an emulsion generated by zirconium-H_3PO_4 stabilised by zirconium-H_2MBP precipitates. This emulsion is permanently degraded, chemically unreactive, and can contain radionuclides present from TBP and zirconium-HDBP extraction. Final solvent disposal involves solvent incineration to leave behind radioactive phosphate residues. Replacing TBP may alleviate these issues and improve the economics of reprocessing. Aliphatic monoamides are promising replacements for TBP. They are mechanistically similar extractants, simple to synthesise, and can be completely incinerated upon solvent degradation to leave no phosphate residue. The degradation products of monoamides are innocuous to reprocessing chemistry. Monoamides also generally have higher decontamination factors than TBP. Monoamide extraction performance for plutonium(IV) far surpasses TBP but it is poorer for uranium(VI). This has been attributed to poor organic solubility of the extracted complex. Altering the hydrophobicity of the complex by adding other CHON ligands may enhance uranium(VI) extraction, but this may come at the cost of selectivity (Nash, et al., 2010d). The addition of a second ligand as a phase modifier may also boost uranium(VI) extraction with monoamides by increasing the organic phase polarity.

The idea of an enhanced monoamide-PUREX flowsheet is novel; there are many advanced reprocessing flowsheets proposed for different applications, but most are focused on trivalent lanthanide/actinide separations for easier management of vitrified HLW. GANEX uses branched monoamides to extract uranium(VI) from dissolved SNF but leaves plutonium(IV) to be recovered with other TRUs by diamide/diglycolamide extraction. This leaves a gap for the sustainable recovery of uranium and plutonium in a single step extraction process similar to current PUREX processes. This similarity is

important because the closer a flowsheet is to current PUREX processes, the easier it could be implemented into industrial scale.

CHAPTER 3   Assessment of Uranyl Nitrate Complexes in Single- and Dual-Ligand Monoamide Systems.

The aim of this chapter was to prove the formation of exploitable ternary complexes with uranyl nitrate, monoamides and selected ligands. The selected ligands were diamides, diglycolamides, phosphates and phosphine oxides; these ligands were chosen due to their affinity for uranium(VI). Within this, the objectives are to:

1. Understand how uranyl nitrate is complexed in single-ligand systems using monoamides, diamides, diglycolamides, phosphates or phosphine oxides.

2. Use single-ligand system data to assess the formation of ternary complexes with uranyl nitrate, monoamides and selected ligands in dual-ligand systems.

3. Assess the effect of changing media and monoamide size on produced species.

4. Identify suitable dual-ligand systems to carry forward to solvent extraction tests.

To that end, the following work tests the first half of sub-hypotheses 1, 2, 3 and 5 in Section 1.3.

3.1   Introduction

Dual-ligand complexes with monoamides are of interest to the field of nuclear fuel reprocessing as they may enhance the performance of monoamides as extractants for uranium. One of the key limiting factors for replacing tri-*n*-butyl phosphate (TBP) with monoamides in reprocessing is the limited solubility of the uranyl-nitrate-monoamide complex in the organic phase. Based on previous literature, it is hypothesized that using monoamides alongside other adduct forming ligands, such as diamides, diglycolamides, phosphates or phosphine oxides, will boost the hydrophobicity of the extracted complex and either eliminate or reduce phosphorus waste in fuel reprocessing. Diamides, diglycolamides and phosphine oxides are not entirely selective for uranium from spent fuel liquors, but monoamides have shown remarkable selectivity (Gasparini & Grossi, 1986); (Manchanda, et al., 2001). Synergism often comes at the cost of selectivity (Nash, et al., 2010d), so it is hypothesized that the right monoamide-based system may boost uranyl extraction with sufficient separation factors.

This chapter is the first step towards determining the applicability of utilising amide and/or organophosphorus ligand mixtures to improve the extractive performance of monoamides for uranium from spent fuel liquors. It investigates whether these kind of dual-ligand uranyl complexes exist in solution. However, to adequately assess whether dual-ligand complexes have been produced, the complexation of uranyl nitrate in single ligand systems must first be investigated. Once it is defined how the uranyl cation interacts with different ligands, this can then go on to inform the viability of any proposed dual-ligand species found experimentally. Below is a recap on the relevant literature for this section that will be compared with the present results.

Most studies have found that up to 4 M nitric acid, monoamides definitively form a disolvate complex with uranyl cations (Gupta, et al., 2000a); (Prabhu, et al., 1997). Beyond 4 M, potential protonation of the monoamide results in the formation of the ionic complex $(UO_2(NO_3)_3)^+(HL)^-$ where $(HL)^-$ is the protonated ligand. The acidity at which the monoamide is protonated changes depending on monoamide structure, but it is worth noting that this ionic complex does not dominate speciation until over 12 M nitric acid for aliphatic amides (Berger, et al., 2020). Diamides like *N,N'*-dimethyl-*N,N'*-dibutyl-2-tetradecyl-malonamide (DMDBTDMA) have been reported to form monosolvate (Wahu, et al., 2012), (Cui, et al., 2010) and disolvate (Chen, et al., 2019) complexes with uranyl nitrate. No ionic complexes are reported due to the lower basicity of these ligands. As the disolvate complex appears to be by far the most common, the formation of a dual-ligand species will likely depend on the substitution of a diamide molecule with a monoamide; the likelihood of this will depend on the relative stability of the formed species. Diglycolamides like tetraoctyl diglycolamide (TODGA) have been reported to form mono-, di- and trisolvate complexes in solution (Gong, et al., 2013); (Boltoeva, et al., 2018); (Sasaki, et al., 2015); (Liu, et al., 2015); (Peng, et al., 2017). These values have typically been determined from solvent extraction slope analysis plots. Theoretically, the monosolvate species is susceptible to form dual-ligand species when considering steric hinderance and uranyl coordination number. Phosphates and phosphine oxides (such as tri-*n*-octyl phosphine oxide, TOPO) have been reported to form disolvate complexes with uranyl cations, similar to monoamides (Durain, et al., 2019); (Bagnall & Wakerley, 1974). Due to the much lower basicity of these ligands when compared with monoamides, protonated

ligand complexes have not been reported. As with the diamides, the formation of a dual-ligand species will likely depend on the substitution of an organophosphorus molecule with a monoamide which is dependent on complex stabilities.

The ligands used in this spectrophotometric study are model ligands for those considered for dual-ligand solvent extraction tests, i.e., monoamides, diamides, diglycolamides, phosphates, and phosphine oxides. The purpose of this chapter is to identify monoamide systems that demonstrate dual-ligand interactions after the introduction of a 'secondary' ligand. Successful systems will then inform what hydrophobic ligands to synthesise for the solvent extraction tests presented later in this thesis. Small ligands were used because the focus of this study was to investigate fundamental interactions. The tested ligands are shown in Scheme 3.1 and 3.2. *N,N*-dimethylacetamide (DMAA), *N,N*-diethyl acetamide (DEAA), N,N-dibutyl acetamide (DBAA), and *N,N*-dibutyl butanamide (DBBA) have been selected to act as DHOA analogues. For the CHON 'secondary' ligands, N^1,N^1,N^3,N^3-tetraethyl malonamide (TEMA) has been selected to act as a DMDBTDMA analogue, and N^1,N^1,N^5,N^5-tetraethyl diglycolamide (TEDGA) has been selected to act as a TODGA analogue. For the organophosphorus 'secondary' ligands, tri-*n*-ethyl phosphate (TEP) has been selected to act as a TBP analogue, and trimethyl phosphine oxide (TMPO) has been selected to act as a TOPO analogue.

The interactions and complex strengths between uranyl nitrate and each of these ligands separately have been investigated in two diluents of differing hydrophobicity to inform any proposed dual-ligand complexes found in this study, and to also inform solvent extraction (SX) behaviour both later in this thesis and in literature. Spectrophotometric titrations (SPTs) were conducted to assess complex stoichiometry and stability of these single ligand systems. Job plots were also conducted to assess the most dominant complex in these systems. The interactions between uranyl nitrate and the ligand mixtures previously mentioned were then investigated through Jobs plots and discussed with the previous results. Results from this chapter go on to inform ligand selection for SX systems. Some of this chapter is based on an article published by the author of this thesis (Canner, et al., 2020), namely the tests conducted in the more hydrophilic diluent, but the present work extends upon this publication by investigating organophosphorus ligands as well in a more hydrophobic solvent.
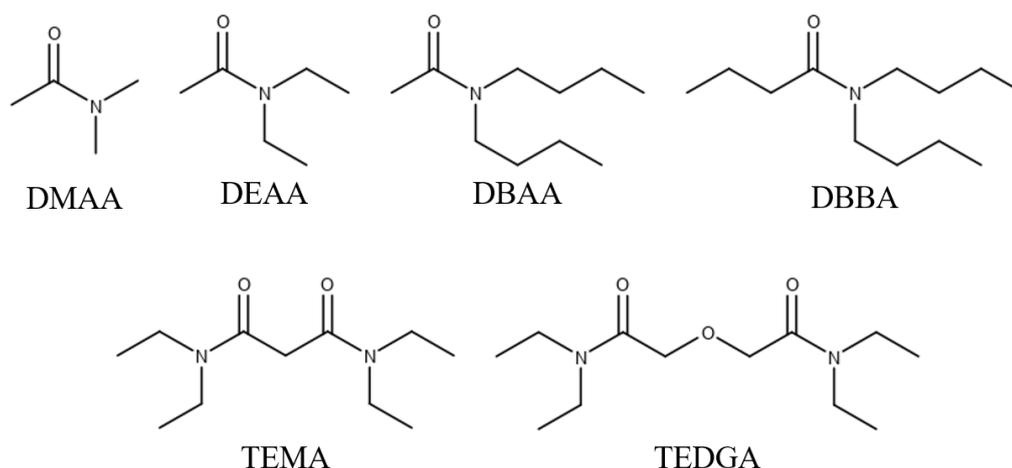
Scheme 3.1. *Structure and abbreviation of the ligands used in diluent A tests.*
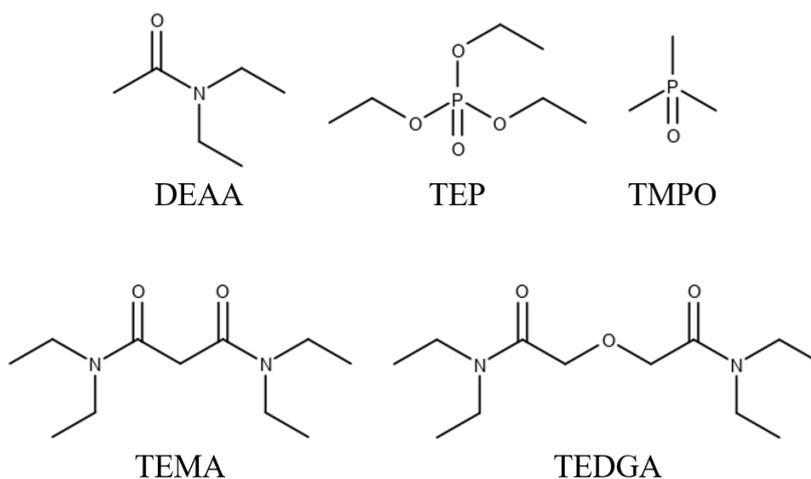
Scheme 3.2. *Structure and abbreviation of the ligands used in diluent B tests.*

3.2   Experimental Method and Materials

All reagents were ACS reagent grade or higher purity. Nitric acid (70%, Merck), methanol (99.8%, Merck), DMAA (99.8%, Sigma-Aldrich), DEAA (95%, Fluorochem), TEP (99.8% Merck) and TMPO (Alfa Aesar) were used as received. Uranyl nitrate hexahydrate was supplied by the Immobilisation Science Laboratory at Sheffield University and was dissolved in pH 1 nitric acid to generate a concentrated mother solution of uranyl nitrate. Aliquots from this solution were used to generate uranyl nitrate working solutions of the required concentration in pH 1 methanolic nitric media. All aliquots were taken from the same mother solution, and it was assumed that uranium concentration of the mother solution (and subsequent initial working solutions) remained constant throughout the work. All tests were conducted at pH 1 and 0.20 M ionic strength controlled by addition of nitric acid and sodium

nitrate, respectively. Ligand solutions were prepared by diluting the required mass of ligand with pre-prepared methanolic nitric acid diluent.

In order to test the hypotheses stated in Chapter 1, two sets of spectroscopy experiments were conducted to investigate:

A. Monoamide-diamide and monoamide-diglycolamide ligand mixtures (towards *eliminating* phosphorus waste in reprocessing). The effect of changing monoamide size on complex speciation was also investigated here.

B. Monoamide-organophosphorus complexes with uranyl nitrate (towards *reducing* phosphorus waste in reprocessing) using a single model monoamide (DEAA).

The former tests were conducted in a 50 vol% water diluent with methanol ('diluent A'), but due to water interference with organophosphorus complex formation, the latter tests were conducted at 4.5 vol% water diluent ('diluent B'). To aid comparability between the two sets of tests, diamide and diglycolamide tests were run in diluent B as well. Comparing these results would also give insight to complex changes in increasingly hydrophobic environments. Ultraviolet-visible (UV-vis) spectra have been analysed to assess what uranyl complexes form in the above systems in the pseudo-aqueous media. The pseudo-aqueous methanolic nitric acid media were used to aid the dissolution of some of the more hydrophobic ligands and have also been reported to give clearer absorbance readings (Rabinowitch & Belford, 1964a).

3.2.1 Ligand synthesis

DBAA and DBBA were synthesised through the reaction of the acetyl chloride (98%, Alfa Aesar) or butyryl chloride (99%, Acros Organics) respectively with equimolar dibutylamine (99.5%, Sigma-Aldrich) in chloroform ($CHCl_3$) under a nitrogen atmosphere. This was carried out in the presence of equimolar triethylamine base (99%, Acros Organics) in a stirred ice bath (Thiollet & Musikas, 1989). The solution was then heated to reflux at the boiling point of the mixture, roughly 68°C, for at least two hours. The organic product was washed with deionised water, 10wt% Na_2CO_3 solution, 1.2 M HCl solution and a final deionised water wash. The organic layer was dried over anhydrous Na_2SO_4, filtered,

and the solvent was removed under reduced pressure. Both ligands were >95% pure as determined by nuclear magnetic spectroscopy (NMR, Table 3.1). The DBAA yield was 76.5% and DBBA yield was 81.9%.

Table 3.1. *^{1}H NMR (500 MHz, CDCl$_3$) chemical shifts for DBAA (top) and DBBA (bottom). Structure labels indicate atom and position (e.g. H2 = proton group identified at chemical shift position 2 for ^{1}H). NMR spectra recorded in the Department of Chemistry at the University of Sheffield. An example NMR spectrum can be seen in Appendix A in Figure A.1.*

Position	^{1}H δ	Structure (top: DBAA, bottom: DBBA)
1	3.05 (t, 2H)	
2	2.98 (t, 2H)	
3	1.82 (s, 3H)	
4	1.27 (m, 4H)	
5	1.07 (m, 4H)	
6	0.68 (m, 6H)	
1	3.19 (t, 2H)	
2	3.10 (t, 2H)	
3	2.15 (t, 2H)	
4	1.55 (m, 2H)	
5	1.40 (m, 4H)	
6	1.12 (m, 4H)	
7	0.82 (m, 9H)	
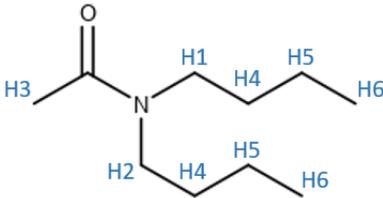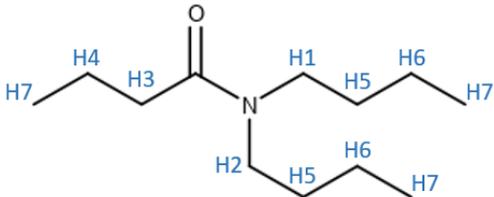
TEMA and TEDGA syntheses were carried out and supplied by Reading University, UK. TEMA was synthesised by the addition of 2 mole equivalents of hydroxybenzotriazole (HOBt), triethylamine, diethylamine and N-(3-dimethylaminopropyl)-N′-ethylcarbodiimide hydrochloride (EDC.HCl) to a suspension of malonic acid in CHCl$_3$. TEDGA was synthesised by the addition of 2 mole equivalents of HOBt, triethylamine, diethylamine and EDC.HCl to a suspension of 2,2'-oxydiacetic acid in CHCl$_3$. Both reactions were stirred at room temperature for 18 hours. Crude products were washed with 1 M HCl and 1 M NaOH. The combined organic layers were separately dried over MgSO$_4$, filtered, and the solvent was removed under reduced pressure. The TEMA yield was 86% and was found to be pure by NMR (Table 3.2) and probe electrospray ionisation-fourier transform mass spectrometry (pESI+FTMS, calculated: C$_{11}$H$_{22}$N$_2$O$_2$Na [M+Na]$^+$: 237.1573; observed: 237.1578). TEDGA yield was 95% and found to be pure with pESI+FTMS (calculated: C$_{12}$H$_{24}$N$_2$O$_3$Na [M+Na]$^+$: 267.1679; observed: 267.1687).

Table 3.2. *^{1}H NMR (400 MHz, CDCl$_3$) and ^{13}C NMR (101 MHz, CDCl$_3$) chemical shifts for TEMA (top) and TEDGA (bottom). Structure labels indicate atom and position (e.g. H2 = proton group identified at chemical shift position 2 for ^{1}H). NMR spectra recorded in the Department of Chemistry at the University of Reading.*

Position	^{1}H δ	^{13}C δ	Structure (top: TEMA, bottom: TEDGA)
1	3.46-3.37 (m, 10H)	166.4	
2	1.20 (t, 6H)	42.6	
3	1.14 (t, 6H)	40.6	
4	-	40.3	
5	-	14.1	
6	-	12.8	
1	4.30 (s, 4H)	167.9	
2	3.35 (app dq, 8H)	77.5	
3	1.16 (app dt, 12H)	77.4	
4	-	77.2	
5	-	76.9	
6	-	69.4	
7	-	41.0	
8	-	40.0	
9	-	14.2	
10	-	12.9	

3.2.2 SPTs and stability constants

For diluent A tests, incremental additions of 0.125 M ligand solution were made via burette into a stirred 0.025 M uranyl nitrate solution. For diluent B tests, lower water content in the diluent required a lower initial uranium concentration; therefore, incremental additions of 0.04 M ligand solution were made via burette into a stirred 0.008 M uranyl nitrate solution in order to keep uranium: ligand mole ratios equal to previous tests. After each addition, a small aliquot was taken, and its absorption spectrum recorded in a 1 cm path length quartz or UV-transparent plastic cuvette against the suitable diluent blank (transparency of the plastic cuvette in the measurement range was confirmed prior to use). The aliquot was then reintroduced into the experiment; volume losses were minimal. The cuvette was washed several times with deionised water (DI), followed by acetone, and then dried with compressed air to ensure no cross-sample contamination. Spectra were recorded on a VWR UV-6300PC Double Beam Spectrophotometer calibrated between 190-1100 nm. Absorption across this entire range was recorded, however, extreme absorption from the nitrate anions prevented reliable readings below ~330 nm. Concentrations of the initial uranium solution were confirmed against a calibration curve (Figure 3.1). Solutions were found to adhere to Beer's Law over the concentration range investigated (< 0.025 M uranyl). It was assumed that pH and ionic strength remained constant throughout the experiments.
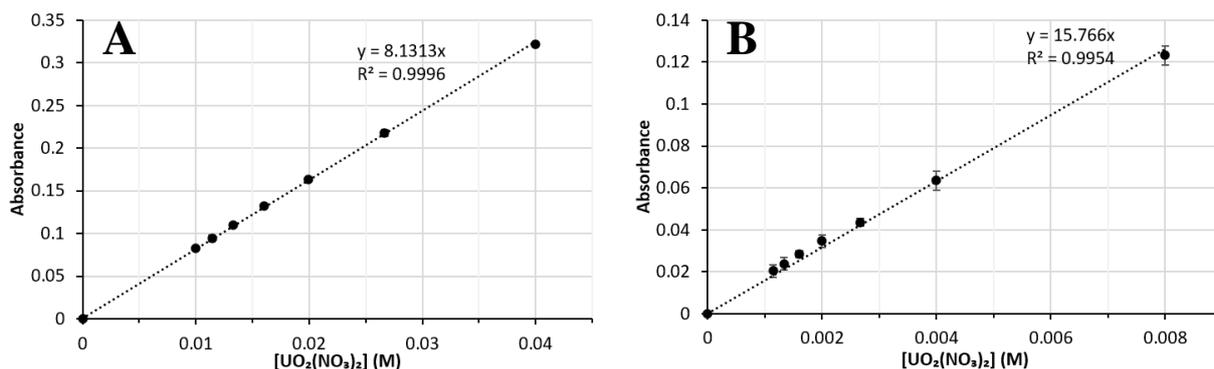
Figure 3.1. *Concentration calibrations at constant wavelength of uranyl nitrate in A) diluent A measured at 402 nm, and B) diluent B measured at 421 nm. Error bars indicate $\pm 2\sigma$ uncertainty.*

For each test, 24 sample spectra were taken (at different [metal]:[ligand]) as this was the upper limit of sample inputs for the MODSQUAD version of the SQUAD (Stability Quotients Using Absorbance Data) program. Stability constants were determined from titration data through the MODSQUAD version of the SQUAD program considering metal dilution (Leggett, 1985). SQUAD utilises a nonlinear least-squares approach to calculate the best values for complex stability constants in a proposed model by reducing the standard deviation of the absorbance data, refined stability constant and of each spectrum through an iterative process. Along with the experimental spectral data, a user inputs a model into SQUAD containing the proposed complexes produced in solution and an estimated stability constant which can be defined as fixed or variable (by SQUAD). An example annotated SQUAD input file can be seen in Appendix A. SQUAD then attempts to model spectra of complexes in the user-inputted model by assigning them a set of molar absorptivities. The standard deviation between the superimposed modelled spectra and the overall experimental data for each data point is recorded and, if it is too large, a new stability constant (if variable) and set of molar absorptivities are applied to reduce this standard deviation. This process repeats until either the standard deviation cannot be sufficiently reduced (indicating wrong model assumptions), or the standard deviation is reduced sufficiently to achieve model convergence (indicating a valid scenario). While model convergence confirmed the validity of each tested model, but this validity was also checked through comparison of the outputted molar absorptivities for the proposed complexes and concentrations of each model component with the experimentally determined spectra.

All stability constants reported in this work were calculated over the range 350-499 nm using the 72 spectra (24 in triplicate) per tested system. As it was found in preliminary tests that dilution effects dominate the spectral changes above a ligand molar excess of ~4.6 (which reduces the accuracy of SQUAD modelling), ligand was added in 0.2 molar steps to uranyl nitrate. All tests were carried out in triplicate at ambient temperature (19°C ± 2°C).

3.2.3 Job plots

Job's method is an established method for the determination of metal complex stoichiometry (Job, 1928); (Gullekson, et al., 2017). By varying the concentration of metal to ligand, or ligand to ligand, the stoichiometry of the dominant species can be determined by monitoring the absorbance of the solution. 'Corrected' absorbance is found by subtracting solution component contributions from the raw absorbance of a solution:

$$Corrected\ Absorbance_\lambda = Absorbance_\lambda - \varepsilon_{metal,\lambda} c_{metal,\lambda} - \varepsilon_{ligand,\lambda} c_{ligand,\lambda} \qquad (Eq\ 3.1)$$

where λ is a specific wavelength (nm), ε is the molar absorptivity of a solution component and c is the solution component concentration. The remaining 'corrected' absorbance is due to the complexed species. When plotting corrected absorbance against mole fraction of ligand, a peak in this absorbance (and hence species concentration) describes the stoichiometry of the dominant species. For example, a peak at 0.5 mole fraction ligand indicates a monosolvate species, i.e. (metal)(ligand), and a peak at 0.67 indicates a disolvate species, i.e. (metal)(ligand)$_2$, etc. Examples of these ideal peaks are shown in Figure 3.2.

For single ligand Job plots, separate stock solutions of uranyl nitrate and single ligand solutions were generated at equal concentration, pH, and ionic strength. Varying volumes of uranyl nitrate and ligand solutions were mixed in separate vials to result in the required mole fraction of metal and ligand. Spectra were recorded as above. pH and ionic strength were assumed to be constant throughout the experiments. All tests were carried out in triplicate at ambient temperature (19°C ± 2°C).

73
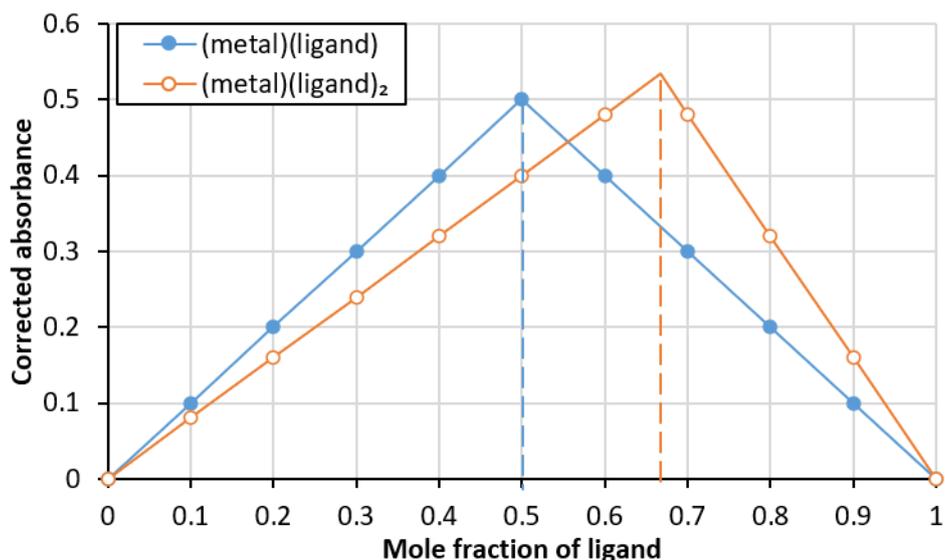
Figure 3.2. *Example ideal Jobs plots for a monosolvate and disolvate metal species.*

For dual ligand Job plots, uranyl-ligand stock solutions were prepared such that the ligand was in $4.6\times$ molar excess to uranium, thus mimicking the end point of the SPTs. Varying volumes of uranyl-monoamide/uranyl-diamide, uranyl-monoamide/uranyl-diglycolamide, uranyl-monoamide/uranyl-phosphate or uranyl-monoamide/uranyl-phosphine oxide solutions were mixed in separate vials to result in the required mole fraction of monoamide. Uranium concentration, pH and ionic strength were assumed to be constant throughout the experiments. Spectra were recorded as above. All tests were carried out in triplicate at room temperature ($19°C \pm 2°C$). Absorbance has been corrected through multiple steps; (1) subtracting the effects of the uranyl cation and both ligands on absorption as per Equation 3.1, (2) zeroing at 700 nm to minimise the effects of any baseline deviation, (3) baseline correct to ensure absorption is zero when mole fraction of a ligand is 0 and 1. Step 3 is a crude but necessary step to take account of absorption changes resulting from the single-ligand uranyl species identified earlier (e.g. $UO_2(NO_3)_2$-diglycolamide species).

3.3　Results

Figure 3.3 shows the molar absorptivity of uranyl nitrate in pH 1 nitric acid in both aqueous and pseudo-aqueous media at 0.2 M total ionic strength. This test was to confirm that no uranyl hydrolysis has taken place when introduced into the methanolic nitric acid media, as has been previously reported (Ogden, et al., 2012); (Ogden, et al., 2011). It can be seen that diluent A gives very similar results to a purely aqueous system which indicates that no hydrolysis is taking place in this diluent. Diluent B results in a larger, broader molar absorptivity spectrum which could either indicate hydrolysis or is simply the result of the differing solvation of the uranyl cation; this is discussed later on.
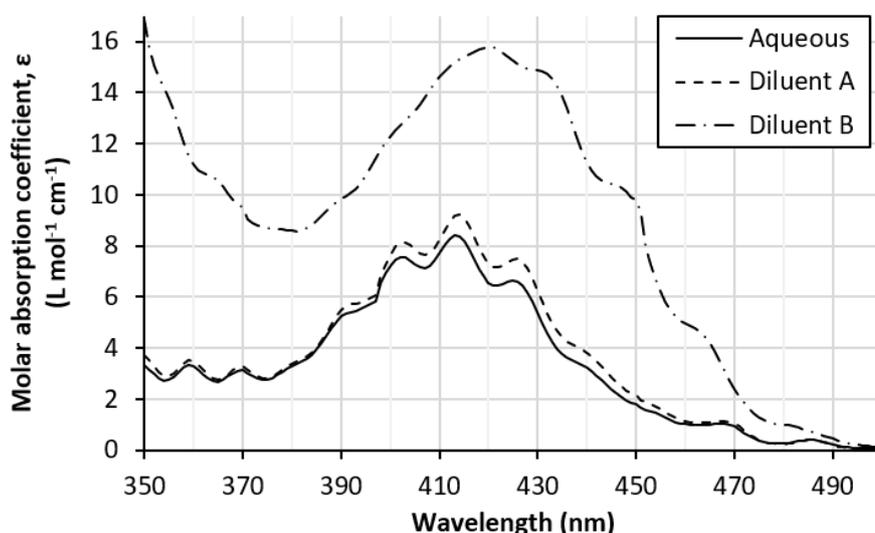
Figure 3.3. *Molar absorptivity of uranyl nitrate in different pH 1 diluents at 0.2 M total ionic strength.*

The results for the diluent A and B SPTs can be seen in Figures 3.4 and 3.5, respectively. The displayed spectral region is dominated by a ligand to metal charge transfer band (LMCT) (Libuś, 1962), and as such, it is sensitive to the ligand environment in the uranyl equatorial plane. As this band is not the result of f-f electronic transitions, it is not subject to selection rules; therefore, 'silent' complexes with linear actinyl cations identified by previous studies need not be considered in the modelling process (Tian, et al., 2005); (Rao & Tian, 2010). The initial and final solutions are denoted by the thick and dashed black lines, respectively. The grey lines denote 0.4 molar steps of ligand to uranium. The data from these titrations were used to determine the stability constants for the uranium(VI) complexes with

the tested ligands using the SQUAD software; these are shown in Table 3.3. Note that Table 3.3 defines complex stability constants in the K_{xyz} convention, where x is the number of metal centers, y is the number of protons, and z is the number of ligands in the complex. For example, K_{102} would be the stability constant for a disolvate complex.

In diluent A (Figure 3.4), both the monoamides and TEMA are found to only form disolvate complexes with uranyl nitrate. Typically, the monosolvate species would also be expected as the disolvate complex can be a product of the further solvation of the monosolvate. As it is not seen here indicates that the monosolvate is either not stable, or much less stable than the disolvate complex. Similar findings were observed for DEAA and TEP in diluent B (Figure 3.5), but TEMA was shown to also form monosolvate species in this more hydrophobic diluent. TEDGA in diluent A is shown to produce three species: a mono-, di- and tetrasolvate. In diluent B, these species are reduced to only the mono- and disolvate. TMPO was also shown to form mono- and disolvate species in diluent B.

Table 3.3. *Uranium(VI) stability constants $\pm 2\sigma$ at 19°C in pH 1 methanolic nitric at 0.2 M ionic strength. "-" indicates that no successful SQUAD model incorporated this complex. For K_{xyz}, x, y and z denote the number of metal ions, protons and ligands involved in the complex respectively, i.e. '102' is a disolvate species.*

Diluent	Ligand	$\log_{10}K_{101}$	$\log_{10}K_{102}$	$\log_{10}K_{104}$
A	DMAA	-	3.74 ± 0.02	-
	DEAA	-	3.86 ± 0.02	-
	DBAA	-	3.72 ± 0.02	-
	DBBA	-	4.03 ± 0.03	-
	TEMA	-	4.28 ± 0.02	-
	TEDGA	2.44 ± 0.03	4.85 ± 0.04	9.0 ± 0.1
B	DEAA	-	4.10 ± 0.06	-
	TEP	-	4.94 ± 0.08	-
	TMPO	3.59 ± 0.07	5.1 ± 0.1	-
	TEMA	2.2 ± 0.1	5.40 ± 0.04	-
	TEDGA	3.9 ± 0.2	4.9 ± 0.2	-
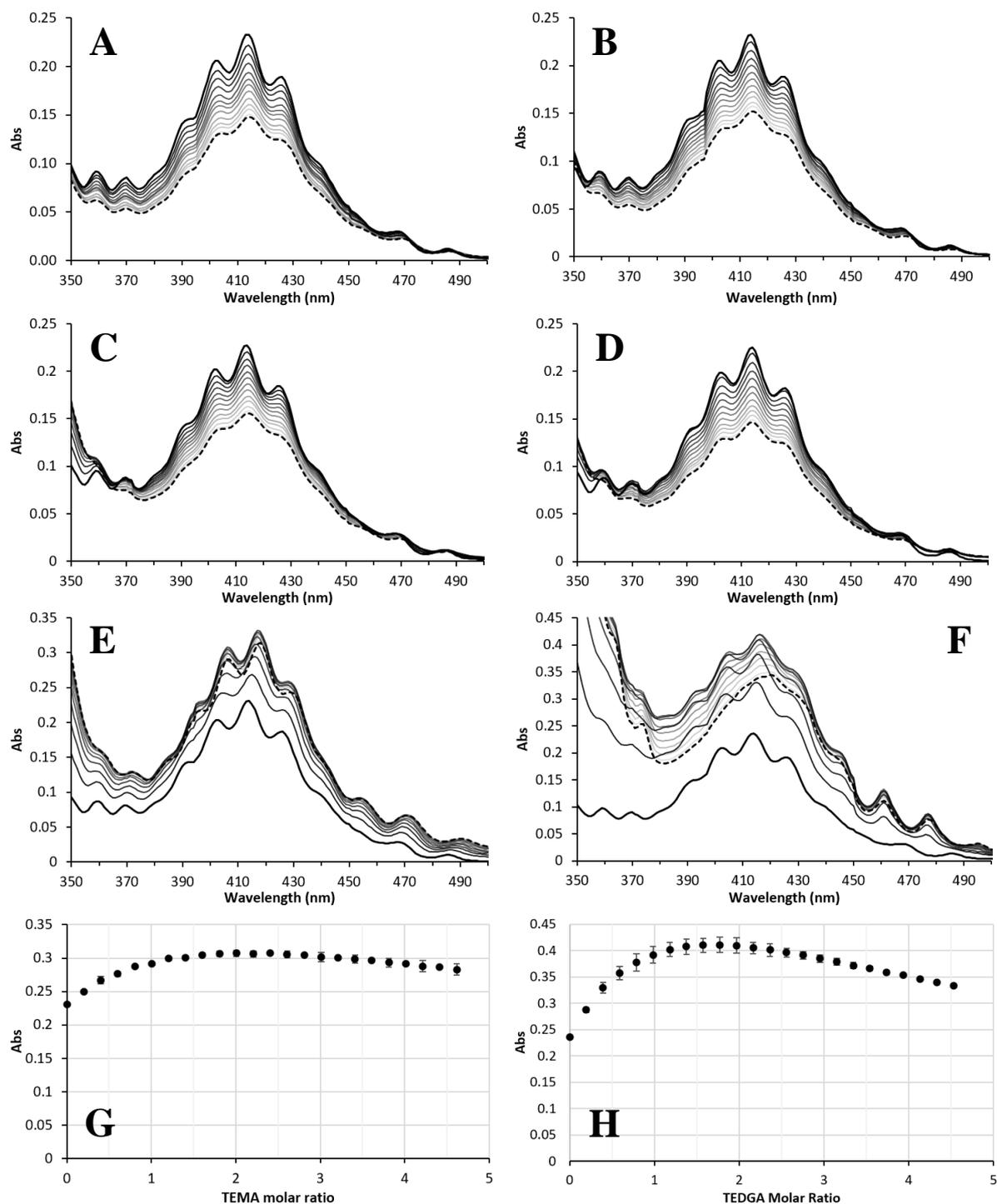
Figure 3.4. *SPTs with incremental additions of 0.125 M ligand into 0.025 M UO₂²⁺ in diluent A. The solid and dashed black lines denote the start and end points, respectively. Grey lines indicate 0.4 molar steps of ligand to metal. Lighter greyscale indicates a higher [ligand]:[metal]. A) DMAA, B) DEAA, C) DBAA, D) DBBA, E) TEMA and F) TEDGA. G) Absorption at 414 nm with increasing [TEMA]:[U] to clarify the trend. H) Absorption at 414 nm with increasing [TEDGA]:[U] to clarify the trend.*
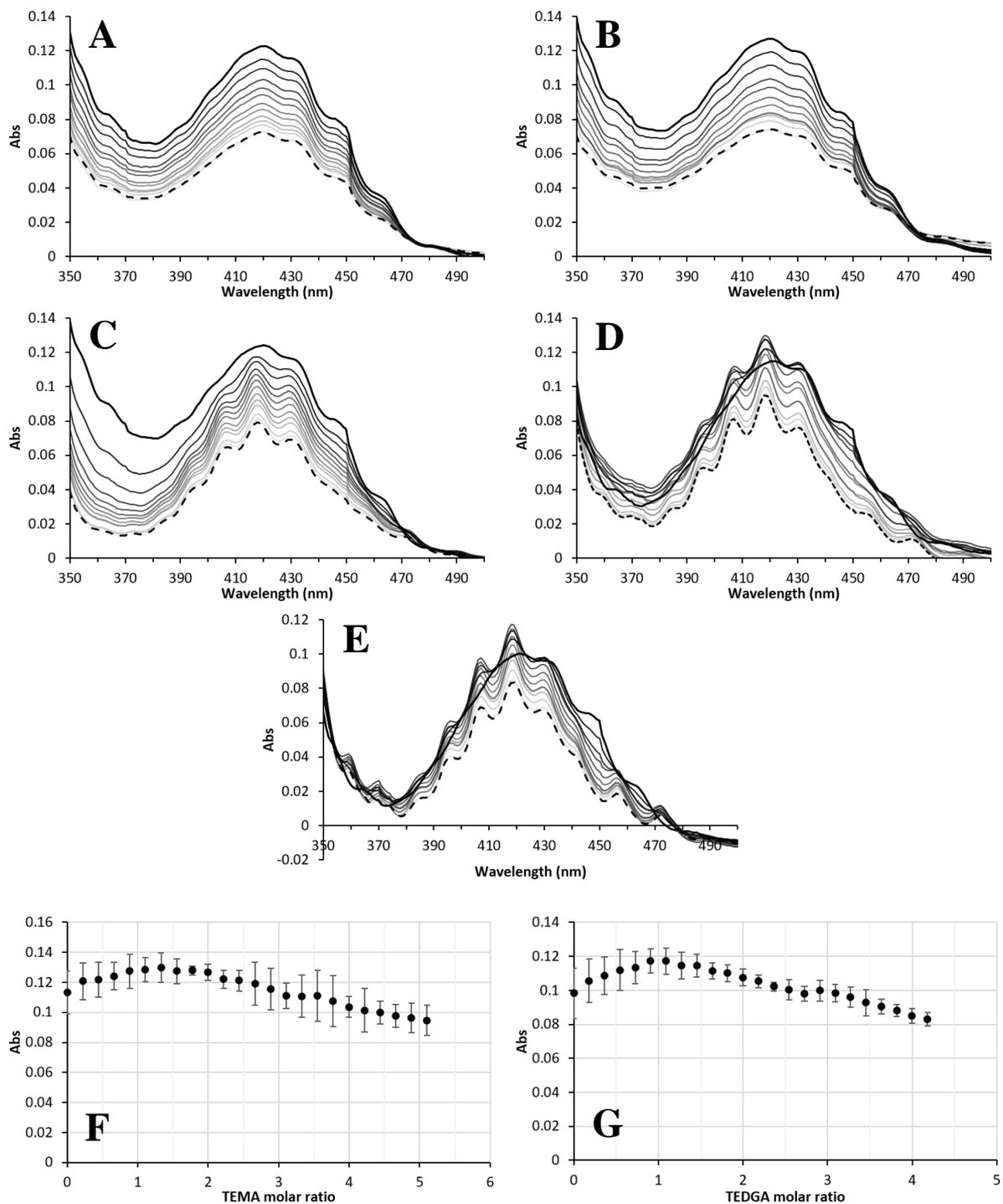
Figure 3.5. *SPTs with incremental additions of 0.04 M ligand into 0.008 M UO$_2$$^{2+}$ in diluent B. The solid and dashed black lines denote the start and end points, respectively. Grey lines indicate 0.4 molar steps of ligand to metal. Lighter greyscale indicates a higher [ligand]:[metal]. A) DEAA, B) TEP, C) TMPO, D) TEMA and E) TEDGA. F) Absorption at 418 nm with increasing [TEMA]:[U] to clarify the trend. G) Absorption at 418 nm with increasing [TEDGA]:[U] to clarify the trend.*

The molar extinction coefficients of the SQUAD-proposed complexes for the diluent A and B tests are shown in Figure 3.6 and 3.7, respectively. These more clearly show the effects of the ligands on the uranyl cation. Concentration profiles from MODSQUAD can be seen in Appendix A.
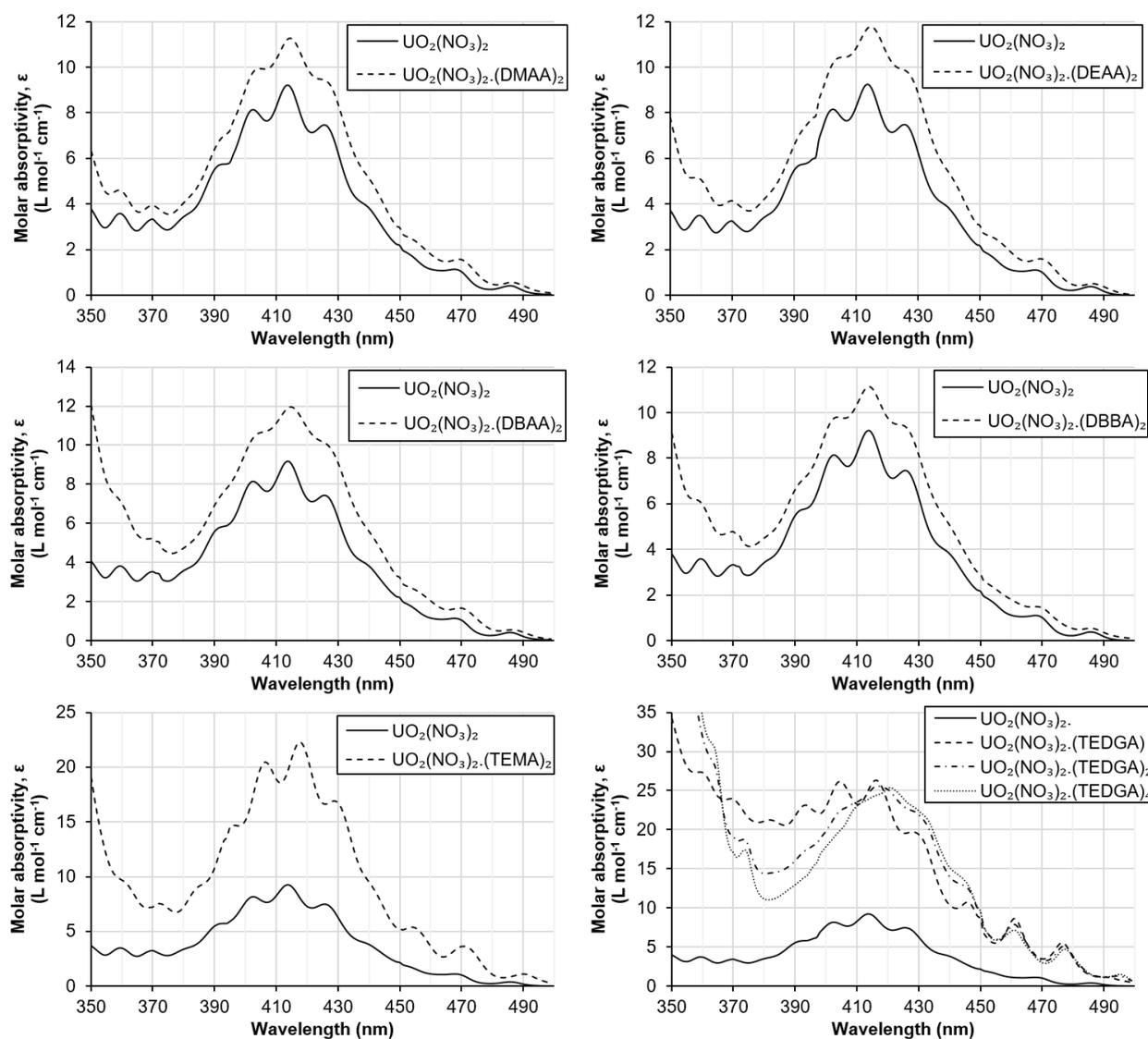
Figure 3.6. *Molar absorptivities of generated complexes in diluent A determined from SQUAD analysis.*
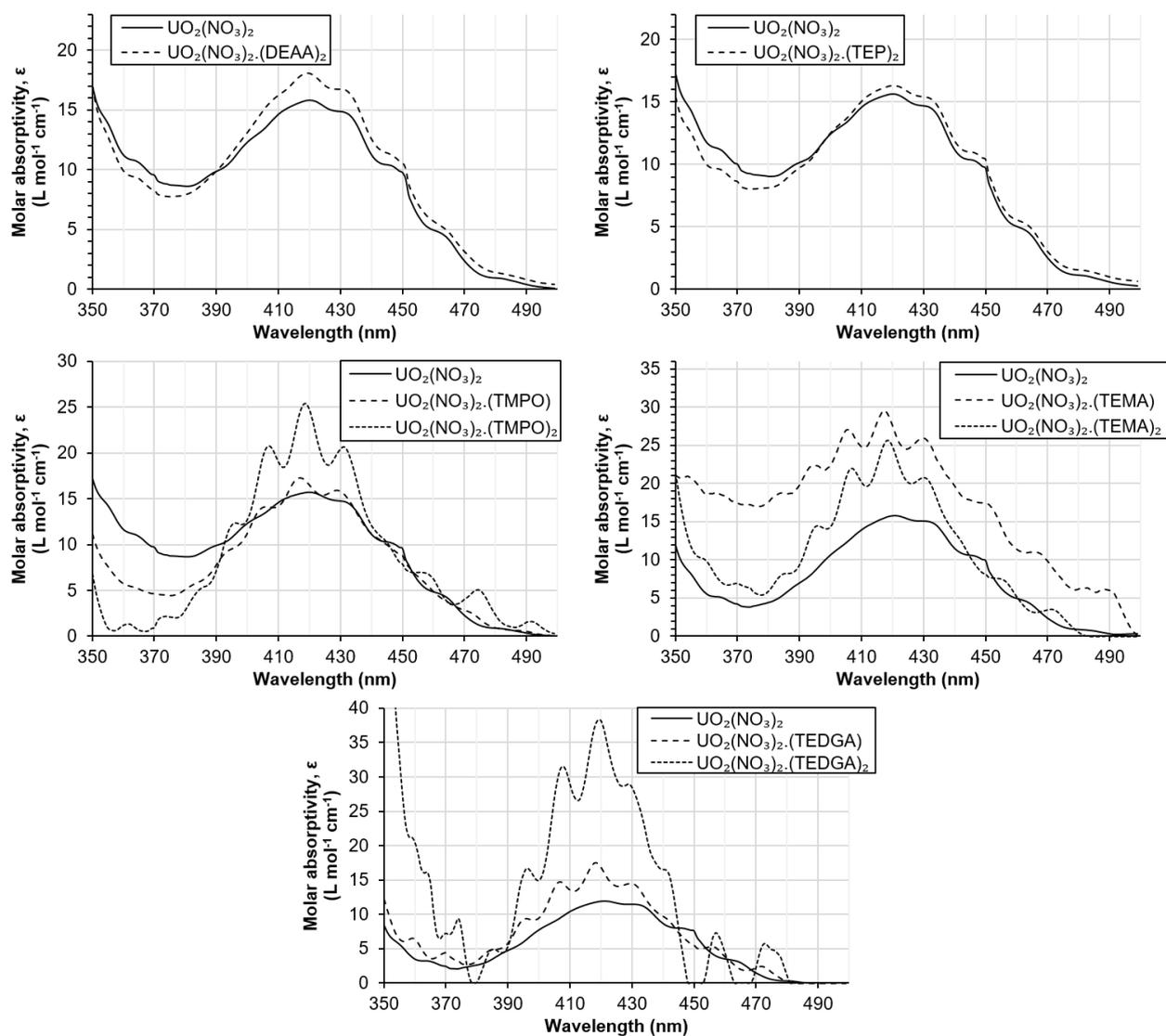
Figure 3.7. *Molar absorptivities of generated complexes in diluent B determined from SQUAD analysis.*

Speciation of the dominant single-ligand complex with uranyl nitrate and each of the tested ligands in the diluent A and B systems are shown in the single-ligand Job plots in Figure 3.8 and 3.9, respectively, to confirm the validity of reported species from MODSQUAD. The large relative uncertainty in the monoamide-uranyl and TEP-uranyl Jobs plots make it difficult to infer a trend, but some monoamide-uranyl plots indicate a dominant disolvate species due to the peak around 0.67. The TEMA-uranyl Jobs plot in diluent A appears to peak at around 0.5 TEMA mole fraction; however, based on the shape of the data, it could be argued that the true peak is at higher TEMA mole fractions. A peak at 0.5 TEMA mole fraction indicates a monosolvate species is dominant, but this is not reflected by the SQUAD modelling. A dominant disolvate TEMA species is reported in diluent B. The dominating TEDGA species is shown to be the monosolvate in both tested diluents. The TMPO-uranyl Jobs plots are largely inconclusive due to the high absorption readings at lower TMPO mole fractions. A peak at these low ligand mole fractions implies a nonsensical complex, and ignoring these readings indicates a rough peak around 0.6. This may mean that both a mono- and disolvate species are roughly equally as dominant under the tested conditions and the super positioning of their trends forms a peak at 0.6 rather than 0.5 or 0.67.
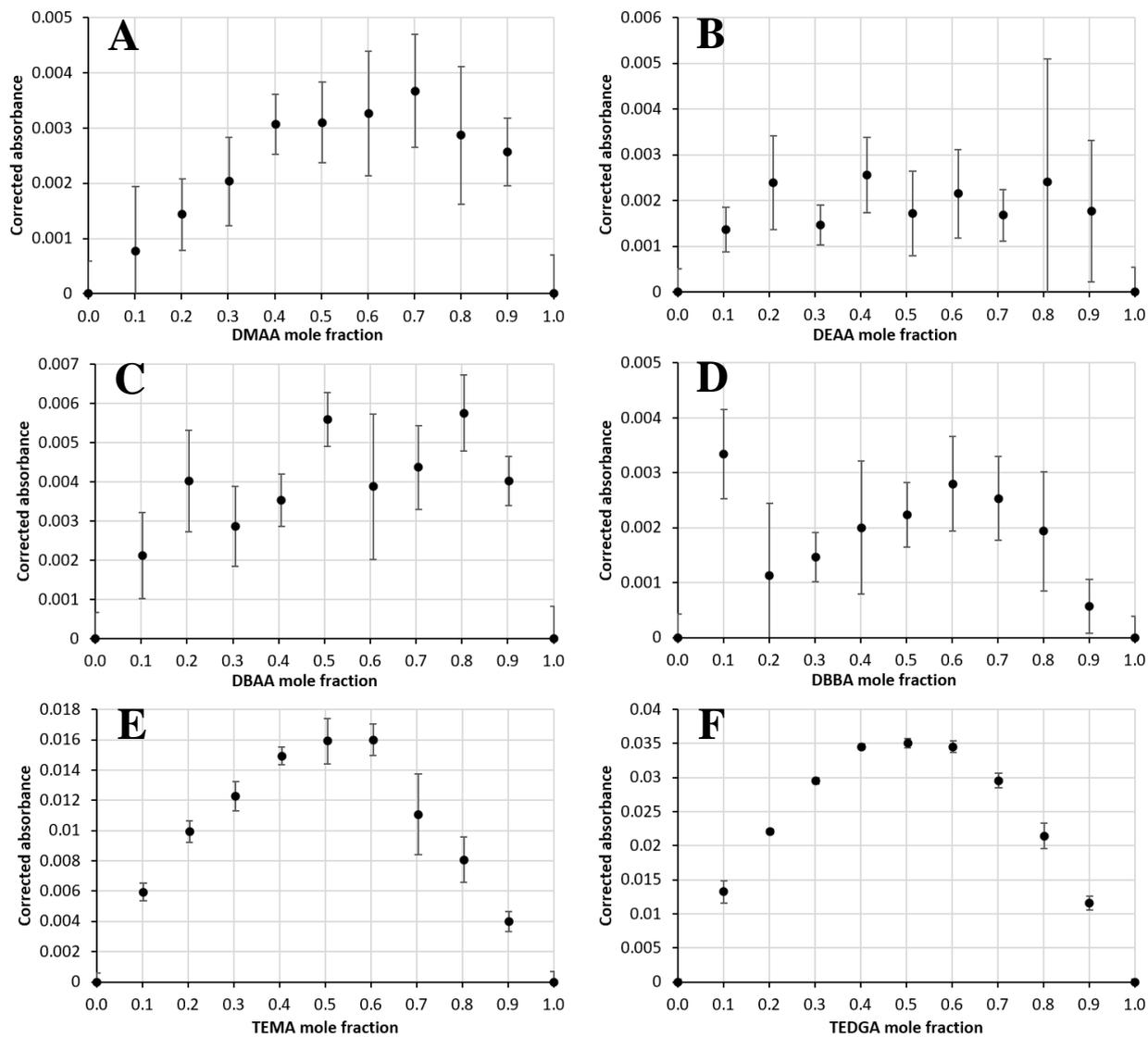
Figure 3.8. *Job plots of tested ligands with uranyl nitrate in diluent A. A) DMAA, B) DEAA, C) DBAA, D) DBBA, E) TEMA, F) TEDGA.*
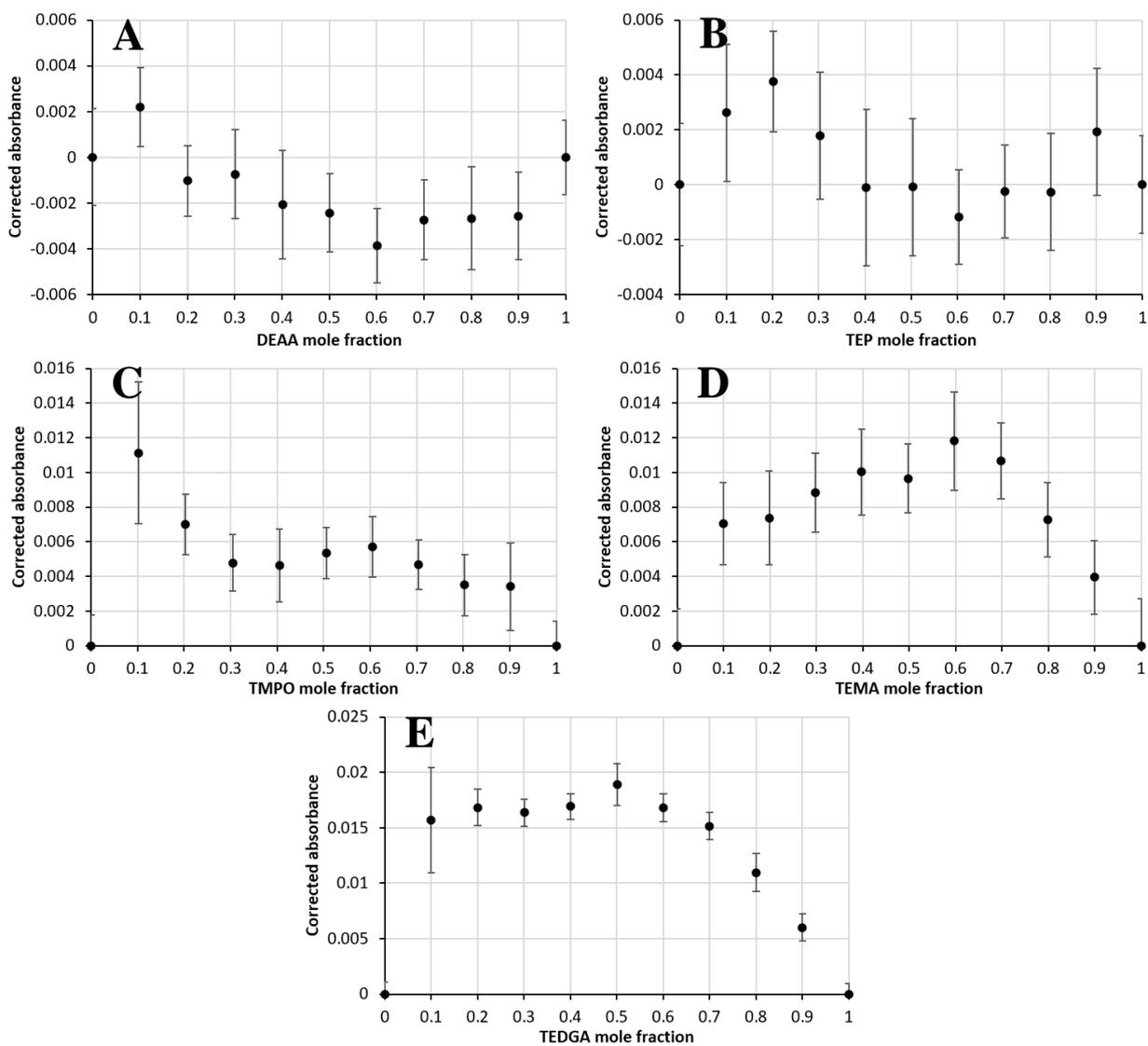
Figure 3.9. *Job plots of tested ligands with uranyl nitrate in diluent B. A) DEAA, B) TEP, C) TMPO, D) TEMA and E) TEDGA.*

Figures 3.10 and 3.11 show the dual-ligand Job plots for the tested monoamide-TEMA and monoamide-TEDGA systems, respectively, with uranyl nitrate in diluent A. Monoamide-TEMA system measurements are much lower than those of the monoamide-TEDGA systems; this indicates a lower concentration of any monoamide-TEMA dual-ligand species. Both tested dual-ligand systems generally peak around 0.6. Similar to the TMPO results, this may indicate that both (monoamide)(TEMA or TEDGA) and (monoamide)$_2$(TEMA or TEDGA) complexes with uranyl nitrate are formed in solution; this is discussed in more detail further into the chapter in Section 3.4.4.

Fig. 3.12 shows the dual-ligand Job plots for the tested DEAA-'second ligand' systems in diluent B. No direct measurements could be made for a DEAA-TEP dual-ligand complex, and no concrete trend could be ascertained from the DEAA-TMPO and DEAA-TEMA Jobs plots. This indicates that monoamides do not form dual-ligand complexes with phosphates, phosphine oxides or diamides in this more hydrophobic diluent. The DEAA-TEDGA Jobs plot still peaks around 0.6 which indicates the formation of the same dual-ligand complexes seen in diluent A for DEAA-TEDGA.
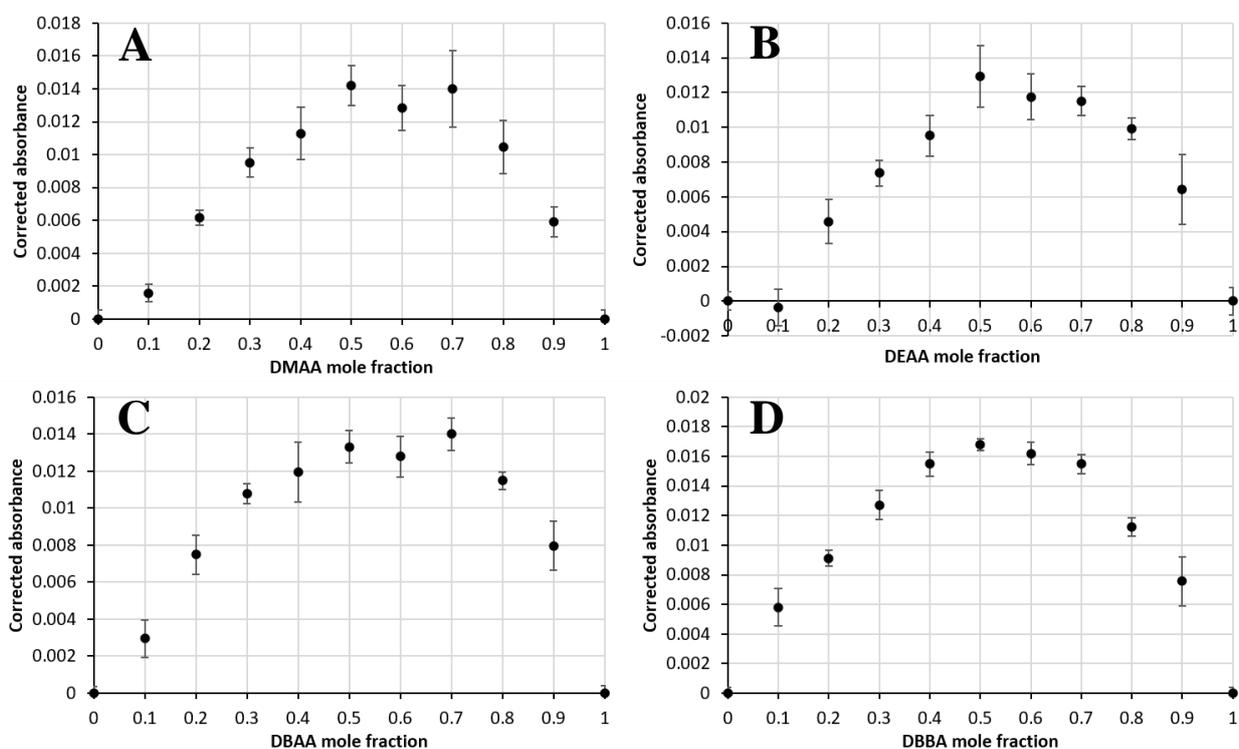
Figure 3.10. *Job plots of tested monoamides with TEMA in diluent A at constant [uranyl nitrate]. A) DMAA, B) DEAA, C) DBAA and D) DBBA.*
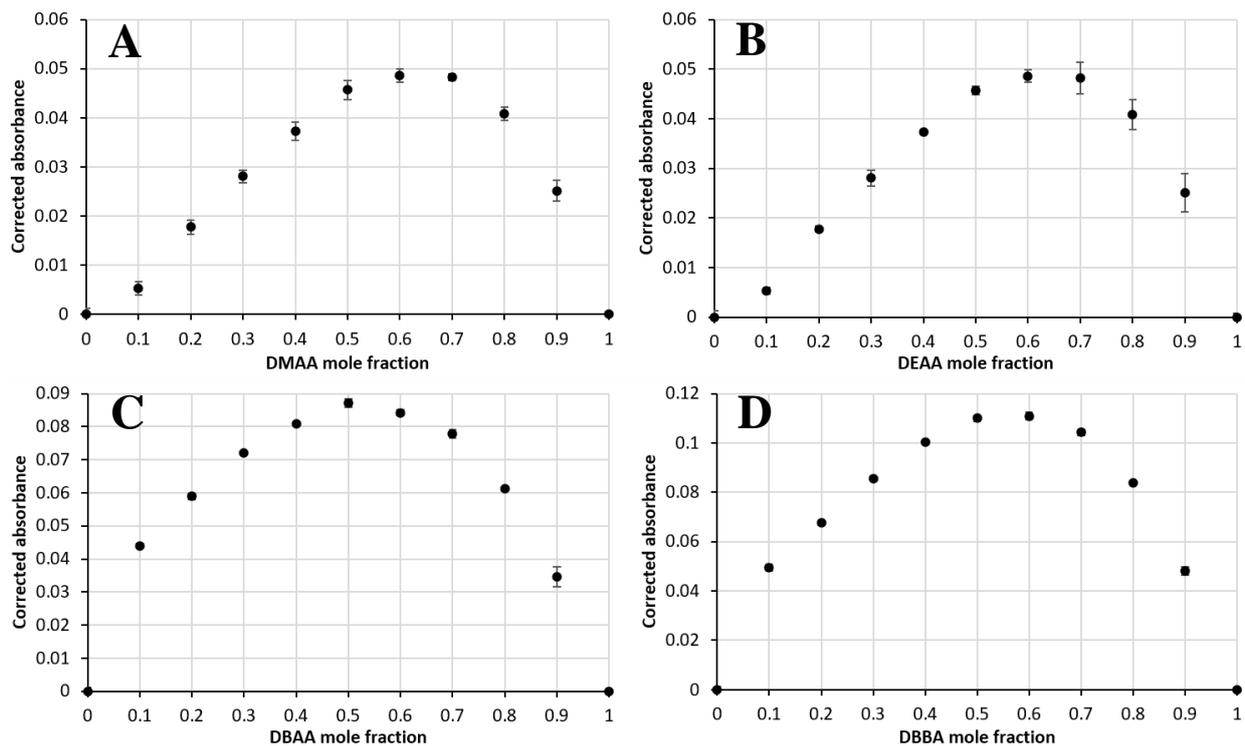
Figure 3.11. *Job plots of tested monoamides with TEDGA in diluent A at constant [uranyl nitrate]. A) DMAA, B) DEAA, C) DBAA and D) DBBA.*
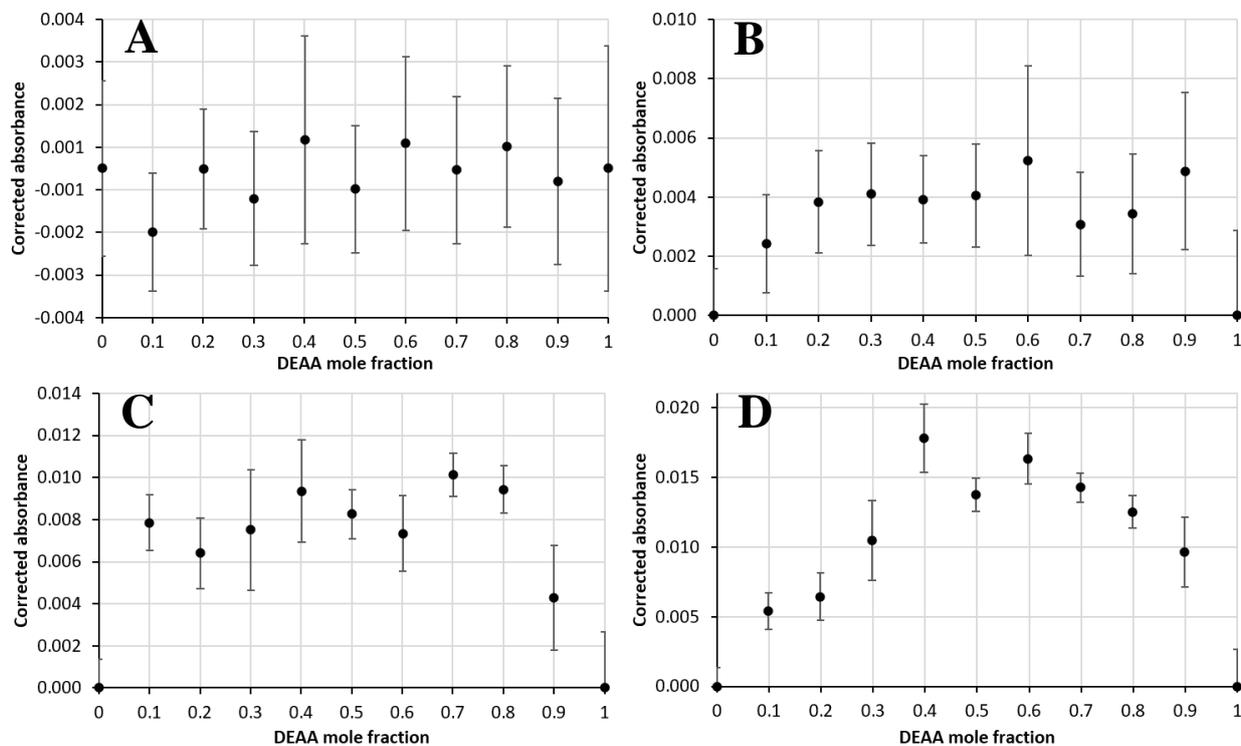
Figure 3.12. *Job plots of tested ligand with DEAA in diluent B at constant [uranyl nitrate]. A) TEP, B) TMPO, C) TEMA and D) TEDGA.*

3.4 Discussion

3.4.1 Uranyl speciation

The absorption spectra of the uranyl cation in aqueous solution depicts a distinct LMCT 'fingerprint' band usually between 350-500 nm (Rabinowitch, 1953). It has previously been reported that the uranyl cation in purely methanolic media exists as a hydrolysed $(UO_2)_2O^{2+}$ dimer shown in Scheme 3.3 (Ogden, et al., 2012). The dimer formation can be inferred from the complete loss of the fingerprint region and peak broadening across the measured absorption range (376-476 nm). In the case of this work, the retention of the distinct fingerprint in the LMCT (~350-500 nm) indicates there is no hydrolysis of the uranyl species in diluent A. In diluent B, the LMCT band loses a large amount of fingerprint detail but is still present. It is unlikely this change indicates hydrolysis and is simply the result of differing solvation environments. This phenomenon is first noted by Jones & Strong (1912) and Jones (1913) who state that the broadened and shifted bands are the result of the superposition of the methanolate and hydrate bands. The molar absorptivities of the observed shoulders in diluent B are also like those reported in literature (Rabinowitch, 1953). This implies that the extracted metal cation can still be treated as a uranyl cation. However, over time, this band broadens similar to the spectra reported by Ogden et al. (2012) which indicates the production of hydrolysed species. To that end, fresh uranium stocks in diluent B were generated prior to tests to ensure all subsequent SQUAD models can consider a single UO_2^{2+} at the centre of the complex.
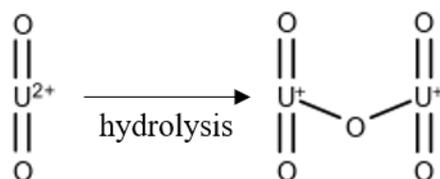
Scheme 3.3. *Structure of the linear uranyl cation and its first hydrolysis product.*

Due to the uranyl cation existing in solution as a linear dioxo cation (Rabinowitch & Belford, 1964b), any bonding is restricted to the equatorial plane. It is unusual for the bonding/coordination number of uranium(VI) to exceed 8; i.e., 6 + 2 from covalently double-bonded oxygens (Cotton, 2006). However, it has been reported that di- and trisolvate uranyl nitrate species are produced with TODGA in acidic

nitric media, potentially indicating the formation of higher coordinated uranium species (Zhu, et al., 2004); (Sasaki, et al., 2001); (Liu, et al., 2015); (Peng, et al., 2017). Therefore, assuming charge neutralisation by two nitrate anions each via at least one oxygen donor, it follows that formed complexes can contain no more than four coordination bonds from adduct-forming ligands. To this end, this was the limiting factor for models considered within SQUAD.

3.4.2 Single-ligand complex speciation and stability in diluent A

Monoamide complexes in diluent A (Figure 3.4 A-D) all produce very similar responses in the UV-vis absorption spectra; a slight bathochromic shifting of the peaks, apparent loss in vibrational coupling and the potential production of at least one isosbestic point at longer wavelengths. As only one set of new peaks appear to be arising, this indicates that only one complex is formed in solution. The isosbestic points observed in the monoamide spectra are good evidence that at least two absorbing (i.e. metallic) species are present in solution (Smith, 2010); this includes the uranyl cation. The best fitting model indicates that only a disolvate complex is produced as shown in Table 3.3. It appears that a disolvate complex is strongly preferred over a potential monosolvate complex even when ligand concentration is less than uranyl concentration. These findings correlate with many studies that use slope analysis to determine complex stoichiometry (Gupta, et al., 2000a); (Gupta, et al., 2000b); (Pathak, et al., 2001); (Prabhu, et al., 1997). They also correlate with more recent structural and spectroscopic studies of uranyl-monoamide complexes (Loubert, et al., 2017); (Verma, et al., 2018), as well as previous spectrophotometric studies with hexavalent actinides at $[HNO_3] < 4$ M (Condamines & Musikas, 1992); (McCann, et al., 2018).

It is difficult to infer any kind of trend for the U-monoamide Job plots (Figure 3.8 A-D). Due to the relatively small amount of measurable interaction, even small amounts of error dominate any perceivable trend in the data. There is no discernible trend in UO_2-monoamide stability constant as the amine-side chain increases in size. However, it is observed that increasing the carbonyl-side chain slightly increases stability. The larger carbonyl-side chain likely provides stability to the amide bond, resulting in a larger donor strength from the carbonyl oxygen. The stability constants determined by

SQUAD are comparable to those determined by Prabhu et al. (1997), which lends validity to the SQUAD methodology for constant determination.

The SPT results for TEMA in diluent A (Figure 3.4E) indicate that diamide interactions with the uranyl cation are similar to those of monoamide interactions; however, there are significant differences. The more significant bathochromic shifting of the peaks indicates the formation of more stable species; this is inferred by the species absorbing a lower energy photon. Like the monoamides, the nature of the peak shift indicates that only one complex is formed in solution. Modelling shows the most likely scenario is the formation of the disolvate complex, as seen in Table 3.3. This agrees with the similar monoamide spectra previously discussed, and also with previous literature (Ruikar & Nagar, 1995). The higher stability of the diamide complex comes from the bidentate nature of the ligands. It should be noted that monosolvate models were also seen to be possible but are less likely due to larger amounts of error in the stability constant and molar absorptivities. The Job plot of TEMA and uranyl nitrate is inconclusive; when taking error into account, it could be argued that a peak lies at either 0.5 or 0.67. Considering all data, it seems most likely that a disolvate complex is the only species formed in solution in this diluent. Sterically speaking, it cannot be expected that this disolvate species can form dual-ligand complexes with monoamides due to the higher stability constant reported for diamides.

Initially in the spectrophotometric results for TEDGA, the fingerprint is maintained with a large increase in molar absorptivity. As [metal]:[ligand] ratio increases, peak broadening and significant bathochromic shifting is observed. While this could be a sign uranyl hydrolysis, SQUAD modelling revealed it may be the formation of di- and tetrasolvate complexes. The molar absorptivities indicate that these species both have broadened spectral peaks. This could possibly be due to Jahn-Teller distortions; this implies that fitting these ligands around the metal centre distorts the bond length of the double bonded oxygens. This would cause band splitting which ultimately results in a peak broadening effect when the spectra are superimposed. The $\log_{10}(K_{101})$ and $\log_{10}(K_{102})$ values reported in Table 3.3 are roughly twice as large as those reported for the linear NpO_2^+ with tetramethyl diglycolamide (Rao & Tian, 2010). This difference is likely due to the larger formal charge on the uranyl cation.

The Job plot of TEDGA and uranyl nitrate definitively shows the dominant solution complex is a monosolvate species which is a good sign from a steric perspective; this is the only TEDGA complex that could reasonably form dual-ligand complexes with monoamides. Literature reports many uranyl-diglycolamide species in solution dependent on different conditions. Mono- and disolvate species have been found to be dominant in polar solvents at high and low nitric acid concentration respectively by slope analysis of solvent extraction distribution plots (Sasaki, et al., 2015). Di- and trisolvate species have been reported for non-polar solvents; these were also determined by slope analysis (Sasaki, et al., 2015); (Sasaki, et al., 2013); (Liu, et al., 2015); (Peng, et al., 2017). However, Liu et al. (2015) and Peng et al. (2017) make no mention of organic phase pre-equilibration with nitric acid so their stoichiometry data may be inaccurate. All models tested with a trisolvate complex with the present data resulted in large amounts of error. As such, it was decided that these results likely do not suggest the presence of a trisolvate complex with TEDGA. Due to the oversimplified nature of the slope analysis method, it is entirely possible that the literature gradient was due to a mixture of diglycolamide species, such as the range of species reported in the present work, rather than a definitive trisolvate complex.

A spectroscopic study into uranyl-TODGA speciation concluded that the mono- and disolvate species were the two species formed in conventional extraction systems in 1,2-dichloroethane (Boltoeva, et al., 2018). The former was found to be the only species formed at high acidity (5 M HNO_3), whereas a mixture of species was found at low acidity (1 M HNO_3). The monosolvate species was also found to have both a bidentate and monodentate nitrate anion associated with the metal centre. It is therefore not inconceivable that, as acidity reduces to that of the present work, a tetrasolvate species with monodentate nitrate ligands is possible.

3.4.3 Single-ligand complex speciation and stability in diluent B

As the media becomes more hydrophobic, monoamides do not behave significantly differently (Figure 3.5A). Similar spectral responses were observed at a lower resolution due to the lower concentrations of uranyl cations and ligands. The modelling indicates similar strength complexes are generated. Molar absorptivities of the produced disolvate complex are similar to that previously seen in diluent A. Again, it seems the monosolvate complex is not generated prior to the disolvate, or perhaps its detection is

beyond the limits of the SQUAD software. Due to the small absorbance changes observed, the Job plot of DEAA and uranyl nitrate is dominated by error (Figure 3.9A) which is similar to that seen in diluent A.

TEP complexation with uranyl nitrate results in very similar spectral changes as the monoamide (Figure 3.5B); this is more clearly seen by comparing the molar absorptivity spectra (Figure 3.7). The similarity in spectral behaviour support the inference that both of these ligands behave in a similar manner with respect to uranyl binding. Again, due to the small absorption changes in the measured spectra, the Job plot of TEP with uranyl nitrate is dominated by uncertainty. It is likely that the small absorption changes could be indicative of the coordination environment of the uranyl cation in both the monoamide and phosphate systems. The uranyl cation sees exceptionally symmetrical binding along the equatorial plane from the disolvate species, leading to very small changes to the LMCT band. The one major difference between the monoamide and phosphate systems is the stability of the produced complex; the disolvate stability constant for the phosphate complex is markedly higher than that of the monoamide, which explains why phosphates generally have better uranyl extraction performance in SX systems.

TMPO, TEMA and TEDGA complexation results in the regeneration of the distinctive spectral fingerprint (Figure 3.5C, D and E, respectively). It could be that the polar nature of these complexes results in a higher solvation of water from the diluent than the uranyl cation initially had in diluent B, negating the broadening effect that the higher methanol content had. This theory is supported by the peaks in the molar absorptivities of these complexes shifting to lower wavelengths, towards that of uranyl species in diluent A. This theory is based on the findings of Jones & Strong (1910) reported by Rabinowitch (1953); they found that as little as 8% water in a solution of uranyl chloride in methanol produced absorption bands similar to aqueous solution. The total water content of the diluent B tests is 4.5 vol%, which is why both methanolate and hydrate absorption bands are observed in the uranyl nitrate spectrum (and superimposed resulting in apparent peak broadening). TMPO, TEMA, and TEDGA are all either strong donors or multidentate ligands. The polar centre of complexes formed with these ligands may result in an environment that is more favourably solvated by water, leading to a higher concentration of water around the uranyl cation and resulting in spectra alluding to a hydrated system.

All three of the above ligands form mono- and disolvate complexes. TMPO and TEDGA both appear to prefer the monosolvate complex, as seen in Appendix A, and the Job plot for TEDGA and uranyl nitrate agrees with this. The Job plot of TMPO with uranyl nitrate shows there are much more complicated interactions occurring in solution beyond complex formation. Even when considering experimental error, there is a clear peak around 0.1 mole fraction TMPO. Clearly a complex of this stoichiometry could not be generated in solution and could instead point towards aggregation. Aside from this feature, the peak around 0.6 suggests that either a '203' species is formed (two uranyl cations with zero protons and three solvating ligands), or both a mono- and disolvate species are formed. MODSQUAD modelling suggests the latter is far more likely; a model containing mono- and disolvate species converged whereas a '203' species did not. That said, it is surprising that the SQUAD model reports the monosolvate TMPO species to be so dominant in pseudo-aqueous solutions (as seen in Appendix A) given that extraction studies generally report phosphine oxides to have a dominant disolvate complex (Laskorin, et al., 1970); (Breshears, et al., 2015). This could be an effect of the diluent and the difference between one-phase and two-phase systems. To that end, phosphine oxides have been incorporated into the later solvent extraction tests to determine if this behaviour carries forward into uranyl extraction.

Modelling indicates that TEMA produces both the mono- and disolvate species in the more hydrophobic diluent. This is backed up by the Job plot of TEMA with uranyl nitrate which peaks around 0.6, like that of TMPO. It seems that the differing solvation environment of the uranyl cation facilitates the formation of the monosolvate complex which is not seen in diluent A. The monosolvate species has been shown to exist in a crystallographic study investigating how the change in carbon chain between carbonyl bonds affects uranyl nitrate complexation (Wahu, et al., 2012). In the case of TEMA, it was found that the uranyl centre was complexed by two bidentate nitrate anions and a single chelating bidentate TEMA molecule. In the present study, while this complex appears relatively prevalent at low [metal]:[ligand] ratios (Appendix A), the abundance of the disolvate complex quickly overtakes the monosolvate as [metal]:[ligand] ratios increase. Therefore, it could be that in high uranyl loading systems, the monosolvate complex dominates, but in most extraction cases the ligand will be in excess.

Sterically speaking, the monosolvate species should be prone to forming dual-ligand complexes with monoamides, but the same cannot be expected for the disolvate complex.

It appears the tetrasolvate TEDGA complex previously seen in diluent A is not generated in diluent B. Due to the more hydrophobic nature of diluent B, the polar high order tetrasolvate complex does not form. Mono- and disolvate complexes are still formed in diluent B. The monosolvate species looks very stable compared with other ligands, and this species is seen to be dominant from the TEDGA and uranyl nitrate Job plot. It seems the diluent has little effect on the dominating complex and is promising for dual-ligand complexes with monoamides.

3.4.4 Dual-ligand complex speciation in diluent A

Figures 3.10 and 3.11 were conducted with the aim of determining the ratio of monoamide to diamide/diglycolamide in any dual-ligand uranyl complexes in diluent A. It should be noted that the diglycolamide solutions used for the Job plot tests already contain multiple uranyl species, as is evident from Appendix A. This immediately arises as a source of error when correcting for the effect of the initial and final complexes in solution from purely a dual-ligand perspective. To correct these figures, a straight line was drawn from monoamide mole fraction = 0 and 1.0 and this was taken to be the baseline. While total ligand concentration remained constant throughout the test, the changing concentrations of each individual ligand may cause a change in complex speciation. This may mean taking a linear baseline lends some inaccuracy; however, it is suitable to use as a good approximation of the solution chemistry.

The low absorption changes in the monoamide-diamide Job plots (Figure 3.10) indicate there is little mixed interaction between the uranyl cation and both ligands. It appears the uranyl centre prefers to bond with either the monoamide or the diamide. This is not entirely unexpected given that the most likely TEMA species in solution in this diluent is the disolvate complex. In order to form a dual-ligand species, one TEMA molecule would have to be replaced with one monoamide, switching from a bidentate ligand to a monodentate one. As per the stability constants in Table 3.3, this would result in a less stable complex, so it is unlikely to form. Isosbestic points were observed in the Job plot spectra of

DBAA-TEMA and DBBA-TEMA, indicating the presence of multiple uranyl species; likely the disolvate complex of both the mono- and diamide. Absorption generally peaks at a TEMA mole fraction of 0.5 indicating the formation of a (monoamide)(diamide) complex with uranyl nitrate. This species is certainly possible from a steric perspective, but this complex either relies on either i) the addition of a monoamide molecule to a monosolvate diamide complex which is not shown to exist in this diluent, or ii) the substitution of a monoamide from a disolvate monoamide complex. The latter scenario means that a monosolvate monoamide complex has to be created as an intermediate which is not seen in the single-ligand tests. These points and the small amount of absorption in Figure 3.10 suggest that this species is in relatively low concentration.

The monoamide-diglycolamide Job plots shown in Figure 3.11 indicate that this system is much more complex than the monoamide-diamide system. The relatively large increases in absorption immediately indicate the presence of dual-ligand complexes. As monoamide size increases, an increased absorbance change is observed which indicates an increase in complex concentration, inferring greater stability. Absorbance peaks at 0.5 mole fraction of monoamide for the DBAA-TEDGA system which indicates the formation of a (monoamide)(diglycolamide) complex. However, the other three tested systems all clearly peak between 0.6 – 0.7 mole fraction of monoamide. Similar observations were made for the single ligand Job plot of uranyl nitrate with TMPO, so similar conclusions can be drawn. They either mean the predominant uranyl complex in solution is (monoamide)$_3$(diglycolamide)$_2$, or there is a mixture of (monoamide)(diglycolamide) and (monoamide)$_2$(diglycolamide) species. From a steric perspective, it can be argued that the latter scenario is much more likely because fitting five ligands around the uranyl cation would not be possible. This also follows from the results of the uranyl nitrate and TEDGA Job plot, which found the monosolvate diglycolamide species to be the dominant complex in solution. Nitrate anions are likely bidentate in the monosolvate TEDGA complex, but the addition of one or two monoamides would most likely cause one or both nitrates to become monodentate ligands, respectively. Monodentate nitrates have been observed in uranyl-TEDGA complexes before (Boltoeva, et al., 2018).

It appears that the stoichiometry of the dual ligand complex is not based on the stability of the single ligand complexes; if it were, it would be expected that DMAA-TEDGA systems would solely produce (DMAA)(TEDGA) complexes; this is not seen in the data. Nevertheless, it appears that dual-ligand species are present in solution in these systems, and the difference in speciation would undoubtedly result in a change in complex hydrophobicity.

3.4.5 Dual-ligand complex speciation in diluent B

As the diluent becomes more hydrophobic, it becomes increasingly difficult to determine whether there are interactions with monoamide-diamide systems. There is no particular trend in the Job plot that would infer any kind of dominating species (Figure 3.12C). The relatively flat nature of the Job plot could infer that there is a systematic error for this system in the crude baseline correction step of calculating corrected absorbance in the dual-ligand Job plots. This assumption relies on species concentrations being proportional throughout the Job plot which may not be the case. The presence of the extra monosolvate TEMA species may complicate this step when compared with the diluent A dual-ligand Job plot. So, similar to the conclusion drawn in diluent A, it appears that the uranyl cation prefers to bond only with either the monoamide or the diamide in diluent B. This is not entirely surprising given that the dominant TEMA species in solution is disolvate, leaving little room around the metal centre for monoamide complexation. In diluent B, monoamide substitution of a diamide molecule is even less unlikely owing to the much higher stability of the disolvate diamide complex.

Monoamide-diglycolamide behaviour does not appear to change as the diluent becomes more hydrophobic (Figure 3.12D); absorbance still peaks around 0.6 mole fraction of monoamide if the outlier point at 0.4 mole fraction is disregarded. Again, this likely points to the formation of (monoamide)(diglycolamide) and (monoamide)$_2$(diglycolamide) species likely for the same reasons outlined for diluent A. The results for the monoamide-phosphate Job plot indicate that there is zero observable dual-ligand interaction occurring in solution with the uranyl cation (Figure 3.12A). This may be expected as the $\log_{10}(K_{102})$ for the uranyl-nitrate-TEP complex is roughly 20% higher than that of DEAA in diluent B. However, as previously discussed, this may be a symptom of the lack of absorption associated with both of these ligands and the uranyl cation; it appears that these monodentate

ligands struggle to produce spectral changes which can be qualitatively discussed. SQUAD modelling has shown that these relatively unchanging spectra indicate stable monoamide and phosphate complexes. Therefore, it can be determined from the monoamide-phosphate Job plot that either: i) there is zero observable interaction between these ligands and the metal centre, ii) there are dual ligand complexes forming, but they are undetectable with the current experimental set up, or iii) there are dual-ligand interactions, but not necessarily complexation. The true outcome can be tested by SX Job plot methodology where uranium distribution can be used to determine speciation rather than direct measurement of complex absorption. The latter two points consider outer sphere complexation or interactions that may help a ligand act as a phase transfer catalyst; systems where a ligand helps a complex pass through a phase boundary or remain in a phase.

The results for the monoamide-phosphine oxide Job plot (Figure 3.12B) are similar to that of the monoamide-diamide; there appears to be no trend that would indicate a dual-ligand species. The flat line may again indicate a slight systematic error in the baseline correction of the Job plot. It is expected that there would be some measurable spectral change in the Job plot given the changes observed in the TMPO SPT. This means that the discussion points raised for the monoamide-phosphate Job plot cannot be applied here. SQUAD modelling revealed that the monosolvate TMPO complex was far more dominant than the disolvate, which should be susceptible to the generation of a dual-ligand complex; however, that does not mean that one will form. It may be that the monosolvate TMPO complex is particularly stable in diluent B, however, no literature support on monosolvate phosphine oxide complexes or phosphine oxide complexes in methanol could be found. The results ascertaining to uranyl complexation by TMPO remain inconclusive, so these systems have been taken forward to solvent extraction tests.

3.5   Conclusions

Monoamides have been studied as potential replacements for TBP in nuclear fuel reprocessing towards the goal of a more sustainable and economic process. However, monoamides generally suffer poorer uranium extraction performance than TBP due to the poorer organic solubility of the uranyl-nitrate-monoamide complex. It is hypothesised that the addition of other adduct forming ligands (such as

diamides, diglycolamides, phosphates and phosphine oxides) into monoamide extraction systems will form new, ternary complexes with higher hydrophobicity which will enhance the performance of these monoamide systems and allow movement towards reducing or eliminating phosphorus in reprocessing. As there is little information in the literature associated with interactions between monoamides with amide- and organophosphorus-based ligands, this work investigates the interactions between monoamides with diamides, diglycolamides, phosphates and phosphine oxides with UO_2^{2+} in in two types of pseudo-aqueous media to determine whether the desired ternary complexes are generated. The effect of changing the monoamide structure on these interactions was also investigated.

In the more hydrophilic media, monoamides were confirmed to produce disolvate complexes with the uranyl cation, and diamides followed this trend. Diglycolamides were seen to produce multiple species of uranyl complexes, up to tetrasolvate, leading to more complex solution chemistry than previously thought. While diamides have similar complex behaviour to monoamides, Job plots suggest that the uranyl cation strongly prefers to bond exclusively with only monoamide or diamide species regardless of monoamide structure; however, a (monoamide)(diamide) species may be present in solution. Diglycolamides were shown to produce stronger complexes with UO_2 than monoamides. However, Job plots suggest that multiple dual-ligand species are produced in UO_2-monoamide-diglycolamide systems, with no clear indication on the dominant species in solution. It is likely both (monoamide)(diglycolamide) and (monoamide)$_2$(diglycolamide) species are produced.

In the more hydrophobic media, stability constants were seen to be slightly higher. Monoamide speciation was the same. Diamides were shown to also form monosolvate complexes, but monoamide-diamide complexes were no longer observed with the uranyl cation. The tetrasolvate diglycolamide complex is no longer generated. This is likely due to the decreased dielectric constant of the media. (Monoamide)(diglycolamide) and (monoamide)$_2$(diglycolamide) species were still shown to be formed in this media. Phosphates were seen to behave like monoamides but generate stronger complexes. Job plots on dual-ligand interactions were inconclusive. Phosphine oxides were reported to generate a monosolvate complex as the dominant species, which goes against that reported in the literature. Job plots did not infer dual-ligand interactions with monoamides.

Based on the data discussed in this chapter, the systems to be taken forward to solvent extraction tests are monoamide-diglycolamide, monoamide-phosphate and monoamide-phosphine oxide. Monoamide-diglycolamide systems have been selected due to the positive results found for the presence of dual-ligand complexes. The (monoamide)(diglycolamide) and (monoamide)$_2$(diglycolamide) uranyl species may be exploitable in a SX setting by changing complex hydrophobicity and increasing solubility of monoamide complexes. Monoamide-phosphate systems have been selected to test whether the current spectrophotometric methodology was unable to identify dual-ligand interactions. The lack of any measurable interaction may not indicate the lack of a generated complex in this case. This is evidenced by the SQUAD modelling of single-ligand complexes based on very little measurable change in absorbance. Therefore, sub-hypotheses 2 and 3 concerning monoamide-diglycolamide and monoamide-phosphate dual-ligand synergic systems are taken forward for further testing.

Monoamide-phosphine oxide systems were initially selected for further investigation into why the present data goes against the reported consensus on phosphine oxide complexes. The present data strongly indicates that monosolvate TMPO complexes are dominant which are feasibly prone to dual-ligand complex formation with the uranyl cation. This is not seen in the dual-ligand Job plots, so further data was advised to underpin what is occurring in solution. However, SX tests with trioctylphosphine oxide also gave inconclusive data due to consistent quantitative extraction of uranium. This is discussed further in Chapter 4. Monoamide-diamide systems have not been selected due to the low interaction seen in the diluent A tests, and the lack of interaction seen in the diluent B tests. Dual-ligand complexes should have been observable with these systems so it has been determined that these systems should not be carried forward. Therefore, sub-hypotheses 1 and 5 concerning monoamide-diamide and monoamide-phosphine oxide dual-ligand synergic systems can be considered tested and found to be incorrect.

CHAPTER 4   Solvent Extraction of Uranyl Nitrate with Single-Ligand Systems

The aims of this chapter are to confirm the synergistic effects of the monoamide-diglycolamide, and monoamide-phosphate systems proposed from Chapter 3 and to determine the likely extraction mechanisms of these solvents. Within this, the objectives are to:

1. Understand the solvent extraction (SX) behaviour of single-ligand systems.

2. Conduct slope analysis to determine extraction mechanisms of the single-ligand systems.

3. Use single-ligand extraction data and dual-ligand Jobs plots to assess synergic effects and likely extraction mechanisms of dual-ligand solvents.

4. Identify suitable dual-ligand solvents to carry forward for further SX testing.

To that end, this chapter works towards testing sub-hypotheses 2, 3 and 4 in Section 1.3.

4.1   Introduction

To maximise the usage of finite uranium sources on Earth, the nuclear power industry requires sustainable and economic spent nuclear fuel (SNF) reprocessing options. Current reprocessing flowsheets use tri-n-butyl phosphate (TBP) to extract uranium(VI) and plutonium(IV) from nitric acid solutions (Phillips, 1992). During this operation, TBP degrades under radiolysis and hydrolysis to form acidic phosphates. These degradation products, as well as TBP itself, can extract undesired metals into the organic phase which reduce uranium(VI) and plutonium(IV) separation factors and therefore requires extra process steps to achieve the required product purity (Alcock, et al., 1957); (Sugai, et al., 1992); (Zilberman, et al., 2003); (Herbst, et al., 2011d). The presence of phosphate also complicates waste disposal as degraded solvent incineration forms secondary phosphate wastes (Todd, et al., 2000). The removal of the extra process steps and secondary wastes will help reduce costs and make the process more economically viable.

Monoamides have been studied as potential replacements for TBP in nuclear fuel reprocessing since the 1960's (Siddall, 1960) due to their numerous benefits over TBP. Firstly, they have much higher separation factors for uranium and plutonium with common fission product contaminants such as Zr(IV)

and RuNO(III) which will increase product stream purity (Gasparini & Grossi, 1986); (Manchanda, et al., 2001); (Kulkarni, et al., 2006). Secondly, degradation products of monoamides are generally carboxylic acids, ketones and disubstituted amines; these have little to no effect on separation factors of uranium and plutonium (Kulkarni, et al., 2006); (Parikh, et al., 2009). Thirdly, they adhere to the CHON principle which means any degraded solvent can be completely incinerated to leave a non-phosphate residue and reduce secondary waste streams. Many studies cited above and in Chapter 2 look into different monoamide performances; these reveal that *N,N*-dihexyl octanamide (DHOA) performs the best. However, while monoamides are excellent extractants for plutonium(IV), poorer extraction yield of uranium(VI) limits the industrial applications of monoamides (Manchanda, et al., 2001); (Manchanda & Pathak, 2004); this has been attributed to poor organic phase solubility of the uranyl-nitrate-monoamide complex (Musikas, 1987). There are two ways to improve this solubility: i) modify the organic phase to increase complex solubility by increasing its polarity without causing third phase formation, or ii) modify the extracted complex by introducing a synergic ligand into the monoamide reaction scheme. Monoamides and phosphates have both been previously used as phase modifiers in diglycolamide systems that look to recover trivalent lanthanides and actinides (Tachimori, et al., 2002); (Sasaki, et al., 2005); (Ansari, et al., 2009); (Raut & Mohapatra, 2013), so it follows that phosphates may act as phase modifiers in a monoamide extraction scheme. This will not eliminate secondary phosphorus waste, but it will reduce it.

Diglycolamides, such as *N,N,N',N'*-tetraoctyl diglycolamide (TODGA), have been used for uranium(VI) extraction and have been shown to form monosolvate species both in literature (Ren, et al., 2017); (Boltoeva, et al., 2018) and previously in Chapter 3. Although, higher solvate species have also been reported which would have a direct impact on uptake capacity (Sasaki, et al., 2013); (Sasaki, et al., 2015); (Liu, et al., 2015); (Peng, et al., 2017). From a steric perspective, this monosolvate complex is vulnerable to further complexation with a monoamide which would produce a far more hydrophobic species that should be more soluble in an organic phase. The formation of (monoamide)(diglycolamide) and (monoamide)$_2$(diglycolamide) dual-ligand complexes were observed in pseudo-aqueous media in Chapter 3, but these species have not been reported in a SX setting. It is also possible that a dual-ligand

monoamide-phosphate complex is formed. Data from Chapter 3 was inconclusive, so SX distribution data will be used to underpin the mechanistic behaviour occurring in solution.

Following from Chapter 3, the aim of this work was to assess the synergistic behaviour of monoamide-diglycolamide and monoamide-phosphate solvents using DHOA, TBP and TODGA (Scheme 4.1). In order to fully explain dual-ligand behaviour, single-ligand extraction behaviour must first be defined. Therefore, extraction mechanisms for uranyl nitrate and nitric acid from acidic nitric media using DHOA, TBP and TODGA are investigated. The influence of acidity, initial ligand concentrations, initial uranium concentration and influence of nitrate concentration on uranyl nitrate extraction were investigated to determine reaction mechanisms. Slope analysis was employed to determine stoichiometric values. Jobs plots of DHOA-TBP and DHOA-TODGA systems were conducted to confirm whether these mixtures form synergic SX systems and compared with the findings of Chapter 3. Confirmed synergic systems were carried forward into Chapter 5 to fully assess the performance of dual-ligand systems and the data for the single-ligand systems presented in this chapter are required to fully describe dual-ligand performance. DHOA and TBP system data are compared with the several published studies on these extraction mechanisms and contradictions with these studies are explored. The current literature on uranyl extraction with TODGA appears divided, particularly on complex speciation, so this work will add to the current literature on TODGA-uranium(VI) interactions in acidic nitrate media.
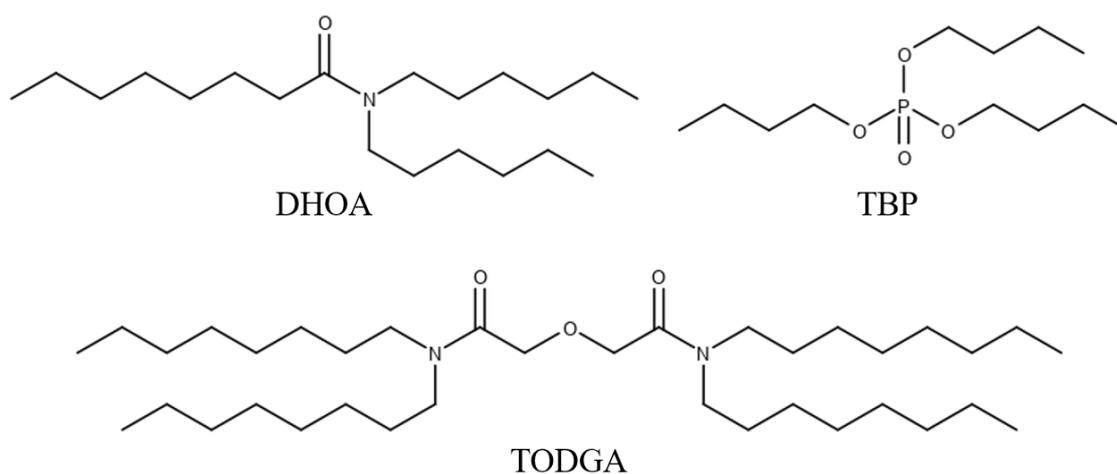
Scheme 4.1. *Chemical structure of the ligands used in this SX study: DHOA, TBP, and TODGA.*

The intriguing data for phosphine oxide systems in Chapter 3 also led the author to assess TOPO behaviour. However, due to extremely high uranium extraction and the requirement for a more polar organic diluent, attempts to underpin phosphine oxide mechanisms were unsuccessful. The data are available in Appendix B in the hope it may be valuable to some readers of this thesis.

4.2   Experimental Method and Materials

All reagents were ACS reagent grade or higher purity. Nitric acid (70%, Merck), sodium hydroxide solution (50%, Sigma Aldrich), *n*-dodecane (99%, Acros Organics), TBP (99%, Acros Organics) and sodium nitrate (99%, Sigma Aldrich) were used as received. Uranyl nitrate hexahydrate was supplied by the Immobilisation Science Laboratory at Sheffield University and was dissolved in pH 1 nitric acid to generate a concentrated mother solution of uranyl nitrate. Aliquots from this solution were used to generate uranyl nitrate working solutions in required nitric acid concentrations. All aliquots were taken from the same mother solution, and it was assumed that uranium concentration of the mother solution (and subsequent initial working solutions) remained constant throughout the work. Ligand solutions were prepared by diluting the required mass of ligand with *n*-dodecane diluent.

4.2.1   Ligand Synthesis

DHOA was synthesised through the reaction of octanoyl chloride (98%, Alfa Aesar) with equimolar dihexylamine (99.5%, Sigma-Aldrich) in chloroform under a nitrogen atmosphere. This was carried out in the presence of equimolar triethylamine base (99%, Acros Organics) in a stirred ice bath (Thiollet & Musikas, 1989). The solution was then heated to reflux at the boiling point of the mixture, around 71℃, for at least two hours. The organic product was washed with deionised water (DI), 10wt% Na_2CO_3 solution, 1.2 M HCl solution and a final DI wash. The organic layer was dried over anhydrous Mg_2SO_4, filtered, and the solvent was removed under reduced pressure. DHOA was consistently >96% pure and yields were generally 43-49%. DHOA ^{1}H NMR data is shown in Table 4.1.

Table 4.1. *^{1}H NMR (500 MHz, CDCl[3]) chemical shifts for DHOA. Structure labels indicate atom and position (e.g. H2 = proton group identified at chemical shift position 2 for ^{1}H).*

Position	^1H δ	DHOA Structure
1	3.10 & 3.18 (dt, 4H)	
2	2.17 (t, 2H)	
3	1.41 & 1.53 (dt, 6H)	
4	1.19 (m, 20H)	
5	0.77 (m, 9H)	

TODGA was synthesised by collaborators at Northumbria University by the following method. Diglycolic acid was dissolved in thionyl chloride and the mixture was heated under reflux for 24 hours. The flask was allowed to cool, and the resulting clear solution was evaporated. The residue was dissolved in dichloromethane, cooled to 0°C using an ice-bath and a solution of dioctylamine and triethylamine in dichloromethane was slowly added dropwise. The solution was allowed to warm to room temperature and stirring was continued for 24 hours. The insoluble solid was filtered and the filtrate was washed sequentially with 1 M hydrochloric acid and sodium hydrogen carbonate before being dried over anhydrous magnesium sulfate, filtered, and evaporated to produce crude TODGA as a clear liquid. The crude product was dissolved in diethyl ether and the solution was washed with 1 M hydrochloric acid. The insoluble solid that formed in the organic phase (dioctylammonium chloride salt) after each washing was filtered and washed with diethyl ether until no more solid formation was visible. The solution was washed with 1 M sodium hydroxide and then dried over anhydrous magnesium sulfate, filtered, and evaporated to afford TODGA as a clear, yellow oil at a 77% yield.

4.2.2   General SX Procedure

All acids were standardised by titration against standardised NaOH using a Mettler-Toledo Titrator Excellence T7 auto-titrator. NaOH solutions were standardised by titration against a known mass of anhydrous potassium hydrogen phthalate (usually 2 g) dissolved in 40 mL DI using the same equipment.

All SX tests were conducted triplicate at room temperature (20 ± 2 °C). 0.5 mL of an organic phase was contacted with 0.5 mL of an aqueous phase in a 5 mL glass scintillation vial and shaken for 5 minutes. 1 minute shaking time was found to be sufficient to reach equilibrium with DHOA and TBP (Figure 4.1). 5 minutes was used as a precaution in case future tested ligands required more contact time.
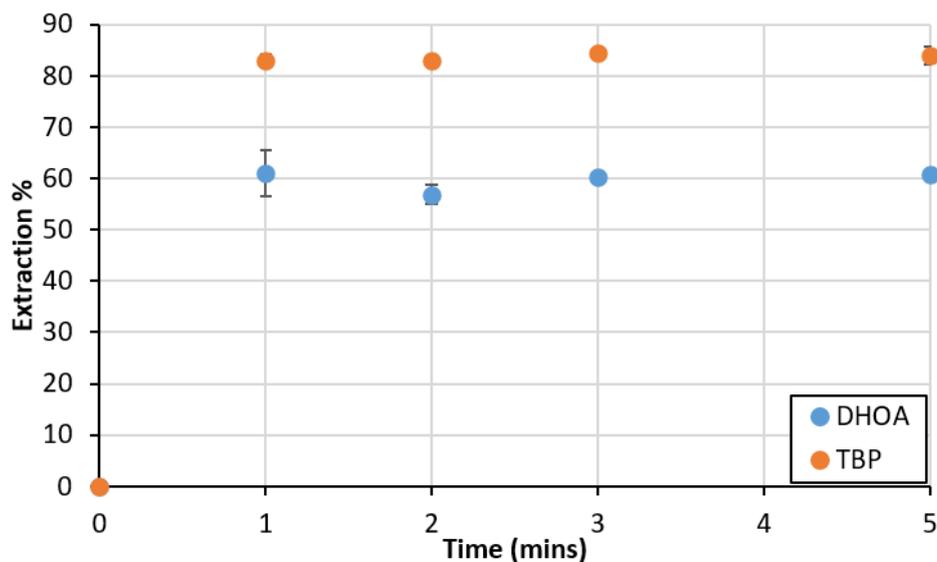
Figure 4.1. *Extraction percentage of uranium from 5.70 M nitric acid into 0.2 M ligand in n-dodecane against vial shaking time at 21±2°C. Initial [uranium] = 493±0.4 ppm.*

Each SX test deviates slightly from the following general procedure in order to provide the required data, however for most tests, the organic phase was contacted with the required standardised nitric acid and shaken to pre-equilibrate the phases. This step not only ensures that nitric acid extraction does not interfere with uranium extraction in the subsequent step, but also that nitric acid/nitrate concentrations remain constant during uranium extraction as the ligand will not extract any more acid. The importance of this is identified in Section 4.2.3. The pre-equilibration aqueous phase was carefully removed with glass pipette tips. The organic phase was then contacted with the same concentration of required standardised nitric acid and a 10,000 ppm uranium solution spike. The phases were shaken to allow mass transfer. Resultant aqueous phases were carefully separated using glass pipette tips. These aqueous phases were analysed with visible light absorption spectroscopy using an arsenazo(III) method adapted from (Wang, et al., 2009). 0.05 mL of a sample aqueous phase was mixed with 0.4 mL of a 0.1 mass% arsenazo(III) solution in deionised water (DI) and 5 mL of 2 M sodium acetate–chloroacetic acid buffer and made up to 10 mL with DI. The cocktail was mixed until homogenous and left to equilibrate for at least 15 minutes before a sample was taken and its absorption spectra was recorded against a non-spiked arsenazo(III) cocktail blank between 500 – 900 nm. The peak at 652 nm was used to determine the uranium content in ppm. Both pre- and post-contact solutions were tested. As the acidity range for the

103
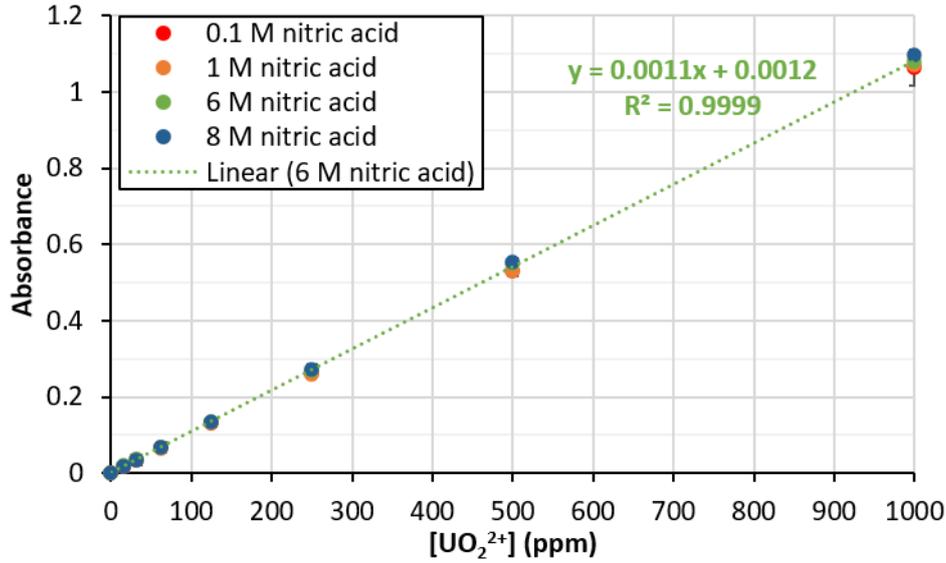
Figure 4.2. *Aqueous phase uranium concentration calibrations using the arsenazo(III) method at 0.1 M, 1 M, 6 M, and 8 M nitric acid at 21±2°C.*

pH screening was large and concentrated, 4 uranyl nitrate concentration calibration curves were conducted between 0.1 M and 8 M nitric acid to ensure the buffer was concentrated enough to consistently buffer through the acidity range (Figure 4.2). All linear trend line equations fit within ± 2σ error with an $R^2 \geq 0.9999$, but the trend line for the 6 M nitric acid extractions had the least amount of uncertainty in the data. Therefore, all aqueous-phase uranium concentrations were calculated using Eq. 4.1:

$$[UO_2^{2+}]_{sample} = \frac{Abs_{652\,nm} - 0.0012}{0.00108} \qquad (Eq\ 4.1)$$

Equilibrium organic phase uranium concentrations were calculated by difference (Eq. 4.2):

$$\overline{[UO_2^{2+}]_{eq}} = [UO_2^{2+}]_i - [UO_2^{2+}]_{eq} \qquad (Eq\ 4.2)$$

where subscript eq indicates the point of equilibrium, subscript i indicates the initial condition and an overbar denotes organic phase species; this equation can be used as phase volumes are equal. Equilibrium extraction percentages ($E\%$) and distribution coefficients (D) were calculated with Eq. 4.3 and 4.4 respectively:

104

$$E\% = \left(\frac{\overline{[UO_2^{2+}]_{eq}}}{[UO_2^{2+}]_i} \right) \times 100 \qquad\qquad (Eq\ 4.3)$$

$$D = \frac{\overline{[UO_2^{2+}]_{eq}}}{[UO_2^{2+}]_{eq}} \frac{V_{aq}}{V_{org}} \quad \rightarrow \quad if\ V_{aq} = V_{org},\ then\ D = \frac{\overline{[UO_2^{2+}]_{eq}}}{[UO_2^{2+}]_{eq}} \qquad\qquad (Eq\ 4.4)$$

where V_{aq} and V_{org} are the volumes of the aqueous and organic phases, respectively. Samples expected

to be over 1500 ppm were diluted by 10 times to ensure $[U]_{eq}$ was within acceptable detection limits as

inferred from Figure 4.3.
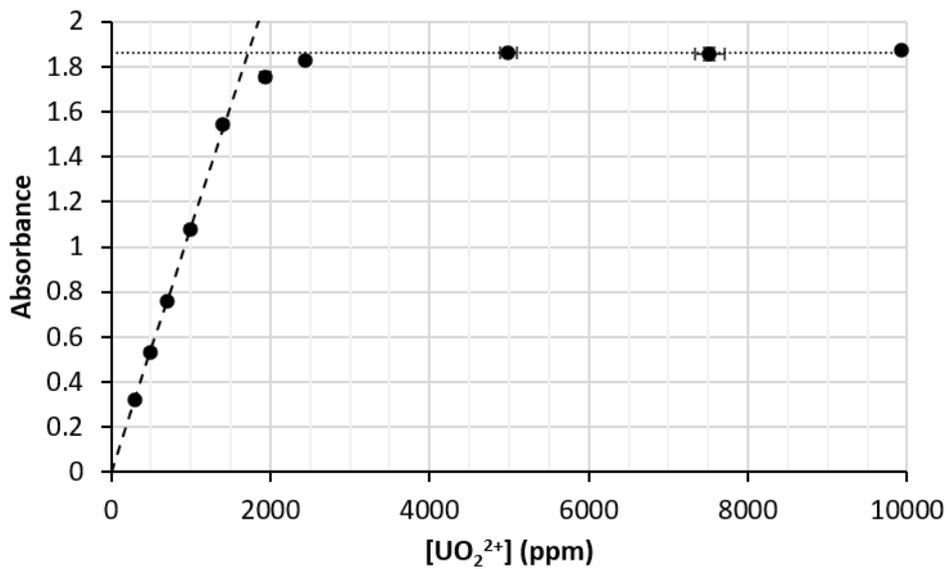
Figure 4.3. *Uranium(VI) saturation of the arsenazo(III) method at 21±2°C. The dashed line depicts the calibration equation determined from Figure 4.2 and the dotted line indicates the arsenazo(III) saturation absorption measurement.*

4.2.3 Slope analysis

Some of the following experimental methods require slope analysis during data processing. Slope

analysis utilises straight-line sections of appropriate plots to determine stoichiometries of proposed

equilibria. For example, if it is assumed that the extraction of uranium in nitrate media by a ligand, L,

follows the solvation mechanism (Eq. 4.5):

$$UO_2^{2+} + 2NO_3^- + \overline{nL} \rightleftharpoons \overline{UO_2(NO_3)L_n} \qquad\qquad (Eq\ 4.5)$$

where n is the stoichiometric coefficient for the extracting ligand. The conditional equilibrium (or

extraction) constant, K'_{eq}, for Eq. 4.5 would therefore be:

$$K'_{eq} = \frac{\overline{[UO_2(NO_3)L_n]_{eq}}}{[UO_2^{2+}]_{eq}[NO_3^-]_{eq}^2\overline{[L]_{eq}^n}}$$

<div align="right">(Eq. 4.6)</div>

The constant is considered conditional as concentrations are used rather than chemical activities. Combining Eq. 4.4 with Eq. 4.6 gives:

$$K'_{eq} = \frac{D}{[NO_3]_{eq}^2\overline{[L]_{eq}^n}}$$

$$D = [NO_3]_{eq}^2\overline{[L]_{eq}^n}K'_{eq}$$

$$\log_{10}(D) = 2\log_{10}([NO_3]_{eq}) + n\log_{10}(\overline{[L]_{eq}}) + \log_{10}(K'_{eq})$$

<div align="right">(Eq 4.7)</div>

If it is said that nitrate concentration is held constant throughout extraction tests, Eq 4.7 reduces to:

$$\log_{10}(D) = n\log_{10}(\overline{\overline{[L]_{eq}}}) + c$$

where c is a constant. A plot of $\log_{10}(D)$ against $\log_{10}(\overline{[L]_{eq}})$ would yield a straight line with a slope of n. D and $\overline{[L]_{eq}}$ are determined by extraction data and mass balances. Changing the experimental conditions allows for different stoichiometries or species to be investigated. The above equations underpin why pre-equilibration of the organic phases is critical to slope analysis. Without direct measurement of all concentrations, namely the nitrate anion, the assumptions that underpin this method cannot be made. It is assumed that after an organic phase has been pre-equilibrated with nitric acid, the nitric acid and nitrate concentrations remain constant during uranium extraction.

While slope analysis is simple and robust, its simplicity can also mask complexities in the system (Moyer, et al., 1991). Non-integer values for n can be indicative of more complicated systems, which can be related to the organic phase activity (Danesi, et al., 1970) and as such would be more qualitative in nature. Conducting experiments at low loadings, concentrations and/or constant ionic strength can offset this disadvantage as extraction is usually simpler under these conditions.

4.2.4   Acid extraction isotherms

Organic phases ranging from 0.025 M – 0.6 M ligand pre-equilibrated with DI were contacted with a standardised nitric acid and shaken. Several initial acidities were tested with each ligand system, ranging from 3 M – 8 M nitric acid. Slope analysis was used to determine speciation of the extracted nitric acid

complexes. For this, the relationship between initial and equilibrium concentrations of ligand over the tested range was used to determine free ligand concentrations (Appendix B) rather than relying on individual data points as this led to large uncertainties. Because determining the relationship between initial and equilibrium ligand concentrations first requires assumption of the complex stoichiometry, this method was conducted iteratively until reasonable results with low error in the slope analysis plots were obtained. The slope analysis gradient, along with the relationship between initial ligand concentration and organic nitric acid concentration, is used to calculate 'free ligand' concentration after pre-equilibration in further SX tests.

4.2.5   Influence of acidity

0.2 M ligand solutions pre-equilibrated with the required nitric acid were contacted with a uranium-spiked nitric acid and shaken. Initial uranium concentration was 500 ppm. Nitric acid concentrations ranged from 0.1 M to 8 M. Uranium content in pre- and post-contact solutions was measured with the arsenazo(III) method in Section 4.2.2. These tests identify optimal acidity for extraction and pH sensitivity of systems.

4.2.6   [Ligand] isotherms

Organic phases ranging from 0.025 M – 0.6 M ligand pre-equilibrated with the required nitric acid were contacted with a uranium-spiked nitric acid and shaken. Initial uranium concentration was 500 ppm. Uranium content in pre- and post-contact solutions was measured with the arsenazo(III) method in Section 4.2.2. Slope analysis was used to determine speciation of extracted uranyl complexes after determining free ligand concentration from the previous acid extraction tests outlined in Section 4.2.4. These results also feed into the uranium loading isotherms.

4.2.7   Uranium loading isotherms

0.2 M ligand solutions pre-equilibrated with the required nitric acid concentrations were contacted with a uranium-spiked nitric acid and shaken. Initial uranium concentration ranged from 250 ppm to 10,000 ppm. Uranium content in pre- and post-contact solutions was measured with the arsenazo(III) method. High $[UO_2^{2+}]_{eq}$ samples ($>$ 1500 ppm) were diluted by 10 times its volume to avoid arsenazo oversaturation observed in Figure 4.3. Loading isotherms were modelled based on the extraction

mechanism determined from earlier SX tests and the K'_{eq} determined from the uranium loading isotherm data. Concentrations of products and reactants were determined at each point of the isotherm and plotted using Eq 4.6 such that the gradient of the slope is K'_{eq} (Appendix B). From this, theoretical free ligand concentration, $\overline{[L]_{eq}}$, for a given value of $\overline{[UO_2^{2+}]_{eq}}$ was determined by:

$$\overline{[L]_{eq}} = \overline{[L]_\iota} - m\overline{[HNO_3]_{eq}} - n\overline{[UO_2^{2+}]_{eq}} \qquad (Eq\ 4.8)$$

Where $\overline{[L]_\iota}$ is the initial ligand concentration, m is the stoichiometric coefficient for the acid-ligand complex determined from acid extraction slope analysis, and n is the stoichiometric coefficient for the metal-ligand determined from metal extraction slope analysis. $[UO_2^{2+}]_{eq}$ could then be found by rearranging Eq 4.6 to Eq 4.9:

$$[UO_2^{2+}]_{eq} = \frac{\overline{[UO_2(NO_3)L_n]}_{eq}}{K'_{eq}[NO_3]_{eq}^2\overline{[L]}_{eq}^n} \qquad (Eq\ 4.9)$$

This model was plotted against experimental data for validation. As discussed later, this model fits for low loading but deviates from higher loading data. A second model was constructed by tweaking the amount of extracted acid in Eq 4.8 until suitable fits with experimental data were obtained. McCabe-Thiele diagrams were constructed with the better fitting model. Operating lines were constructed using Eq 4.10 adapted from (Warade, et al., 2011):

$$\overline{[UO_2^{2+}]}_{N+1} = \frac{V_{aq}}{V_{org}}([UO_2^{2+}]_N - [UO_2^{2+}]_F) + \overline{[UO_2^{2+}]}_1 \qquad (Eq\ 4.10)$$

where V_{aq} and V_{org} are the volumes (or volumetric flowrates) of the aqueous or organic phases respectively, $\overline{[UO_2^{2+}]}_{N+1}$ is the organic uranium concentration leaving the Nth stage, $\overline{[UO_2^{2+}]}_1$ is the organic uranium concentration entering the 1st stage, $[UO_2^{2+}]_N$ is the aqueous uranium concentration leaving the Nth stage and $[UO_2^{2+}]_F$ is the aqueous uranium concentration of the feed.

4.2.8 Influence of ionic strength

0.2 M ligand solutions pre-equilibrated with the required 'nitrated' nitric acid were contacted with a uranium-spiked nitric acid and shaken. Nitrated solutions were prepared by dissolving sodium nitrate in nitric acid. Nitric acid concentration was held constant through each test, but several acidities were

studied from 2 M to 4 M nitric acid. Initial aqueous nitrate concentration ranged from 2 M to 7 M including the contribution from nitric acid. Initial uranium concentration was 500 ppm. Uranium content in pre- and post-contact solutions was measured with the arsenazo(III) method.

4.2.9   Jobs plots

Mixed DHOA-TBP and DHOA-TODGA solutions were prepared by mixing required volumes of 0.2 M single-ligand solutions; as such, total ligand concentration remained constant at 0.2 M. These mixed-ligand solutions were pre-equilibrated with the required nitric acid before being contacted uranium-spiked nitric acid and shaken. Initial uranium concentration was 500 ppm. Molar ratios from pure monoamide to pure 'other ligand' were tested. Uranium content in pre- and post-contact solutions was measured with the arsenazo(III) method. Corrected distribution values were determined by calculating the expected $\overline{[UO_2^{2+}]}_{eq}$ assuming no interaction between the mixed ligands which would result in a linear relationship between the pure ligand tests. Eq. 4.11 takes the DHOA-TBP Job plot as an example:

$$\overline{[UO_2^{2+}]}_{eq,x} = \left(x \frac{\overline{[UO_2^{2+}]_{eq,pure\ DHOA}} - \overline{[UO_2^{2+}]_{eq,pure\ TBP}}}{x_{pure\ DHOA} - x_{pure\ TBP}} \right) + \overline{[UO_2^{2+}]_{eq,pure\ TBP}} \qquad (Eq.\ 4.11)$$

where x indicates a mole fraction of DHOA and subscript $pure\ DHOA$ and $pure\ TBP$ indicate DHOA mole fractions of 1 and 0 respectively. Analysis for the DHOA-TODGA Job plot was conducted the same way but with the suitable TODGA data.

4.3   Results

An extraction screen was conducted to determine suitable ligand concentrations and contact volumes for general SX tests; Table 4.2 shows these results. DHOA and TBP were used as screening ligands as they were available during initial testing. Contact volume does not seem to have any effect on the point of equilibrium, and uranium extraction increases with increasing ligand concentration. As the aim of this chapter is to compare ligand performances, it is desirable to pick conditions where changes in extractive performance can easily be seen. To that end, and in the interest of using material economically, 0.5 mL contacts of each phase at 0.2 M ligand were chosen as standard experimental conditions except where ligand concentration had to be varied. Equal phase volumes were used to simplify Equation 4.4.

Table 4.2. *Uranyl nitrate extraction screening data with DHOA and TBP in 5.97 M HNO₃.*

Ligand	Concentration (M)	Phase volume (mL)	E%	D
DHOA	0.1	1	38.2 ± 7.4	0.62 ± 0.05
	0.2	0.5	66.8 ± 2.1	1.91 ± 0.07
	0.2	1	68.2 ± 1.5	2.04 ± 0.04
	0.3	0.5	82.1 ± 1.6	4.4 ± 0.2
	0.3	1	83.4 ± 1.2	4.8 ± 0.1
	0.5	0.5	94.5 ± 2.3	17 ± 2
	0.5	1	94.7 ± 2.9	17.7 ± 0.7
TBP	0.1	1	66.1 ± 5.7	2.0 ± 0.2
	0.2	0.5	85.2 ± 2.2	5.7 ± 0.6
	0.2	1	85.8 ± 1.1	6.0 ± 0.1
	0.3	0.5	91.3 ± 1.3	10.5 ± 0.5
	0.3	1	91.9 ± 1.1	11.4 ± 0.5
	0.5	0.5	96.1 ± 2.4	25 ± 4
	0.5	1	95.7 ± 2.9	22.2 ± 0.5

Figure 4.4A shows the organic nitric acid concentrations after contact with varying DHOA, TBP or TODGA concentrations; initial nitric acid concentrations were 5.69 M, 5.60 M, and 4.68 M, respectively. DHOA and TBP were found to linearly extract acid with increasing ligand concentration, but acid extraction with TODGA was found to fit a second order polynomial, potentially due to a change in speciation as ligand concentration increases. The equations of the trends seen in Figure 4.4A are used to determine free ligand concentration after pre-equilibration in subsequent SX tests. Figure 4.4B shows the slope analysis from log-log plots for DHOA, TBP and TODGA acid extraction. Values derived from slope analyses are presented in Table 4.3. Both DHOA and TBP appear to form monosolvate complexes with nitric acid. TODGA appears to generate both mono- and di-*acid* complexes. It is likely that a varying speciation profile results in the polynomial nitric acid extraction profile. Data shown in Figure 4.4B assumes $\overline{\overline{[TODGA]}}_{eq}$ is dominated by (TODGA)(HNO₃)₂ species (assuming dominant (TODGA)(HNO₃) species gave negative free [TODGA] which cannot be feasible). However, the non-integer slope analysis reveals that the speciation is not that simple over the tested ligand concentration range; this is discussed further in Section 4.4.1.

Table 4.3. *Slope analysis values for nitric acid extraction and uranyl nitrate extraction with single ligand systems.*

Test	System	Slope	Intercept	R^2
Nitric acid extraction	DHOA	1.06 ± 0.08	-0.55 ± 0.09	0.9890
	TBP	1.1 ± 0.1	-0.6 ± 0.1	0.9859
	TODGA	0.75 ± 0.04	-0.08 ± 0.05	0.9966
Uranyl nitrate extraction	DHOA	1.93 ± 0.02	2.27 ± 0.03	0.9996
	TBP	1.57 ± 0.08	2.9 ± 0.1	0.9964
	TODGA	1.0 ± 0.2	2.9 ± 0.3	0.9592
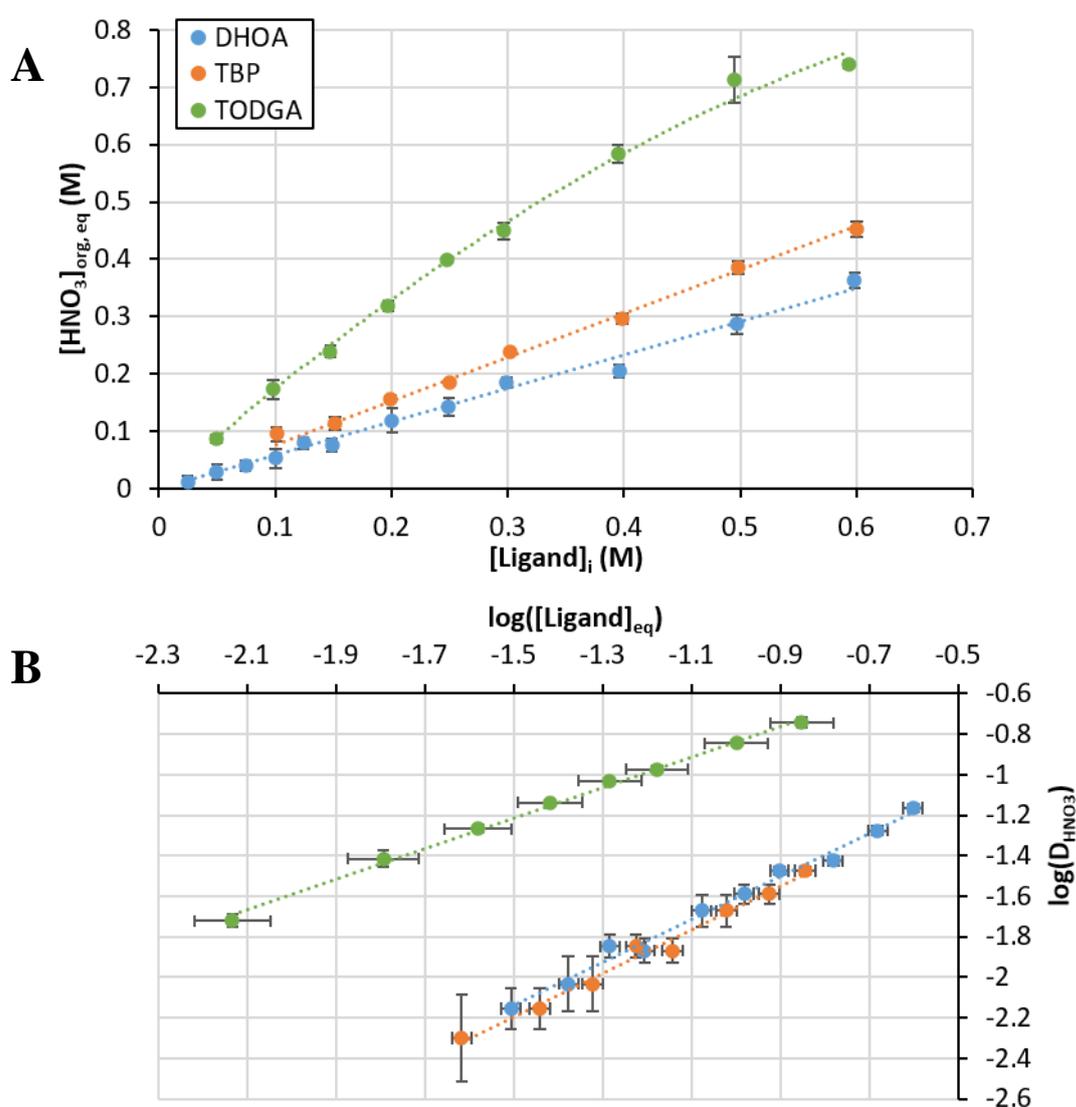
Figure 4.4. *Nitric acid A) extraction isotherms and B) slope analysis for 0.2 M DHOA (from 5.69 M HNO3), TBP (from 5.60 M HNO₃) and TODGA (from 4.68 M HNO₃) at 21±2°C.*

Figure 4.5 shows how DHOA, TBP and TODGA extraction of uranyl nitrate is influenced by acidity, whereas Figure 4.6 shows the distribution profiles. DHOA was found to produce a stable emulsion after contact with 0.1 M nitric acid; globules of the aqueous phase were held up in the organic phase. The same was found for 1 M nitric acid, but to a much lower extent and the phases were still separable after gentle agitation. TBP formed no third phases over the tested acidity range. TODGA was found to be very sensitive to acidity. TODGA solvents behaved normally between 4 – 5.5 M nitric acid. Below this range, acid contact resulted in a cloudy organic phase. Above this range, acid contact clearly split the organic into a TODGA-rich phase and a diluent-rich phase. Contact with uranium did not change this, but the two organic phases were readily soluble in each other after the initial 5 minute shake for SX.
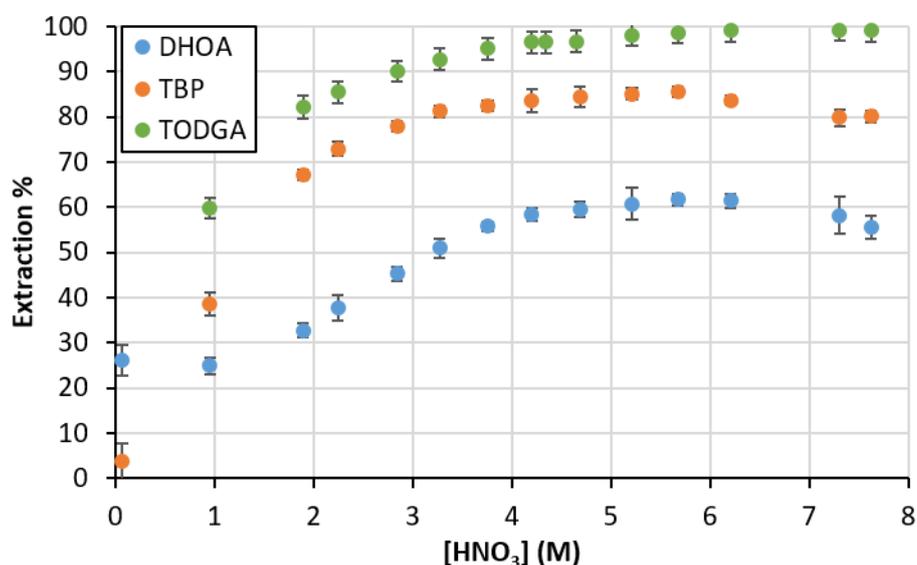
Figure 4.5. *pH profiles of uranyl nitrate extraction by 0.2 M DHOA, TBP and TODGA at 21±2°C. Initial [uranium] for DHOA, TBP and TODGA tests are 490±3, 490±3 and 504±9 ppm respectively.*
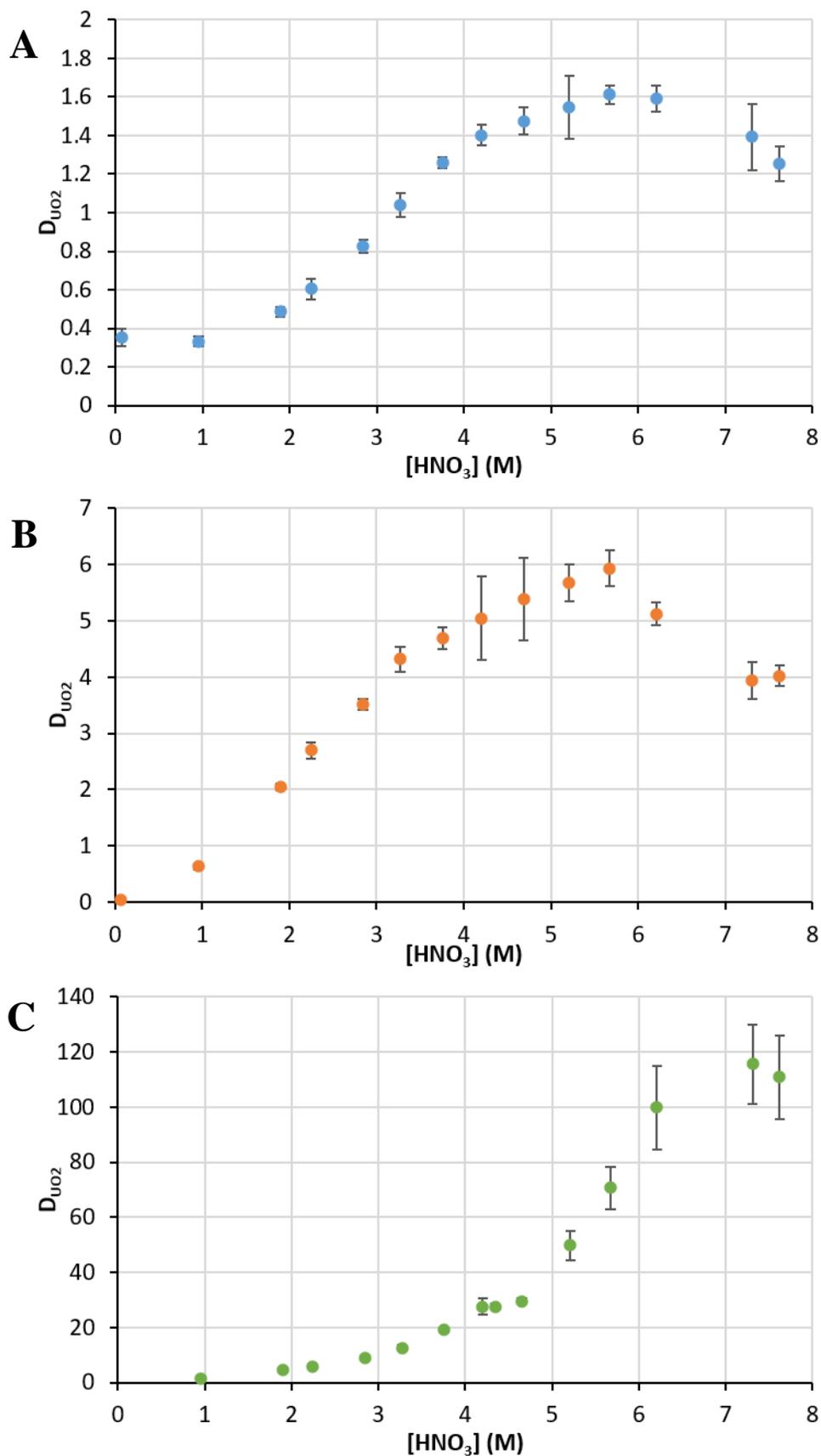
Figure 4.6. *pH profiles of uranyl nitrate distribution coefficient by 0.2 M A) DHOA, B) TBP and C) TODGA at 21±2°C. Initial [uranium] for DHOA, TBP and TODGA tests are 490±3, 490±3 and 504±9 ppm respectively.*

Figure 4.7A and B shows uranium extraction and distribution, respectively, with varying DHOA, TBP and TODGA concentrations. Extraction is consistently in the order DHOA < TBP < TODGA; this is expected given the donor strengths of the ligands. The large errors on the last distribution points for TODGA systems are due to the very low absorbance readings measured in the post-contact solutions. The standard deviations of these points are small, but error propagation causes high uncertainty values due to the small raw data values. Figure 4.7C shows slope analysis of the ligand isotherm tests. Equilibrium free ligand concentrations were calculated by accounting for ligand complexed with acid (determined from the trends in Figure 4.4A) and of the ligand complexed with uranyl nitrate. Values determined from slope analysis are presented in Table 4.3. It can clearly be seen that DHOA and TODGA form di- and monosolvate complexes with uranyl nitrate respectively. TBP is seen to form a mixture of di- and monosolvate complexes with uranyl nitrate seemingly at roughly equal concentrations. Triplicate TBP extraction tests were repeated a second time to confirm this finding.
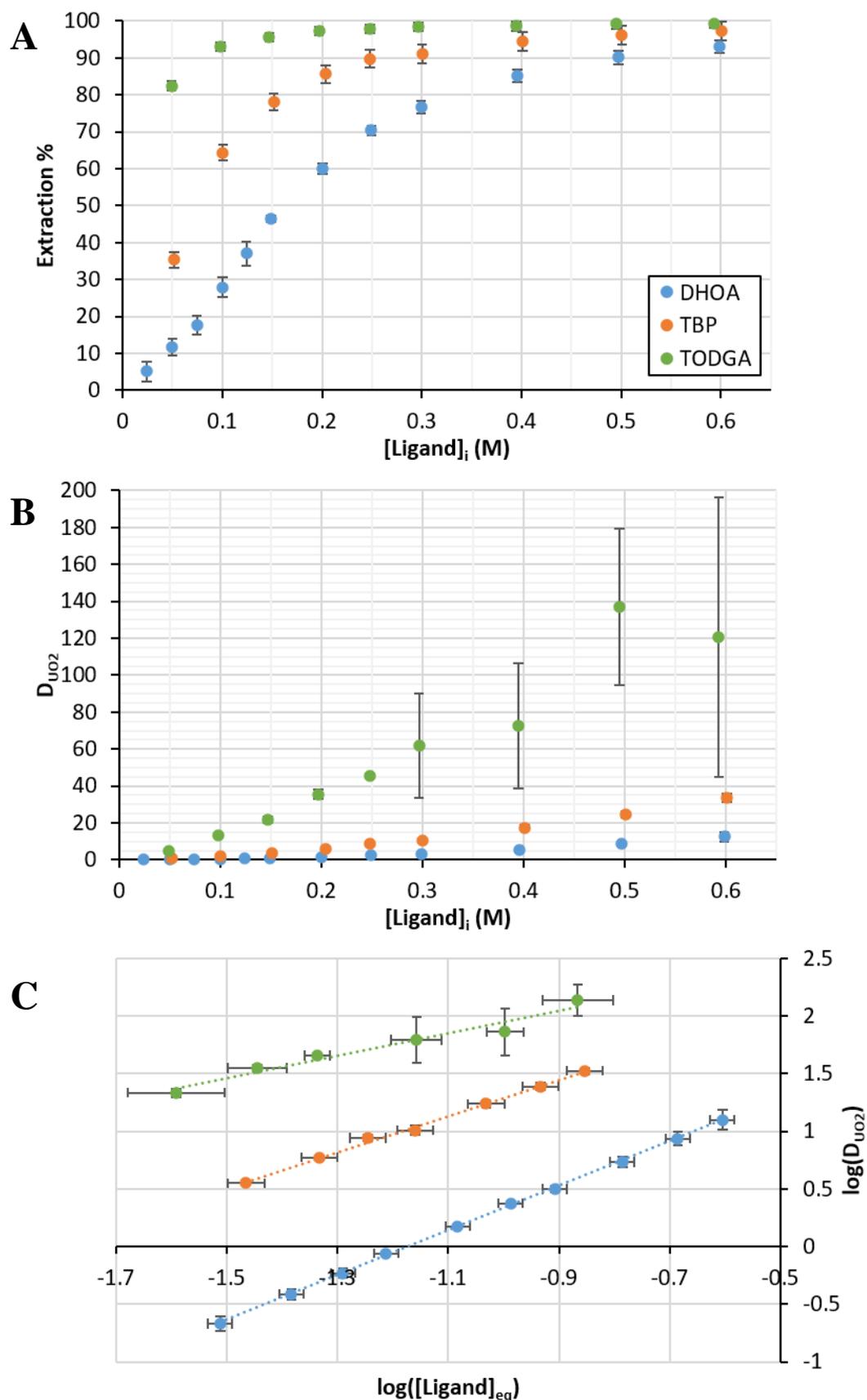
Figure 4.7. *Ligand isotherms of uranyl nitrate A) extraction and B) distribution coefficient by DHOA from 5.69 M HNO₃, TBP from 5.60 M HNO₃ and TODGA from 4.68 M HNO₃ at 21±2°C. Initial [uranium] for DHOA, TBP and TODGA tests are 490±3, 500±9 and 498±5 ppm respectively. C) shows slope analysis plots of these systems.*

Figure 4.8 shows the uranium loading isotherms for the DHOA, TBP and TODGA systems at both low loading (0-3 g/L U) and through the entire tested range (0-10 g/L U). Calculated models based purely on the proposed reaction mechanism fit the data well under low loading conditions but deviate as organic uranium loading exceeds ~3 g/L. This is likely due to exchange of complexed acid for uranyl nitrate and is discussed later. Models that account for changing organic acid concentrations are shown in Figure 4.8C and fit the data well. McCabe-Thiele diagrams were constructed using Figure 4.8C equilibrium models; the operating lines assumed a feed of 10 g/L uranium with a desired 95% recovery and varying aqueous/organic (A/O) phase flow rates to compare the performance of the tested systems. The number of theoretical stages for the 0.2 M ligand systems is presented in Table 4.4, as well as estimations of number of theoretical stages for 1.1 M ligand systems discussed later for A/O phase volume ratios of 0.5 and 1. An A/O phase volume ratio of 1 indicates equal phase volumes, whereas an A/O phase volume ratio of 0.5 indicates twice the organic phase volume relative to the aqueous phase.

Table 4.4. *Loading capacities and number of theoretical extraction stages as determined by the McCabe-Thiele method for >95% uranium recovery with 0.2 M ligand solutions from nitric acid at 21±2°C. Theoretical stages in brackets indicate estimated stages at 1.1 M ligand using Figure 4.13.*

System	[HNO$_3$] (M)	Maximum capacity (g/L)	Theoretical extraction stages	
			A/O = 0.5	A/O = 1
DHOA	5.63	17.4	3 (1)	N/A (2)
TBP	5.63	23.6	2 (1)	3 (1)
TODGA	4.65	17.8	1 (1)	1 (1)
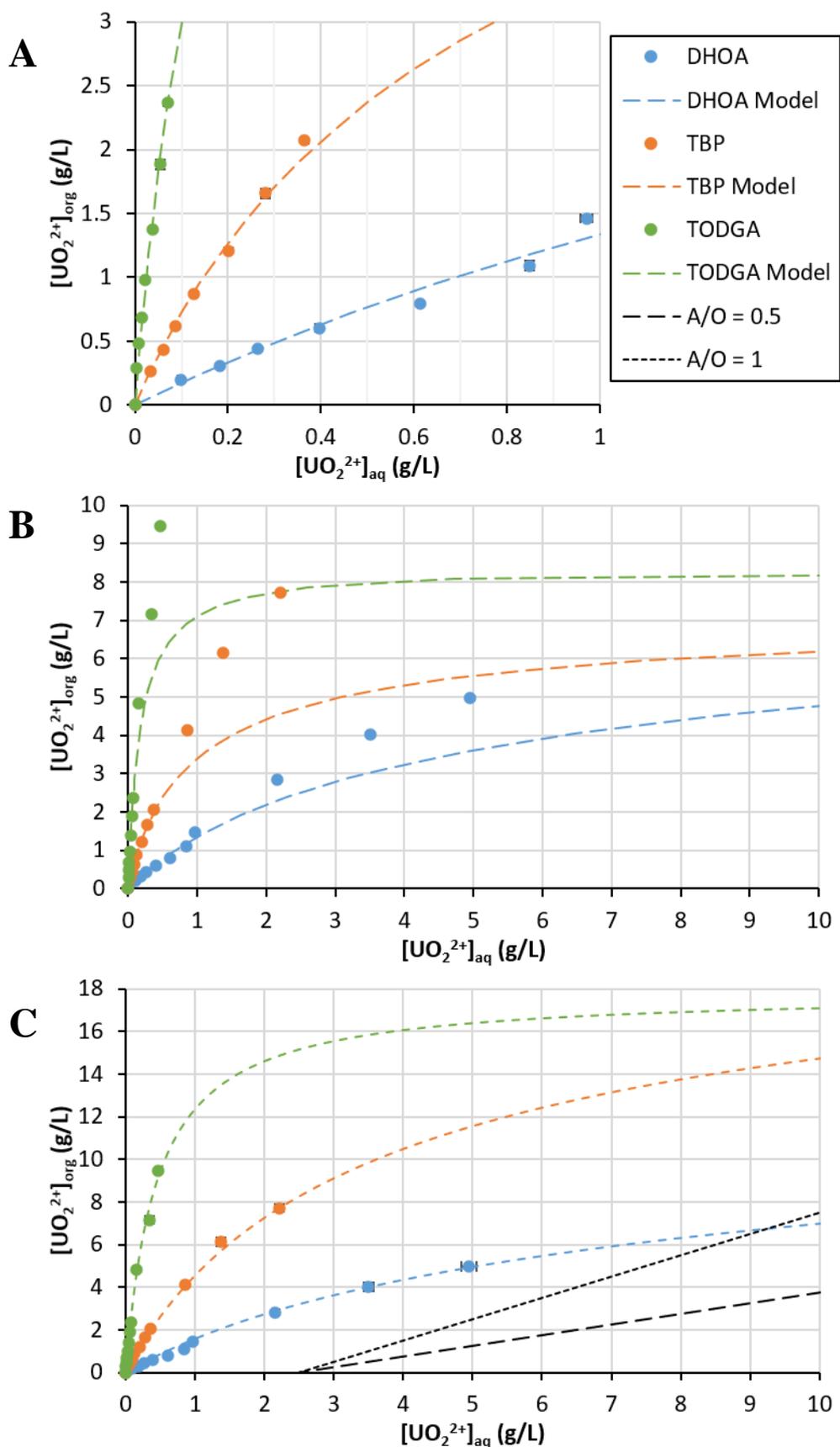
Figure 4.8. *Uranyl nitrate loading isotherms with 0.2 M DHOA (at 5.63 M HNO₃), TBP (at 5.63M M HNO₃) and TODGA (at 4.65 M HNO₃) at 21±2°C. A) depicts low loading with models based on the extraction mechanism, B) shows entire tested range with models based on the extraction mechanism, and C) shows modified model fits with two operating lines constructed from Equation 4.10 assuming the specified A/O.*

Figure 4.9 shows uranyl nitrate distribution in 0.2 M DHOA, TBP and TODGA systems with varying sodium nitrate concentrations. Both DHOA and TBP are shown to have enhanced extraction at lower acidities when sodium nitrate concentration is increased. This is due to less acid competition and shifting of the equilibrium position because of the higher equilibrium nitrate concentrations. This observation is not seen in TODGA systems; the nitric acid concentration appears to have no effect on uranyl extraction and nitrate concentration seems to be the dominating factor.

Figure 4.10 shows the slope analysis for the tested systems at the three tested acidities. Values determined from slope analysis are presented in Table 4.5, although these are generally qualitative and discussed further later in this chapter.

Table 4.5. *Slope analysis values for the influence of ionic strength tests conducted at 21±2°C.*

System	[HNO_3] (M)	Slope	Intercept	R^2
DHOA	2	2.0 ± 0.2	-0.9 ± 0.1	0.9884
	3	1.8 ± 0.3	-0.9 ± 0.2	0.9820
	4	1.74 ± 0.06	-0.91 ± 0.04	0.9994
TBP	2	2.2 ± 0.2	-0.3 ± 0.1	0.9927
	3	1.9 ± 0.1	-0.3 ± 0.1	0.9957
	4	1.6 ± 0.5	-0.3 ± 0.3	0.9634
	2	2.6 ± 0.4	-0.1 ± 0.1	0.9715
TODGA	3	2.5 ± 0.1	-0.17 ± 0.07	0.9991
	4	2.8 ± 0.3	-0.3 ± 0.2	0.995
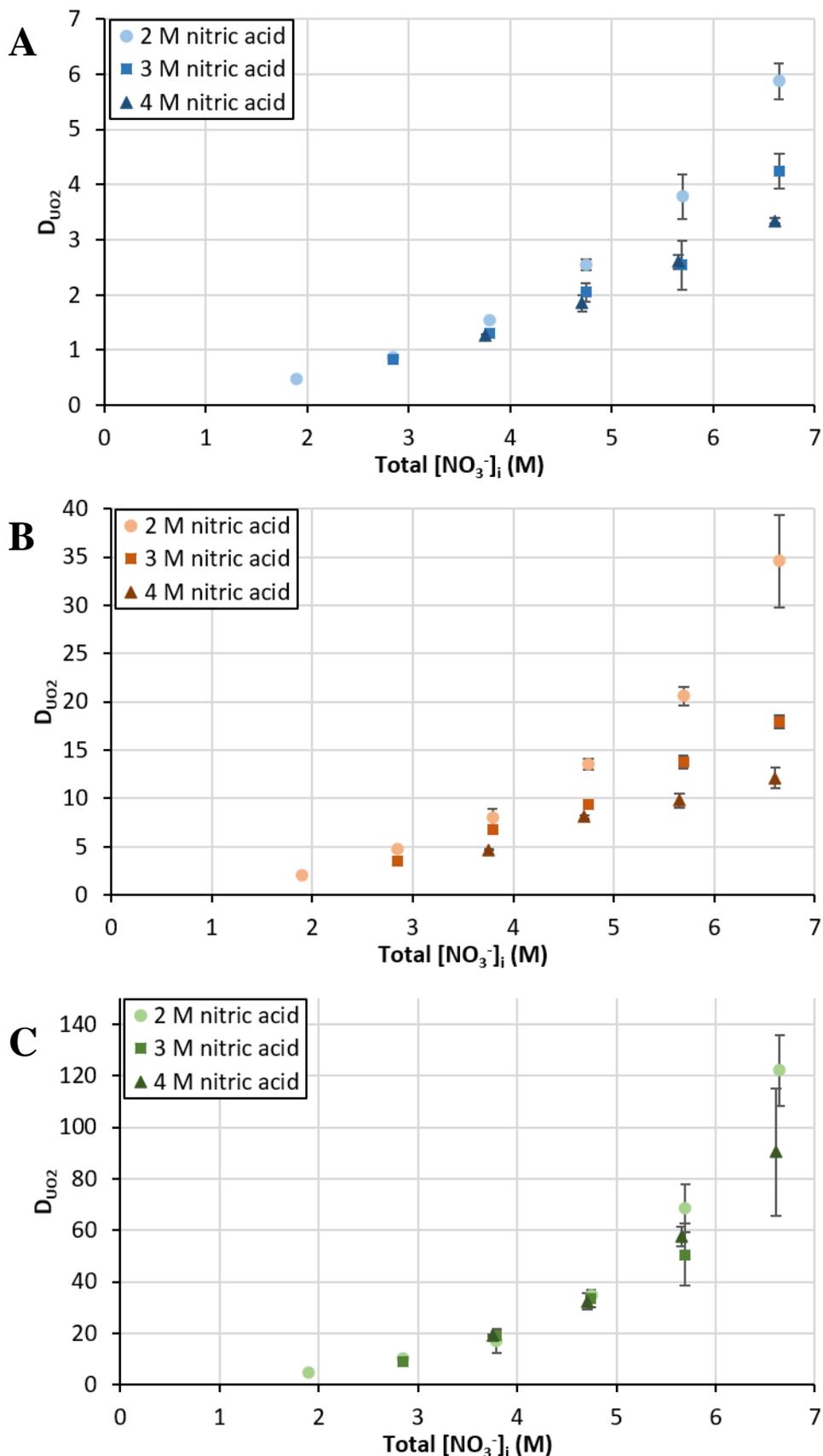
Figure 4.9. *Uranyl nitrate extraction with varying nitrate concentrations in different nitric acid concentrations with 0.2 M A) DHOA, B) TBP and C) TODGA at 21±2°C. Initial [uranium] for DHOA, TBP and TODGA tests are 486±3, 475±3 and 482±4 ppm respectively.*
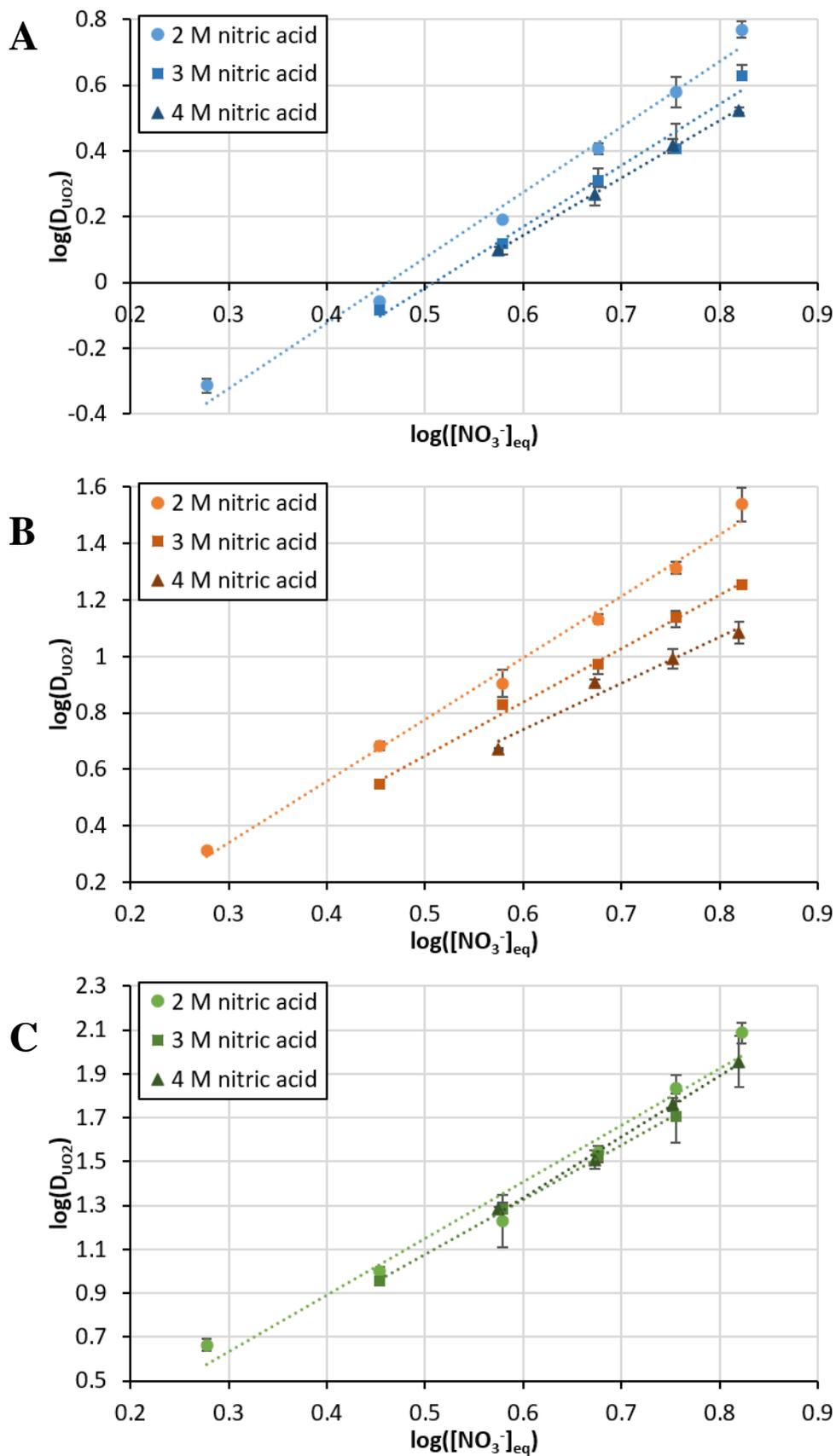
Figure 4.10. *Slope analysis for 0.2 M A) DHOA, B) TBP and C) TODGA from nitric acid with varying total nitrate concentration at 21±2°C. Initial [uranium] for DHOA, TBP and TODGA tests are 486±3, 475±3 and 482±4 ppm respectively.*

Figure 4.11 shows the distribution and organic uranium concentration Jobs plots for DHOA-TBP. It can be seen that no mixture of DHOA and TBP results in a system that extracts uranium better than pure TBP, but some synergic interaction is observed throughout the Job plot. This can be seen because mixtures perform better than expected if no interaction is assumed. The organic uranium Job plot hints at mixed ligand complexes but the large error relative to the small changes in measurements makes it difficult to definitively draw these conclusions.
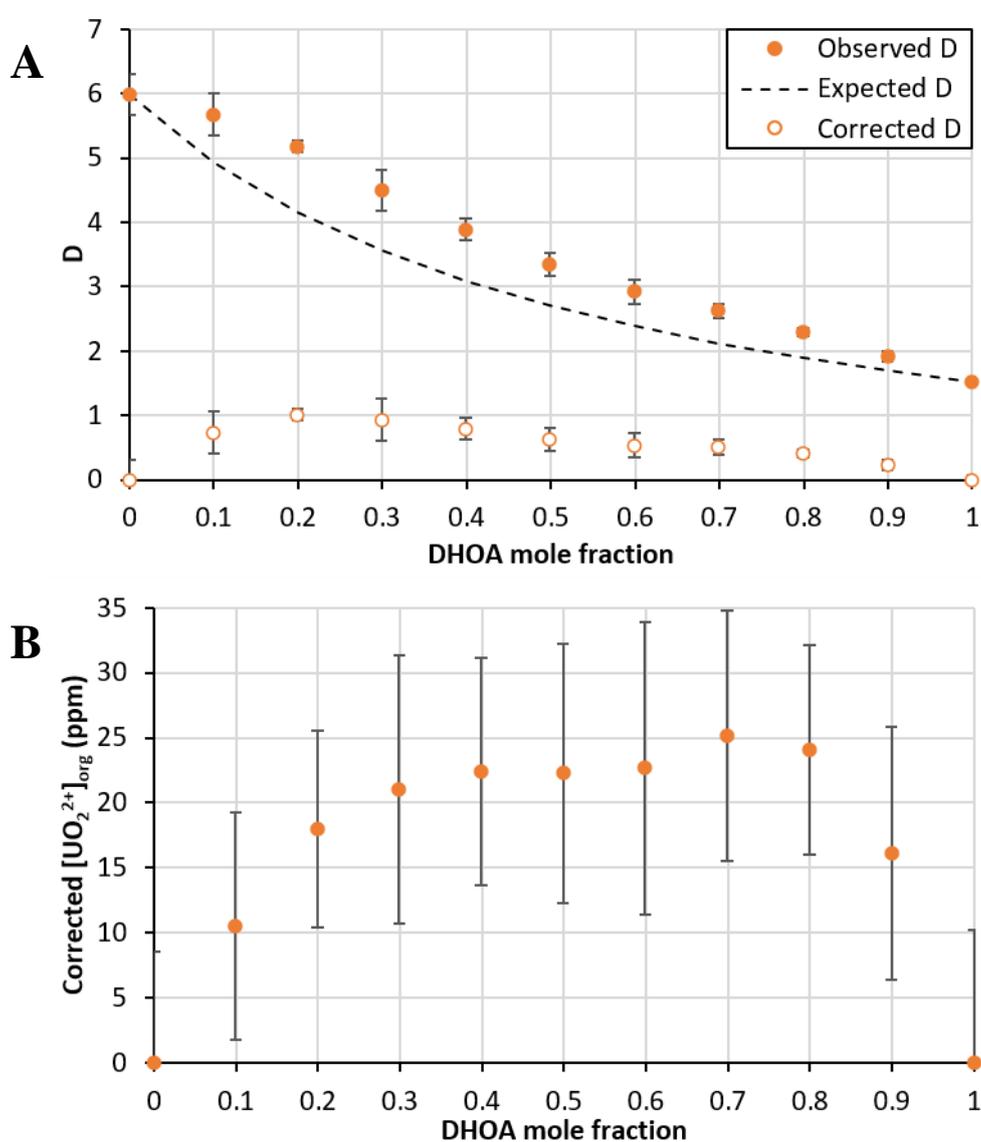
Figure 4.11. *DHOA-TBP Job plot at 5.7 M nitric acid at 21±2°C. Initial [uranium] = 568±8 ppm. A) depicts the distribution Job plot. B) depicts the organic [uranium] Job plot.*

Figure 4.12 shows the distribution and organic uranium concentration Jobs plots for DHOA-TODGA systems. DHOA-TODGA systems appear to have synergic interactions especially at low mole fractions of DHOA. Uranium extraction is enhanced beyond pure systems up until ~35% DHOA, after which pure TODGA systems extract more uranium. Similar to DHOA-TBP systems, uranium extraction is seen to be consistently better than if no mixed ligand interaction is assumed. The organic uranium Job plot indicates that a $(DHOA)_2(TODGA)$ complex is generated which supports the findings of Chapter 3.
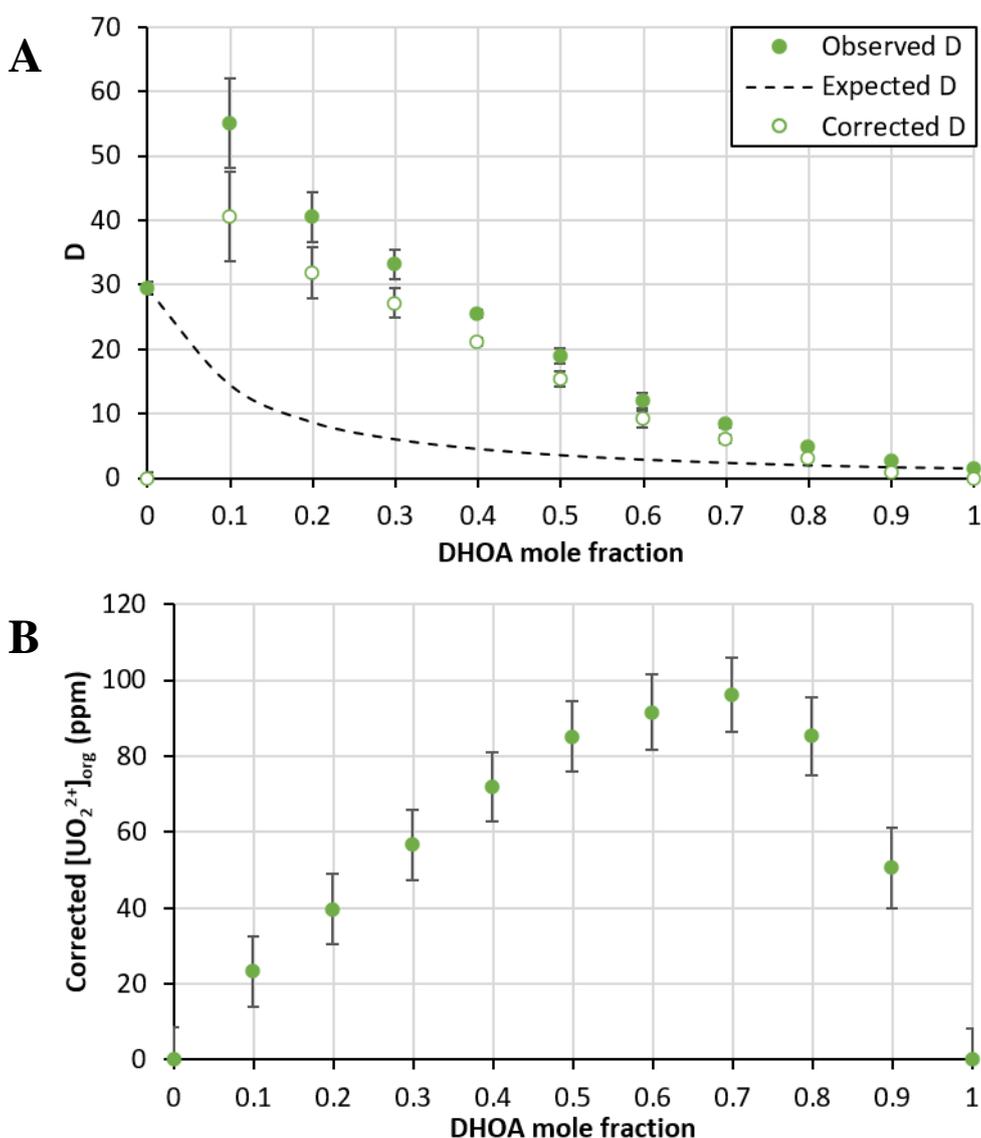
Figure 4.12. *DHOA-TODGA Job plot at 4.7 M nitric acid at 21±2°C. Initial [uranium] = 500±9 ppm. A) depicts the distribution Job plot. B) depicts the organic [uranium] Job plot.*

4.4   Discussion

4.4.1   Acid extraction isotherms

TBP is found to consistently be a slightly stronger extractant for nitric acid than DHOA, which is supported by previous research (Gasparini & Grossi, 1986). While the monoamide has a higher basicity, the weaker donor strength of the carbonyl relative to the phosphoryl likely results in the weaker extraction of acid. Slope analysis reveals both of these ligands produce monosolvate species at the tested acidities which is supported by literature (Alcock, et al., 1956); (Nukada, et al., 1960); (Prabhu, et al., 1993).

It is unsurprising that TODGA outperforms TBP given the number of hard donor sites on the molecule. It was initially thought that the slope of 0.75 for TODGA acid extraction meant that both $(TODGA)(HNO_3)$ and $(TODGA)(HNO_3)_2$ were present. However, while models assuming 2 extracted acid molecules gave reasonable results, modelling 1 extracted acid molecule was not possible. Despite this, the second order relationship between initial $[TODGA]$ and $[HNO_3]_{org}$ indicates that acid complex speciation does indeed change with ligand concentration. This phenomenon has been noted previously by (Modolo, et al., 2007a) who tested organic nitric concentration with different initial TODGA concentrations over a range of acidities. They did not present slope analysis, but they find that at 6 M nitric acid, 0.1 M TODGA results in a dominant $(TODGA)(HNO_3)_2$ complex, whereas 0.6 M TODGA results in a dominant $(TODGA)(HNO_3)_{1.5}$ species. This not only supports the findings of the current work, but it also explains why attempting to model $(TODGA)(HNO_3)$ species was not possible. The slope for 0.2 M TODGA in Modolo et al.'s work is nearly identical to that of 0.1 M TODGA, so $(TODGA)(HNO_3)_2$ is taken to be the extracted complex in the current 0.2 M ligand SX tests. Excellent fits in the acid extraction slope analysis and later loading models support this assumption.

4.4.2   Influence of acidity

Influence of acidity on DHOA agrees with reported behaviour in literature (Gasparini & Grossi, 1986); (Condamines & Musikas, 1992); (Nair, et al., 1995); (Gupta, et al., 2000b). Extraction peaks between 5.5-6 M nitric acid beyond which acid extraction begins to dominate and anionic uranyl species form which can only be extracted by protonated ligand. Emulsions were observed at low acidity, yet the

123

stability of the monoamide solvent at low acidity has not been discussed in the literature before. Condamines & Musikas (1992) conducted uranyl nitrate extractions at and below 0.1 M nitric acid with branched and aliphatic monoamides but did not report the formation of a stable emulsion or third phase under these conditions. All other studies appear to begin pH profile extractions from 0.5 M nitric acid, potentially to avoid the emulsion issue observed in this study. This emulsion was observed to a much lower extent at 1 M nitric acid, but gentle agitation easily formed two distinct phases and the phases were still completely separable. It is unlikely that precipitates were formed to stabilise an emulsion at these conditions, therefore, these third phases are likely the result of micellar interactions.

TBP is seen to be a consistently better extractant for uranyl nitrate than DHOA and did not form third phases throughout the tested range, which is supported by previous literature (Gasparini & Grossi, 1986); (Manchanda, et al., 2001); (Manchanda & Pathak, 2004). Aside from the better performance of TBP, the extraction profiles are fairly similar owing to their similar extraction mechanisms. TBP extraction also peaks around 5.5 M nitric acid before acid extraction begins to dominate and uranium extraction decreases. The drop after 5.5 M nitric acid appears shearer than that of DHOA which might be due to TBP's lower ability to extract the anionic uranyl trinitrate species formed under these conditions. That said, it has been reported that TBP forms a complex of $HUO_2(NO_3)_3 \cdot TBP$ under these conditions (Woodhead, 1965); (Zilberman & Ferorov, 1991) which can explain why distribution is still relatively high at high acid concentrations.

TODGA systems were found to be incredibly sensitive to acid pre-equilibration. Pre-equilibration below 4 M nitric acid formed a cloudy organic phase, yet the two phases were still completely separable. Pre-equilibration above 5.5 M nitric acid split the organic phase into a denser TODGA-rich phase and a lighter diluent-rich phase. After phase separation, the two organic phases were still readily soluble in one another despite the initial splitting; this was also observed during some unreported acid extraction tests. Contact with uranium after pre-equilibration did not change this observation. TODGA solvent third phases have been reported before (Tachimori, et al., 2002); (Modolo, et al., 2007a) and attractive interactions between reverse micelles have been shown to be the cause (Nave, et al., 2004). Modolo, et al. (2007a) found that branched diluents suppressed third phase formation but also found that 0.2 M

TODGA in *n*-dodecane starts to form third phases at 4 M nitric acid which contradicts what was observed in the present work. It is possible that the differing reaction methodology (Sasaki & Choppin, 1996) means there is an impurity difference that causes third phase stability/instability. Solvent stability aside, TODGA is seen to extract uranium far better than DHOA and TBP due to its higher number of hard oxygen donors. It is unclear whether the profile peaks around 7.5 M nitric acid or whether distribution continues to increase. Either way, acid competition at high nitric acid concentrations is seen to be much less of an issue in TODGA systems than for DHOA or TBP. This could be a result of TODGA solvents higher capacity for acid.

4.4.3   [Ligand] isotherms

The ligand isotherms for DHOA definitively show that the disolvate uranyl species is dominant which is supported by Chapter 3 findings as well as many literature studies (Gasparini & Grossi, 1986); (Condamines & Musikas, 1992); (Prabhu, et al., 1993); (Nair, et al., 1994); (Prabhu, et al., 1997). The slope of 1.93 gives little indication that the ionic $UO_2(NO_3)_3^-\cdot H\text{-}DHOA^+$ is formed under the tested conditions; if it were, the slope would tend more towards a value of 1. Berger et al. (2020) indicate that these complexes may not dominate until well over 12 M nitric acid. Assuming that the present slope of 1.93 ± 0.02 means $7\pm2\%$ of uranyl complexes are monosolvate ionic, this fits relatively well with Berger et al.'s findings for aliphatic amides at ~5.5 M nitric acid.

The slope of 1.57 for the TBP ligand isotherm indicates that both mono- and disolvate complexes are formed under the tested conditions. It is generally reported that TBP forms disolvate complexes in acidic nitrate media (Sato, 1958); (Nukada, et al., 1960); (Alibrahim & Shlewit, 2007), so these triplicate tests were repeated but yielded the same result. It has been noted previously that TBP may form a complex of $HUO_2(NO_3)_3\cdot TBP$ where uranyl nitrate is extracted with an undissociated nitric acid molecule at high acidities due to the high content of nitric acid in the organic phase (Zilberman & Ferorov, 1991); (Woodhead, 1965). In the present study, it appears that both this monosolvate and the disolvate species are formed in roughly equal proportions at 5.6 M nitric acid. This assumption was used to inform the TBP uranium loading isotherm seen in Figure 4.8 and the good fits support that both complexes are formed.

The slope of 1 for the TODGA ligand isotherm at 4.7 M nitric acid indicates that only the monosolvate species is formed in solution which is supported by some diglycolamide literature (Panja, et al., 2009); (Ren, et al., 2017); (Boltoeva, et al., 2018) but contradicts some other studies (Sasaki, et al., 2013); (Sasaki, et al., 2015); (Liu, et al., 2015); (Peng, et al., 2017). As stated in Chapter 3, it is worth noting that Liu, et al. (2015) and Peng, et al. (2017) stated no methodology for organic phase pre-equilibration with nitric acid, so the higher initial free ligand may be affecting the equilibrium position and result in a differing value for complex stoichiometry. Sasaki et al. (2015) found a slope of 3.0±0.2 for TODGA in *n*-dodecane with uranyl nitrate at 1 M nitric acid and found this value is highly dependent on the organic diluent. Sasaki et al. (2013) conducted a large study into the speciation of many elements with four different diglycolamides and found that both mono- and disolvate uranyl species form in varying quantities depending on ligand structure. They found a slope of 1.9 for TODGA at 3 M nitric acid, indicating a dominant disolvate species. Again, there was no methodology stated for organic phase pre-equilibration which may affect speciation, but organic phases were shaken for 30 minutes to ensure that equilibrium was reached. It is also unclear whether free or initial ligand concentration has been used for the slope analysis. Using initial TODGA concentrations for the present work rather than equilibrium values increases the slope analysis value to 1.35, so this could be a factor causing the discrepancy. It may be that complex speciation changes drastically with acidity, similar to that seen with nitric acid extraction. The trend from literature and the current data shows that low aqueous acidity favours higher solvate complexes and increasing the acidity leads to a decreasing solvate complex. This rough pattern was observed by Boltoeva et al. (2018) who found that a mixture of mono- and disolvate species were formed at 1 M nitric acid in 1,2-dichloroethane, but only the monosolvate complex was present at 5 M nitric acid. It is clear that TODGA speciation is complex and depends on many factors, but the present data was used to inform uranium loading isotherm models.

4.4.4   Uranium loading isotherms

The theoretical models for uranyl loading shown in Figure 4.8 were constructed using the free ligand concentrations prior to metal extraction determined from the acid extraction isotherms (Figure 4.4A)

and the stoichiometric coefficients determined from the ligand isotherms. The TBP model considered the dual extraction mechanism proposed by the [TBP] isotherm at equal proportion:

$$UO_2^{2+} + 2NO_3^- + \overline{(HNO_3) \cdot (TBP)} \leftrightarrow \overline{HUO_2(NO_3)_3 \cdot TBP}$$

$$UO_2^{2+} + 2NO_3^- + 2\overline{TBP} \leftrightarrow \overline{UO_2(NO_3)_2 \cdot 2TBP}$$
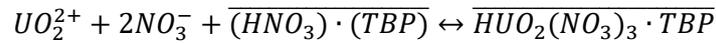
Note that the extra nitrate anion molecule involved in the former reaction scheme is already in the organic phase after pre-equilibration, so nitric acid concentration during metal extraction can still be assumed to be constant. Metal extraction K'_{eq} values were determined from the uranium loading isotherm data by constructing graphs of [products]$_{eq}$ against [reactants]$_{eq}$ and can be seen in Appendix B. The slope of the straight-line portions of these figures was taken to be the respective K'_{eq}. From this, theoretical models were built using Eq 4.9 for given values of $\overline{[UO_2^{2+}]}_{eq}$.

The theoretical models fit the experimental data very well at low loadings (≤ 3 g/L), after which the models significantly underestimate the amount of uranium loaded into the organic phase. This is likely due to the underlying assumptions no longer being valid under high loading conditions, namely, constant aqueous acidity and ionic strength. It is likely that the ligands have higher affinity for uranyl nitrate, and the higher initial metal concentration shifts the equilibrium such that nitric acid bound by ligands from the pre-conditioning is released into the aqueous phase in favour for uranyl nitrate. In this case, acidity and ionic strength can no longer be considered to be constant, free ligand concentrations will vary and the K'_{eq} value will change for two reasons: i) the changing reactant concentration values, and ii) the introduction of a new reaction (the substitution of acid for metal nitrate). Therefore, it is proposed that the reaction schemes at the tested acidities adhere to the following equilibria:

For DHOA:

$$UO_2^{2+} + 2NO_3^- + \overline{2DHOA} \leftrightarrow \overline{UO_2(NO_3)_2 \cdot 2DHOA}$$

$$\overline{(HNO_3)(DHOA)} \leftrightarrow HNO_3 + \overline{DHOA}$$

For TBP:

$$UO_2^{2+} + 2NO_3^- + \overline{2TBP} \leftrightarrow \overline{UO_2(NO_3) \cdot 2TBP}$$

$$UO_2^{2+} + 2NO_3^- + \overline{(HNO_3)(TBP)} \leftrightarrow \overline{HUO_2(NO_3)_3 \cdot TBP}$$

$$\overline{(HNO_3)(TBP)} \leftrightarrow HNO_3 + \overline{TBP}$$

For TODGA:

$$UO_2^{2+} + 2NO_3^- + \overline{TODGA} \leftrightarrow \overline{UO_2(NO_3)_2 \cdot TODGA}$$
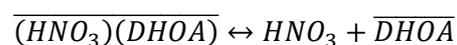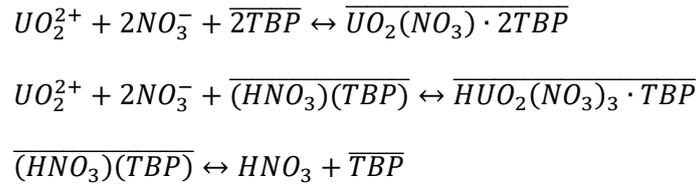
$$\overline{(HNO_3)_2(TODGA)} \leftrightarrow 2HNO_3 + \overline{TODGA}$$
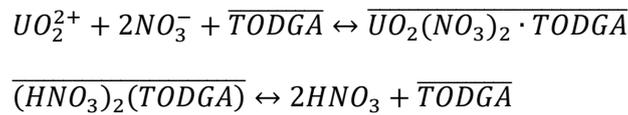
Although TODGA speciation may change with varying conditions as seen previously in the acid extraction and ligand isotherms. It is worth noting that the K_{eq}' values were determined from the slope of the data points which do not deviate from the initial theoretical models (i.e., constant ionic strength). Using the data points at high loading did not produce a linear trend which further supports the changing conditions of the system.

Attempts were made to model these theoretical systems at high uranium loading but the added degrees of freedom from non-constant ionic strength and unknown changes to free ligand concentrations rendered this unsuccessful. However, equilibrium lines were constructed that better fit all the collected data by modifying the amount of extracted acid (Figure 4.8C) to estimate solvent loading capacities and number of mass transfer stages for varying organic/aqueous phase volume ratios which can be seen in Table 4.4. These lines are still based on the initial model equations (assuming constant ionic strength/acidity), so the extrapolations may deviate from true values but are better estimates than the original models.

TBP performs far better at uranium loading than DHOA at the tested ligand concentrations which supports reported literature (Manchanda, et al., 2001); (Manchanda & Pathak, 2004). However, despite the higher performance of TBP, a study by Pathak, et al. (2010) that compared the multi-stage extraction of uranium with 1.1 M DHOA and TBP solvents indicated that both solvents only need 2 contact stages to recover 99.9% from a 300 g/L uranium feed at 4 M nitric acid with an aqueous/organic phase volumetric flowrate ratio of 0.2. In order to compare the present loading data with literature, the modified equilibrium lines in Figure 4.8C were multiplied to account for the different initial ligand

concentrations (Figure 4.13). As determined by Gasparini & Grossi (1986), doubling the monoamide concentration doubles the organic phase capacity and this assumption has been extended to TBP and TODGA. The data indicate that only one stage is required for all three of the tested systems to achieve >95%. This implies that uranium loading may not actually be the main issue with monoamide systems. Using the conditions stated by Pathak et al. (2010) and Figure 4.13, it is predicted that DHOA and TBP systems will recover 99.6% and ≤99.9% uranium respectively, which supports their findings. However, disparity between the solvents is observed by altering the A/O in a given stage. By manipulation of the operating line in Figure 4.13, it is estimated that a 1.1 M DHOA, TBP, or TODGA solvent could achieve an effective separation up to an A/O = 3.5, 8, or 9.5, respectively. This indicates that TBP and TODGA solvents require far less solvent for the same separation efficiencies when compared with DHOA when considering high ligand concentrations or even high metal loadings.

The DHOA loading data fits well with a study by Kumari, et al. (2013) who report 1.1 M DHOA extract 96% and 91.1% of uranium from a feed concentration of 20 g/L and 54.5 g/L respectively in 4 M nitric acid feed with two contact stages and equal aqueous/organic phase volumetric flowrates in a centrifugal contactor. A McCabe-Thiele diagram using Figure 4.13 with these conditions predicts 98.7% and 96.3% respectively; a slight overestimation is expected due to the higher acidity of the present work. The larger degree of deviation from the more concentrated feed may also be attributed to the model equation not accounting for changing ionic strength which would be more prevalent at higher initial uranium feeds. Kumari et al. also report 1.1 M TBP extract 97.6% and 95.4% under the same conditions above and prediction with Figure 4.13 indicates <99.8% recovery. Again, the 20 g/L feed values fit well when accounting for the higher acidity, but there is a larger deviation with the more concentrated initial feed that likely stems from uncertainty in the models. Raut & Mohapatra (2013) report that 1.1 M DHOA extracted 88.2% of uranium from a 10.6 g/L uranium feed at 3 M nitric acid using a single contact and equal aqueous/organic phase volumetric flowrates in a hollow fibre contactor, and 89.6% was predicted with the current data. This all indicates that the present data suitably predicts contact stages for DHOA and TBP systems with feeds at least ≤ 20 g/L uranium (roughly equivalent to the ≤ 3.6 g/L region of Figure 4.8C) but may deviate above this value.

TODGA solvents can load far more uranium and therefore would only require 1 extraction stage to achieve 95% recovery from a 10 g/L feed. This can be attributed to the inherent affinity for uranium from its many oxygen donors and the requirement of only 1 molecule of TODGA per extracted metal ion. Despite this, maximum loading for TODGA solvents is reportedly the same as that for DHOA solvents. It is likely that the loading capacity for TODGA is underestimated due to the changing speciation and extraction mechanisms of TODGA under varying conditions. Post-contact acidity measurements for these isotherms should help clarify this value. No uranyl loading data could be found for TODGA systems in the literature and, while it is likely that the high capacity will result in low numbers of contact stages, there is more uncertainty with these models due to the variability of TODGA speciation with different conditions.
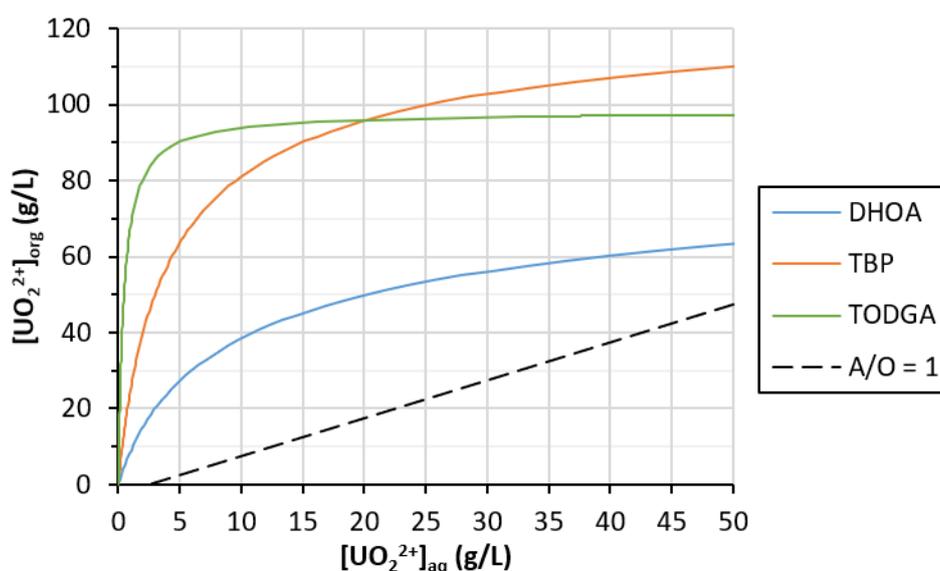
Figure 4.13. *Equilibrium loading models for 1.1 M ligand systems estimated from Figure 4.8C. The dashed line is an example operating line calculated from Eq 4.10 assuming a 50 g/L uranium feed and a desired recovery of 95% at an A/O of 1.*

4.4.5 Influence of ionic strength

Both DHOA and TBP see an increase in uranium distribution as nitrate concentration increases following the shift in equilibrium position from the increased reactant concentrations. Both systems perform better at lower acidities due to the reduced competition from nitric acid. These findings are supported by the reaction mechanism and previous studies looking at influence of ionic strength (Cui, et al., 2005); (Lin, et al., 2005). It has been reported by Gupta, et al. (2000a) that the ion-pair species

$UO_2(NO_3)_3^-\cdot HDHOA^+$ may be prominent at higher nitrate concentrations after they observed decreasing limiting organic content of uranium with DHOA from 3 M nitric acid. The present data does not support this conclusion as the values for slope analysis indicate that there is no increase in nitrate extraction with metal extraction when error is considered. It should be noted that higher initial nitrate concentrations through these tests mean that the free ligand concentrations will not remain constant due to a shift in the acid extraction equilibria; this means that the slope values may not be entirely accurate from a quantitative perspective. However, from a qualitative perspective, the values of these slopes should still at least show an increasing trend toward a value of 3 if the ion-pair complex is being favoured. This is due to the larger dependence on the nitrate stoichiometry relative to ligand concentrations (3:1) and the much larger nitrate concentrations. That said, the present extractions are conducted at low loading to underpin the extraction mechanisms, so perhaps ion-pair complexes are more prevalent in the more complicated, higher metal-loading environments.

While TODGA performs better at higher nitrate concentrations due to the shifted equilibrium as seen in literature (Panja, et al., 2011), there is hardly any change as acidity is reduced from 4 M to 2 M nitric acid when error is considered. This indicates very little competition between the acid and uranyl nitrate for TODGA complexation. It also supports the previous slope analysis results showing that TODGA species with acid and uranyl nitrate have low solvation numbers when compared with that of DHOA and TBP. It is interesting that the slope analysis values are well above 2. As stated previously, these are not true values, but it is indicative of another reaction mechanism involving nitrate anions. It is very unlikely that the diglycolamide is protonated under these conditions, but perhaps the increased nitrate favours a uranyl-nitrate and nitric acid co-extraction like that seen with TBP but without the high acidity requirements.

4.4.6 Job plots

Some previous studies have used a distribution Job plot to attempt to describe complex stoichiometry and extractive behaviour of mixed ligand systems (Gannaz, et al., 2007); (Gullekson, et al., 2017) rather than correlating mole fraction to absorbance/concentration or molar absorptivity (Irving & Edgington, 1959); (Wall, 2017). However, complex stoichiometry cannot be directly determined from a distribution

Job plot, so instead, two Job plots are presented per system. The distribution Job plot describes the performance of the dual-ligand systems relative to expected values assuming independent ligand interactions with changing monoamide mole fraction. The organic uranium content Job plot is directly related to absorbance, similar to the Job plots presented in Chapter 3, and as such describe the speciation of any ternary complexes formed in solution.

The DHOA-TBP distribution Job plot (Figure 4.11A) shows that no mixture of these ligands performs better than pure TBP, however, all mixtures perform better than expected if both ligands are assumed to be independent of each other which indicates a level of synergic interaction. The peak of this synergic interaction is at 20 mol% DHOA. The organic uranium Job plot (Figure 4.11B) hints at a peak around 0.5-0.7 which in turn hints at the formation of (DHOA)(TBP) and (DHOA)$_2$(TBP) solvated uranyl species, however, uncertainty makes it difficult to draw this conclusion definitively. Therefore, it is proposed that the synergic interaction observed in the distribution Job plot is due to phase modifying behaviour of the mixed ligand system rather than the production of a more hydrophobic or stable monoamide complex which supports the findings of Chapter 3. This behaviour may stem from the increased polarity of the DHOA organic phase introduced by the more polar TBP; higher polarity of the organic phase favours the solubility of the uranyl-nitrate-monoamide complex (Musikas, 1987); (Sasaki, et al., 2005). The 20 mol% DHOA – 80 mol% TBP system was selected for Chapter 5 dual-ligand SX tests as a compromise between adequate solvent performance and reduced TBP concentrations. This mixture performed the best after accounting for independent ligand contributions and has comparable performance to pure TBP systems. This solvent also constitutes a 20% decrease in TBP usage which would lessen the amount of secondary phosphate waste formed in reprocessing flowsheets.

The DHOA-TODGA distribution Job plot (Figure 4.12A) shows that uranium extraction is enhanced at low DHOA mole fractions up to ~35 mol% after which pure TODGA systems perform better. Like in the DHOA-TBP system, all mixtures are seen to perform better than expected if independent ligand interactions are assumed. The organic uranium Job plot (Figure 4.12B) peaks between 0.65 and 0.7 which indicates the formation of a (DHOA)$_2$(TODGA) solvated uranyl species; this is in accordance

with the findings of Chapter 3. The large enhancement in distribution at lower DHOA mole fractions must be due to the formation of this complex in the presence of a large excess of TODGA. As TODGA concentrations decrease, less of the ternary complex is formed and a decrease in distribution is observed. The enhanced uranyl extraction is supported by previous literature studying the performance of a DHOA-TODGA mixture in a dynamic extraction process (Raut & Mohapatra, 2013), but no mechanism was proposed to explain this and the enhancement was simply put down to a synergistic interaction or phase modifying effect of DHOA (Ansari, et al., 2009). The 80 mol% DHOA – 20 mol% TODGA system was selected for Chapter 5 dual-ligand SX tests for two main reasons: i) performance is comparable to the previously selected DHOA-TBP system which enables direct comparison, and ii) decreased total TODGA concentrations limits the threat of undesired extraction in a competitive setting.

4.5 Conclusions

The future of nuclear power requires sustainable and economic SNF reprocessing so that usage of the limited amount of available uranium fuel can be maximised. One of the key drawbacks of current reprocessing is the use of TBP which extracts undesired metals, complicates phase separation and results in difficult-to-handle secondary phosphate waste after degraded solvent treatment. Monoamides have been studied as potential TBP replacements due to their i) higher uranium and plutonium selectivity, ii) innocuous degradation products which do not affect phase separations, and iii) adherence to the CHON principle meaning that degraded solvent can be completely incinerated leaving no phosphate residue. However, applications of monoamides to reprocessing are limited due to the lower extraction of uranium attributable to the lower solubility of the uranyl-nitrate-monoamide complex in organic phases. It is hypothesised that the addition of a phosphate or diglycolamide to a monoamide solvent will enhance the extractive performance of monoamides due to the increased polarity of the organic phase (aiding complex solubility) or through synergic complex formation; this is towards the reduction or elimination of phosphates in reprocessing flowsheets.

In order to properly assess these dual-ligand monoamide-phosphate or monoamide-diglycolamide solvents, the single-ligand systems themselves must first be evaluated. A solid basis of data for the single-ligand systems goes on to inform the models used to describe dual-ligand behaviour. This chapter

comprehensively evaluated the extractive performance of DHOA, TBP and TODGA for uranyl nitrate from acidic nitrate media into *n*-dodecane and determines the mechanisms behind extraction. Generally, DHOA and TBP data confirm those found in literature. Both ligands form monosolvate species with nitric acid and TBP is the stronger extractant of acid due to the higher donor strength of the phosphoryl bond. DHOA is shown to form disolvate species with uranyl nitrate in accordance with Chapter 3 and literature. The presence of the monosolvate ion-pair species is discussed and fits literature concentration profiles for aliphatic amides. TBP is shown to form mono- and disolvate complexes with uranyl nitrate at 5.7 M nitric acid. Acidity dependence for DHOA and TBP are similar owing to their similar extraction mechanisms and fit well with published trends. There was no evidence for the presence of the monosolvate ion-pair DHOA complex at high ionic strength solutions, but this may be a symptom of using low uranium loadings for the mechanistic studies. Uranium loading isotherms indicate TBP solvents have a much higher capacity for uranium than DHOA solvents, but consideration of higher ligand concentrations show that this disparity does not generally translate to dynamic multi-stage extractions. Comparison of these conditions to literature values supports this, but higher uranium feeds generally deviate more from expected values. This is attributed to the uncertainty present in the equilibrium models from the changing extraction mechanisms at higher uranium loading in the organic phase.

TODGA behaviour is seen to be much more complicated than the monodentate ligands. Acid extractions indicate $(HNO_3)_2(TODGA)$ and $(HNO_3)_{1.5}(TODGA)$ species are formed dependent on ligand concentration and, likely, initial acidity. TODGA forms monosolvate complexes with uranyl nitrate under the tested conditions which supports some literature and contradicts others. These low solvate complexes and number of hard donor sites are the main factors for the high loading capacity of TODGA solvents. Influence of ionic strength tests indicate that acidity has little effect on uranyl uptake, likely owing to the high capacity of TODGA for both uranium and nitric acid. TODGA is seen to have the same uranium capacity as DHOA solvents, but this value is likely vastly underestimated due to the changing speciation and extraction mechanisms of TODGA under varying conditions. More data is required to adequately describe these parameters.

DHOA-TBP Job plots indicate that the synergic interaction observed between the two ligands is more likely to be due to phase modifying factors rather than the generation of a ternary complex which supports the finding of Chapter 3. This means that sub-hypothesis 3 (concerning monoamide-phosphate dual-ligand synergic systems) can be considered tested and found to be incorrect. However, sub-hypothesis 4 (concerning the phase modifying effect of phosphates on a monoamide solvent) can be tested further. DHOA-TODGA Job plots indicate the formation of a $(DHOA)_2(TODGA)$ ternary uranyl species, which is also in accordance with Chapter 3 findings. This means that sub-hypothesis 2 (concerning monoamide-diglycolamide dual-ligand synergic systems) can be carried forward for further testing. 20 mol% DHOA – 80 mol% TBP and 80 mol% DHOA – 20 mol% TODGA solvents were selected for assessment in dual-ligand extraction scenarios as they both have comparable performance with a pure TBP solvent but with reduced or no amount of phosphorus in the solvent.

CHAPTER 5   Solvent Extraction of Uranyl Nitrate with Dual-Ligand Monoamide Solvents

The aims of this chapter are to confirm the proposed extraction mechanisms for the dual-ligand solvents shown in Chapter 4, and to prove the dual-ligand monoamide solvents can be comparable with Plutonium Uranium Reduction EXtraction (PUREX) solvents in terms of uranium recovery. Within this, the objectives are to:

1. Use single-ligand extraction data to predict dual-ligand solvent performance assuming no synergic effects (i.e. ligand independence).

2. Compare predictions with actual dual-ligand solvent behaviour to qualitatively assess extraction behaviour and explain the observed enhanced extraction.

3. Use slope analysis scenario modelling to quantitatively determine likelihood of proposed extraction models.

4. Compare dual-ligand solvent loading data with a typical PUREX solvent.

To that end, this work further tests sub-hypotheses 2 and 4 in Section 1.3.

5.1   Introduction

A closed nuclear fuel cycle is required to maximise the use of limited global uranium reserves, but current policy is moving away from spent nuclear fuel (SNF) reprocessing due to complexity and costs associated with current PUREX technologies (Bunn, et al., 2005). PUREX uses tri-n-butyl phosphate (TBP) to selectively extract uranium(VI) and plutonium(IV) from dissolved SNF in nitric acid, but the use of the organophosphorus ligand leads to phase-control issues, extra process steps due to undesired extraction, and difficult-to-handle, radioactive secondary phosphate wastes when the degraded solvent is incinerated at end-of-life (Alcock, et al., 1957); (Garraway, 1984); (Phillips, 1992); (Sugai, 1992); (Sugai, et al., 1992); (Todd, et al., 2000); (Herbst, et al., 2011c); (Herbst, et al., 2011d). The reduction or elimination of phosphorus in SNF reprocessing flowsheets would make the process more economically favourable by reducing secondary wastes and the requirement for extra process stripping steps. Monoamides have been studied as potential TBP replacements due to their higher uranium(VI)

and plutonium(IV) selectivity, innocuous degradation products that reduce phase-control issues, and their adherence to the CHON principle (Gasparini & Grossi, 1986); (Musikas, 1987); (Kulkarni, et al., 2006); (Parikh, et al., 2009); (Pathak, et al., 2010). The CHON principle means the ligand is only comprised of carbon, hydrogen, oxygen and/or nitrogen which means the degraded solvent can be incinerated at end-of-life to leave no phosphate residue. Literature identifies N,N-dihexyl octanamide (DHOA) as one of the best monoamide replacements for TBP; the performance of this ligand was explored earlier in Chapter 4. However, monoamide solvents typically have a much lower loading capacity that traditional TBP solvents which impede their application to current industrial processes and requirements (Manchanda, et al., 2001); (Manchanda & Pathak, 2004). The lower loading is attributed to the lower solubility of the uranyl-nitrate-monoamide complex (Musikas, 1987). It follows that uranium recovery with monoamide solvents can be enhanced if either: i) the organic phase can be modified with a suitable ligand to increase the solvent polarity and increase the complex solubility, or ii) the addition of another ligand will form a more hydrophobic ternary complex with the uranyl-nitrate-monoamide species.

Chapter 4 demonstrated that DHOA-TBP and DHOA-TODGA (N,N,N',N'-tetraoctyl diglycolamide) mixed ligand solvent systems can result in enhanced uranium recovery when compared with pure ligand systems. The DHOA-TBP system is aimed towards reduction of phosphorus in PUREX flowsheets and it is proposed that this system improves recovery based on a phase modifying effect rather than the production of a more hydrophobic ternary complex. Both DHOA and TBP have been used as phase modifiers in solvent extraction (SX) systems before (Tachimori, et al., 2002); (Sasaki, et al., 2005); (Ansari, et al., 2009); (Raut & Mohapatra, 2013), but they have not yet been used together to enhance monoamide solvents. The DHOA-TODGA system is aimed towards elimination of phosphorus and it is proposed that this system improves recovery by producing a more hydrophobic ternary complex, namely $UO_2(NO_3)_2 \cdot (DHOA)_2(TODGA)$. DHOA has been used as a phase modifier in TODGA systems that look to recover trivalent lanthanides and actinides from a PUREX raffinate (Tachimori, et al., 2002); ; (Sasaki, et al., 2005); (Raut & Mohapatra, 2013). However, these mixtures have not been used

for uranium recovery and neither has the changing complexation behaviour of these ligand mixtures been studied.

The present work uses data from Chapter 4 to determine the extraction mechanisms for these dual-ligand systems and compare uranyl extraction performance with the typical PUREX solvent. The selected systems to be tested in this work are 20 mol% DHOA – 80 mol% TBP (herein termed 'DHOA-TBP') and 80 mol% DHOA – 20 mol% TODGA (herein termed 'DHOA-TODGA'). These concentrations were selected based on their comparable performance with the pure TBP solvent shown in Chapter 4 and to mitigate potential competition conducted in further tests (particularly with the DHOA-TODGA solvent).

5.2   Experimental Method and Materials

The same experimental methodology used in Chapter 4 was generally used here unless stated otherwise. The main differences for the present experimental tests are the organic phase ligand concentrations which are either 20 mol% DHOA – 80 mol% TBP ('DHOA-TBP') or 80 mol% DHOA – 20 mol% TODGA ('DHOA-TODGA').

5.2.1   Slope analysis modelling

Slope analysis is used throughout this chapter to assess the extraction behaviour of the dual-ligand systems. While a detailed review of this general method is given in Chapter 4.2.3, the application of slope analysis is different in the present chapter. In Chapter 4, slope analysis was used to directly determine the stoichiometric coefficients of a reaction by using a suitable plot of extraction data. This was possible because all relevant solution component concentrations were either directly measurable or inferable from other component concentrations. However, because the dual-ligand systems tested in the present chapter are inherently more complex than single-ligand extractions (leading to a higher degree of freedom in the reaction scheme), normal slope analysis cannot provide the stoichiometry of components as it has done previously. Therefore, slope analysis was instead utilised to determine the validity of a given extraction scenario with a set of defined assumptions. Extraction behaviour of the single-ligand systems from Chapter 4 was used to inform these scenarios and assumptions. If the given

scenario describes the real extraction well, then the slope provided by slope analysis will be predictable. The methods for building these models are described in the following relevant sub-sections.

While slope analysis can be a powerful tool, it is important to consider the weaknesses of this method. In normal slope analysis, the simplistic nature of the method means that it has difficulty dealing with systems that produce more than one species. This phenomenon usually results in the production of non-integer slopes which must be discussed qualitatively. Because this chapter uses slope analysis to determine the validity of a scenario, rather than directly determine stoichiometric coefficients, this is not a weakness that needs to be considered. However, what must be considered is that ionic strength must remain constant throughout the extraction tests. Shifts in ionic strength will shift the equilibrium position of the reaction during extraction tests and this will lead to changing behaviour that cannot be accurately modelled. It is possible to qualitatively assess data with changing ionic strength, like for the ionic strength tests presented in Chapter 4 and later in this chapter, but this assessment must be taken with caution.

5.2.2   Acid extraction and modelling

These tests were conducted to determine whether ligand mixtures enhance the extraction of acid when compared with their respective single-ligand systems. An understanding of the form and amount of acid-ligand species is critical for the further analysis of the metal-ligand species. 0.5 mL of varying total ligand concentrations were shaken with 0.5 mL of 5.6 M nitric acid for 5 minutes. Pre- and post- contact nitric acid concentrations were analysed using a Mettler-Toledo Titrator Excellence T7 auto-titrator by titrating against sodium hydroxide solution that was itself standardised by titration against a known mass of anhydrous potassium hydrogen phthalate (usually 2g) in 40 mL deionised water using the same equipment.

The remainder of this section details how the slope analysis models were constructed for the extraction of nitric acid with the DHOA-TBP and DHOA-TODGA systems. The reactions presented are based on the findings of Chapter 4 data. In the case of the DHOA-TBP system, if no synergism is assumed, then the extraction scenario can be described as Eq. 5.1:

$$HNO_3 + DHOA \leftrightarrow (HNO_3)(DHOA)$$

$$HNO_3 + TBP \leftrightarrow (HNO_3)(TBP)$$

$$\therefore 2HNO_3 + DHOA + TBP \leftrightarrow (HNO_3)(DHOA) + (HNO_3)(TBP) \qquad (Eq\ 5.1)$$

The conditional extraction constant, K'_{eq} (L mol^{-1}), is therefore:

$$K'_{eq} = \frac{\overline{[(HNO_3)(DHOA)]_{eq}}\,\overline{[(HNO_3)(TBP)]_{eq}}}{[HNO_3]^2_{eq}\,\overline{[DHOA]_{eq}}\,\overline{[TBP]_{eq}}} \qquad (Eq.\ 5.2)$$

where subscript *eq* denotes the point of equilibrium and an overbar indicates organic phase species.

Distribution coefficient, D, can be defined as:

$$D = \frac{\overline{[(HNO_3)(DHOA)]_{eq}} + \overline{[(HNO_3)(TBP)]_{eq}}}{[HNO_3]_{eq}} = \frac{\overline{[HNO_3]_{eq}}}{[HNO_3]_{eq}}$$

$$\therefore [HNO_3]_{eq} = \frac{\overline{[HNO_3]_{eq}}}{D} \qquad (Eq\ 5.3)$$

Substituting Eq. 5.3 into Eq. 5.2 yields:

$$K'_{eq} = D\frac{\overline{[(HNO_3)(DHOA)]_{eq}}\,\overline{[(HNO_3)(TBP)]_{eq}}}{[HNO_3]_{eq}\,\overline{[HNO_3]_{eq}}\,\overline{[DHOA]_{eq}}\,\overline{[TBP]_{eq}}}$$

$$\therefore D = \frac{K'_{eq}[HNO_3]_{eq}\,\overline{[HNO_3]_{eq}}\,\overline{[DHOA]_{eq}}\,\overline{[TBP]_{eq}}}{\overline{[(HNO_3)(DHOA)]_{eq}}\,\overline{[(HNO_3)(TBP)]_{eq}}}$$

$$\therefore \log(D) = \log(K'_{eq}) + \log([HNO_3]_{eq}) + \log(\overline{[HNO_3]_{eq}}) + \log([DHOA]_{eq}) +$$

$$\log([TBP]_{eq}) - \log([(HNO_3)(DHOA)]_{eq}) - \log(\overline{[(HNO_3)(TBP)]_{eq}}) \qquad (Eq\ 5.4)$$

If we define the dimensionless coefficient α as:

$$\alpha = \log([HNO_3]_{eq}) + \log(\overline{[HNO_3]_{eq}}) + \log([DHOA]_{eq}) + \log([TBP]_{eq}) -$$

$$\log([(HNO_3)(DHOA)]_{eq}) - \log(\overline{[(HNO_3)(TBP)]_{eq}})$$

then Eq 5.4 becomes:

$$\log(D) = \alpha + \log(K'_{eq}) \qquad (Eq\ 5.5)$$

If the given extraction scenario models the real system well, then plotting $\log(D)$ against α should yield a slope of 1 with an intercept of $\log(K'_{eq})$. α can be calculated from the acid extraction data from the dual-ligand acid extraction tests and data from the single-ligand acid extraction tests.

In the case of DHOA-TODGA systems, if no synergism is assumed, then the extraction scenario can be described as Eq. 5.6:

$$HNO_3 + DHOA \leftrightarrow (HNO_3)(DHOA)$$

$$2HNO_3 + TODGA \leftrightarrow (HNO_3)_2(TODGA)$$

$$\therefore 3HNO_3 + DHOA + TODGA \leftrightarrow (HNO_3)(DHOA) + (HNO_3)_2(TODGA) \qquad (Eq\ 5.6)$$
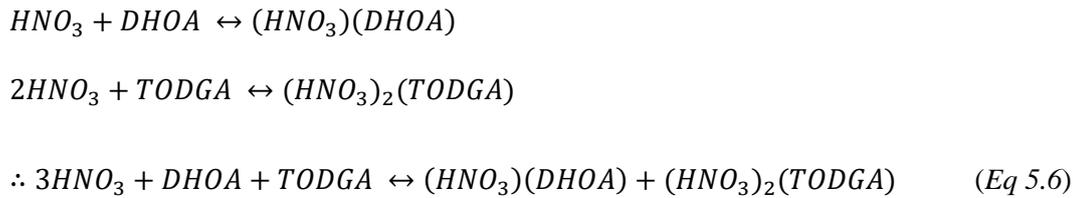
Following the same procedure as above, it can be found that:

$$\log(D) = \log(K'_{eq}) + 2\log([HNO_3]_{eq}) + \log(\overline{[HNO_3]_{eq}}) + \log([DHOA]_{eq}) +$$

$$\log([TODGA]_{eq}) - \log([(HNO_3)(DHOA)]_{eq}) - \log(\overline{[(HNO_3)(TODGA)]_{eq}}) \quad (Eq\ 5.7)$$

If we define dimensionless coefficient β as:

$$\beta = 2\log([HNO_3]_{eq}) + \log(\overline{[HNO_3]_{eq}}) + \log([DHOA]_{eq}) + \log([TODGA]_{eq}) -$$

$$\log([(HNO_3)(DHOA)]_{eq}) - \log(\overline{[(HNO_3)(TODGA)]_{eq}})$$

then Eq 5.7 becomes:

$$\log(D) = \beta + \log(K'_{eq}) \qquad\qquad (Eq\ 5.8)$$

Like before, the slope of $\log(D)$ against β should be 1 if the given scenario fits the real extraction well. β can be calculated from the acid extraction data from the dual-ligand acid extraction tests and data from the single-ligand acid extraction tests.

5.2.3 Influence of acidity

0.5 mL of pre-equilibrated 0.2 M total ligand in *n*-dodecane was hand shaken with 500 ppm uranyl nitrate in varying concentrations of nitric acid. Pre- and post-contact uranyl solutions were analysed using the arsenazo(III) method outlined in Chapter 4.2.2. These tests were conducted to determine

whether uranium extraction is enhanced or diminished between 0.1 M and 8 M nitric acid when compared with previous single-ligand studies. They are also used to assess organic phase stability within this range.

'Expected' extraction (indicated by subscript 'exp') at each pH point was calculated assuming no mixed-ligand interaction from single-ligand extraction data using Eq. 5.9:

$$\overline{[UO_2^{2+}]}_{exp,eq,Dual-ligand} = x\overline{[UO_2^{2+}]}_{eq,Ligand\ 1} + y\overline{[UO_2^{2+}]}_{eq,Ligand\ 2} \qquad (Eq.\ 5.9)$$

where subscript $Dual - ligand$, $Ligand\ 1$ and $Ligand\ 2$ refer to the dual-ligand system and each of the suitable single-ligand systems, x is the mole fraction of ligand 1 and y is the mole fraction of ligand 2. The resultant organic uranium concentration (ppm) was used to calculate extraction percentage ($E\%$) and D using the initial aqueous uranium concentration from the single-ligand studies. Mean averages of these values were taken in the case that they were different.

5.2.4 [Total ligand] isotherms and modelling

0.5 mL of pre-equilibrated organic phase containing varying total ligand (0.05 - 0.6 M) in n-dodecane was hand shaken with 500 ppm uranyl nitrate in 5.6 M nitric acid. Pre- and post-contact uranyl solutions were analysed using the arsenazo(III) method. These tests were conducted to validate the proposed complex speciation from the Job plots in Figures 4.11 and 4.12 in Chapter 4. As stated in Section 5.2.1, the complexity of these systems means that slope analysis cannot provide stoichiometric values. Therefore, like for the acid extraction analysis, slope analysis was instead used to determine the validity of a given extraction scenario. If the scenario describes the real extraction well, then the slope generated from slope analysis should be predictable. Three different extraction scenarios were tested as outlined in Table 5.1 which were informed by the single-ligand extraction mechanisms determined from Chapter 4. The construction of these scenario models is outlined below.

Table 5.1. *General extraction scenarios constructed for the dual-ligand ligand isotherms.*

Scenario	Assumption(s)	Systems tested
1	Only single-ligand complex formation	DHOA-TODGA, DHOA-TBP
2	Only dual-ligand complex formation	DHOA-TODGA
3	Both single- and dual-ligand complex formation	DHOA-TODGA

DHOA-TODGA Scenario 1 was modelled using findings from single-ligand isotherm data:

$$UO_2^{2+} + 2(NO_3) + 2DHOA \leftrightarrow UO_2(NO_3)_2 \cdot 2DHOA$$

$$UO_2^{2+} + 2(NO_3) + TODGA \leftrightarrow UO_2(NO_3)_2 \cdot TODGA$$

$$\therefore 2UO_2^{2+} + 4(NO_3) + 2DHOA + TODGA \leftrightarrow UO_2(NO_3)_2 \cdot 2DHOA + UO_2(NO_3)_2 \cdot TODGA$$
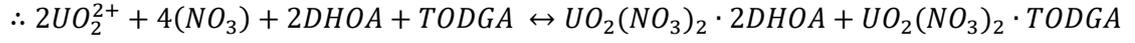
Using the same methodology as with the acid extraction analysis, it can be found that:

$$\log(D) = \gamma_1 + c_1 \qquad\qquad (Eq.\ 5.10)$$

where the dimensionless coefficient γ_1 is defined as:

$$\gamma_1 = \log\left(\overline{[UO_2^{2+}]_{eq}}\right) + \log\left([UO_2^{2+}]_{eq}\right) + 2\log\left(\overline{[DHOA]_{eq}}\right) + \log\left(\overline{[TODGA]_{eq}}\right) -$$
$$\log\left(\overline{[UO_2(NO_3)_2 \cdot 2DHOA]}\right) - \log\left(\overline{[UO_2(NO_3)_2 \cdot TODGA]}\right)$$

and the dimensionless intercept c_1 is defined as:

$$c_1 = \log\left(K'_{eq}\right) + 4\log\left([NO_3^-]\right)$$

If this scenario is representative of the real extraction, a plot of $\log(D)$ against γ_1 should yield a slope of 1. For these calculations, it was assumed that both ligands extract independent of each other. Therefore, single-ligand isotherm data was used to calculate the amount of free ligand at each tested ligand concentration.

DHOA-TODGA Scenario 2 was modelled using the finding from Chapter 4 Jobs plots:

$$UO_2^{2+} + 2(NO_3) + 2DHOA + TODGA \leftrightarrow UO_2(NO_3)_2 \cdot 2DHOA \cdot TODGA$$

Therefore:

$$\log(D) = \gamma_2 + c_2 \qquad\qquad (Eq\ 5.11)$$

where the dimensionless coefficient γ_2 is defined as:

$$\gamma_2 = 2\log\left(\overline{[DHOA]_{eq}}\right) + \log\left(\overline{[TODGA]_{eq}}\right)$$

and the dimensionless intercept c_2 is defined as:

$$c_2 = \log(K'_{eq}) + 2\log([NO_3^-])$$

If this scenario is representative of the real extraction, a plot of $\log(D)$ against γ_2 should yield a slope of 1. As the only reaction here is adduct-forming, it is similar to single-ligand slope analysis. Equilibrium free ligand concentrations were calculated using the initial free ligand concentrations calculated from the DHOA-TODGA acid extraction tests and the resultant $\overline{[U]}_{eq}$ from the present test.

DHOA-TODGA Scenario 3 was modelled using both reaction pathways from the previous two models:

$$UO_2^{2+} + 2(NO_3) + 2DHOA \leftrightarrow UO_2(NO_3)_2 \cdot 2DHOA$$

$$UO_2^{2+} + 2(NO_3) + TODGA \leftrightarrow UO_2(NO_3)_2 \cdot TODGA$$

$$UO_2^{2+} + 2(NO_3) + 2DHOA + TODGA \leftrightarrow UO_2(NO_3)_2 \cdot 2DHOA \cdot TODGA$$

$$\therefore 3UO_2^{2+} + 6(NO_3) + 4DHOA + 2TODGA \leftrightarrow UO_2(NO_3)_2 \cdot 2DHOA +$$

$$UO_2(NO_3)_2 \cdot TODGA + UO_2(NO_3)_2 \cdot 2DHOA \cdot TODGA$$
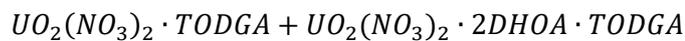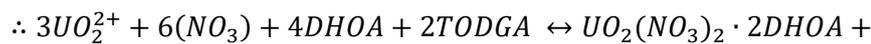
Therefore:

$$\log(D) = \gamma_3 + c_3 \qquad\qquad (Eq\ 5.12)$$

where the dimensionless coefficient γ_3 is defined as:

$$\gamma_3 = \log(\overline{[UO_2^{2+}]}_{eq}) + 2\log([UO_2^{2+}]_{eq}) + 4\log(\overline{[DHOA]}_{eq}) + 2\log(\overline{[TODGA]}_{eq}) -$$

$$\log(\overline{[UO_2(NO_3)_2 \cdot 2DHOA]}_{eq}) - \log(\overline{[UO_2(NO_3)_2 \cdot TODGA]}_{eq}) -$$

$$\log(\overline{[UO_2(NO_3)_2 \cdot 2DHOA \cdot TODGA]}_{eq})$$

and the dimensionless intercept c_3 is defined as:

$$c_3 = \log(K'_{eq}) + 6\log([NO_3^-])$$

If this scenario is representative of the real extraction, a plot of $\log(D)$ against γ_3 should yield a slope of 1. Modelling this system is more complex than those previously as there is no available data on the ratios of the produced species. To decrease the degrees of freedom in the model, it was initially assumed

that concentrations of the three generated complexes would be proportional to initial ligand concentration. This was not found to be the case as no successful model could be generated.

Hence, the Microsoft Excel GRG Nonlinear Solver was employed to refine variables to find a scenario where these three complexes could be produced. To this end, it was first assumed that the summation of the three newly generated complex concentrations at each tested extraction system (i.e., data point) equalled the $\overline{[UO_2^{2+}]_{eq}}$ measured for that system. Each of the three newly generated complexes was assigned a 'concentration factor' (CF) for each data point, which was a value between 0 and 1. For each point, the CFs of all three species must sum to 1, i.e., complex concentrations equal 100% of measured $\overline{[UO_2^{2+}]_{eq}}$ for that point. The calculated concentration of each complex at a given point was then found to be the product of the suitable CF with $\overline{[UO_2^{2+}]_{eq}}$ at that point. These values were calculated over the collected data set for the [ligand] isotherm and allowed for the calculation of free ligand concentrations. From these values, γ_3 was calculated and plotted against log(D). The linear trendline slope and R^2 value of this plot was also calculated. Up until this point, the assigned CFs were arbitrary, so the GRG Nonlinear Solver in Microsoft Excel was used to refine these CFs to satisfy the requirement that the slope of log(D) against γ_3 trendline have an $R^2 > 0.999$. This was chosen as it would mean that the outputted model data points would fit well along a linear trend. Additional constraints were set to ensure that the CF values were between 0.0001 (a sufficiently low but non-zero value) and 1; this was to avoid nonsensical conditions in the produced model. Unlike previous models, the outcome of this model was to determine if there were a set of CFs that would result in Scenario 3 being feasible, rather than directly determining whether Scenario 3 was feasible in itself. The resultant CFs were converted into complex concentration profiles and compared with previous data to determine viability.

DHOA-TBP Scenario 1 was modelled using findings from single-ligand isotherm data:

$$UO_2^{2+} + 2(NO_3) + 2DHOA \leftrightarrow UO_2(NO_3)_2 \cdot 2DHOA$$

$$UO_2^{2+} + 2(NO_3) + TBP \leftrightarrow UO_2(NO_3)_2 \cdot TBP$$

$$UO_2^{2+} + 2(NO_3) + 2TBP \leftrightarrow UO_2(NO_3)_2 \cdot 2TBP$$

$$\therefore 3UO_2^{2+} + 6(NO_3) + 2DHOA + 3TBP \leftrightarrow UO_2(NO_3)_2 \cdot 2DHOA + UO_2(NO_3)_2 \cdot TBP +$$
$$UO_2(NO_3)_2 \cdot 2TBP$$

Therefore:

$$\log(D) = \delta + c_3 \qquad\qquad (Eq.\ 5.13)$$

where the dimensionless coefficient δ is defined as:

$$\delta = \log\left(\overline{[UO_2^{2+}]_{eq}}\right) + 2\log\left([UO_2^{2+}]_{eq}\right) + 2\log\left(\overline{[DHOA]_{eq}}\right) + 3\log\left(\overline{[TBP]_{eq}}\right) -$$
$$\log\left(\overline{[UO_2(NO_3)_2 \cdot 2DHOA]}\right) - \log\left(\overline{[UO_2(NO_3)_2 \cdot TBP]}\right) - \log\left(\overline{[UO_2(NO_3)_2 \cdot 2TBP]}\right)$$

and the dimensionless intercept c_3 is the same as that in DHOA-TODGA Scenario 3.
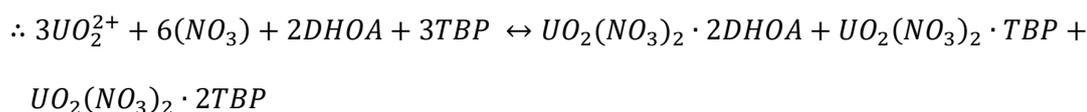
If this scenario is representative of the real extraction, a plot of $\log(D)$ against δ should yield a slope of 1. For these calculations, it was assumed that both ligands extract independent of each other. Therefore, single-ligand isotherm data was used to calculate the amount of free ligand at each tested ligand concentration. No other extraction scenarios were modelled for the DHOA-TBP system.

5.2.5   Uranium loading isotherms

0.5 mL of pre-equilibrated 0.2 M total ligand in *n*-dodecane was shaken with varying concentrations of uranyl nitrate (300-10,000 ppm) in 5.6 M nitric acid. Pre- and post-contact uranyl solutions were analysed using the arsenazo(III) method. These tests were conducted to assess loading of the tested systems and to inform required extraction stages determined from a McCabe-Thiele diagram. Operating lines for the McCabe-Thiele diagram were determined using Equation 4.10 along with suitable process conditions that are defined where necessary. Isotherm loading models were constructed according to the reaction mechanisms determined by previous experiments. Models assumed that acidity, ionic strength, and temperature remained constant and that the phases were immiscible.

The DHOA-TBP model assumed that the ratios of formed complexes did not change with varying initial uranyl concentration. The concentration ratios of the complexes formed in this system were determined from the dual-ligand [ligand] isotherm data. Free ligand concentrations were determined by subtracting

metal-bound and acid-bound ligand concentrations from the initial value. From this, K'_{eq} can be determined. The DHOA-TBP isotherm model used was Eq. 5.14:

$$[UO_2^{2+}]_{eq} = \sqrt[3]{\frac{\overline{[UO_2(NO_3)_2 \cdot 2DHOA]_{eq}}\ \overline{[UO_2(NO_3)_2 \cdot TBP]_{eq}}\ \overline{[UO_2(NO_3)_2 \cdot 2TBP]_{eq}}}{K'_{eq}[NO_3^-]_{eq}^6 \overline{[DHOA]_{eq}^2}\overline{[TBP]_{eq}^3}}}$$ (Eq. 5.14)

Complex concentrations were calculated for a given $\overline{[UO_2^{2+}]_{eq}}$. Free ligand concentrations were determined by taking account of this metal-bound ligand as well as acid-bound ligand.

For the DHOA-TODGA model, it was initially assumed that the ratios of formed complexes also did not change with varying initial uranyl concentration. Modelling attempts with this assumption were unsuccessful as no viable K'_{eq} could be determined, so it was then assumed that the ratios of formed complexes varied with varying uranyl concentration. To account for this, CFs were approximated using linear interpolation from the DHOA-TODGA [ligand] isotherm data using the ratio of total ligand to initial uranyl concentration as a basis. However, no viable K'_{eq} value could be determined from this methodology either and the implications of this are discussed later in Section 5.4.4.

5.2.6 Influence of ionic strength

0.5 mL of pre-equilibrated 0.2 M total ligand in *n*-dodecane was shaken with 500 ppm uranyl nitrate in 2, 3 and 4 M nitric acid at varying concentrations of nitrate between 2 – 7 M. Nitrate concentrations were controlled through addition of sodium nitrate. Pre- and post-contact uranyl solutions were analysed using the arsenazo(III) method. These tests were conducted to determine whether uranium extraction is enhanced through addition of nitrate when compared with previous single-ligand studies. Expected extraction at each nitrate concentration was calculated assuming no mixed-ligand interaction from single-ligand extraction data using Eq. 5.9 similar to the analysis for influence of pH.

5.3 Results

Most figures in this chapter compare observed behaviour of the dual-ligand systems with their expected behaviour. In all of these cases, expected behaviour assumes that the two extracting ligands behave completely independently of each other when extracting nitric acid or uranyl nitrate. Expected

behaviour was determined using a mass balance from suitable extraction data from the single-ligand systems presented in Chapter 4 like that described by Equation 5.9.

Figure 5.1A shows the expected and observed nitric acid extraction isotherms for the 0.2 M DHOA-TBP system. The isotherms lie largely within error of each other indicating that the ligands do indeed behave independent of one another in terms of nitric acid extraction. The slope of 1.09 from the scenario slope analysis using Equation 5.5 and presented in Figure 5.1B confirms this (a slope of 1 would indicate a perfectly modelled system); values derived from this slope analysis are presented in Table 5.2.
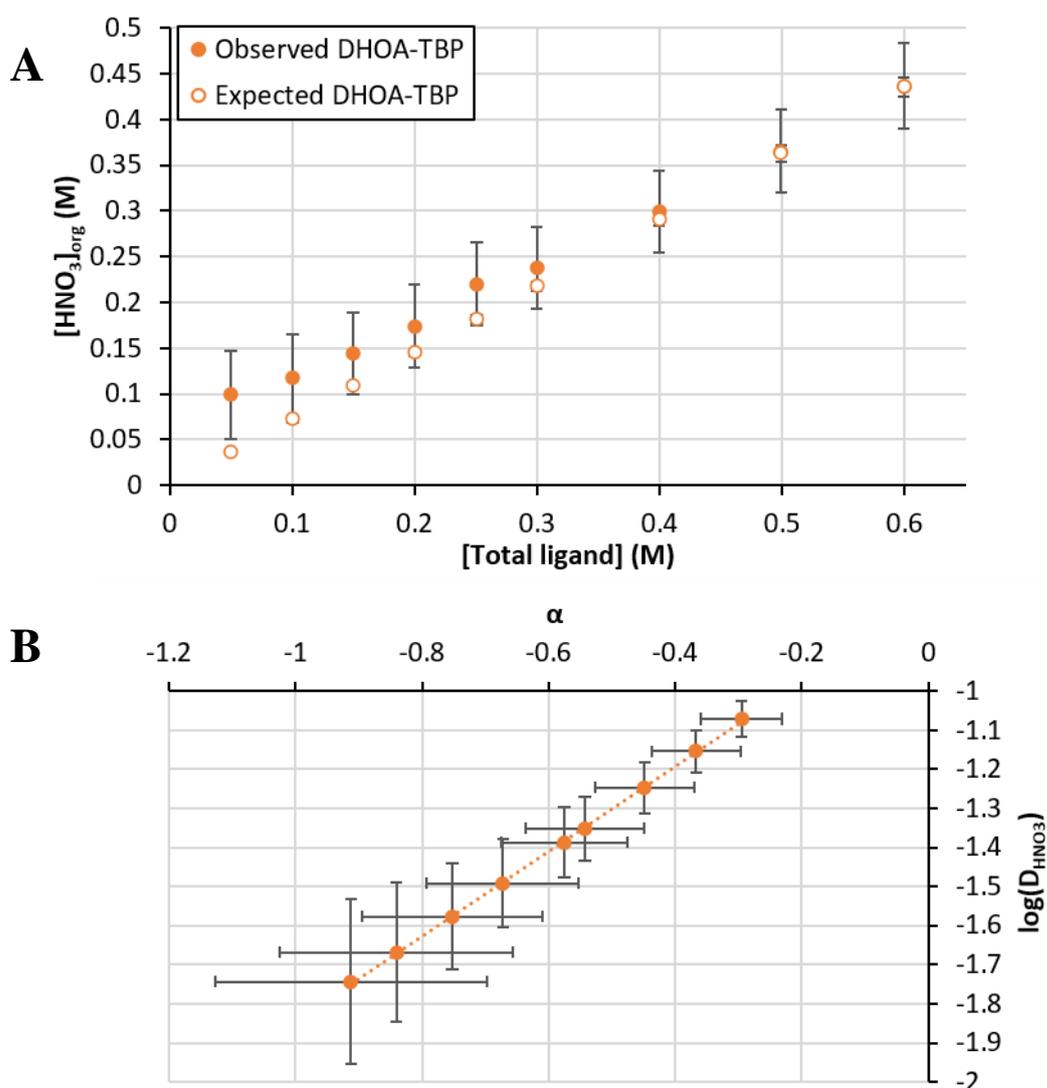
Figure 5.1. *Nitric acid A) extraction isotherms and B) scenario slope analysis using Equation 5.5 for 20 mol% DHOA- 80 mol% TBP at 0.2 M total ligand from 5.58 M HNO3 at 21±2°C.*

Table 5.2. *Scenario slope analysis values determined for nitric acid extraction with the DHOA-TBP and DHOA-TODGA systems from 5.58 M nitric acid at 21±2°C.*

System	Slope	Intercept	R^2
DHOA-TBP	1.09 ± 0.02	-0.76 ± 0.01	0.9997
DHOA-TODGA	0.999 ± 0.008	-1.284 ± 0.002	0.9999

Figure 5.2A shows the expected and observed nitric acid extraction isotherms for the 0.2 M DHOA-TODGA system. As with the DHOA-TBP extractions, the expected isotherm lies within error of the observed behaviour which indicates these ligands also behave independently when extracting nitric acid. The slope of 0.999 from the scenario slope analysis using Equation 5.8 and presented in Figure 5.2B also confirms this; values derived from slope analysis are presented in Table 5.2.
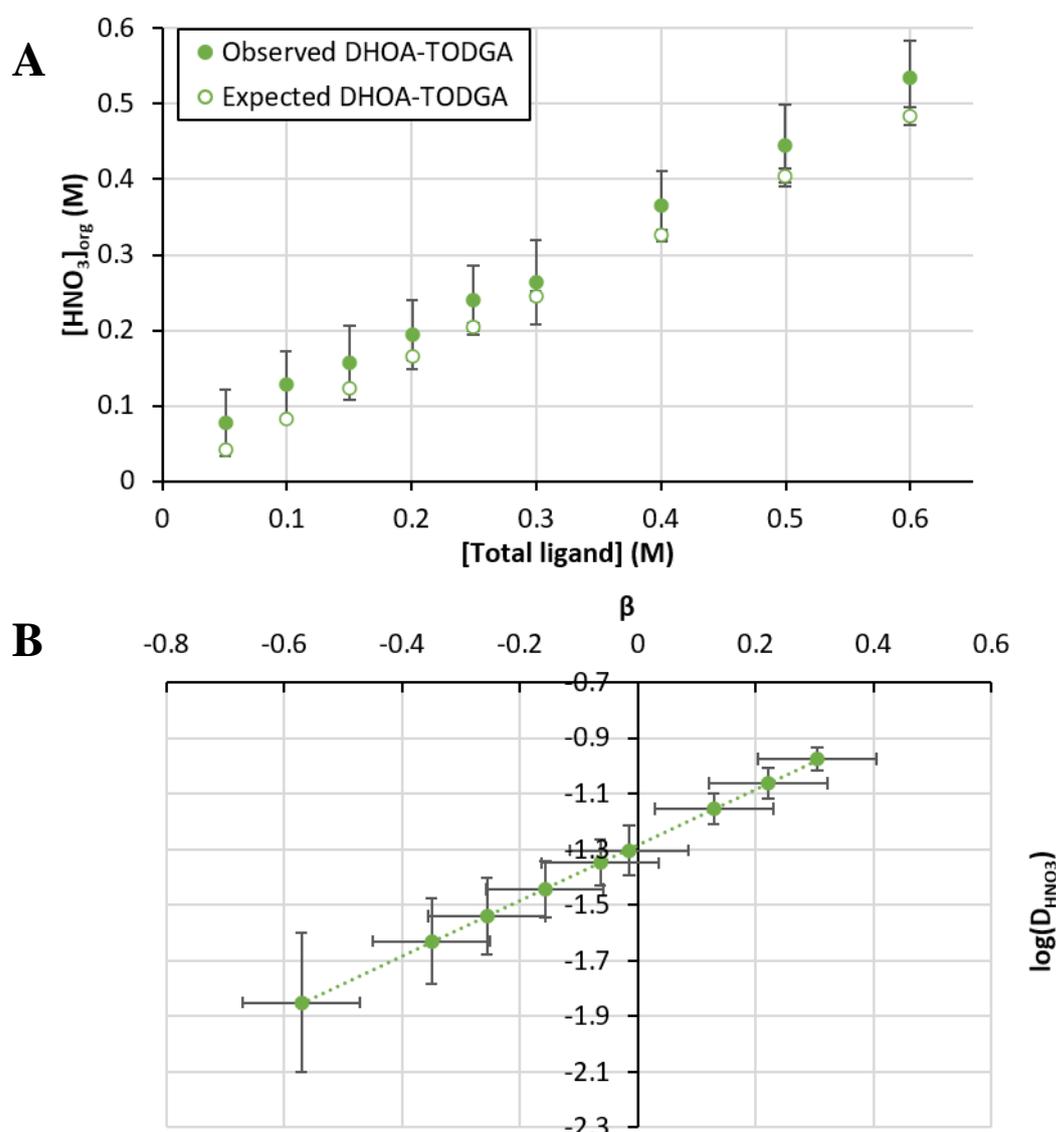
Figure 5.2. *Nitric acid A) extraction isotherms and B) scenario slope analysis using Equation 5.8 for 80 mol% DHOA- 20 mol% TODGA at 0.2 M total ligand from 5.58 M HNO3 at 21±2°C.*

Figure 5.3 shows the expected and observed extraction and distribution of uranyl nitrate with varying acidity for the 0.2 M DHOA-TBP system. Both profiles share similar shapes and both peak around 5.5 M nitric acid. Observed extraction in Figure 5.3A is as expected when acidity is ≤ 1 M which indicates the ligands behave completely independently at these conditions. As acidity increases, an enhancement in uranium distribution is observed with the dual-ligand system in Figure 5.3B by as much as 38% between 3 and 4 M nitric acid. Peak observed extraction at ~5.5 M nitric acid is 27% higher than expected.
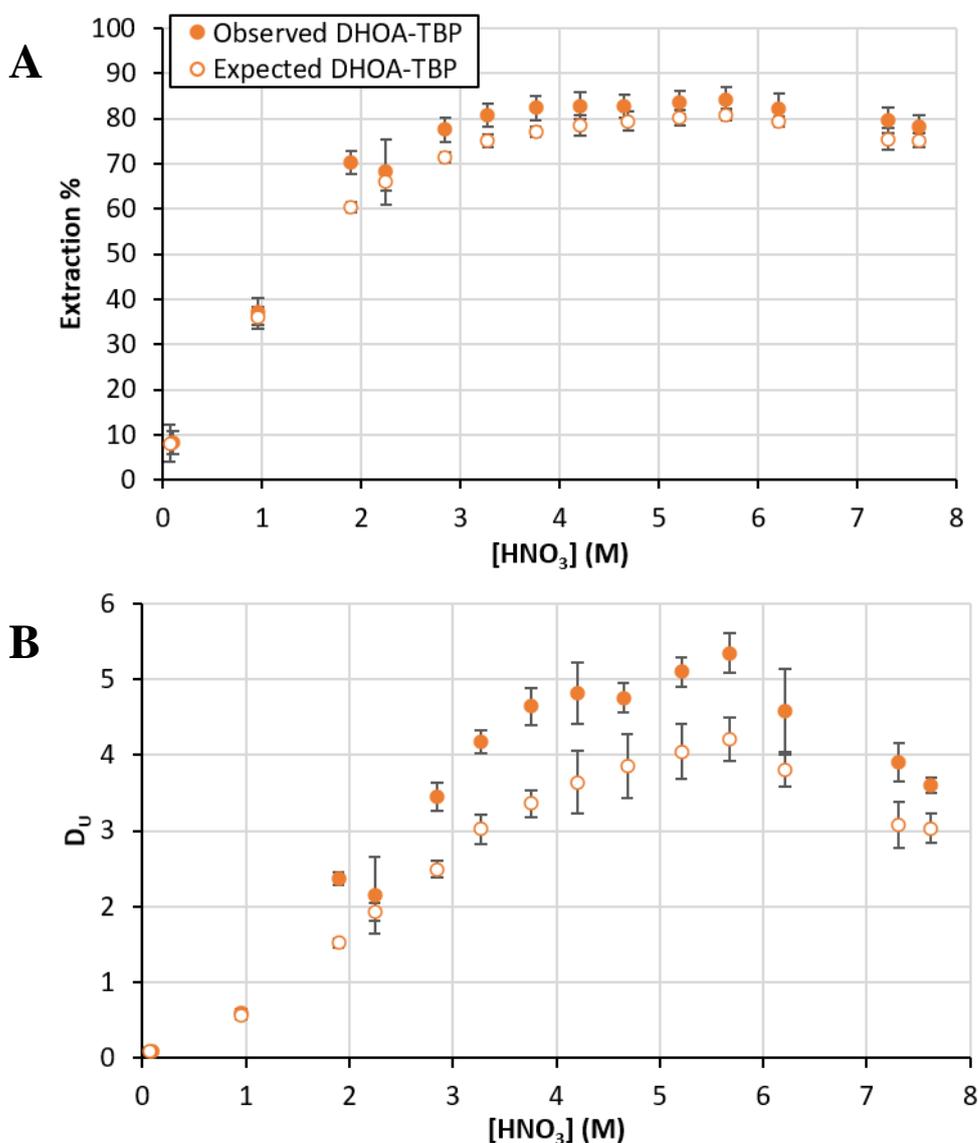
Figure 5.3. *pH profiles of uranyl nitrate A) extraction and B) distribution coefficient by 20 mol% DHOA- 80 mol% TBP at 0.2 M total ligand and 21±2°C. Initial [uranium] = 490±10 ppm.*

Figure 5.4 shows the expected and observed extraction percentage and distribution of uranyl nitrate with varying acidity for the 0.2 M DHOA-TODGA system. The dual-ligand system distribution does not peak as expected and instead continues to increase with increasing acidity. As seen with the DHOA-TBP system, observed extraction in Figure 5.4A is as expected when acidity is ≤ 1 M which indicates the ligands behave completely independently at these conditions. After this point, observed uranium distribution in Figure 5.4B is consistently enhanced over expected values by as much as 490% at the highest tested acidity. It is likely that distribution is even more enhanced at > 8 M nitric acid, but these conditions were deemed too extreme for industrial processing equipment and were not tested. It should be noted that the phase splitting issues observed previously with the TODGA solvents were not observed with this dual-ligand solvent.
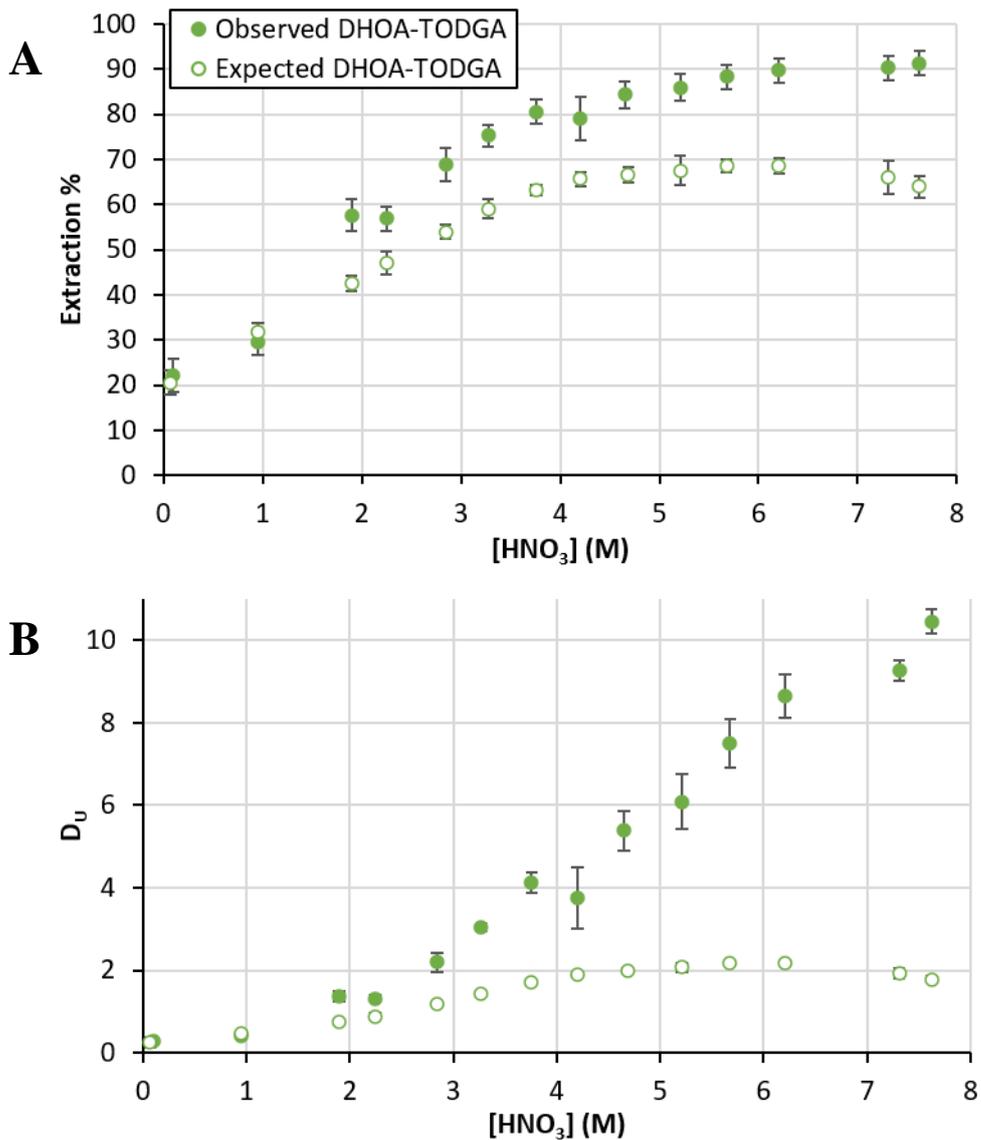
Figure 5.4. *pH profiles of uranyl nitrate A) extraction and B) distribution coefficient by 80 mol% DHOA- 20 mol% TODGA at 0.2 M total ligand and 21±2°C. Initial [uranium] = 490±10 ppm.*

Figure 5.5A and B show the expected and observed extraction and distribution of uranyl nitrate with varying total ligand concentrations for the DHOA-TBP system at 5.6 M nitric acid. Observed extraction is consistently higher than expected when assuming independent ligand interactions, but large uncertainty in the expected extraction at total ligand concentrations > 0.4 M makes it impossible to confirm this trend at these conditions. Before the uncertainty overtakes the trend, observed distribution is 40-46% higher than expected indicating a generally consistent boost to uranyl extraction from the presence of the dual-ligand solvent. Figure 5.5C shows the scenario slope modelling using Equation 5.13 which assumes no dual-ligand complex formation; the slope of 0.98 indicates that this model adequately describes the extraction mechanism (Table 5.3).

Table 5.3. *Scenario slope analysis values determined for uranyl nitrate extraction from the DHOA-TBP and DHOA-TODGA [ligand] isotherms from 5.58 M nitric acid at 21±2°C.*

System	Scenario	Slope	Intercept	R^2
DHOA-TBP	1	0.98 ± 0.09	8.3 ± 0.2	0.9893
DHOA-TODGA	1	-7.6 ± 0.8	-34 ± 4	0.9874
	2	0.49 ± 0.01	3.24 ± 0.06	0.9989
	3	1.02 ± 0.02	10.1 ± 0.2	0.9992
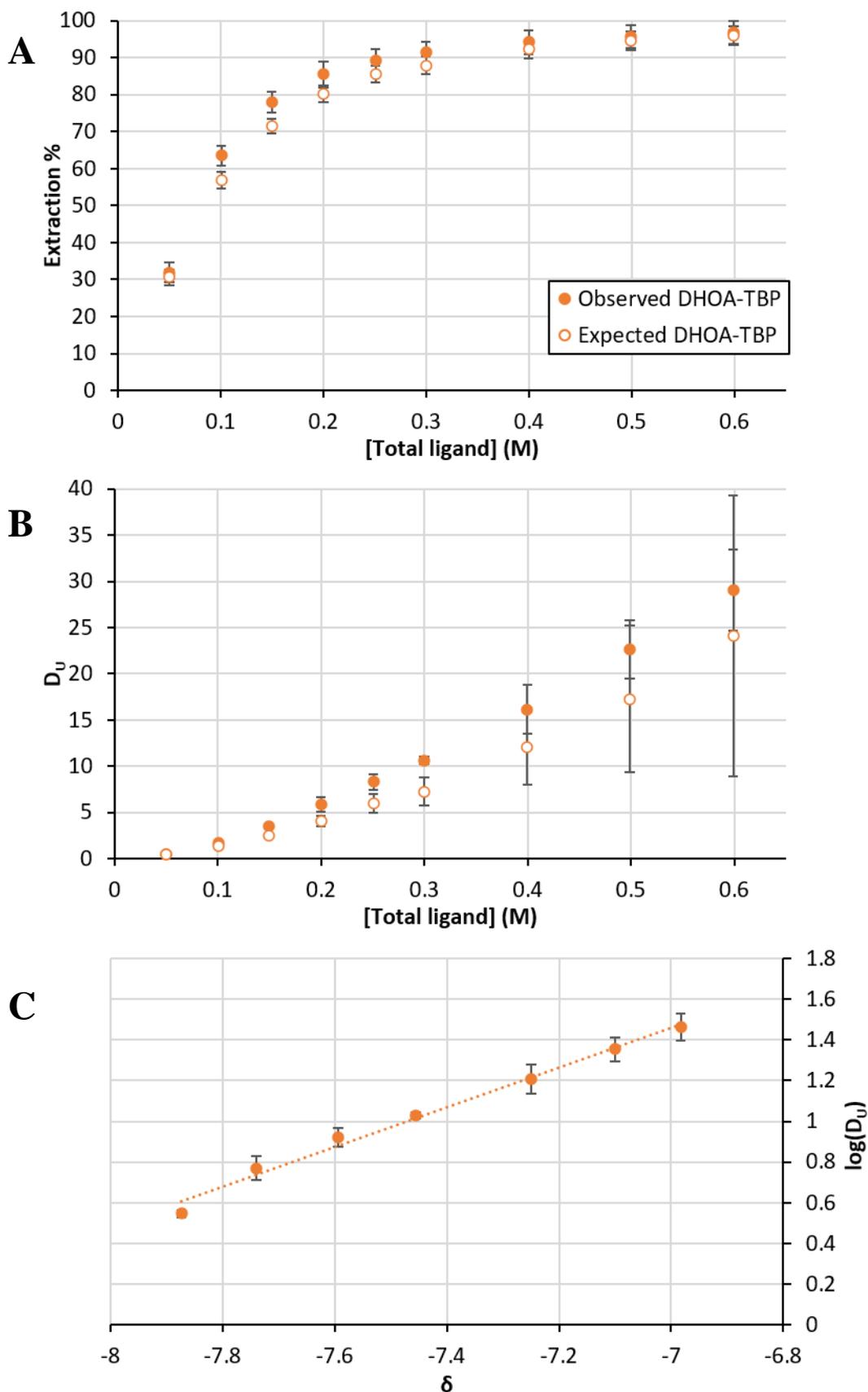
Figure 5.5. *[Total ligand] isotherm of expected and observed uranyl nitrate A) extraction and B) distribution coefficient by 20 mol% DHOA- 80 mol% TBP from 5.58 M nitric acid at 21±2°C. Initial [uranium] = 480±10 ppm. C) shows the scenario slope analysis of DHOA-TBP Scenario 1 determined from Equation 5.13.*

Figure 5.6 shows the expected and observed extraction and distribution of uranyl nitrate with varying total ligand concentrations for the DHOA-TODGA system at 5.6 M nitric acid. Like with the DHOA-TBP system, observed extraction is consistently higher than expected even after accounting for the large uncertainty in observed measurements at high ligand concentration; this large uncertainty comes from the very small raw absorbance readings. Before the large uncertainties, observed distribution is seen to increase up to 300% higher than expected which indicates a significant enhancement with the dual-ligand system.
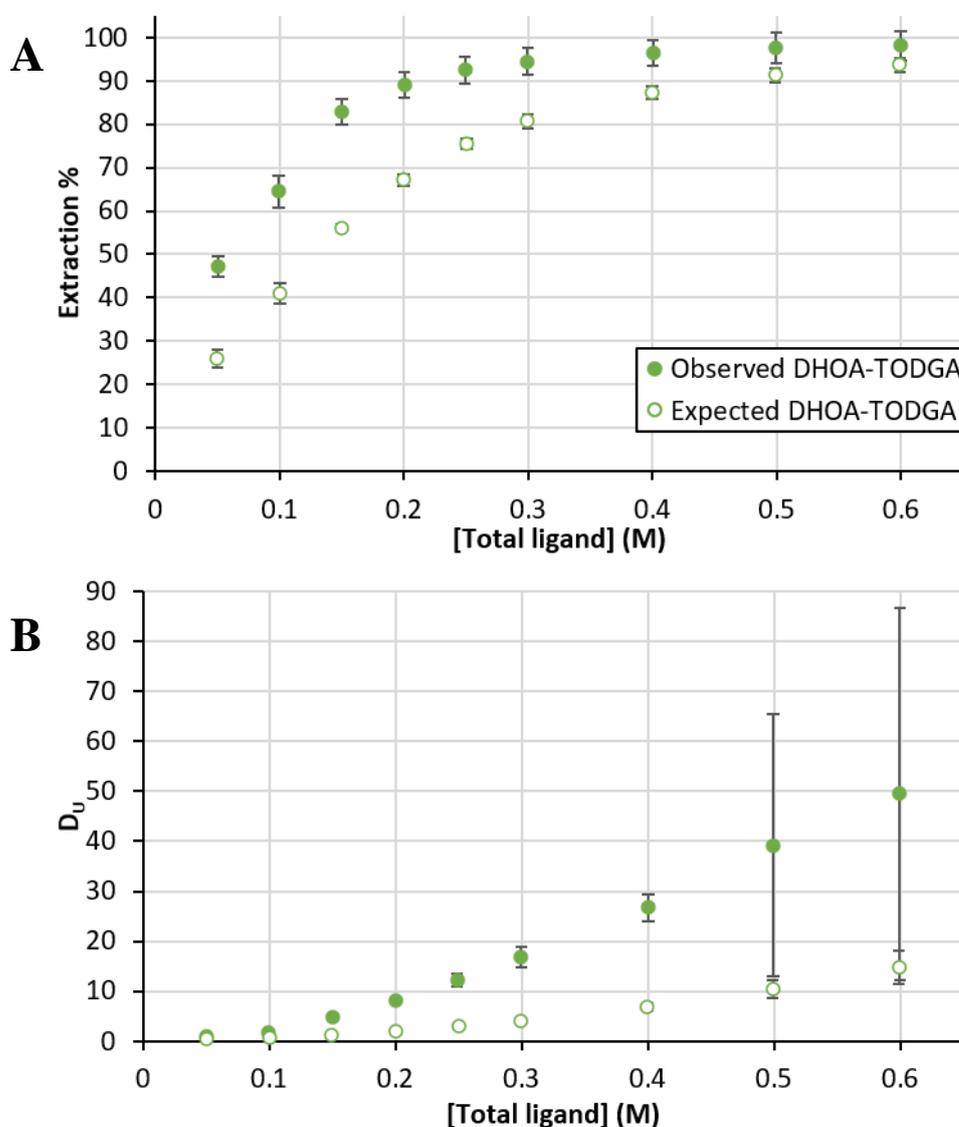
Figure 5.6. *[Total ligand] isotherm of expected and observed uranyl nitrate A) extraction and B) distribution coefficient by 80 mol% DHOA- 20 mol% TODGA from 5.58 M nitric acid at 21±2°C. Initial [uranium] = 480±10 ppm.*
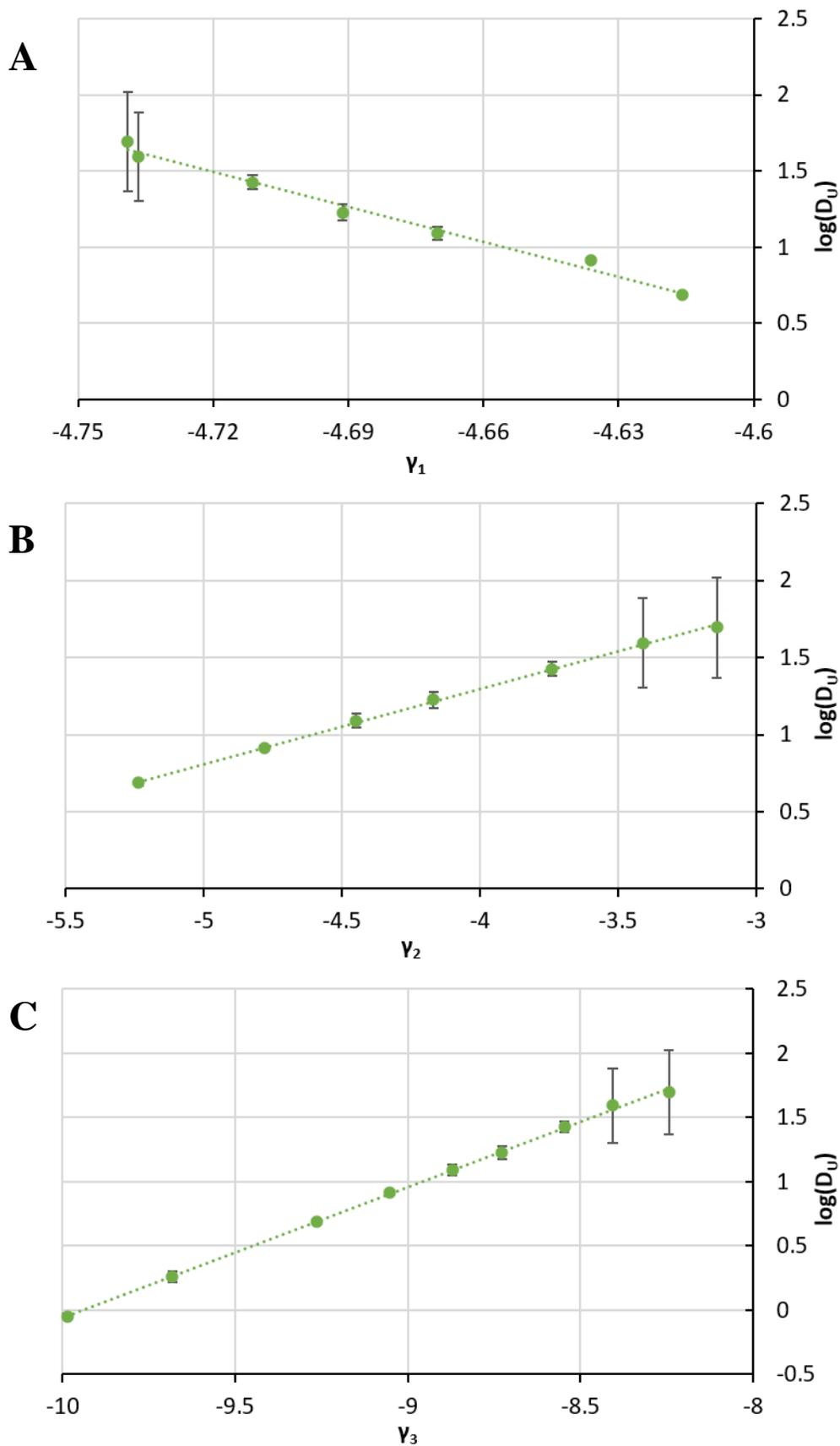
Figure 5.7. *Scenario slope analyses of the [total ligand] isotherm of 80 mol% DHOA- 20 mol% TODGA from 5.58 M nitric acid at 21±2°C determined from A) Scenario 1 (Equation 5.10), B) Scenario 2 (Equation 5.11) and C) Scenario 3 (Equation 5.12).*

Figure 5.7 shows the scenario slope modelling conducted using Equations 5.10-12; values derived from these slope analyses are presented in Table 5.3. It can be seen that no synergistic interaction (Scenario 1, Figure 5.7A) and only synergistic interaction (Scenario 2, Figure 5.7B) do not adequately describe the extraction mechanism. However, the slope of 1.02 for the mixture of species scenario indicates that this model does describe the extraction well (Scenario 3, Figure 5.7C).

Figure 5.8 shows the concentrations profiles of the complexes modelled in Scenario 3 and indicates that the dual-ligand complex is in large abundance at low total ligand concentrations. As total ligand concentration increases, the concentration of the dual-ligand species decreases as other single-ligand complexes are also formed in solution.
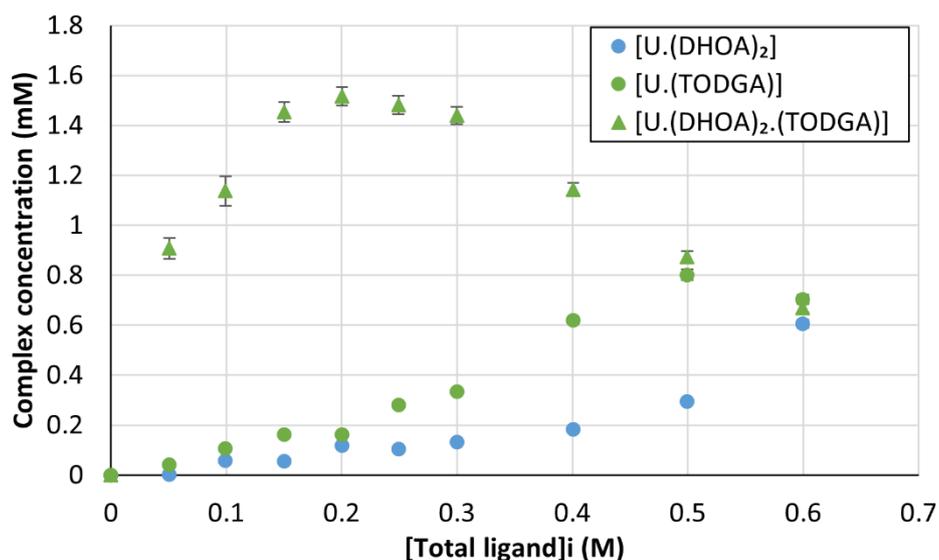
Figure 5.8. *Concentration profiles of the proposed complexes in the modelled Scenario 3 for the DHOA-TODGA system from the [total ligand] isotherm at 21±2°C.*

Figure 5.9 shows the uranium loading isotherms and calculated equilibrium lines for the DHOA, TBP, DHOA-TBP and DHOA-TODGA systems at 0.2 M total ligand concentration. Figure 5.9A shows the calculated equilibrium line for the DHOA-TBP system based on the extraction mechanism determined from the previous SX data. Like with the uranium loading isotherms from Chapter 4, a good fit is seen at low loadings but the model deviates from observed distributions at higher uranium loading. No model based on the determined extraction mechanism could be obtained for the DHOA-TODGA system because no viable K_{eq} value could be determined from the uranium loading isotherm data; this is discussed in Section 5.4.4. Figure 5.9B shows the modified equilibrium models for DHOA, TBP, DHOA- TBP and DHOA-TODGA systems at 0.2 M total ligand concentration. The data for DHOA and TBP were taken from Chapter 4. The DHOA-TBP model was modified to fit the observed data points and DHOA-TODGA system was found to fit to a second-order polynomial through the origin ($R^2 = 0.9955$) and these were deemed suitable for use in a McCabe-Thiele diagram. The operating lines in Figure 5.9 use Equation 4.10 and assume a 10 g/L aqueous uranium feed, a desired recovery of 95% and an aqueous/organic phase volumetric flowrate that is defined on the figure legend. Required extraction stages for >95% recovery using the 0.2 M systems are presented in Table 5.4; estimated extraction stages for 1.1 M ligand systems assuming proportional uptake are also presented (Gasparini & Grossi, 1986). Generally, the dual-ligand systems require fewer extraction stages than DHOA to achieve over 95% recovery except when assuming 1.1 M total ligand concentration and an aqueous / organic (A/O) phase volumetric flowrate ratio of 0.5 where all systems are estimated to require a single contact stage similar to that determined in Chapter 4. This may mean that monoamide solvent loading is not as large an issue as previously considered and is further discussed in Section 5.4.4. Both dual-ligand solvent loadings are similar to that of pure TBP, and this is portrayed by the same number of extraction stages required.
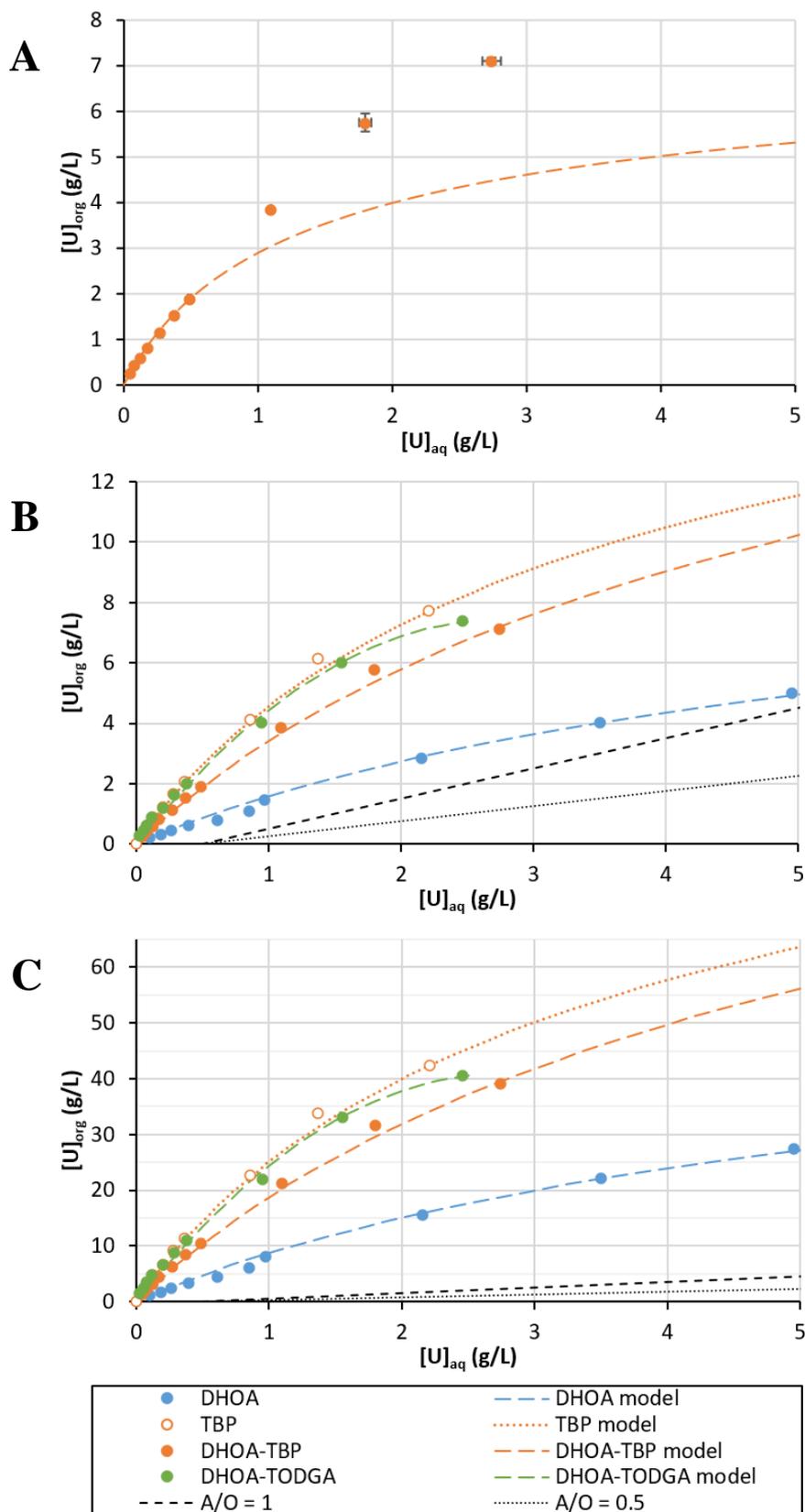
Figure 5.9. *Uranyl nitrate loading isotherms with 0.2 M DHOA (at 5.63 M HNO₃), DHOA-TBP (at 5.68M M HNO₃) and DHOA-TODGA (at 5.68 M HNO₃) at 21±2°C. A) depicts the low loading DHOA-TBP model based on the extraction mechanism, B) shows entire tested range with modified models and C) shows concentration-amended model fits. Operating lines were determined assuming a feed of 10 g/L uranium and a recovery of 95% at the specified A/O phase volume ratio.*

Table 5.4. *Number of estimated extraction stages for >95% uranium recovery of a 10 g/L uranium feed at 5.7 M nitric acid with 0.2 M ligand systems and 1.1 M system estimations at 21±2°C.*

System	Theoretical extraction stages			
	[total ligand] = 0.2 M		[total ligand] = 1.1 M	
	A/O = 0.5	A/O = 1	A/O = 0.5	A/O = 1
DHOA	3	-	1	2
TBP	2	3	1	1
DHOA-TBP	2	3	1	1
DHOA-TODGA	2	3	1	1

Figure 5.10A shows the expected and observed uranyl nitrate distribution with varying total nitrate concentrations from nitric acid using the DHOA-TBP solvent at 0.2 M total ligand. Similar to the single-ligand behaviour, increasing nitrate concentrations causes an increase in uranyl distribution due to a shift in equilibrium position. The increasing acidity causes a decrease in uranyl distribution due to acid competition. Observed distribution is consistently higher than expected except for at the lowest nitrate concentration (1.90 M) where it is roughly equal. This is similar to that observed in the pH profiling and indicates that both ligands operate completely independently under low ionic strength conditions. Figure 5.11B shows the expected and observed slope analyses of the nitrate isotherms with the DHOA-TBP solvent at 0.2 M total ligand. The slopes of two indicate that it is likely that extraction does not involve the ion-pair monoamide complex, so predictive models can ignore this species under the tested conditions; values derived from slope analysis can be seen in Table 5.5.

Table 5.5. *Slope analysis values determined for uranyl nitrate extraction from the DHOA-TBP and DHOA-TODGA [nitrate] isotherms from 5.58 M nitric acid at 21±2°C.*

System	Acidity (M)	Slope	Intercept	R^2
DHOA-TBP	1.90	2.12 ± 0.09	-0.41 ± 0.05	0.9983
	2.85	2.00 ± 0.2	-0.5 ± 0.1	0.9931
	3.76	1.9 ± 0.5	-0.5 ± 0.4	0.9672
DHOA-TODGA	1.90	2.0 ± 0.4	-0.5 ± 0.2	0.9719
	2.85	2.0 ± 0.1	-0.57 ± 0.9	0.9963
	3.76	1.6 ± 0.3	-0.3 ± 0.2	0.9858
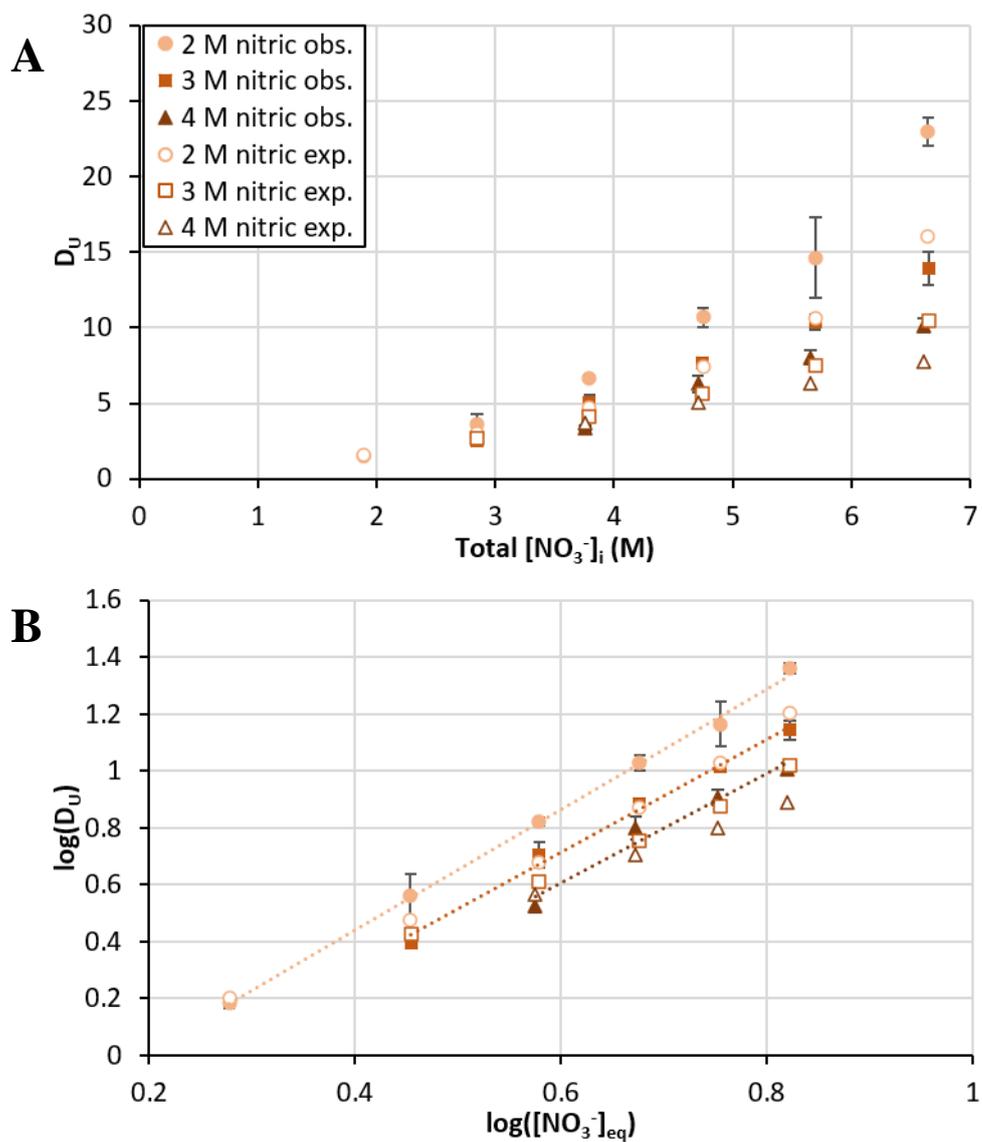
Figure 5.10. *A) Expected and observed uranyl nitrate distribution with varying nitrate concentrations in different nitric acid concentrations with 20 mol% DHOA- 80 mol% TBP at 0.2 M total ligand and 21±2°C. Initial [uranium] = 494±8 ppm. B) depicts observed and expected slope analyses of these systems.*

Figure 5.11A shows the expected and observed uranyl nitrate distribution with varying total nitrate concentrations from nitric acid using the DHOA-TODGA solvent at 0.2 M total ligand. Unlike TODGA behaviour, acidity seems to affect the extractive performance of this solvent, albeit less than that of the DHOA-TBP solvent. Observed distribution is consistently higher than expected. Figure 5.11B shows the expected and observed slope analyses of the nitrate isotherms with the DHOA-TODGA solvent at 0.2 M total ligand. The slopes of two (Table 5.5) at 2 M and 3 M nitric acid indicate that extraction likely involves two nitrate anions overall considering all extraction mechanisms. However, the slope value decreases to 1.6 at 4 M nitric acid indicating a change in extraction mechanism; this is discussed in Section 5.4.5.
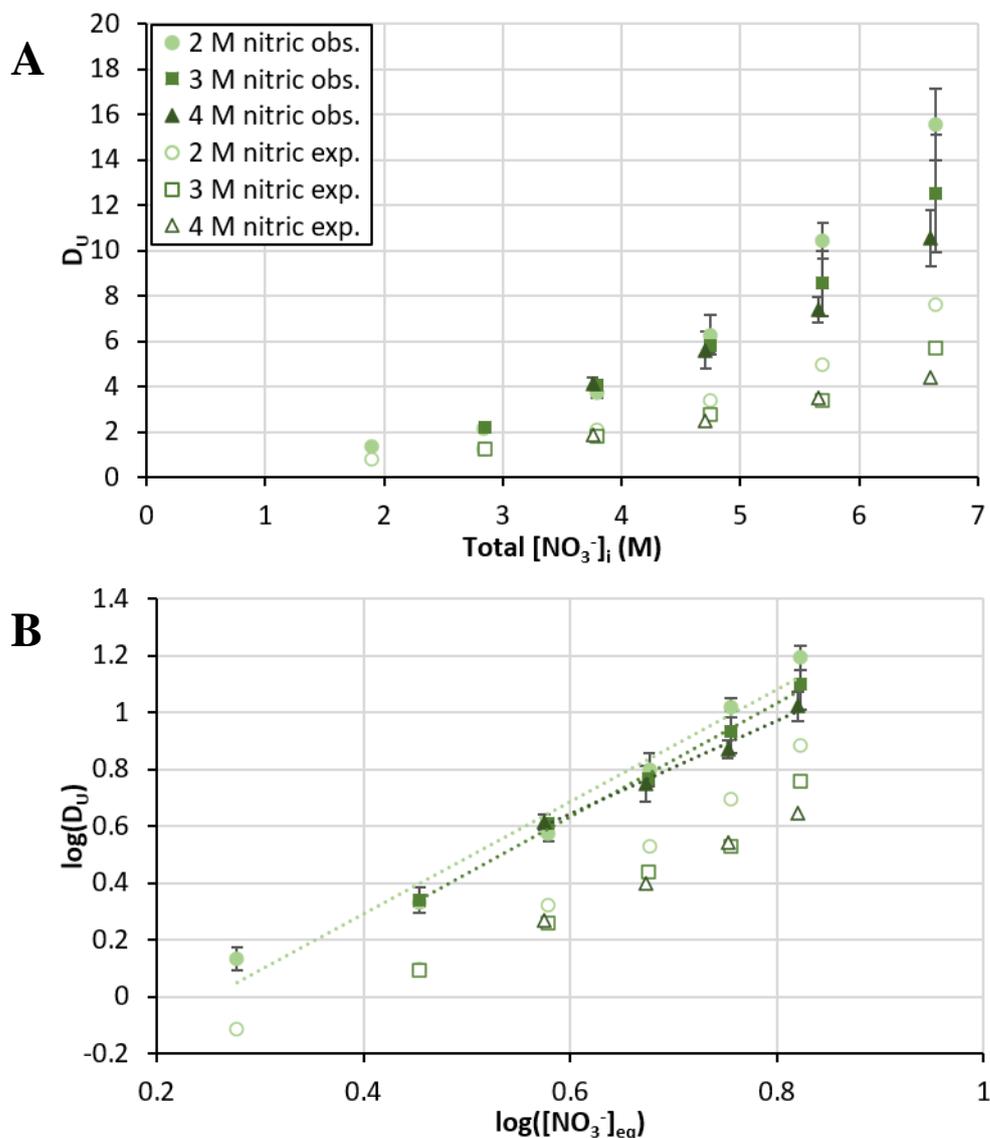
Figure 5.11. *A) Expected and observed uranyl nitrate distribution with varying nitrate concentrations in different nitric acid concentrations with 80 mol% DHOA- 20 mol% TODGA at 0.2 M total ligand and 21±2°C. Initial [uranium] = 494±8 ppm. B) depicts observed and expected slope analyses of these systems.*

5.4 Discussion

5.4.1 Acid extraction isotherms

It was determined that DHOA and TBP are independent of each other in terms of nitric acid extraction because expected behaviour generally lies within the error of observed measurements. However, it should be noted that the two isotherms do deviate at low ligand concentrations as the observed extraction is consistently slightly higher than the expected values when not considering the uncertainties. Equation 5.5 was constructed to confirm whether these ligands are truly independent with regards to acid extraction via slope analysis. This equation assumes nitric acid is extracted as separate monosolvate complexes with DHOA and TBP at the ratios of their concentrations (20 mol% DHOA and 80 mol% TBP). The slope of 1.09 produced from the plot of α against $\log(D)$ indicates that this model adequately describes the extraction environment; a slope of exactly 1 means that the model perfectly describes the extraction environment. This provides good qualitative evidence that DHOA and TBP act independent of one another for nitric acid extraction forming the same complexes determined from Chapter 4 and those described in literature (Prabhu, et al., 1993); (Nair, et al., 1994); (Prabhu, et al., 1997); (Nukada, et al., 1960); (Alibrahim & Shlewit, 2007); (Zilberman & Ferorov, 1991); (Woodhead, 1965). This means that free DHOA and TBP concentrations after pre-equilibration of the dual-ligand system can be suitably determined from the single-ligand acid extraction correlations in Appendix B rather than more complex correlations based on present data. There are too many degrees of freedom to discuss what the 0.09 slope deviation truly relates to as it is most likely a variety of factors involved in the calculation of α.

Like with the DHOA-TBP system, expected nitric acid extraction with the DHOA-TODGA solvent is within the error of observed measurements but observed extraction is consistently higher. Equation 5.8 was constructed assuming only $(HNO_3)(DHOA)$ and $(HNO_3)_2(TODGA)$ are produced at the ratios of their concentrations (80 mol% DHOA and 20 mol% TODGA); these were the acid-ligand species identified in Chapter 4. The slope of 0.999 indicates that this model perfectly describes the extraction mechanism and the two ligands can be assumed to be completely independent of each other with regards to nitric acid extraction and form the species identified in Chapter 4. As above, this means that free

163

DHOA and TODGA concentrations after pre-equilibration of the dual-ligand system can be suitably determined from the single-ligand acid extraction correlations in Appendix B.

5.4.2   Influence of acidity

The DHOA-TBP pH profile shows that the dual-ligand system is consistently better than expected when acidity is between 1 and 8 M. When acidity is ≤ 1 M, extractive performance is exactly as expected which indicates ligand independence under these conditions. As stated previously, the expected and observed profiles share some similarities: both profiles peak around 5.5 M nitric acid (observed distribution is 27% higher than expected at this point) and both profiles have the same shape with changing acidity. This implies that the mechanism of extraction with the dual-ligand system is largely the same as the independent systems which supports the previous claim that the DHOA-TBP system is likely enhanced by a phase modifying effect of the TBP rather than the formation of a more hydrophobic ternary complex. The observation that there is no enhancement when acidity is ≤ 1 M implies that acidity also plays a role in the extent of enhancement. It could be that sufficient concentrations of either the $(HNO_3)(DHOA)$ or $(HNO_3)(TBP)$ complex are required to facilitate the enhancement, either by sufficiently increasing the polarity of the organic phase or potentially by acting as a phase transfer catalyst. It has been observed before that the $(HNO_3)(TBP)$ species extracts uranyl nitrate; it could be that uranium is extracted by the $(HNO_3)(TBP)$ complex and then complexed as an arguably more stable disolvate monoamide species in the organic phase rather than relying on solubisation at the aqueous-organic interface.

Like that of the DHOA-TBP pH profile, the DHOA-TODGA shows that the dual-ligand system is consistently better than expected when acidity is between 1 and 8 M. When acidity is ≤ 1 M, extractive performance is as expected which indicates ligand independence under these conditions. It may be that the lower concentration of extracted acid under these conditions means that the organic phase cannot support enough formation of the dual-ligand complex identified in Chapter 4 to exceed expected extraction. Unlike that of the DHOA-TBP profile, the observed DHOA-TODGA distribution continues to increase past 5.5 M nitric acid instead of peaking and then slowly decreasing as expected. This indicates one of two things: i) the dual-ligand system is far more selective for uranium and hence acid

competition is vastly reduced, or ii) the dual-ligand solvent simply has a much higher capacity for both uranium and acid. There is not much difference between the acid extraction performance of the DHOA-TBP and DHOA-TODGA solvents at 0.2 M total ligand, so the latter point may not be valid, but the DHOA-TODGA distribution profile is fairly similar to the shape of the TODGA profile from Section 4.3 which was attributed to TODGA's high acid capacity. It is likely that the cause of the observation is a mixture of the two above points; the dual-ligand complex has a higher affinity for the metal centre due to the many hard oxygen donors present in the complex, and any free TODGA is still available to extract nitric acid and reduce competition.

5.4.3   [Ligand] isotherms

The DHOA-TBP ligand isotherm shows that uranyl distribution is observed to be consistently higher than expected with the dual-ligand system, however, uncertainty in the expected values at total ligand concentrations above 0.4 M makes it impossible to confirm this trend at these conditions. As stated previously, the distribution enhancement before this point increases from 6% (at 0.05 M total ligand) up to 40-45% (0.2-0.3 M total ligand). The increasing concentrations of the ligands, and therefore extracted acid and uranium, will lead to increased organic phase polarity which should enable the dissolution of more uranyl-nitrate-monoamide species. Chapter 4 found that the DHOA-TBP dual-ligand solvent likely enhances uranium recovery via a phase modifying effect rather than by the formation of a new complex. To support this, Equation 5.13 was constructed to determine whether the phase modifier scenario is likely using the dual-ligand extraction data presented in Figure 5.5. The model assumes that $(UO_2)(NO_3)_2 \cdot (DHOA)_2$, $(UO_2)(NO_3)_2 \cdot (TBP)_2$ and $H(UO_2)(NO_3)_3 \cdot (TBP)$ complexes are formed independently. Free DHOA concentrations were determined from Chapter 4 acid extractions and the single-ligand DHOA isotherm. Due to the multiple TBP species, free TBP concentrations were then determined via a uranium mass balance assuming equal concentrations of the mono- and disolvate TBP species as determined from Chapter 4. The slope of 0.98 ($R^2 = 0.99$) for this scenario indicates it describes the extraction mechanism well; no ternary complexes are formed so the distribution enhancement must come from a phase modifier or phase transfer catalyst effect. No further extraction

scenarios were modelled for the DHOA-TBP system as Equation 5.13 gave a suitable slope and there is no evidence to suggest that a ternary complex is generated.

The DHOA-TODGA ligand isotherm shows that uranyl distribution is consistently higher than expected throughout the tested ligand concentration range (0.05 – 0.6 M total ligand) up to 300% at 0.4 M total ligand which indicates a vast enhancement with increasing ligand concentrations. Large uncertainties in the ligand concentrations above this point make it difficult to report a concrete enhancement at these conditions. Regardless, the overall large enhancement in uranium extraction indicates that the ternary complex has a much higher affinity for the uranyl cation than the two ligands alone. In order to confirm whether this ternary complex is generated, Equations 5.10, 5.11 and 5.12 were constructed to model only independent ligand complexation (Scenario 1), only ternary complexation (Scenario 2), and both independent and ternary complex formation (Scenario 3) respectively. A slope of 1 on the slope analysis plot would indicate that the underlying assumptions of that model perfectly describe the extraction mechanism. As Scenario 1 assumes ligand independence, free ligand concentrations were determined by a suitable mass balance using acid extraction and single-ligand isotherm data. The slope of -7.6 reveals that this scenario does not describe the extraction behaviour of this dual-ligand system. Scenario 2 assumes only ternary complex formation; this mechanism is a simple adduct-forming reaction like those seen in the single-ligand systems so free ligand concentrations can be directly determined from the organic uranium content and the proposed complex stoichiometry. Modelling with these assumptions gives a slope of 0.49 which reveals that this scenario does not adequately describe the extraction mechanism either.

Scenario 3 is based on the previous two models but is much more complicated due to the higher degrees of freedom present in the model. Initially, it was assumed that the species concentrations throughout the isotherm test would be proportional; however, modelling with this assumption was unsuccessful as no adequate solution could be determined. It follows that the proportion of species concentrations is very dependent on initial ligand concentrations. Therefore, the modelling for Scenario 3 was constructed in reverse as outlined in Section 5.2.3; briefly, the reaction mechanism was assumed to be correct and CFs were assigned to each complex for each data point. These were then refined using the

GRG Nonlinear Solver add-in in Microsoft Excel to assess whether varying complex speciation could result in a linear slope for log(D) against γ_3 with an $R^2 > 0.999$. So, whereas Scenario 1 and 2 were modelled to see if their mechanisms fit the observed behaviour, Scenario 3 was modelled assuming it fit observed behaviour to determine whether there is a possible mechanism. The Scenario 3 model was successful; slope analysis yielded a slope of 1.02 ($R^2 = 0.999$) and the concentration profile based on the refined CFs is presented in Figure 5.8. This indicates that the extraction mechanism is indeed a mixture of single-ligand and dual-ligand complexations identified in Chapter 4. It is possible that different concentration profiles would also yield a slope of 1 with the slope analysis but no evidence of this was found during data processing. The peak enhancement in the DHOA-TODGA ligand isotherm is between 0.2-0.3 M total ligand which corresponds to the ternary complex concentration peak in Figure 5.8. The ternary complex concentration begins to decrease at 0.3 M total ligand, but the increase in the monosolvate TODGA species likely makes up for this in terms of uranyl extraction. There is large uncertainty in the extraction measurements at 0.5 and 0.6 M total ligand due to the very small amount of aqueous uranyl after contact, so, the corresponding points on Figure 5.8 likely have uncertainty associated with them too. Nevertheless, it is clearly shown that complex speciation changes with total ligand concentrations; this casts doubt on whether it can be assumed that doubling the ligand concentration will lead to a doubling in loading capacity for this system when considering the metal loading isotherms, which is an assumption previously used for monoamide systems (Gasparini & Grossi, 1986).

5.4.4   Uranium loading isotherms

The metal loading isotherm model calculated for the DHOA-TBP system is based on the proposed extraction mechanism involving no ternary complex. The good fit at low metal loading is further evidence that this is the true extraction behaviour and that the enhancement is due to phase modifying effects. Similar to the metal loading isotherms presented in Chapter 4, the model deviates and vastly underestimates the uranium extraction at higher metal loading. This is expected given that the ligands are thought to extract independently; similar extraction behaviour to the single-ligand systems is likely. Uranyl nitrate must substitute for extracted nitric acid at higher metal loading conditions which changes

the aqueous acidity and ionic strength. These are assumed to be constant in the model, so changes to these conditions will lead to deviations in the model. Post-contact acidity measurements of the metal loading isotherms should confirm this mechanism and provide enough data for a better fitting model for McCabe-Thiele assessment of extraction stages. A handle on the changing acidity is also important for process design; changing pH may change plutonium speciation or affect uranium and plutonium separation factors from competitive metals (Kulkarni, et al., 2006). Given that this behaviour is already seen for the pure TBP system, this behaviour will already be accounted for in process design. However, differences between a TBP system and a dual-ligand system will be required to adequately control pH in a dual-ligand extraction process. No metal loading model could be constructed for the DHOA-TODGA system as no viable K_{eq} could be determined from any of the metal isotherm data. It is likely that the $(HNO_3)_2(TODGA)$ complex dissociates in favour of uranyl nitrate even at low metal loading conditions. This is inferred from the small total concentration of TODGA and the very small free TODGA concentrations calculated even at low metal loading. The TODGA metal loading isotherm presented in Chapter 4 began deviating away from the model when free TODGA was roughly >0.02 M and all free TODGA concentrations in the present study are far below this value meaning that acid is likely replaced by metal under all loading conditions. The total ligand concentration in this test was 0.2 M so two methods were employed to determine free TODGA concentrations: i) assuming constant complex speciation proportional to the CFs determined for 0.2 M total ligand from Figure 5.8, or ii) assuming changing complex speciation as the metal-to-ligand ratio changes throughout the metal loading isotherm. Linear interpolation between the data points was employed for the latter method using the [ligand]/[metal] ratios from the data points in Figure 5.8 as a basis. Neither method allowed for the estimation of a viable K_{eq} and free TODGA concentrations were often negative which indicates that the underlying assumptions of the model (i.e. constant acidity) are not correct for the majority of the isotherm. As before, post-contact acidity measurements would allow for the more accurate determination of the extraction mechanisms and model behaviour.

Metal loading with the dual-ligand systems are shown to be much higher than that of DHOA which means less solvent can be required in a process scale for effective separations (i.e. a higher A/O phase

volume ratio). 0.2 M DHOA-TBP and DHOA-TODGA solvents are estimated to be suitable for a multi-stage extraction process with an A/O phase volume ratio of 1 at a feed concentration of 10 g/L uranium whereas the data shows that the use of a 0.2 M DHOA solvent would lead to the enrichment of the aqueous phase. Through manipulation of the operating line in Figure 5.9C, it is estimated that the 1.1 M DHOA solvent with the same feed conditions could achieve an effective separation up to an A/O = 3.5, whereas the DHOA-TBP and the DHOA-TODGA solvents could operating comfortably up to A/O = 7.5-8. This indicates a potential reduction in solvent volume over a pure monoamide extraction process leading to lower operating costs or smaller equipment requirements.

The tested dual-ligand solvents behave very similar to the PUREX solvent (pure TBP); their loading isotherms are similar and the same number of contact stages are estimated to achieve >95% recovery of uranium from a 10 g/L feed with both the 0.2 M and 1.1 M total ligand conditions. This indicates that implementation of a dual-ligand solvent to reduce or eliminate phosphorus in reprocessing may be simpler as there would be less disparity between the current PUREX solvent and those proposed in this work. However, this also relies on hydrodynamical parameters of the solvents as well; similar loading behaviour is an advantage, but the solvents need to be similar to transport and handle as well. Monoamide solvents have been shown to have higher phase separation times mainly due to the higher solvent viscosities (Pathak, et al., 2009); (Parikh, et al., 2009). An assessment of the dual-ligand solvents hydrodynamic parameters is therefore needed for a full assessment of ease of implementation of a dual-ligand solvent into PUREX operations.

5.4.5   Influence of ionic strength

As seen with the single-ligand tests, increasing nitrate concentrations leads to an increased uranium extraction with the DHOA-TBP solvent, and increased nitric acid content reduces uranium recovery due to acid competition. Similar behaviour between the dual- and single-ligand systems is in-line with the concept of these ligands extracting uranium separately. Generally, there is an enhancement in uranium distribution across the tested range, however, extraction is roughly as expected when there is no addition of sodium nitrate. This was observed in the pH profile but only at lower acidities. This may be further evidence of the requirement for extracted acid to facilitate the enhanced uranyl nitrate

extractions observed with these systems. Ionic strength is usually increased during PUREX processing to allow for plutonium redox control (Gupta, et al., 2000a), so these lower nitrate condition points may not be relevant to PUREX processing and the enhanced extraction with this dual-ligand solvent can be expected if used in reprocessing operations.

Like in Chapter 4, the slope analysis values based on the nitrate isotherms for the DHOA-TBP solvent may not be quantitatively accurate as there is no way to account for changing free ligand concentrations with the current experimental set-up; however, they should still present a qualitative picture of the extraction process due to the large nitrate concentrations and influence of nitrate on extraction compared with free ligand. The slopes of two indicate that extraction likely does not involve the ion-pair monoamide complex even at high nitrate concentrations, so predictive models can ignore this species at these conditions. This species is only expected to dominate at >12 M nitric acid (Berger, et al., 2020), so it is not unexpected that no evidence of its formation was found here or in the ligand isotherms.

The consistently enhanced extraction observed in the ionic strength isotherm with the DHOA-TODGA solvent indicates there is no ligand independence under these conditions with regards to uranyl nitrate extraction which is consistent with the formation of the ternary complex at these conditions. Unlike TODGA behaviour, acidity seems to affect the extractive performance of the DHOA-TODGA solvent, albeit less than that of the DHOA-TBP solvent. This demonstrates that there is still acid competition with the DHOA-TODGA solvent despite the insights from the pH profile in Figure 5.4. Given that the ligands behave independently with regards to acid extraction, this deviation from acid independence at high ionic strength must be from the DHOA like that seen in Chapter 4.

Generally, the slope analyses show two nitrate anions are involved with the overall uranyl nitrate extraction with the DHOA-TODGA solvent, but they also potentially indicate the formation of a complex featuring a single nitrate anion at 4 M nitric acid. No evidence of such a complex could be found in the literature and no feasible charge-neutral structure could be conceived to explain this phenomenon, especially in the concentrations required to deviate the slope by 0.4 units. It is more likely that the uncertainty in the experiment and from the assumption of constant free ligand concentration has led to the lower calculated value.

5.5   Conclusions

A closed nuclear fuel cycle is required to efficiently use the limited amount of producible nuclear fuel. Process complications in the current PUREX flowsheet and low uranium costs mean that reprocessing SNF is not currently economically favourable. The replacement of the TBP solvent in reprocessing with a more sustainable monoamide-based alternative could cut down on process steps and secondary wastes to reduce overall process costs. However, monoamide solvents do not load as much as TBP and more organic phase would be required for equal separations which may not work with existing reprocessing equipment and required throughputs.

Using ligand mixtures with monoamides may enhance the solvent performance and enable the reduction or elimination of phosphorus in reprocessing flowsheets which lead to the expensive secondary wastes. The extraction enhancement would either come from a change in solvent polarity to increase the solubility of the uranyl-nitrate-monoamide complex, or through the production of a more hydrophobic mixed-ligand complex. It has previously been demonstrated in Chapter 4 that mixtures of 20 mol% DHOA – 80 mol% TBP and 80 mol% DHOA – 20 mol% TODGA perform as well as TBP alone in *n*-dodecane. Based on previous data, it was theorised that the DHOA-TBP solvent led to enhanced extraction based on the phase modifying effect of TBP. The DHOA-TODGA solvent was theorised to produce a more hydrophobic ternary complex with uranyl nitrate. The current work aims to prove these extraction mechanisms and provide data on the loading performance of these mixed ligand solvents. Slope analysis was used alongside modelled extraction scenarios to determine likely mechanisms. Loading behaviour of the dual-ligand solvents were compared with pure DHOA and TBP solvents to inform viability of solvent implementation.

The present data for the extractive behaviour of the DHOA-TBP solvent is consistent with expected phase modifying behaviour. Modelling extraction scenarios for nitric acid and uranyl nitrate extraction indicate that the same complexes are formed in the single-ligand systems identified in Chapter 4. Similar extraction behaviour to single-ligand systems with changing acidity indicate that the extraction mechanism is similar. Observed uranyl distribution is consistently greater than expected when complete ligand independence is assumed except at low acidity or nitrate concentration. This points towards a

requirement for organic nitric acid content before the enhanced extraction can be seen. It is possible that the phase modifying effect relies on a certain amount of extracted acid to increase solvent polarity, or acid-ligand complexes may aid in the transfer of metal-ligand complexes to the organic phase. This should not be a concern at the high acidity that the initial PUREX separation is generally operated at, however, this may mean that the DHOA-TBP solvent will not suffer reduced uranium recovery from the dilute nitric acid strips after the initial PUREX separation.

DHOA and TODGA are shown to act independently with regards to acid extraction; the shift in extraction behaviour with acidity points to a new extraction mechanism than those identified for the single-ligand systems. Modelling from the ligand isotherms indicate that the previously identified $UO_2(NO_3)_2 \cdot (DHOA)_2(TODGA)$ complex is responsible for the large enhancement to extractive performance. Models assuming no ternary complex or only a ternary complex were unsuccessful, so this solvent involves a mixture of single- and dual-ligand extracted species.

The uranium loading behaviour of both of the dual-ligand solvents is shown to be comparable to that of the PUREX solvent and much better than a pure DHOA solvent. It is estimated from the current data that the same number of extraction steps are required for the dual-ligand solvents and the PUREX solvent which means that retrofitting one of the dual-ligand solvents into existing technology may be possible, as long as phase separation times are not adversely affected, leading to reduction or elimination of phosphorus in reprocessing flowsheets.

CHAPTER 6   Thesis Conclusions

This chapter includes the thesis conclusions and proposes future work. The chapter begins by summarising the background and context for this work and is followed by the research hypotheses that were tested in this thesis. This is followed by a summary and conclusion of each of the presented results chapters and linked back to the research hypotheses. Research hypotheses are identified to be either correct or incorrect, and the achievement of the thesis aims are discussed. Proposed future work areas are then summarised and discussed in two main sections: i) work to further the efforts of this thesis, and ii) new areas to investigate relevant to the work in this thesis that have not been explored.

6.1   Conclusions

A sustainable fully-closed nuclear fuel cycle is required in order to fully utilise the limited amount of natural, fissile uranium fuel on Earth. It also allows for the significant volume and heat load reduction of high level waste (HLW) due to the removal of the actinide elements. This will make the storage requirements of HLW in a geological disposal facility drastically simpler. Many countries operate on a once-through nuclear fuel cycle which leads to large wastage of uranium-235 and other fuel elements produced during the operation of a nuclear reactor. There are some countries that operate a partially-closed fuel cycle, where the fuel is reprocessed once before disposal, but high process costs and low uranium product prices mean that reprocessing can be economically unfavourable and cause reprocessing plants to shut down. For example, in the UK, the Thermal Oxide Reprocessing Plant closed in 2019 and the Magnox plant is due to close in 2020; no other reprocessing capability is currently planned.

Current reprocessing flowsheets use the Plutonium Uranium Reduction EXtraction (PUREX) solvent extraction (SX) process to recover uranium(VI) and plutonium(IV) from dissolved SNF in nitric acid using the extractant tri-*n*-butyl phosphate (TBP) in an aliphatic organic diluent. This process achieves high recoveries and purity uranium(VI) and plutonium(IV) products but requires extra stripping steps due to undesired metal extraction (mainly neptunium, zirconium, technetium, and ruthenium) and suffers from phase forming issues when the solvent degrades. The solvent degrades via radiolysis and hydrolysis, due to the high radiation field and acidity present in the process, to form several

organophosphorus degradation products that form precipitates and stable emulsions as well as extract undesired metals (mainly Zr, Mo, lanthanides, minor actinides). The degraded solvent is incinerated at end-of-life which produces a highly radioactive phosphate residue. It is radioactive due to the undesired extraction facilitated by the organophosphorus degradation products and the chemical nature of the residue makes it difficult to process. It follows that the reduction or replacement of TBP with a more selective and sustainable ligand should reduce the need for extra process steps and reduce or eliminate the difficult secondary phosphate wastes, thereby reducing the costs of the overall process.

Monoamides are a set of extractants that are structurally analogous to TBP but adhere to the CHON principle (they only contain carbon, hydrogen, oxygen, and/or nitrogen), meaning that they behave like TBP but can be incinerated to leave no phosphate residue. N,N-dihexyl octanamide (DHOA) has been identified as one of the best monoamide replacements for TBP; DHOA has been shown to be much more selective for uranium(VI) and plutonium(IV) than TBP and has impressive plutonium recoveries. However, uranium loading with DHOA is far less than TBP which means that more organic solvent would be required in order to achieve the same performance with high uranium feed concentrations, and this may not work with existing reprocessing equipment and flowsheets. The lower loading of the uranyl-nitrate-monoamide complex is generally attributed to the lower solubility of this complex in the organic phase, so it follows that there are two ways to improve uranium(VI) recovery with monoamides:

- Employ a phase modifier to increase the polarity of the organic phase and increase complex solubility.
- Employ a secondary extractant that forms a ternary complex (i.e. uranyl-nitrate-monoamide-ligand) with a higher hydrophobicity to increase mass transfer of uranium to the organic phase.

The overarching aim of this thesis was to identify viable SX systems to replace the traditional PUREX solvent to reduce or eliminate phosphorus in spent nuclear fuel reprocessing. The focus was to improve the uranium(VI) recovery of monoamide solvents through the addition of either amide-based ligands (diamide or diglycolamide) or organophosphorus ligands (phosphate or phosphine oxide) as a phase modifier or secondary extractant. These types of ligands were selected due to their affinity for uranium(VI); amide-based ligand mixtures with monoamides would allow for the elimination of

phosphorus in reprocessing flowsheets, and organophosphorus ligands mixtures with monoamides would reduce it. The reduction or elimination of phosphorus is key to reduce or eliminate the secondary phosphate wastes produced from incinerating the degraded PUREX solvent. There are many different advanced flowsheets that look to further process PUREX raffinate, but there is no official process being developed to improve the sustainability and cost effectiveness of PUREX itself using monoamide-based ligand mixtures, which is where the novelty of this work lies.

The research hypothesis tested in this thesis was:

"The addition of amide-based or organophosphorus adduct-forming ligands to monoamide solvents will enhance the uranium recovery of these solvents and allow for the reduction or elimination of phosphorus from reprocessing flowsheets"

This was split into the following sub-hypotheses:

1. Diamides can form ternary complexes with uranyl nitrate and monoamides which enhances uranium recovery with a monoamide solvent during SX.

2. Diglycolamides can form ternary complexes with uranyl nitrate and monoamides which enhances uranium recovery with a monoamide solvent during SX.

3. Phosphates can form ternary complexes with uranyl nitrate and monoamides which enhances uranium recovery with a monoamide solvent during SX.

4. Phosphates can modify a monoamide solvent to increase uranyl-nitrate-monoamide solubility which enhances uranium recovery with a monoamide solvent during SX.

5. Phosphine oxides can form ternary complexes with uranyl nitrate and monoamides which enhances uranium recovery with a monoamide solvent during SX.

The complex formation of uranyl nitrate with monoamides and selected ligands was investigated in Chapter 3 to assess whether ternary complexes are indeed generated; this chapter tests the first half of sub-hypotheses 1, 2, 3 and 5. Measurements were made in pseudo-aqueous media to allow clear absorbance readings and to ensure all tested ligands were soluble. Two pseudo-aqueous media were investigated to assess how complexes change as media hydrophobicity changes. Despite very small

observable changes in the UV-vis spectra, four tested monoamides were found to generate only the disolvate complexes with uranyl nitrate in both media which is expected from literature and supports the validity of the methodology.

Tetraethyl malonamide was shown to likely not produce ternary complexes with monoamides and uranyl nitrate in either media; the metal centre prefers to bond with only the diamide or the monoamide. In a reprocessing flowsheet, it is expected that diamides will also extract undesired elements (namely lanthanides or minor actinides) as well as uranium which means that a monoamide-diamide system would have to produce a ternary complex with uranium in order to be viable; a phase modifying effect would not be enough to overcome the inevitable lack of selectivity. As this is not the case, monoamide-diamide systems were not carried forward to SX tests and sub-hypothesis 1 was found to be incorrect.

Tetraethyl diglycolamide (TEDGA) was shown to produce a variety of species up to tetrasolvate, which adds to the already ambiguous literature on diglycolamide-uranyl-nitrate speciation. Jobs plots from tests in both pseudo-aqueous media showed that monoamide-TEDGA systems generate both the (monoamide)(TEDGA) and (monoamide)$_2$(TEDGA) ternary uranyl nitrate species, which indicates that these systems may form a more hydrophobic, soluble monoamide complex in a SX setting. Changing the monoamide structure did little to change the speciation of these ternary complexes. Like with the diamides, it would be expected that diglycolamides would also extract undesired elements in a reprocessing flowsheet. This means that the presence of a ternary complex is required in order for a monoamide-diglycolamide system to be viable, as relying on phase modifying effects would not overcome the inevitable lower separation factors. As evidence for ternary complexes was consistently found, these systems were carried forward to SX tests to further test sub-hypothesis 2.

Triethyl phosphate (TEP) was found to behave similarly to the tested monoamides but produced a stronger complex. This is expected given their similar structure and the stronger phosphate phosphoryl donor relative to the monoamide carbonyl. Like that of monoamides, TEP produced very small observable changes in UV-vis spectra. Jobs plots of TEP and diethyl acetamide showed zero observable absorbance change as ligand mole fractions were varied. This either means no ternary complex is formed, or the detection of this complex is outside the capability of this experimental method. The latter

is implied from the prediction of the disolvate phosphate and monoamide species from the SQUAD software based on very small absorbance changes in the inputted spectra from the spectrophotometric titrations. As phosphates are already used in reprocessing flowsheets, it may be possible to introduce phosphates as a phase modifier rather than a secondary extractant. Due to this reasoning and the inconclusive Jobs plot results, monoamide-phosphate systems were carried forward to further test sub-hypothesis 3.

Trimethyl phosphine oxide (TMPO) was reported to generate monosolvate complexes with uranyl nitrate which goes against that reported in literature. There were large absorbance changes observed in the spectrophotometric titrations, but no trend was observable in the Jobs plot of TMPO and diethyl acetamide. Due to the conflicting phosphine oxide speciation and the inconclusive trend from the Jobs plot, monoamide-phosphine oxide systems were initially carried forward to SX tests in order to underpin what is occurring in solution. However, these tests were subject to a large amount of error stemming from the quantitative uranium extraction by the phosphine oxide; this data can be seen in Appendix B. It was found that no ternary complex was formed with DHOA and tri-n-octyl phosphine oxide; with this finding and the TMPO results, it was determined that sub-hypothesis 5 was incorrect.

The systems carried forward for SX tests were the monoamide-phosphate and monoamide-diglycolamide systems; DHOA, TBP and *N,N,N',N'*-tetraoctyl diglycolamide (TODGA) were selected as ligands for the SX tests. An understanding of the uranium extraction mechanisms of DHOA, TBP and TODGA systems alone is required to properly explain and model extraction behaviour of the dual-ligand systems. To that end, Chapter 4 studied the extraction behaviour and mechanisms of these single ligand systems to test sub-hypotheses 2, 3 and 4.

It was generally found that DHOA and TBP extraction mechanisms for uranium adhere to that reported in literature. Both ligands form monosolvate complexes with nitric acid and TBP was found to extract more acid, likely owing to the stronger donor strength of the phosphoryl bond. DHOA was shown to form disolvate species with uranyl nitrate through slope analysis at equilibrium concentrations which supports the findings of Chapter 3. Formation of the ion-pair species $UO_2(NO_3)_3^-\cdot HDHOA^+$ is hinted at in 5.7 M nitric acid and fits with literature trends. No evidence of this species could be found from slope

analysis at elevated nitrate concentrations, but these tests relied on qualitative analysis due to free ligand concentrations being incalculable. TBP slope analysis revealed the formation of mono- and disolvate uranyl nitrate species at 5.7 M nitric acid which is rarely discussed in the literature. The much lower acidity used in Chapter 3 tests are likely why this species was not found through UV-vis analysis. Acidity dependence for both DHOA and TBP are similar owing to their similar structure and extraction mechanisms; a peak is observed around 5.7 M nitric acid after which acid competition decreases uranium(VI) recovery. Loading isotherms indicate TBP solvents can hold ~36% more uranium(VI) than DHOA solvents and would require less solvent for a given flowrate at high uranium feed concentrations. This disparity lessens at higher ligand concentrations and lower feed uranium concentrations. Estimations for the number of contact stages required for a given separation were determined by a modified McCabe-Thiele method using a calculated operating line and an equilibrium model. Models were initially constructed based on the determined extraction mechanisms and loading isotherm data which fit well at low loading but deviated largely as loading increased above ~3.5 g/L. It was proposed that the underpinning assumptions of the model (i.e. constant ionic strength/ aqueous acidity) were no longer valid as uranyl nitrate substituted for extracted nitric acid at higher initial uranium concentrations. Models fitting the higher loading data points were used to determine stages numbers as this gives a more realistic value for a real process.

TODGA solvent extraction behaviour was shown to be much more complicated than that of DHOA and TBP. Data indicates both $(HNO_3)_2(TODGA)$ and $(HNO_3)_{1.5}(TODGA)$ are formed dependent on ligand and acid concentration, but that the disolvate species dominates at the conditions for most tests. TODGA slope analysis revealed that the monosolvate uranyl nitrate species is formed which supports Chapter 3 findings and some literature but contradicts some other studies; it is clear from literature and this study that uranyl-nitrate-TODGA speciation is complex and reliant on many factors. Acidity dependence revealed little to no acid competition with TODGA as no peak was observed in the tested range (0.1 - 8 M nitric acid). Elevated ionic strength tests up top 7 M nitrate showed that higher nitrate concentrations increased uranium(VI) recovery, but higher acidity also had no effect under these conditions which further indicates that acid competition is negligible with this system. Like with DHOA

and TBP, uranium loading models based on the determined extraction mechanism fit well at low loading but deviate at higher loadings; this is likely due to the same reasoning given above for DHOA and TBP solvents. This has resulted in a large underestimation of the TODGA solvent capacity for uranium(VI). Nevertheless, the presented loading data show that this solvent has a much higher capacity than both DHOA and TBP owing to the number of hard donor sites on the molecule and the low solvation numbers of both the acid and metal complexes.

The DHOA-TBP Job plot show that uranium(VI) extraction is consistently better than expected assuming independent ligand interactions, but there is no clear peak at a viable complex stoichiometry. From this observation and Chapter 3 data, it was proposed that the enhanced extraction seen with this system is from a phase modifying effect of the ligands rather than the production of a ternary complex. The system selected for dual-ligand solvent assessment was 20 mol% DHOA – 80 mol% TBP as this system has comparable performance to the pure TBP solvent with 20% less organophosphorus ligand. This means that sub-hypotheses 3 and 4 are taken forward for further testing.

The DHOA-TODGA Job plot also shows that uranium(VI) extraction is consistently better than expected assuming independent ligand interactions with a clear peak in enhanced extracted uranium around 0.67, indicating the production of a $UO_2(NO_2)_2 \cdot (DHOA)_2(TODGA)$ ternary complex, which supports the findings of Chapter 3. The system selected for dual-ligand solvent assessment was 80 mol% DHOA – 20 mol% TODGA as this system has comparable performance to the DHOA-TBP solvent selected previously, and the lower concentrations of TODGA should limit the amount of any potential undesired extraction. This means that sub-hypothesis 2 is taken forward for further testing.

The data from Chapter 4 was used to predict and model the behaviour of the dual ligand systems in Chapter 5. Due to the increased complexity of these systems, slope analysis could no longer be used to quantitatively describe the speciation in solution from SX data. Therefore, slope analysis was used as a qualitative tool to determine the validity of a given extraction 'scenario'; a model was built on a set of assumptions and mechanisms in order to produce a predictable slope if they were correct. The gradient of the resultant slope on a suitable plot demonstrated the validity of those assumptions and mechanisms.

Both DHOA-TBP and DHOA-TODGA systems were shown to independently extract acid; this finding allows the use of single-ligand acid extraction relations and significantly reduces the complexity of modelling the metal extraction behaviour of these systems. DHOA-TBP extraction data were found to fit well to mechanisms assuming phase modifying behaviour, i.e. independent yet enhanced extraction. Similar acidity dependence profiles with single-ligand tests indicate that extraction mechanisms have not changed, and that acid competition begins to dominate at higher acidities. From these findings and that from earlier chapters, it was concluded that sub-hypothesis 3 is incorrect, but that sub-hypothesis 4 is correct. Extraction was generally enhanced except at low acidity or low ionic strength in nitrate isotherm tests. This indicates that there is a level of extracted acid that must be achieved before the phase modifying phenomenon takes effect; perhaps the polarity of the solvent must be at a certain value for enhanced metal extraction. This may mean that the DHOA-TBP solvent will not suffer reduced uranium recovery from the dilute nitric acid strips after the initial PUREX separation.

The shift in the acidity dependence behaviour of the DHOA-TODGA systems indicates a change in extraction mechanism. Modelling the ligand isotherm assuming either ligand independence or only the ternary complex formation showed that these scenarios do not explain the extraction behaviour. Fitting a model under the assumption of both independent and ternary complex formation was successful. From these findings and that from earlier chapters, it was concluded that sub-hypothesis 2 is correct. Concentration profiles of the produced complexes were estimated from the ligand isotherm model and show that complex speciation is very dependent on the [metal]:[ligand] ratio. Assessment of this solvent for a process should therefore be conducted on a case-by-case basis as changing feed conditions may have drastic effects on performance.

The loading performance of the dual-ligand solvents were comparable to that of pure TBP and much better than that of pure DHOA. Current data suggests that the same number of steps are required for the dual-ligand solvents and the PUREX solvent which means that retrofitting a process may be possible as long as phase separation times and metal competition are within acceptable ranges. It is concluded that the tested DHOA-TBP and DHOA-TODGA solvents are viable, promising solvents for SNF

reprocessing but there is still plenty to test before these solvents can be implemented which is discussed in Section 6.2.

To summarise the main findings of this work, two flowsheets have been proposed based on the chemistry and chemical engineering principles investigated throughout this thesis. These flowsheets are towards either the reduction or elimination of phosphorus by relying on DHOA-based solvents but improving upon DHOA's uranium recovery with the addition of either TBP or TODGA. To link back to the advanced reprocessing flowsheets depicted in the literature review, Figure 6.1 displays the proposed Advanced PUREX flowsheet towards the reduction of phosphorus based on the findings of this work with a 20 mol% DHOA – 80 mol% TBP solvent. This solvent achieves comparable performance with the standard PUREX solvent with a 20% reduction in phosphorus. A further reduction in phosphorus could be possible, but this may be at the cost of uranium distribution. Therefore, a clear understanding on the minimum allowable uranium distribution coefficient would be required when choosing solvents with higher DHOA content. It should be noted that the transport of problematic fission products or transuranics are still depicted in Figure 6.1, however, the introduction of DHOA within a TBP solvent should reduce contaminant extraction. That said, since this has not yet been explored, it is assumed that a proportion of these contaminants will still be taken past the U/Pu extraction step.

Figure 6.2 displays the proposed Advanced PUREX flowsheet towards the elimination of phosphorus based on the findings of this work with an 80 mol% DHOA – 20 mol% TODGA solvent. This solvent also achieves comparable performance with the standard PUREX TBP solvent. This process allows for simpler spent solvent management due to the absence of phosphorus, as well as simpler process management from the absence of problematic acidic phosphate degradation products. The caveat with this solvent that has not been explored in this work is that the present TODGA may very well extract Ln(III) and An(III) from spent fuel liquors in the Primary U/Pu extraction step. This can be mitigated through the addition of aqueous holdback reagents that are seen in current advanced flowsheets such as TALKSPEAK, ALSEP, and EXAm described in Chapter 2.
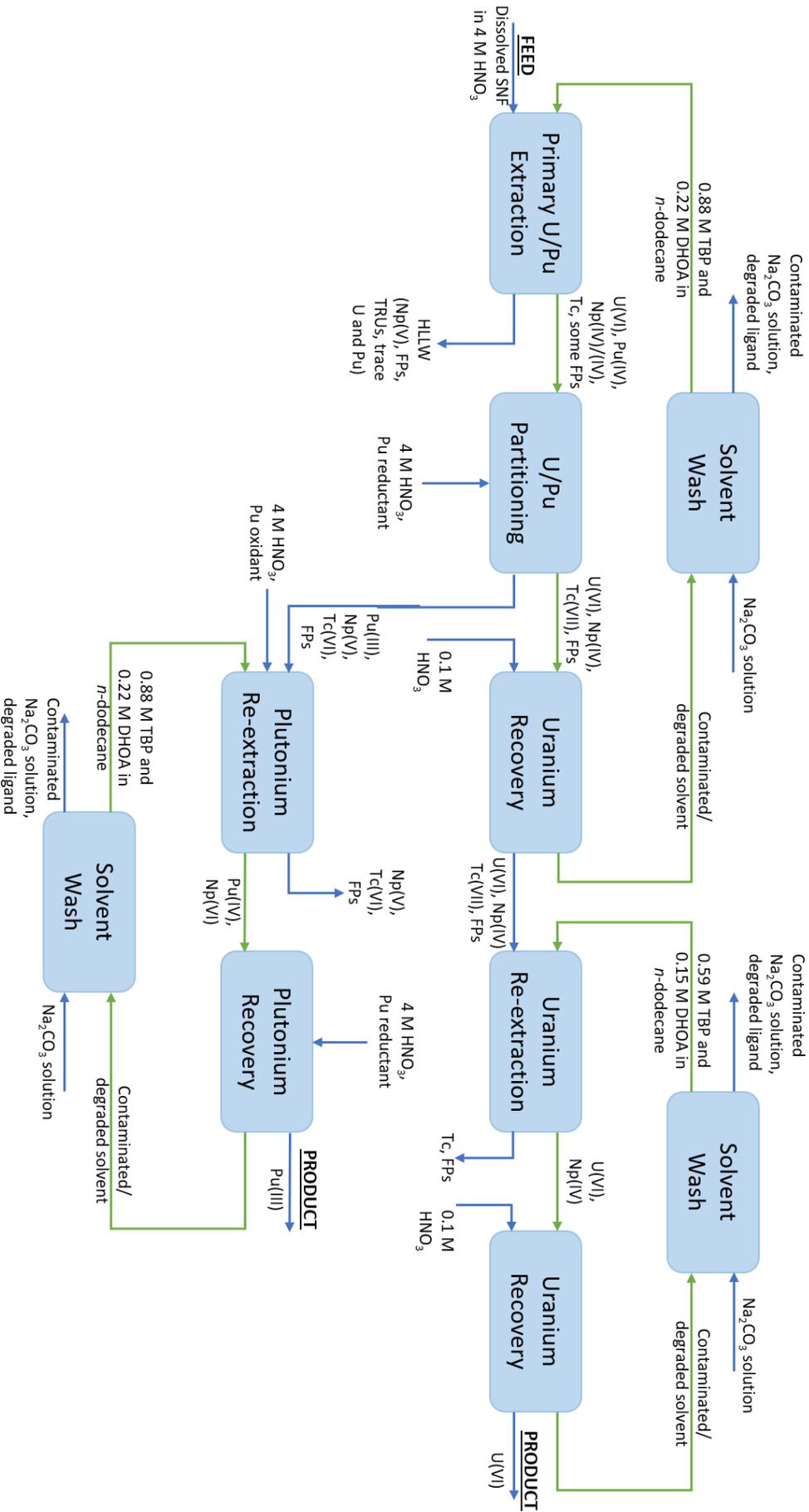
Figure 6.1. *A proposed DHOA-TBP PUREX process based on the work conducted in this thesis. Blue arrows show aqueous flows. Green arrows show organic flows.*
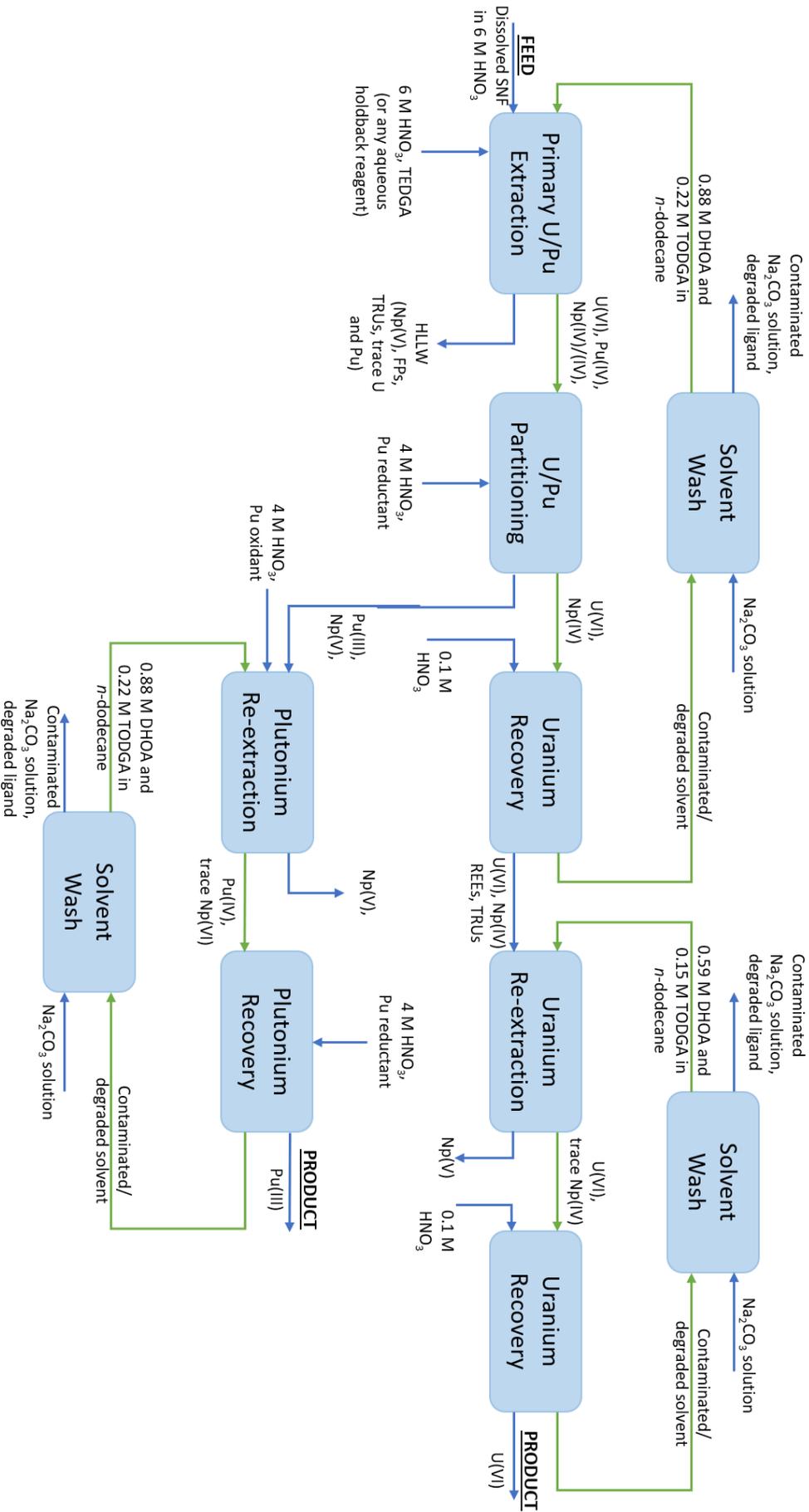
Figure 6.2. *A proposed DHOA-TODGA PUREX process based on the work conducted in this thesis. Blue arrows show aqueous flows. Green arrows show organic flows.*

In terms of which solvent performs better than the other, that depends on the perspective. The DHOA-TODGA solvent may very well be the better performing solvent from a waste management and uranium extraction point of view, but competitive extraction of contaminants will likely be an issue. The application of aqueous holdback reagents to limit this contaminant extraction have been mentioned previously, however this has not been explored in this context. The DHOA-TBP solvent may not have the selectivity of a pure DHOA solvent, and as such it will suffer the disadvantages of a TBP solvent, albeit to a lesser extent. That said, there is knowledge and skills around dealing with this within industry, and there may be the option to increase the DHOA fraction in the solvent beyond that tested in Chapter 5.

To end this summary, the aims of thesis were:

1. To prove the formation of exploitable ternary complexes with uranyl nitrate, monoamides and selected ligands using spectroscopic methods.

2. To confirm the synergistic effects of promising dual-ligand solvent systems proposed from spectroscopic tests using single-ligand SX tests and Jobs plots to determine the likely extraction mechanisms of these solvents.

3. To confirm the proposed extraction mechanisms for the dual-ligand solvents using dual-ligand SX tests.

4. To prove the dual-ligand monoamide solvents can be comparable with PUREX solvents in terms of uranium recovery.

It can be seen from this conclusion that these aims have been achieved by first assessing the formation of ternary complexes with uranyl nitrate, monoamides, and selected adduct-forming ligands (diamides, diglycolamides, phosphates and phosphine oxides). Successful or promising systems were taken forward to SX tests; these were the monoamide-phosphate and monoamide-diglycolamide systems. Single-ligand SX data was generated and used to predict and model the behaviour of the chosen dual-ligand systems. Comparison of these data sets allowed for the determination of extraction mechanisms that describe the solvent behaviour. The novel solvents were also compared with pure DHOA and TBP solvents as industry benchmarks. The chosen solvents are better than pure DHOA and comparable with

pure TBP in terms of uranium(VI) extraction and should be further assessed in a competitive extraction environment.

6.2   Future Work

This section is split into two types of future work; work to further that described in this thesis, and new areas to explore relevant to this work that have not been investigated in this thesis.

6.2.1   Further work areas

Chapter 3 data suggested the formation of two ternary uranyl-nitrate-monoamide-diglycolamide complexes, but there were many systems that had inconclusive results. Some of these systems were taken forward to solvent extraction test to clarify behaviour (phosphates and phosphine oxides), but diamide systems were not. While it is likely from the presented data that monoamide-diamide systems likely did not produce ternary complexes to a sufficient extent, further tests that do not rely on UV-visible (UV-vis) analysis could be conducted to confirm this. ^{1}H nuclear magnetic resonance (NMR) titrations could be conducted to support or clarify the current findings on complex speciation with UV-vis analysis. Extended X-ray absorption fine structure (EXAFS) measurements could also be conducted to further assess the coordination environment of the metal centre and the geometries of the surrounding ligands.

The effect of further changing monoamide structure could also be investigated. Excessive extension of the carbonyl side-chain would drastically reduce solubility, so small changes or a change in diluent would likely be required. Branching of the monoamide side chains would be a key area to investigate due to the interest of these types of monoamides in uranium/thorium 'THOREX' separations, but this lay outside the scope of this work as branched monoamides would not be useful for PUREX / plutonium extractions.

Changing the acidity/ionic strength of the spectrophotometric tests would allow for complex assessment under changing conditions. This is particularly the case with systems containing diglycolamides; it is shown in the current thesis and in literature that these ligands have complex speciation behaviour with changing system concentrations. PUREX separations are conducted at high acidity to facilitate a

suitable extraction, so a spectrophotometric assessment of the tested ligands at high acidity may prove useful and further line up with the SX findings of this thesis; for example, the (monoamide)-(diglycolamide) and (monoamide)$_2$(diglycolamide) uranyl species were determined spectrophotometrically, but only the latter was observed in SX tests.

Chapter 4 provided a solid basis of SX data on which to base the models of the dual-ligand systems, but there are several aspects of the metal loading isotherms that need addressing. Better fitting models at higher metal loading need to be constructed from extraction data rather than minimising error between the data points and the model. To do this, the loading isotherms should be repeated with post-contact acidity measurements so that acid distribution and substitution by uranyl nitrate can be considered in the isotherm model. This will allow for better predictions of multi-stage SX performance, and therefore, better comparisons of the dual-ligand solvents with PUREX and monoamide solvents. To that end, this further work should also be applied to the loading isotherms presented in Chapter 5.

A second area to further the metal loading isotherms is to use macro-concentrations of uranium (~300 g/L) with higher ligand concentrations (~1.1 M). 0.2 M ligand solvents were used to clearly observe how changing conditions affected extractions, and to allow for the economic use of available ligands. It is shown in the literature that a doubling in monoamide concentration leads to a doubling in solvent capacity, so higher ligand concentration solvents of this type can be estimated by applying a multiplier to the extraction isotherm. While this assumption is likely also true for TBP, the changing speciation of diglycolamide species means this assumption likely is not true for TODGA. Therefore, testing at process concentrations may produce valuable process data for more realistic equilibrium models and subsequent McCabe-Thiele analysis. Again, this further work can also be applied to the metal loading isotherms presented in Chapter 5.

The output of Chapter 5 indicates that DHOA-TBP and DHOA-TODGA solvents can be comparable to standard PUREX solvents, but it is likely that certain fission products may still be problematic. In particular, REEs and TRUs may be extracted with the DHOA-TODGA solvent, and so flowsheet modifications could include aqueous holdback reagents to limit uptake of these contaminants. This is similar to other advanced reprocessing flowsheets currently under study in parts of the world such as

TALSPEAK, ALSEP, and EXAm which use holdback reagents such as HEDTA ((2-hydroxyethyl) ethylenediaminetriacetic acid) or DTPA (diethylenetriamine-*N,N,N',N'',N''*-pentaacetic acid). Testing of these ligands in the DHOA-TODGA flowsheet after determining which contaminants are problematic would be greatly beneficial to simplify the overall flowsheet and improve the purity of the uranium and plutonium products with these newly proposed advanced reprocessing flowsheets.

6.2.2   New work areas

Arguably, the most important and obvious new area of study from this thesis would be to assess the competitive extraction performance of the chosen dual-ligand solvents in Chapter 5. This test should study the extractive performance of the tested dual-ligand solvents with an aqueous phase containing Sr, Zr, Mo, Ru, Pd, Cs, La, and Th as these are either problematic or abundant elements present in SNF. Sr and Cs are not problematic elements in traditional PUREX separations, but they are high heat-generating radionuclides in a relatively large concentration, so it is important to check that they do not partition unfavourably with the novel solvents. Zr, Mo, Ru, Pd and La are identified as problematic elements for either DHOA, TBP and/or TODGA which need to be investigated to assess whether undesired extraction will be an issue for the proposed solvents. La is chosen as a model lanthanide which is expected to have some level of affinity for the DHOA-TODGA solvent due to the presence of TODGA. This is one of the reasons that the TODGA concentration in this dual-ligand solvent is small, but the partitioning behaviour still needs to be investigated. Competitive tests should study the effect of changing acidity, ionic strength, and initial metal concentration. Acidity effects are key to determining optimal pH conditions for an extraction. Ionic strength effects are key to assessing how extraction may change through addition of redox controlling agents or other salts in the process. Effects of initial metal concentration are key to assess whether there is any undesired co-extraction that occurs when certain problematic elements are at a high enough concentration.

Another new area to investigate would be the hydrodynamic parameters of the proposed solvents. A key drawback of monoamide solvents is the higher viscosity that leads to longer separations times which will impede application of these solvents into existing reprocessing equipment. An assessment of solvent viscosity with changing ligand concentrations and metal loading would provide a good basis of

data to recommend viable novel solvents. Generally, monoamide solvents are more viscous, but the enhanced recovery of the dual-ligand solvents may mean that a lower ligand concentration can be used with suitable recoveries. Single-ligand tests should also be conducted to explain observed behaviour.

Loading isotherms were investigated in this report but stripping tests could also be conducted to assess how well metal can be recovered from the novel solvents. It was observed in Chapter 5 that enhanced extractions are not observed at low acidity or low ionic strength. This indicates that dilute nitric acid can still be used as a strippant for uranium(VI) as it is in traditional PUREX; however, this should be confirmed. A carbonate strip could be tested as well, which would also reveal solvent robustness under alkaline conditions which is important for the solvent wash stages in PUREX.

Another new area to investigate would be the effect of dose rate on the novel solvent performance. It is generally known which degradation products are formed, but an assessment of how these degradation products affect extraction and process operational are vital before these new solvents can be introduced into a reprocessing flowsheet. This includes uranium extraction in a both a competitive and non-competitive environment followed by stripping tests; it may be that degradation products can retain uranium(VI). The main novelty here would be the assessment of diglycolamide degradation performance with regards to uranium(VI) recovery which is not well studied in the literature. These systems could also be studied spectrophotometrically to further Chapter 3 findings and to clarify what species are formed with suspected degradation products.

Not all of PUREX is conducted at ambient temperature; dissolution of the fuel takes place in hot nitric acid, so a temperature profile will be present in PUREX processes. Studying the effect of temperature with these systems would provide much useful data but would be a serious undertaking. It would require the repetition of most previous tests but at elevated temperatures. Changing temperatures shifts the equilibrium position of extraction reactions, so it is unlikely that extraction mechanisms would change. This means that acid extractions and ligand isotherms would likely not have to be repeated, but at least pH, metal loading and ionic strength isotherms would be repeated at several temperatures to describe changing extraction behaviour. It is likely that single-ligand behaviour will shift by different amounts,

which will have a knock-on effect for the dual-ligand systems and changing temperatures will affect the hydrodynamic parameters of the solvents too.

Another new area to investigate would be to assess the behaviour of the novel solvents in a multi-stage setting to confirm McCabe-Thiele stage number predictions once acid substitution can be taken account of in the equilibrium model. Initially, this should be conducted as a series of batch equilibrium contacts on a small scale similar to the solvent extraction tests conducted in this thesis. This should be conducted for both a non-competitive and competitive extraction scenario to confirm the validity of proposed models and ensure uranium transport can be adequately predicted. Macro-concentrations of uranium and higher ligand concentrations should be used for these tests to ensure that realistic TODGA behaviour is observed. If good agreement with data and models is observed, a dynamic multi-stage setting with either mixer-settler batteries, centrifugal contactors, or column contactors could be conducted to assess novel solvent performance in a more realistic, non-equilibrium extraction scenario.

A final new area to study once all required SX data has been acquired is a technoeconomic assessment of the proposed SX flowsheet with comparison with current PUREX operations. This assessment should look at both new build and retrofitting options for the process set up, as well as continued operating costs. Operating costs should include the effect of degraded ligands on process operation and performance. A comparison with short-term SNF storage should also be included for reference.

References

Acher, E. et al., 2016. Structure of plutonium(IV) and uranium(VI) with N,N-dialkyl amides from crystallography, X-ray absorption spectra, and theoretical calculations. *Inorganic Chemistry,* 55(11), pp. 5558-5569.

Acher, E. et al., 2017. Inner to outer-sphere cooridination of plutonium(IV) with N,N-dialkyl amide: Influence of nitric acid. *Dalton Transactions,* 46(12), pp. 3812-3815.

Alcock, K., Bedford, F. C., Hardwick, W. H. & McKay, H. A. C., 1957. Tri-n-butyl phosphate as an extracting solvent for inorganic nitrates - I. *Journal of Inorganic Nuclear Chemistry,* 4(2), pp. 100-105.

Alcock, K. et al., 1956. The extraction of nitrates by tri-n-butylphosphate (TBP). Part 1. - The system TBP+diluent+H2O+HNO3. *Transactions of the Faraday Society,* Volume 52, pp. 39-47.

Alibrahim, M. & Shlewit, H., 2007. Solvent extraction of uranium(VI) by tributyl phosphate/dodecane from nitric acid medium. *Periodica Polytechnica,* 51(2), pp. 57-60.

Allen, S., 2011. *Carbon footprint of electricity generation,* s.l.: Parlimentary Office of Science & Technology.

Ansari, S. A. et al., 2005. N,N,N',N-tetraoctyl diglycolamide (TODGA): A promising extractant for actinide-partitioning from high-level waste (HLW). *Solvent Exctraction and Ion Exchange,* 23(4), pp. 463-479.

Ansari, S. A. et al., 2009. Counter-current extraction of uranium and lanthanides from simulated high-level waste using N,N,N',N'-tetraoctyl diglycolamide. *Separation and Purification Technology,* 66(1), pp. 118-124.

Bagnall, K. W. & Wakerley, M. W., 1974. Phosphine oxide complexes of thorium(IV), uranium(IV), neptunium (IV) and dixoxuranium(VI) nitrates. *Dalton Transactions,* Volume 8, pp. 889-895.

Baron, P., Lorrain, B. & Boullis, B., 2006. *Progress in Partitioning: Activities in ATALANTE. 9th IEM on P&T.* Nimes, OECD Nuclear Energy Agency.

Bell, K. et al., 2012. Pogress towards the development of a new GANEX process. *Procedia Chemistry,* Volume 7, pp. 392-397.

Berger, C. et al., 2020. Coordination structures of uranium(VI) and plutonium (IV) in organic solutions with amide derivatives. *Inorganic Chemistry.*

Berger, C. et al., 2020. Coordination structures of uranium(VI) and plutonium(IV) in organic solutions with amide derivatives. *Inorganic Chemistry.*

Berthon, L. et al., 2007. Solvent penetration and sterical stabilization of reverse aggregates based on the DIAMEX process extraction molecule: Consequences for the third phase formation. *Solvent Extraction and Ion Exchange,* Volume 25, pp. 545-576.

Berthon, L. et al., 2001. DIAMEX process for minor actinide partitioning: Hydrolytic and radiolytic degradations of malonamide extractants. *Separation Science and Technology,* 36(5-6), pp. 709-728.

Bisel,, I. et al., 2007. DIAMEX-SANEX solvent bahviour under continuous degradation and regeneration operation. *Advanced Nuclear Fuel Cycles and Systems, GLOBAL-2007.*

Bisel, I. et al., 1998. Inactive DIAMEX test with the optimised extraction agent DMDOHEMA. *International Conference on Future Nuclear Systems, GLOBAL,* pp. 1-17.

Boltoeva, M. et al., 2018. Speciation of uranium(VI) extracted from acidic nitrate media by TODGA into molecular and ionic solvents. *Separation Purification Technology,* Volume 203, pp. 11-19.

Braley, J. C., Grimes, T. S. & Nash, K. L., 2012. Alternatives to HDEHP and DTPA for simplified TALSPEAK separations. *Industrial and Engineering Chemistry Research,* 51(2), pp. 629-638.

Braley, J. C., Lumetta, G. J. & Carter, J. C., 2013. Combining CMPO and HEH[EHP] for separating trivalent lanthanides from the transuranic elements. *Solvent Extraction adn Ion Exchange,* 31(3), pp. 223-236.

Breshears, A. T. et al., 2015. Sturecture and spectroscopy of uranyl and thorium complexes with substituted phosphine oxide ligands. *Radiochimica Acta,* 103(1), pp. 49-56.

Brown, J. et al., 2010. Screening of TODGA/TBP/OK solvent mixtures for the grouped extraction of actinides. *IOP Conference Series: Materials Science and Engineering,* 9(1).

Brown, J. et al., 2012. Plutonium loading of prospective group actinide extraction (GANEX) solvent systems based on diglycolamide agents. *Solvent Extraction and Ion Exchange,* 30(2), pp. 127-141.

Bunn, M., Holdren, J. P., Fetter, S. & Van Der Zwaan, B., 2005. The economics of reprocessingversus direct disposal of spent nuclear fuel. *Nuclear Technology,* 150(3), pp. 209-230.

Burger, L. L. & Money, M. D., 1959. *Nitrous acid behaviour in PUREX systems,* s.l.: General Electric.

Burr, J. G., 1958. The radiolysis of tributyl phosphate. *Radiation Research,* 8(3), pp. 214-221.

Buxton, G. V. & Greenstock, C. L., 1988. Critical review of rate constants for reactions of hydrated electrons, hydrogen atoms and hydroxyl radicals in aqueous solution. *Journal of Physical and Chemical Reference Data,* 17(2), pp. 513-886.

Cames, B. et al., 2004. Long term evaluation of recycled DIAMEX solvent properties under hydrolysis and radiolysis with or without solvent clean-up. *No. INIS-FR-2910. CEA Marcoule.*

Canner, A. J. et al., 2020. Specrophotometric analysis of ternary uranyl systems to replace tri-n-butyl phosphate (TBP) in used fuel reprocessing. *J Sol Chem,* 49(1), pp. 52-67.

Chen, X., Li, Q. & Gong, Y., 2019. Coordination structures of the uranyl(VI)-diamide complexes: A combined mass spectrometric, EXAFS spectroscopic, and theoretical study. *Inorgnic Chemistry,* 58(9), pp. 5695-5702.

Choppin, G., Liljenzin, J.-O. & Rydberg, J., 2002a. The Nuclear Fuel Cycle. In: *Radiochemistry and Nuclear Chemistry.* s.l.:Butterworth-Heinemann, p. 593.

Choppin, G., Liljenzin, J.-O. & Rydberg, J., 2002b. The Nuclear Fuel Cycle. In: *Radiochemistry and Nuclear Chemistry.* Woburn: Butterworth-Heinemann, p. 608.

Choppin, G. R., 2002. Covalency in f-element bonds. *Journal of Alloys and Compounds,* 344(1), pp. 55-59.

Clark, D. L., 2000. The chemical complexities of plutonium. *Los Alamos Science,* Volume 26, pp. 364-381.

Condamines, N. & Musikas, C., 1988. The extraction by N,N-dialkylamides. I. HNO3 and other inorganic acids. *Solvent Extraction and Ion Exchange,* 6(6), pp. 1007-1034.

Condamines, N. & Musikas, C., 1992. The extraction by N,N-dialkylamides. II. Extraction of actinide cations. *Solvent Extraction and Ion Exchange,* 12(1), pp. 69-100.

Cotton, S., 2006. Coordination Chemistry of the Actinides. In: *Lanthanide and Actinide Chemistry.* Chichester: John Wiley & Sons Ltd., p. Chapter 11.

Courson, O. et al., 1998. *Separation of minor actinides from genuine HLLW using the DIAMEX process.* s.l., 5th International Information Exchange Meeting, Mol..

Cui, Y. et al., 2010. Extraction of U(VI) with N,N'-dimethyl-N,N'-dioctylmalonamide from nitrate media. *Russian Journal of Inorganic Chemistry,* 55(3), pp. 468-471.

Cui, Y. et al., 2005. Extraction of U(VI) with unsymmetrical N-methyl-N-decylalkylamide in toluene. *Radiochimica Acta,* 93(5), pp. 287-290.

Danesi, P. R., Chiarizia, R. & Scibona, G., 1970. The meaning of slope analysis in solvent extraction chemistry: The case of zinc extraction by trilaurylammonium chloride. *Journal of Inorganic and Nuclear Chemistry,* 32(7), pp. 2349-2355.

Delpech, M. et al., 1999. *Transmutation of Americium and Curium. Review of solutions and impacts.* Mol, Belgium, International information exchange meeting on actinide and fission product partitioning and transmutation.

Dukes, E. K. & Siddall, T. H., 1966. Tetrabutyl urea as an extractant for nitric acid and some actinide nitrates. *J. Inorg. Nucl. Chem.,* Volume 28, pp. 2307-2312.

Durain, J., Bourgeois, D. & Meyer, D., 2019. Comprehensive studies on third phase formation: Application to U(VI)/Th(IV) mixtures extracted by TBP in n-dodecane. *Solvent Extraction and Ion Exchange,* 37(5), pp. 328-346.

Egorov, G. F. et al., 2005. Radiation chemical behaviour of tributyl phosphate, dibutylphosphoric acidand its zirconium salt in organic solutions and two-phase systems. *Radiochemistry,* 47(4), pp. 392-397.

Facchini, A. et al., 2000. Transient- and seady-state concentration profiles in a DIAMEX-like countercurrent process for An(III) + Ln(III) separation. *Separation Scence and Technology,* 35(7), pp. 1055-1068.

Fuger, J. J., 1958. Ion exchange behaviour and dissociation constants of americium, curium and californium complexes with ethylenediaminetetra acetic acid. *Journal of Inorganic and Nuclear Chemistry,* 5(4), pp. 332-338.

Gannaz, B. et al., 2007. Extraction of lanthanides(III) and Am(III) by mixtures of malonamide and dialkylphosphoric acid. *Solvent Extraction and Ion Exchange,* 25(3), pp. 313-337.

Garraway, J., 1984. *The behaviour of technetium in a nuclear fuel reprocessing plant.* Dounreay, I.Chem.E, pp. 47-56.

Gasparini, G. M. & Grossi, G., 1986. Review Article: Long chain disubstituted aliphatic amides as extracting agents in industrial applications of solvent extraction. *Solvent Extraction and Ion Exchange,* 4(6), pp. 1233-1271.

Geier, R. G., 1979. *Purex Process Solvent Literature Review,* Richland, Washington: United States Department of Energy.

Gong, Y. et al., 2013. Experimental and theoretical studies on the fragmentation of gas-phase uranyl-, neptunyl-, and plutonyl-diglycolamide complexes. *The Journal of Physical Chemistry,* 117(40), pp. 10544-10550.

Guelis, A. V., 2013. *Actinide and lanthanide separation process (ALSEP).* US, Patent No. 8,354,085.

Guillaume, B., Maurice, C. & Moulin, J. P., 1984. *Chemical properties of neptunium applied to neptunium management in extraction cycles of PUREX process.* s.l., CEA Centre d'Etudes Nucleaires de Saclay.

Gujar, R. B. et al., 2012. Radiolytic stability of N,N,N′,N′-tetraoctyl diglycolamide (TODGA) in the presence of phase modifiers dissolved in n-dodecane. *Solvent Extraction and Ion Exchange,* 30(3), pp. 278-290.

Gulevich, A. V. et al., 2020. Possibility of burning americium in fast reactors. *Atomic Energy,* 128(2), pp. 88-94.

Gullekson, B. J., Brown, M. A., Paulenova, A. & Gelis, A. V., 2017. Speciation of select f-element with lipohilic phosphorus acids and diglycol amides in the ALSEP backward-extraction regime. *Industrial and Engineering Chemistry Research,* pp. 12174-12183.

Gupta, K. K. et al., 2000c. Third phase formation in the extraction of the uranyl nitrate by N,N-dialkyl aliphatic amides. *Solvent Extraction and Ion Exchange,* 18(3), pp. 421-439.

Gupta, K. K., Manchanda, V. K., Subramanian, M. S. & Singh, R. K., 2000a. Solvent extraction studies on U(VI), Pu(IV) and fission products using N,N-dihexyloctanamide. *Solvent Extraction and Ion Exchange,* 18(2), pp. 273-292.

Gupta, K. K., Manchanda, V. K., Subramanian, M. S. & Singh, R. K., 2000b. N,N-dihexyl hexanamide: A promising extractant for nuclear fuel reprocessing. *Separation Science and Technology,* 35(10), pp. 1603-1617.

Heionen, J., 2014. Regulatory approach to the construction of ONKALO. *No. NEA-RWM-R-2013-6.*

Herbst, R. S., Baron, P. & Nilsson, M., 2001a. Standard and advanced separation: PUREX processes for nuclear fuel reprocessing. In: K. L. Nash & G. J. Lumetta, eds. *Advanced separation techniques for nuclear fuel reprocessing and radioactive waste treatment.* Cambridge: Woodhead Publishing Ltd., p. 172.

Herbst, R. S., Baron, P. & Nilsson, M., 2011b. Standard and advanced separation: PUREX processes for nuclear fuel reprocessing. In: K. L. Nash & G. J. Lumetta, eds. *Advanced separation techniques for nuclear fuel reprocessing and radioactive waste treatment.* Cambridge: Woodhead Publishing Limited, p. 159.

Herbst, R. S., Baron, P. & Nilsson, M., 2011c. Standard and advanced separation: PUREX processes for nuclear fuel reprocessing. In: K. L. Nash & G. J. Lumetta, eds. *Advanced separation techniques for nuclear fuel reprocessing and radioactive waste treatment.* Cambridge: Woodhead Publishing Ltd., p. 149.

Herbst, R. S., Baron, P. & Nilsson, M., 2011d. Standard and advanced separation: PUREX processes for nuclear fuel reprocessing. In: K. L. Nash & G. J. Lumetta, eds. *Advanced separation tecniques for nuclear fuel reprocessing and radioactive waste treatment.* Cambridge: Woodhead Publishing Ltd, p. 150.

Hérès, X. et al., 2008. The separation of extractants implemented in the DIAMEX-SANEX process. *ATALANTE (Nuclear Fuel Cycles for a Sustainable Future).*

IAEA, 2011. *The Nuclear Fuel Cycle,* Vienna: s.n.

Irish, E. R. & Reas, W. H., 1957. *The PUREX Process - A Solvent Extraction Reprocessing Method for Irradiated uranium,* Richland, Washington: General Electric.

Irving, H. & Edgington, D., 1959. The extraction of some metal chlorides into tri-n-butyl phosphate. *Journal of Inorganic and Nuclear Chemistry,* 10(3-4), pp. 306-318.

Job, P., 1928. Formation and stability of inorganic complexes in solution. *Annales de Chimie,* 9(113), pp. 113-203.

Jones, H. C., 1913. *Franklin Inst.,* Volume 176, pp. 479, 677.

Jones, H. C. & Strong, W. W., 1910. *Carnegie Inst. Wash. Pub.,* Volume 130.

Jones, H. C. & Strong, W. W., 1912. *Am. Chem. J.,* Volume 47, pp. 27, 126.

Kappelmann, F. A. & Weaver, B. S., 1966. *Method for separating americium and curium from the lanthanide rare earths and yttrium.* U.S., Patent No. 3,230,036.

Kirker, I. & Kaltsoyannis, N., 2011. Does covalency really increase across the 5f series? A comparison of molecular orbital, natural population, spin and electron density analysesof AnCp3 (An = Th-Cm; Cp = n5-C5H5). *Dalton Transactions,* 40(1), pp. 124-131.

Kosyakov, V. N. & Yerin, E. A., 1978. Separation of transplutonium and rare-earth elements by extraction with HDEHP from DTPA solutions. *Journl of Radioanalytical Chemistry,* 43(1), pp. 37-51.

Kudo, A. et al., 2017. *Development of U and Pu co-processing process demonstration of U, Pu and Np co-recovery with centrifugal contactors.* Fukui, 2017 international congress on advances in nuclear power plants.

Kulkarni, P. G. et al., 2006. Solvent extraction behaviour of some fission product elements with N,N-dihexyl octanamide and tri-n-butyl phasphate under simulated PUREX process conditions. *Radioachimica Acta,* 94(6-7), pp. 325-329.

Kumari, N., Prabhu, D. R. & Pathak, P. N., 2013. Uranium extraction studies employing tributyl phosphate and N,N-dihexyl octanamide as extractants: counter-current centrifugal contactor runs. *Separation Science and Technology,* 48(16), pp. 2479-2485.

Kumbhare, L. B. et al., 2002. Development of the DIAMEX process for treating PHWR high-level liquid waste. *Nuclear Technology,* Volume 139, pp. 253-262.

Laskorin, B. N., Skorovarov, D. I., Fedorova, L. A. & Shatalov, V. V., 1970. Basic principles in the extraction of uranium by phosphine oxide. *Soviet Atomic Energy,* 28(5), pp. 491-496.

Leafe, M., 2017. *End in sight for reprocessing nuclear fuel at Sellafield.* [Online]
Available at: https://nda.blog.gov.uk/2017/01/24/end-in-sight-for-reprocessing-nuclear-fuel-at-sellafield/
[Accessed 05 September 2017].

Leggett, D. J., 1985. In: *Computational Methods for the Determination of Formation Constants.* New York: Plenum.

Lewis, F. L. et al., 2012. Complexation of lanthanides, actinides and transition metal cations with a 6-(1,2,4-triazin-3-yl)-2,2':6',2''-terpyridine ligand: implications for actinide(III)/lanthanide(III) partitioning. *Dalton Transactions,* 41(30), pp. 9209-9219.

Libuś, Z., 1962. Absorption spectra of uranium(VI) complexes in solution. *J Inorg Nucl Chem,* 24(6), pp. 619-631.

Lin, L. et al., 2005. Synergistic extraction of uranium(VI) with tri-n-butyl phosphate and i-butyldedecylsulfoxide. *Jornal of Radioanalytical and Nuclear Chemistry,* 266(2), pp. 355-359.

Liu, X. et al., 2015. Extraction of U(VI) with N,N,N',N'-tetraoctyl diglycolamide from nitric acid solution. *J Radioanal Nucl Chem, 306:2,* pp. 549-553.

Loubert, G. et al., 2017. Structual studies of a series of uranyl alkylacetamides and piracetam complexes obtained in nitric acid aqueous solution. *Polyhedron,* Volume 138, pp. 7-12.

Loveland, W., Morrissey, D. & Seaborg, G., 2006. Schematic Shell Model. In: *Modern Nuclear Chemistry.* Hoboken, New Jersey: John Wiley % Sons, Inc., pp. 140-152.

Lumetta, G. J. et al., 2013. The TRUSPEAK Concept: Combining CMPO and HDEHP for Separating Trivalent Lanthanides from the Transuranic Elements. *Solvent Extraction and Ion Exchange,* 31(3), pp. 223-236.

Lumetta, G. J. et al., 2014. The Actinide-Lanthanide Separation concept. *Solvent Extraction and Ion Exchange,* 32(4), pp. 333-347.

Lumetta, G. J. et al., 2012. Lipophilic ternary complexes in liquid-liquid extraction of trivalent lanthanides. *Journal of Cordination Chemistry,* Volume 65, pp. 741-753.

Lumetta, G. J. et al., 2011. *Combining Neutral and Acidic Extractants for Recovering Transuranic Elements from Nuclear Fuel.* Santiago, Chile, XIX International Solvent Extraction Conference.

Madic, C. et al., 1994. *Actinide partitioning from high level liquid waste using the DIAMEX process.* s.l., The Fourth International Conference on Nuclear Fuel Reprocessing and Waste Management, RECOD'94 Proceedings.

Magnusson, D. et al., 2009. Demonstration of a SANEX process in centrifugal contactors using the CyMe4-BTBP molecule on a genuine fuel solution. *Solvent Extraction and Ion Exchange,* 27(2), pp. 97-106.

Magnusson, D. et al., 2009. Demonstration of a TODGA based extraction process for the partitioning of minor actinides from a PUREX raffinate. Part III: Centrifugal contactor run using genuine fuel solution. *Solvent Extraction and Ion Exchange,* 27(1), pp. 26-35.

Mahajan, G. R., Prabhu, D. R., Manchanda, V. K. & Badheka, L. P., 1998. Substituted malonamides as extractants for partitioning of actinides from nuclear waste solutions. *Waste Management,* 18(2), pp. 125-133.

Manchanda, V. K. et al., 2001. Distribution behaviour of U(VI), Pu(IV), Am(III) and Zr(IV) with N,N-dihexyl octanamide under uranium-loading conditions. *Nuclear Technology,* 134(3), pp. 231-240.

Manchanda, V. & Pathak, P., 2004. Amides and diamides as promising extractants in the back end of the nuclear fuel cycle. *Separation and Purification Technology,* 35(2), pp. 85-103.

Markandya, A. & Wilkinson, P., 2013. Electricity generation and health. *The Lancet,* 370(9591), pp. 979-990.

McCann, K., Mincher, B. J., Schmitt, N. C. & Braley, J. C., 2017. Hexavalent actinide extraction using N,N-dialkyl amides. *Industrial and Engineering Chemistry Research,* Volume 56, pp. 6515-6519.

McCann, K., Sinkov, S. I., Lumetta, G. J. & Shafer, J. C., 2018. Inner versus outersphere metal-monoamide complexation: Ramification for tetravalent & hexavalent actinide selectivity. *New J Chem,* 42(7), pp. 5415-5424.

Mellinger, P. J., Harmon, K. M. & Lakey, L. T., 1984. *A Summary of Nuclear Fuel Reprocessing Activities Around the World,* s.l.: United States Department of Energy.

Miguirditchian, M. et al., 2008. *Extraction of uranium(VI) by N,N-di(2-ethylhexyl)isobutyramide (DEHIBA): from the batch experimental data to the countercurrent process.* Montreal, Canada, Solvent extraction: fundamentals to industrial applications. Proceedings ISEC 2008 Internaltional Solvent Extraction conference.

Mincher, B. J., Modolo, G. & Mezyk, S. P., 2009a. Review article: The effects of radiation chemistry on solvent extraction: 1. Conditions in acidic solution and a review of TBP radiolysis. *Solvent Extraction and Ion Exchange,* 27(1), pp. 1-25.

Mincher, B. J., Modolo, G. & Mezyk, S. P., 2009b. Review Article: The effects of radiation chemistry on solvent extraction 3: A review of actinide and lanthanide extraction. *Solvent Extraction and Ion Exchange,* 27(5-6), pp. 579-606.

Mincher, B. J., Modolo, G. & Mezyk, S. P., 2010. Review: The effects of radiation chemistry on solvent extraction 4: Separation of the trivalent actinides and considerations for radiation-resistant solvent systems. *Solvent Extraction and Ion Exchange,* 28(4), pp. 415-436.

Modolo, G., Asp, H., Schreinemachers, C. & Vijgen, H., 2007a. Development of a TODGA based process for partitioning of actinides from a PUREX raffinate part I: Batch extraction optimization studies and stability tests. *Solvent Extraction and Ion Exchange,* 25(6), pp. 703-721.

Modolo, G. et al., 2008. Demonstration of a TODGA-based continuous counter-current extraction process for the partitioning of actinides from simulated PUREX raffinate. Part II: Centrifugal contactor runs. *Solvent Extraction and Ion Exchange,* 26(1), pp. 62-76.

Modolo, G., Seekamp, S. & Vijgen, H., 2003. *DIAMEX process development to separate trivalent actinides from high active concentrates.* s.l., The 9th International Conference on Environmental Remediation and Radioactive Waste Management.

Modolo, G. et al., 2007b. DIAMEX counter-current extraction process for recovery of trivalent actinides from simulated high active concentrate. *Separaton Science and Technology,* 42(3), pp. 439-452.

Mowafy, E. A. & Aly, H. F., 2002. Extraction behaviours of Nd(III), Eu(III), La(III), Am(III) and U(VI) with some substituted malonamides from nitrate medium. *Solvent Extraction and Ion Exchange,* 20(2), pp. 177-194.

Mowafy, E. A. & Aly, H. F., 2002. Extraction behavious of Nd(III), Eu(III), La(III), Am(III) and U(VI) with some substituted malonamides from nitrate media. *Solvent Extraction and Ion Exchange,* 20(2), pp. 177-194.

Moyer, B. A. et al., 1991. Liquid-liquid equilibrium analysis in perspective: Part 1. Slope analysis of the extraction of uranyl nitrate from nitric acid by di-2-ethyl-hexylsulfoxide. *Solvent Extraction and Ion Exchange,* 9(5), pp. 833-864.

Musikas, C., 1987. Solvent extraction for the chemical separations of the 5f elements. *Inorganica Chimica Acta,* Volume 140, pp. 197-206.

Nair, G., Mahajan, G. & Prabhu, D., 1995. Extraction of uranium(VI) and plutonium(IV) with some high molecular weight aliphatic monoamides from nitric acid medium. *Journal of Radioanalytical and Nuclear Chemistry,* 191(2), pp. 323-330.

Nair, G. M., Mahajan, G. R. & Prabhu, D. R., 1996. Dioctyl butyramide and dioctyl isobutyramide as extractants for uranium(VI) and plutonium(IV). *Journal of Radioanalytical and Nuclear Chemistry,* 204(1), pp. 103-111.

Nair, G. M., Prabhu, D. R. & Mahajan, G. R., 1994. Extraction of uranium(VI) and plutonium(IV) with dihexylbutyramide and dihexylisobutyramide from nitric acid medium. *Journal of Radioanalytical and Nuclear Chemistry,* 182(2), pp. 393-399.

Nair, G. M., Prabhu, D. R., Mahajan, G. R. & Shukla, J. P., 1993. Tetra-butyl-malonamide and tetra-isobutyl-malonamideas extractants for uranium(VI) and plutonium(IV). *Solvent Extraction and Ion Exchange,* 11(5), pp. 831-847.

Nash, K. L., 2015. The chemistry of TALSPEAK: A review of the science. *Solvent Extraction and Ion Exchange,* 33(1), pp. 1-55.

Nash, K. L., Madic, C., Mathur, J. & Lacquement, J., 2010a. Actinide Separation Science and Technology. In: L. R. Morss, N. M. Edelstein & J. Fuger, eds. *The Chemistry of the Actinde and Transactinide Elements.* Dordrecht: Springer, p. 2645.

Nash, K. L., Madic, C., Mathur, J. & Lacquement, J., 2010b. Actinide separation science and technology. In: L. R. Morss, N. M. Edelstein & J. Fuger, eds. *The Chemistry of the Actinide and Transactinide Elements.* Dordrecht: Springer, pp. 2732-2733.

Nash, K. L., Madic, C., Mathur, J. & Lacquement, J., 2010c. Actinde Separation Science and Technology. In: L. R. Morss, N. M. Edelstein & J. Fuger, eds. *The Chemistry of the Actinide and Transactinide Elements.* Dordrecht: Springer, p. 2634.

Nash, K. L., Madic, C., Mathur, J. N. & Lacquement, J., 2010d. Actinide Separation Science and Technology. In: L. R. Morss, N. M. Edelstein & J. Fuger, eds. *The Chemistry of the Actinide and Transactinide Elements.* Dordrecht: Springer, p. 2647.

Nash, K. L. & Nilsson, M., 2015a. Introduction to the reprocessing and recycling of spent nuclear fuel. In: R. Taylor, ed. *Reprocessing and Recycling of Spent Nuclear Fuel.* Cambridge: Elsevier, p. 9.

Nash, K. L. & Nilsson, M., 2015b. Introduction to the reprocessing and recycling of spent nucelar fuel. In: R. Taylor, ed. *Rerocessing and Recycling of Spent Nuclear Fuel.* Cambridge: Elsevier, pp. 13-14.

Nash, K. L. & Nilsson, M., 2015c. Introduction to the reprocessing and recycling of spent nuclear fuels. In: R. Taylor, ed. *Reprocessing and Recycling of Spent Nuclear Fuel.* Cambridge: Woodhead Publishing, p. 16.

Nave, S., Modolo, G., Madic, C. & Testard, F., 2004. Aggregation properties of N,N,N',N'-tetraoctyl-3-oxapentanediamide (TODGA) in n-dodecane. *Solvent Extraction and Ion Exchange,* 22(4), pp. 527-551.

Neta, P., Huie, R. E. & Ross, A., 1990. Rate constants for reactions of peroxyl radicals in fluid solutions. *Journal of Physical and Chemical Reference Data,* 19(2), pp. 413-513.

Nigond, L., Musikas, C. & Cuillerdier, C., 1994. Extraction by N,N,N',N'-tetraalkyl-2-alkyl propane-1,3-diamides I. H2O, HNO3 and HClO4. *Solvent Extraction Ion Exchange,* 12(2), pp. 261-296.

Nilsson, M. & Nash, K. L., 2007. Review article: A review of the development and operational characteristics ofthe TALSPEAK process. *Solvent Extraction and Ion Exchange,* 25(6), pp. 665-701.

NIST, 2020. *NIST Center for Neutron Research.* [Online]
Available at: https://www.ncnr.nist.gov/resources/n-lengths/list.html
[Accessed 2nd May 2020].

Nukada, K., Naito, K. & Maeda, U., 1960. On the Mechanism of the Extraction of Uranyl Nitrate by Tributyl Phosphate II. Infrared Study. *Bulletin of the Chemical Society of Japan,* 33(7), pp. 894-898.

OECD, 2006. *Physics and Safety of Transmutation Systems, A Status Report, NEA No. 6090,* s.l.: s.n.

OECD & NEA, 2012. *Spent Nuclear Fuel Reprocessing Flowsheet.* [Online]
Available at: https://www.oecd-nea.org/science/docs/pubs/nea6090-transmutation.pdf

Ogden, M. D. et al., 2011. Complexation studies of bidentate heterocyclic N-donor ligands with Nd(III) and Am(III). *Journal of Solution Chemistry,* 40(11), pp. 1874-1888.

Ogden, M. D., Sinkov, S. I., Lumetta, G. J. & Nash, K. L., 2012. Affinity of An(VI) for N4-tetradentate donor ligands: Complexation of the actinyl(VI) ions with N4-tetradentate ligands. *Journal of Solution Chemistry,* 41(4), pp. 616-629.

Panak, P. J. & Geist, A., 2013. Complexation and extraction of trivalent actinides and lanthanides by triazinylpyridine N-donor ligands. *Chemical Reviews,* 113(2), pp. 1199-1236.

Panja, S., Mohapatra, P. K., Tripathi, S. C. & Manchanda, V. K., 2009. Studies on uranium(VI) pertraction across a N,N,N'N'-tetraoctyldiglycolamide (TODGA) suported liquid membrane. *Journal of Membrane Scince,* Volume 337, pp. 274-281.

Panja, S., Mohapatra, P. K., Tripathi, S. C. & Manchanda, V. K., 2011. Facilitated transport of uranium(VI) across supported liquid membranes containing T2EHDGA as the carrier extractant. *Journal of Hazardous Materials,* 188(1-3), pp. 281-287.

Parikh, K. J. et al., 2009. Radiolytic degradation studies on N,N-dihexylactanamide (DHOA) under PUREX process conditions. *Solvent Extraction and Ion Exchange,* 27(2), pp. 244-257.

Pathak, D. R., Kumbhare, L. B. & Manchanda, V. K., 2001. Structural effects in N,N-dialkyl amides on the extraction behaviour toward uranium and thorium. *Solvent Extraction and Ion Exchange,* 19(1), pp. 105-126.

Pathak, P. N., Kanekar, A. S., Prabhu, D. R. & Machanda, V. K., 2009. Comparison of hydrometallurgical parameter of N,N-dialkylamides and of tri-n-butylphosphate. *Solent Extraction and Ion Exchange,* 27(5-6), pp. 683-694.

Pathak, P. N., Prabhu, D. R., Kanekar, A. S. & Manchanda, V. K., 2010. Evaluation of N,N-dialkylamides as promising process extractants. *IOP Conference Series: Materials Science and Engineering,* Volume 9, pp. 1-8.

Pathak, P., Prabhu, D. & Manchanda, V., 2000. Distribution behaviour of U(VI), Th(IV) and Pa(V) from nitric acid mudium using linear and branched hain extractants. *Solvent Extraction and Ion Exchange,* 18(5), pp. 821-840.

Peng, X. et al., 2017. Extraction and separation of uranium(VI) and Fe(III) from lanthanide chlorides with N,N,N',N'-tetrasubstituted alkyl diglycolamide extractants. *Journal of Radioanalytical and Nuclear Chemistry,* 313(2), pp. 327-332.

Phillips, C., 1992. Uranium-plutonium partitioning by pulsed columns in the first cycle of the three cycle thermal oxide reprocessing plant. *Waste Management '92: working towards a cleaner environment: waste processing, transportation, storage and disposal, technical programs and public education.,* Volume 1 and 2, pp. 1041-1045.

Prabhu, D. R., Kumari, N., Kanekar, A. S. & Pathak, P. N., 2013. Biphasic kinetic investigations on th evaluation of non-salt forming reductants for Pu(IV) stripping from tributyl phosphate and N,N-ihexyl octanamide solutions in n-dodecane. *Journal of Radioanalytical and Nuclear Chemistry,* 298(1), pp. 691-698.

Prabhu, D. R., Mahajan, G. R. & Nair, G. M., 1997. Di(2-ethyl hexyl) butyramide and di(2-etyl hexyl)isobutyramide as extractants for uranium(VI) and plutonium(IV). *Journal of Radioanalytical and Nuclear Chemistry,* 224(1-2), pp. 113-117.

Prabhu, D. R., Mahajan, G. R., Nair, G. M. & Subramanian, M. S., 1993. Extraction of uranium(VI) and plutonium(IV) with unsymmetrical monoamides. *Radiochimica Acta,* 60(2-3), pp. 109-113.

Rabinowitch, E., 1953. *Absorption spectra of uranyl compounds in solution,* Lemont, Illinois: Argonne National Laboratory.

Rabinowitch, E. & Belford, R. L., 1964a. In: *Spectroscopy and Photochemistry of Uranyl Compounds, Chapter 2.* New York: Macmillan.

Rabinowitch, E. & Belford, R. L., 1964b. In: *Spectroscopy and Photochemistry of Uranyl Compounds.* New York: Macmillan, p. Chapter 1.

Rao, L. & Tian, G., 2010. Symmetry, optical properties and thermodynamics of neptunium(V) complexes. *Symmetry,* 2(1), pp. 1-14.

Raut, D. & Mohapatra, P., 2013. Non-dispersive solvent extraction of uranium from nitric acid medium by several amides and their mixture with TODGA using a hollow fiber contactor. *Separation Science and Technology,* 48(16), pp. 2436-2443.

Regalbuto, M., 2001a. Alternative separation and extraction: UREX+ processes for acintide and targetted fission product recovery. In: K. L. Nash & G. Lumetta, eds. *Advanced separation techniques for nuclear fuel reprocessing and radioactive waste treatment.* Cambridge: Woodhead Publishing Limited, p. 177.

Regalbuto, M. C., 2011b. Alternative separation and extraction: UREX+ processes for actinide and tagetted fission product recovery. In: K. L. Nash & G. J. Lumetta, eds. *Advanced separation tecniques for nuclear fuel reprocessing and radioactive waste treatment.* Cambridge: Woodhead Publishing Ltd, p. 179.

Regalbuto, M. C., 2011c. Alternative separation and extraction: UREX+ processes for actinide and targeted fission product recovery. In: K. L. Nash & G. J. Lumetta, eds. *Advanced separation tecniques for nuclear fuel reprocessing and radioactive waste treatment.* Cambridge: Woodhead Publishing Ltd, p. 181.

Reif, D. J., 1988. Restoring solvent for nuclear separation processes. *Separation Science and Technology,* 23(12-13), pp. 1285-1295.

Ren, P. et al., 2017. Synthesis and characterization of bisdiglycolamides for comparable extraction of Th4+, UO22+ and Eu3+ from nitric acid solution. *Journal of Radioanalytical and Nuclear Chemistry,* 312(3), pp. 487-494.

Rostaing, C. et al., 2012. Development and validation of the EXAm separation process for single Am recycling. *Procedia Chemistry,* Volume 7, pp. 367-373.

Ruikar, P. B. & Nagar, M. S., 1995. Synthesis and Characterisaion of some new mono- and diamide complexes of plutonium(IV) and dioxouranium(VI) nitrates. *Polyhedron,* 14(20-21), pp. 3125-3132.

Ruikar, P. B. et al., 1995. Extraction behaviour of uranium(VI), plutonium(IV), zirconium(IV), ruthenium(III) and europium(III) with γ-pre-irradiated solutions of N,N-methylbutyl substituted amides in n-dodecane. *Journal of Radioanalytical and Nuclear Chemistry Letters,* 201(2), pp. 125-134.

Sasaki, Y. & Choppin, G. R., 1996. Solvent extraction of Eu, Th, U, Np and Am with N,N'-dimethyl-N,N'-dihexyl-3-oxapentanediamide and its analagous compounds. *Analytical Sciences,* 12(2), pp. 225-230.

Sasaki, Y. & Choppin, G. R., 1996. Solvent extraction of Eu, Th, U, Np and Am with N,N'-dimethyl-N,N'-dihexyl-3-oxapentanediamide and its analogous compounds. *Analytical Sciences,* 12(2), pp. 225-230.

Sasaki, Y., Sugo, Y., Morita, K. & Nash, K. L., 2015. The effect of alkyl substituents on actinide and lanthanide extraction by diglycolamide compounds. *Solvent Extraction and Ion Exchange, 33:7,* pp. 625-641.

Sasaki, Y., Sugo, Y., Suzuki, S. & Kimura, T., 2005. A method for the determination of extraction capacity and its application to N,N,N',N'-tetraalkylderivatives of diglycolamide-monoamide/n-dodecane media. *Analytica Chimica Acta,* 543(1-2), pp. 31-37.

Sasaki, Y., Sugo, Y., Suzuki, S. & Tachimori, S., 2001. The novel extractants, diglycolamide, for the extraction of lanthanides and actinides in HNO3-n-dodecane system. *Solvent Extraction and Ion Exchange,* 19(1), pp. 91-103.

Sasaki, Y. et al., 2013. Extraction behaviour of metal ions by TODGA, DOODA, MIDOA and NTAamide extractants from HNO3 to n-dodecane. *Solvent Extraction and Ion Exchange, 31:4,* pp. 401-415.

Sato, T., 1958. The extraction of uranyl nitrate from nitric acid solutions by tributyl phosphate solvent. *Journal of Inorganic and Nuclear Chemistry,* Volume 6, pp. 334-337.

Schulz, W. W., 1972. Radiolysis of Hanford B plant HDEHP extractant. *Nuclear Technology,* 13(2), pp. 159-167.

Serrano-Purroy, D. et al., 2004. *First DIAMEX partitioning using genuine high active concentrate.* s.l., Atalante 2004 (No. INIS-FR--2874). JRC.

Siddall, T. H., 1960. Effects of structure of N,N-disubstituted amides on their extraction of actinide and zirconium nitrates and of nitric acid. *Journal of Physical Chemistry,* 64(12), pp. 1863-1866.

Smith, B. F. et al., 1997. Amides as phase modifiers for N,N'-tetraalkylmalonamide extraction of actinides and lanthanides from nitric acid solutions. *Separation Science and Technology,* 32(1-4), pp. 149-173.

Smith, N. A., 2010. Speciation and spectroscopy of the urnayl and tetravalent pluonium nitrate systems: Fundamental studies and appliactions to used fuel reprocessing. *PhD thesis, University of Nevada.*

Sugai, H., 1992. Crud in solvent washing process for nuclear fuel reprocessing. *Journal of Nuclear Science and Technology,* 29(5), pp. 445-453.

Sugai, H., Munakata, K., Miyachi, S. & Yasu, S., 1992. Emulsions stabilized by precipitates of zirconium and tributyl phosphate degradation products. *Nuclear Technology,* 98(2), pp. 188-195.

Svantesson, I., Hangstroem, I., Persson, G. & Liljenzin, J. O., 1979. Separation of americium and neodymium by selective stripping and subsequent extraction with HDEHP using DTPA-lactic acid solution in a closed loop. *Radiochemical and Radioanalytical Letters,* 37(4-5), pp. 215-222.

Tachimori, S. & Nakamura, H., 1979. Radiation effects on the separation of lanthanides and transplutonides by the TALSPEAK-type extraction. *Biochemical and Biophysical Research Communications,* 91(2), pp. 498-501.

Tachimori, S., Sasaki, Y. & Suzuki, S., 2002. Modification of TODGA-n-dodecane solvent with a monoamide for high loading of lanthanides(III) and actinides(III). *Solvent Extraction and Ion Exchange,* 20(6), pp. 687-699.

Taylor, R. et al., 2016. The EURO-GANEX process: current status of flowsheet development and process safety studies. *Procedia Chemistry,* Volume 21, pp. 524-529.

Taylor, R. J. et al., 2013. Progress towards the full recovery of neptunium in an advanced PUREX process. *Solvent Extraction and Ion Exchange,* 31(4), pp. 442-462.

Thiollet, G. & Musikas, C., 1989. Synthesis and uses of the amides extractants. *Solvent Extraction and Ion Exchange,* 7(5), pp. 813-827.

Tian, G., Xu, J. & Rao, L., 2005. Optical absorption and structure of a highly symmetrical neptunium(V) diamide complex. *Actinide Chemistry,* 117(38), pp. 6356-6359.

Tkac, P., Vandegrift, G. F., Lumetta, G. J. & Gelis, A. V., 2012. Study of the Interaction between HDEHP and CMPO and its Effect on the Extraction of Selected Lanthanides. *Industrial and Engineering Chemistry Research,* Volume 51, pp. 10433-10444.

Todd, T. A. et al., 2000. Treatment of radioactive wastes using liquid-liquid extraction technologies - Facts, fears and issues. *Waste Management '00.*

Trading Economics, 2020. *Uranium.* [Online]
Available at: https://tradingeconomics.com/commodity/uranium
[Accessed 2nd May 2020].

Tsutsui, N. et al., 2017. Solvent extraction of uranium with N,N-di(2-ethylhexyl)octanamide from nitric acid medium. *Solvent Extraction and Ion Exchange,* 35(6), pp. 439-449.

Vandegrift, G. F. et al., 2004. *Designing and demonstration of the UREX+process using spent nuclear fuel.* Nimes, ATALANTE 2004 conference: Advancements for future nuclear fuel cycles.

Vanel, V. et al., 2012. Modelling of americium stripping in the EXAm process. *Procedia Chemistry,* Volume 7, pp. 404-410.

Verma, P. K. et al., 2018. Structural investigations on uranium(VI) and thorium(IV) complexation with TBP and DHOA: a spectroscopic study. *New J. Chem.,* Volume 42, pp. 5243-5255.

Vidyalakshmi, V., Subramanian, M. S., Srinivasan, T. G. & Vasudeva Rao, P. R., 2001. Effect of extractant structure on third phase formation in the extraction of uranium and nitric acid by N,N-dialkyl amides. *Solvent Extraction and Ion Exchange,* 19(1), pp. 37-49.

Von Sonntag, C., Ansorge, G. & Sugimori, A., 1972. Radiation chemistry of DNA model compounds. Part II. Alkyl phosphate cleavage of aliphatic phosphates induced by hydrated electrons and by OH radicals. *Z. Naturforsch,* 27b(4), pp. 471-472.

Wahu, S. et al., 2012. Structural Versatility of Uranyl(VI) Nitrate Complexes That Involve the Diamide Ligand Et2N(C=O)(CH2)n(C=O)NEt2 (0 < n < 6). *European Journal of Inorganic Chemistry,* Volume 23, pp. 3747-3763.

Wall, N., 2017. *Managing zirconium chemistry and phase compatibility in combined process separations for minor actinide partitioning fuel cycle research and development,* s.l.: Washinton State University.

Wang, G. et al., 2009. Adsorption of uranium (VI) from aqueous solution onto cross-linked chitosan. *Journal of Hazardous Materials,* 168(2-3), pp. 1053-1058.

Wang, Z. et al., 2017. Extraction of trivalent americium and europium with TODGA homologs from HNO3 solution. *Journal of Radioanalytical and Nuclear Chemistry,* 313(2), pp. 309-318.

Warade, A., Gaikwad, R., Sapkal, R. & Sapkal, V., 2011. Simulation of multistage countercurrent liquid-liquid extraction. *Leonardo Journal of Sciences,* Volume 20, pp. 79-94.

Weaver, B. S. & Kappelmann, F. A., 1964. *TALSPEAK, a new method of separation americium and curium from the lananides by extraction from an aqueous solution of an aminopolyacetic acid complexwith a monoacetic organophosphate or phosphate,* Oak Ridge, Tennessee: Oak Ridge National laboratory.

Weaver, B. S. & Kappelmann, F. A., 1968. Preferential extraction of lanthanides over trivalent actinides by monoacetic organophosphates from carboxylic acids and from mixtures of carboxylic and aminopolyacetic acids. *Journal of inorganic and Nuclear Chemistry,* 30(1), pp. 263-272.

Whittaker, D. et al., 2018. Applications of diglycolamide based solvent extraction processes in spent nuclear fuel reprocessing, part 1: TODGA. *Solvent Extraction and Ion Exchange,* 36(3), pp. 223-256.

Wilden, A. et al., 2015. Laboratory-scale counter-current centrifugal contactor demonstration of an innovative-SANEX process using a water soluble BTP. *Solvent Extraction and Ion Exchange,* 33(2), pp. 91-108.

Wilkinson, W. L., 1987. The UK reprocessing and waste management programme. *RECOD 87.*

Wojnárovits, L., 2011. Radiation Chemistry. In: A. Vértes, et al. eds. *Handbook of Nuclear Chemistry, 2nd Ed.* Dordrecht: Springer, p. 1315.

Woodhead, J., 1965. The ultra-violet absorption spectra of nitric acid ad metal nitrates in tri-n-butyl phosphate solutions. *Journal of Inorganic and Nuclear Chemistry,* 27(5), pp. 111-1116.

World Nuclear Association, 2020a. *Nuclear Power in the United Kingdom.* [Online]
Available at: https://www.world-nuclear.org/information-library/country-profiles/countries-t-z/united-kingdom.aspx
[Accessed 2nd May 2020].

World Nuclear Association, 2020b. *Radioactive Waste Treatment.* [Online]
Available at: www.world-nuclear.org/information-library/nuclear-fuel-cycle/nuclear-wastes/radioactive-waste-management.aspx
[Accessed 2nd May 2020].

World Nuclear Association, 2020c. *Processing of Used Nuclear Fuel.* [Online]
Available at: https://www.world-nuclear.org/information-library/nuclear-fuel-cycle/fuel-recycling/processing-of-used-nuclear-fuel.aspx
[Accessed 16th February 2021].

World Nuclear Association, 2020d. *Nuclear Fuel Cycle Overview.* [Online]
Available at: https://www.world-nuclear.org/information-library/nuclear-fuel-cycle/introduction/nuclear-fuel-cycle-overview.aspx
[Accessed 16th February 2021].

Yoshida, Z., Johnson, S. G., Kimura, T. & Krsul, J. R., 2010. Neptunium. In: L. R. Morss, N. M. Edelstein & J. Fuger, eds. *The Chemistry of the Actinide and Transactinide Elements.* Dordrecht: Springer, p. 752.

Zhu, Z.-X.et al., 2004. Cumulative study on the solvent extraction of elements by N,N,N',N'-tetraoctyl-3-oxapentanediamide (TODGA) from nitric acid into n-dodecane. *Analytica Chimica Acta,* 527(2), pp. 163-168.

Zilberman, B. Y. et al., 2003. Extraction of transplutonium and rare-earth elements, molybdenum and iron with zirconium salt of dibutyl phosphoric acid. *Czechoslovak Journal of Physics,* Volume 53, pp. 479-486.

Zilberman, B. Y. & Ferorov, Y. S., 1991. Extraction chemistry of uranyl nitrate and nitric acid in high concentration systems. *Journal of Radioanalytical and Nuclear Chemistry,* 150(2), pp. 357-362.

Appendix A – Spectrophotometric Data and SQUAD Modelling

A.1   Spectral and Spectrophotometric data

A.1.1   NMR spectra
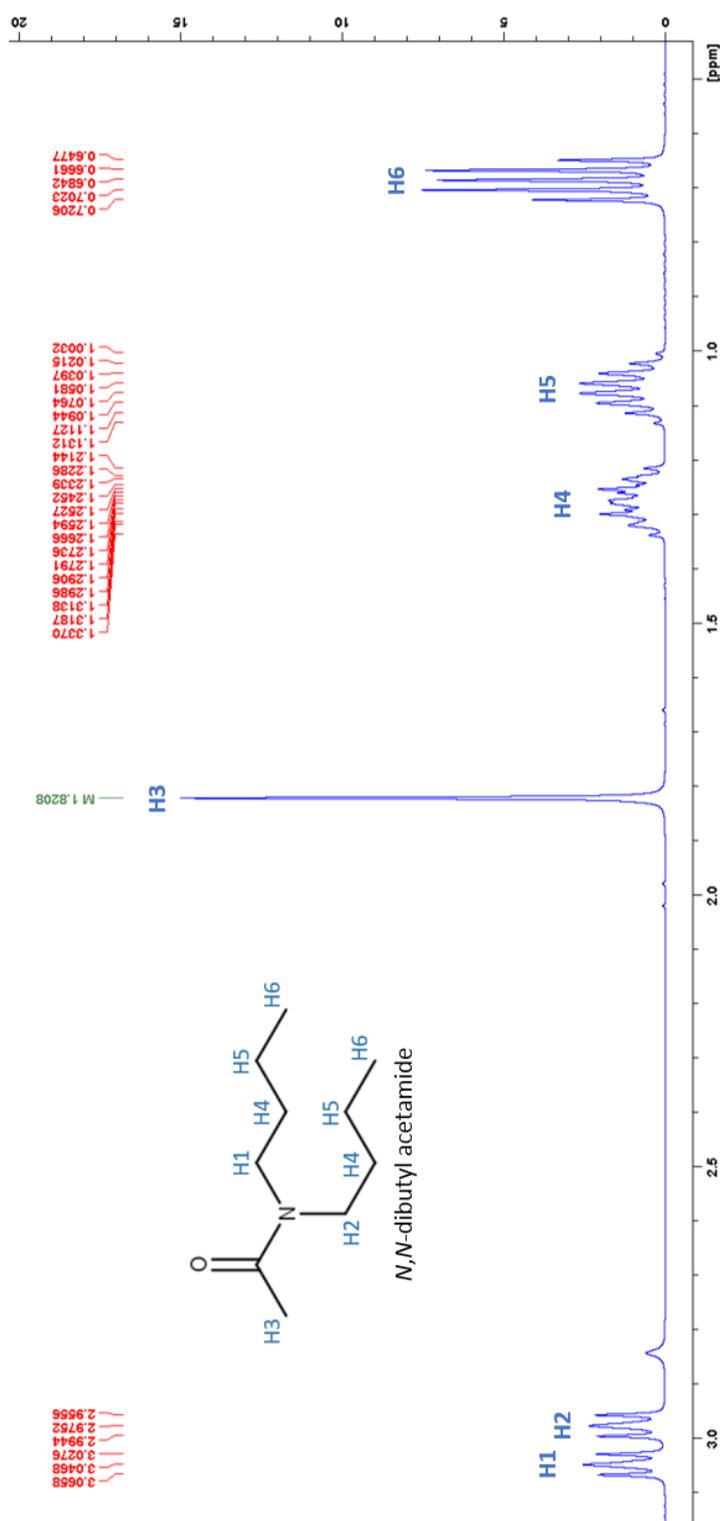
Figure A.1. *An example ^{1}H NMR (500 MHz, CDCl$_3$) spectrum of N,N-dibutyl acetamide taken at the Department of Chemistry at the University of Sheffield and processed in the Topspin software.*

A.1.2 Jobs plot spectra
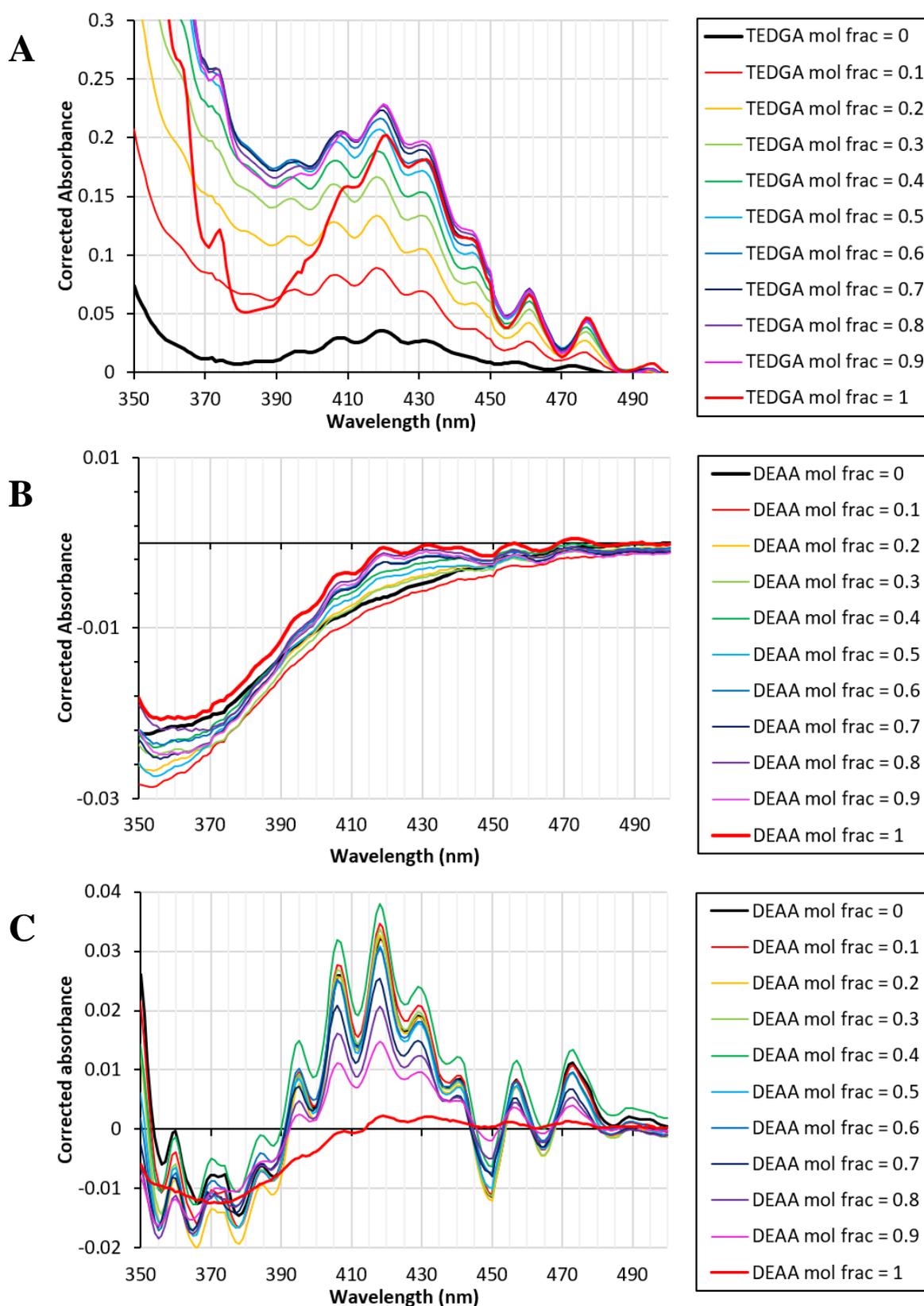
Figure A.2. *Example raw spectra for the dual ligand Jobs plots in Figure 3.11 and 3.12 to showcase spectra that worked and a spectrum that showed no interaction. A) DBBA-TEDGA Jobs plot in diluent A (Jobs plot displayed ligand interaction), B) DEAA-TEP Jobs plot in diluent B (Jobs plot did not display ligand interaction), C) DEAA-TEDGA Jobs plot in diluent B (Jobs plot displayed ligand interaction).*

A.2 SQUAD Modelling

A.2.1 SQUAD Input File

```
Section 1 ──┤ U(VI)-TEMA spectrophotometric titration experiment. Wavelength range: 360..479 nm
            │ System- pH 1 HNO3-MeOH (4.5:95.5 vol%), 0.2 M NO3-. Path length: 10 mm
            ┌ DICTIONARY:
Section 2 ──┤ MTL1=U;LIG1=TEMA;PROT=H;HYDX=OH:
            └ END:
            ┌ SPECIES:
            │ U(1)TEMA(1);3.5;VB;VE:
Section 3 ──┤ U(1)TEMA(2);4.5;VB;VE:
            └ END:
            ┌ OTHER:
Section 4 ──┤ U;VE:
            └ END:
            ┌ DATA:
            │ 350.00       499.00      +1.00
            │ LOGB
            │ PRIN
            │ CARD
Section 5 ──┤ NNLS
            │ NOPL
            │ CRT
            │ 50
            └ 1.0
            ┌ MOL.ABS.:
            │ TEMA:
            │ END:
            │    0.563
            │    0.496
Section 6 ──┤    0.440
            │              One value for each measured λ.
            │              Excess values removed for clarity.
            │    0.034
            │    0.034
            │    0.034
```

```
Section 7 ◄── SPECTRA:
(not included   0.0072          0.0000E-00    1e-19        0.0000E-00    1.000      1.0
in this example)   0.0838  0.0750  0.0693  0.0655  0.0624  0.0593  0.0554  0.0509
                   0.0466  0.0432  0.0406  0.0390  0.0387  0.0385  0.0386  0.0378
                   0.0365  0.0348  0.0334  0.0319  0.0315  0.0297  0.0291  0.0289
                   0.0288  0.0298  0.0304  0.0311  0.0319  0.0326  0.0335  0.0342
                   0.0355  0.0368  0.0387  0.0409  0.0433  0.0456  0.0479  0.0499
                   0.0517  0.0534  0.0552  0.0572  0.0596  0.0624  0.0655  0.0688
                   0.0721  0.0750  0.0777  0.0801  0.0821  0.0841  0.0860  0.0880
                   0.0903  0.0928  0.0956  0.0981  0.1005  0.1027  0.1046  0.1060
                   0.1074  0.1087  0.1098  0.1106  0.1116  0.1124  0.1130  0.1133
                   0.1132  0.1125  0.1117  0.1108  0.1099  0.1093  0.1090  0.1089
                   0.1088  0.1087  0.1082  0.1071  0.1054  0.1026  0.0991  0.0951
Section 8 ──┤      0.0908  0.0869  0.0836  0.0812  0.0795  0.0784  0.0778  0.0777
                   0.0775  0.0768  0.0756  0.0741  0.0731  0.0639  0.0590  0.0542
                   0.0499  0.0463  0.0432  0.0408  0.0388  0.0376  0.0368  0.0360
                   0.0353  0.0344  0.0329  0.0310  0.0285  0.0258  0.0230  0.0203
                   0.0179  0.0158  0.0138  0.0120  0.0105  0.0094  0.0086  0.0080
                   0.0077  0.0075  0.0074  0.0073  0.0072  0.0068  0.0064  0.0060
                   0.0054  0.0050  0.0044  0.0040  0.0034  0.0029  0.0026  0.0023
                   0.0020  0.0018  0.0016  0.0015  0.0013  0.0012
                0.0069          0.0000E-00    0.00153      0.0000E-00    1.000      1.0
                   0.0912  0.0821  0.0757  0.0711  0.0677  0.0643  0.0603  0.0561
                   0.0523  0.0491  0.0467  0.0452  0.0443  0.0440  0.0433  0.0426
                   0.0415  0.0398  0.0385  0.0374  0.0368  0.0353  0.0347  0.0343
                   0.0343  0.0346  0.0350  0.0356  0.0362  0.0368  0.0377  0.0388
                   0.0402  0.0419  0.0436  0.0455  0.0474  0.0493  0.0515  0.0534
```

Figure A.3. *An example input file for the SQUAD program. Descriptions for the identified sections can be seen in Table A.1.*

Table A.1. *Descriptions for each of the sections of the SQUAD input file in Figure A.3.*

| Section	Name	Description
1	Title	File description which has no impact on the model. Two lines for a useful title and subtitle.
2	Dictionary	Define up to 2 metals, 2 ligands, proton, and hydroxide to be used in the model, each separated by a semicolon. 4 characters maximum per definition.
3	Species	Define complexes to be considered in the model with fixed stability constants (FB) or variable stability constants (VB), and to state whether molar absorptivities of these species need to be calculated (VE), or not (FE).
4	Other	Optional section. Can set variable molar absorptivities of other solution components (than those defined in Species), or to set the molar absorptivities of two components equal to one another.
5	Data	Operational data for refining, including the wavelength range (minimum and maximum) and interval, set logarithmic or numerical stability constant reporting, set output method, set multiple regression or non-negative least-squares regression for refining.
6	Mol.Abs.	Optional section. Allows the user to fix molar absorptivities either for components in Species that have been defined as having fixed molar absorptivities, or for components in the Dictionary where molar absorptivities are known.
7	Baseline	Optional section. Allows for baseline corrections to be applied. An absorbance measurement is required per λ measured.
8	Spectra	Absorbance values for each spectrum inputted into the model. Each spectrum is headed by the conditions of that sample: [MTL1], [MTL2], [LIG1], [LIG2], pH, path length. *Note: SQUAD can not interpret zero values for species that are defined in the dictionary, which is why [LIG1] for sample 1 is 1e-19 (a sufficiently low non-zero value), even though no ligand is present in this solution. However, because LIG2 is not defined in the Dictionary, [LIG2] can be set to zero.*
	End	The end of the input file is marked by a "-1" on a new line. When SQUAD reads a -1, it will immediately stop reading data from the input file and attempt to refine stability constants from what it has already read.

A.2.2 Complex Concentration Profiles
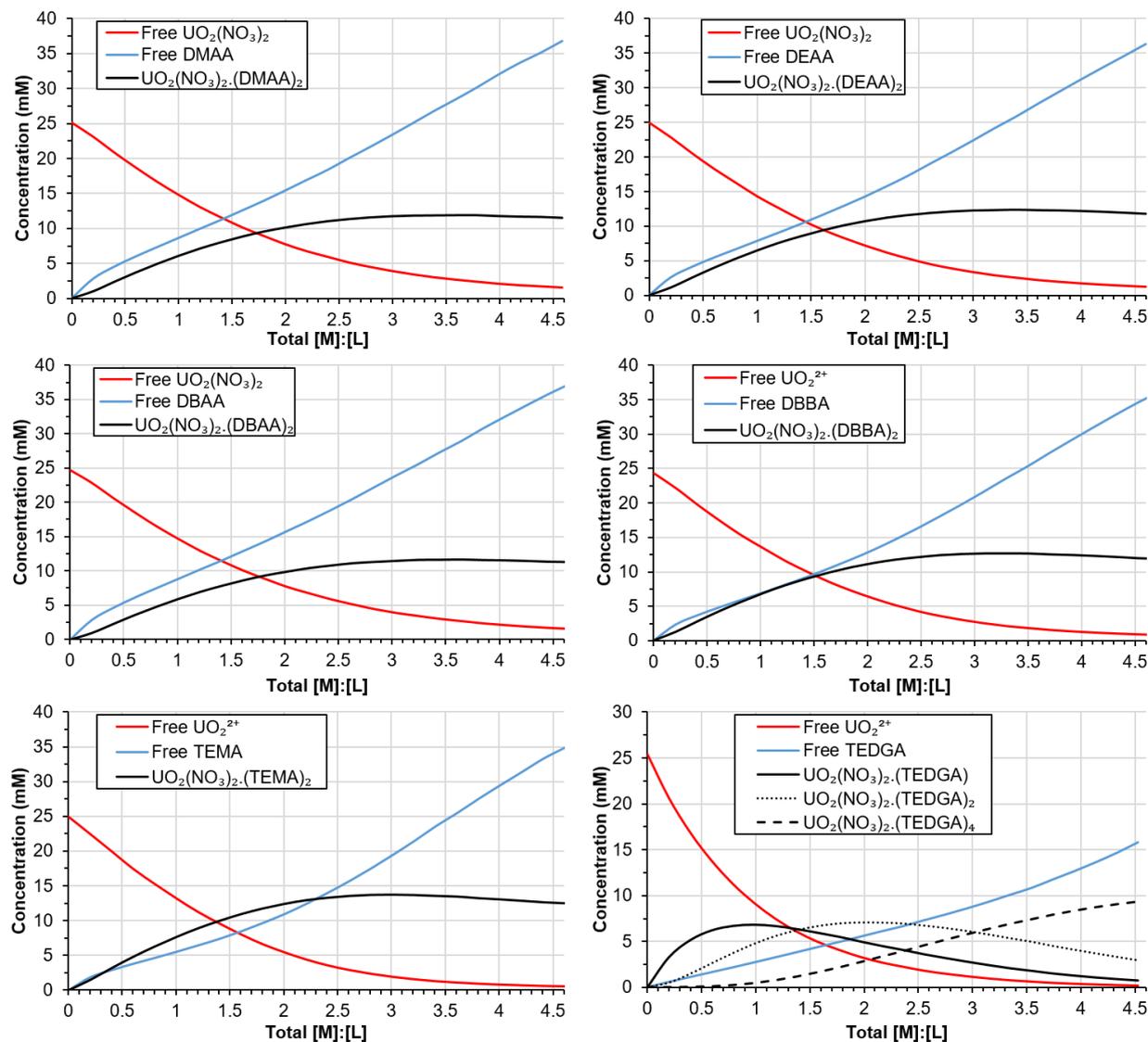
Figure A.4. *Concentration profiles of generated uranyl-nitrate-ligand complexes with changing [metal]:[ligand] in diluent A (pH 1, 50wt% nitric acid, 50wt% methanol at 0.2 M nitrate) determined from SQUAD analysis of spectrophotometric titration spectra.*
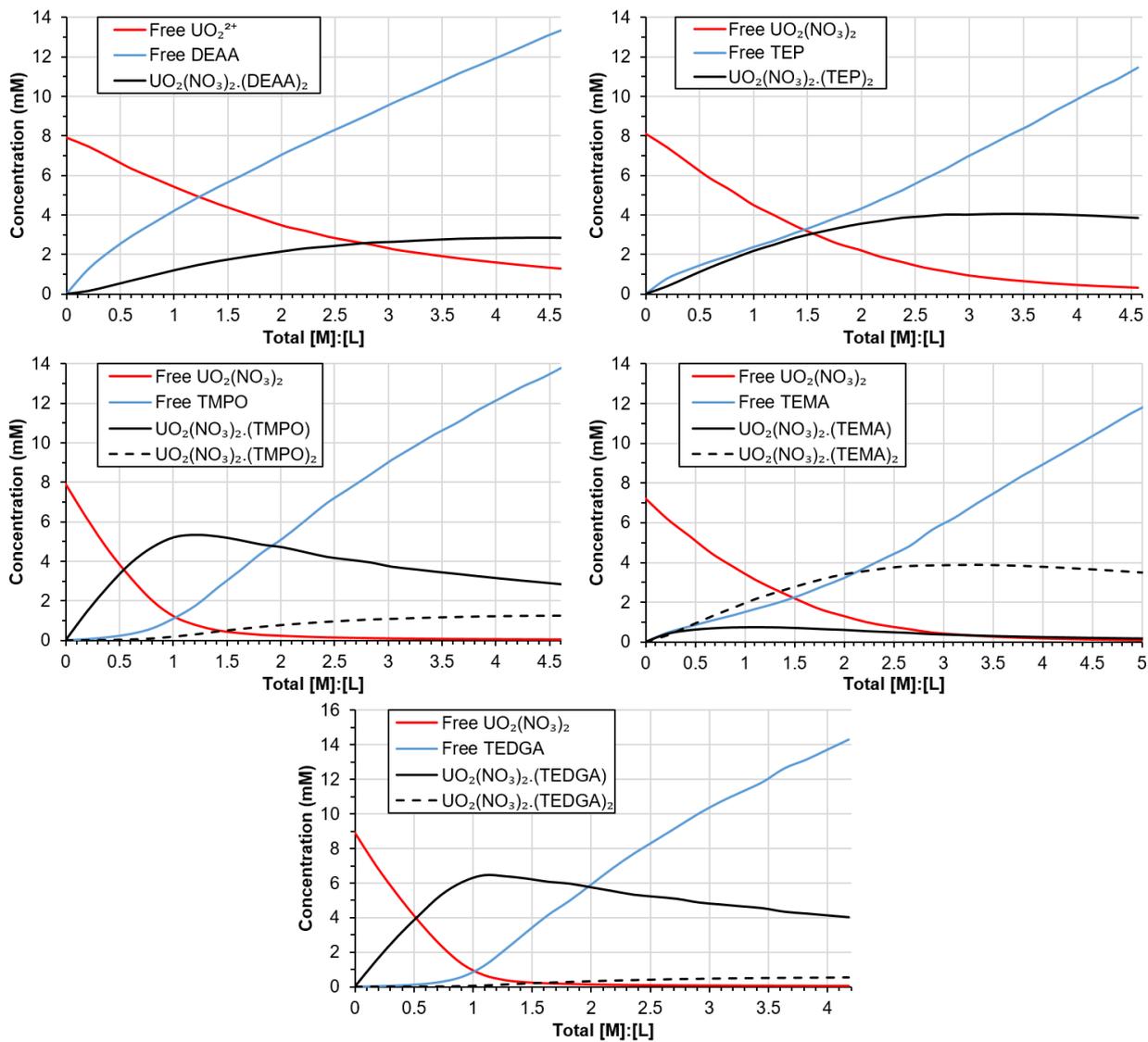
**Figure A.5.** *Concentration profiles of generated uranyl-nitrate-ligand complexes with changing [metal]:[ligand] in diluent B (pH 1, 4.50wt% nitric acid, 95.5wt% methanol at 0.2 M nitrate) determined from SQUAD analysis of spectrophotometric titration spectra.*

Appendix B

B.1   Single-Ligand Acid Extraction Relations
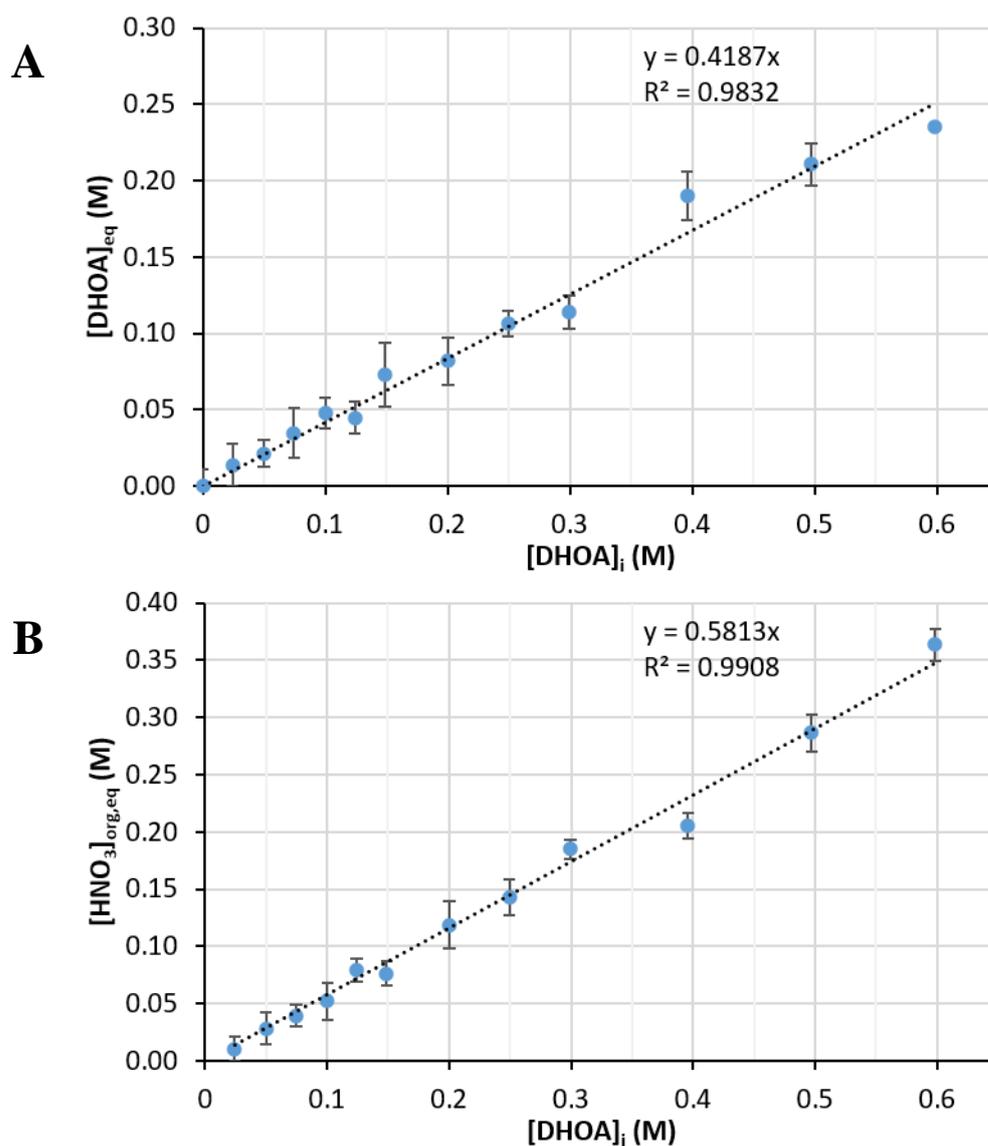
**Figure B.1.** *A) Free DHOA concentration and B) organic acid concentrations with changing initial DHOA concentrations after contact with 5.7 M nitric acid.*
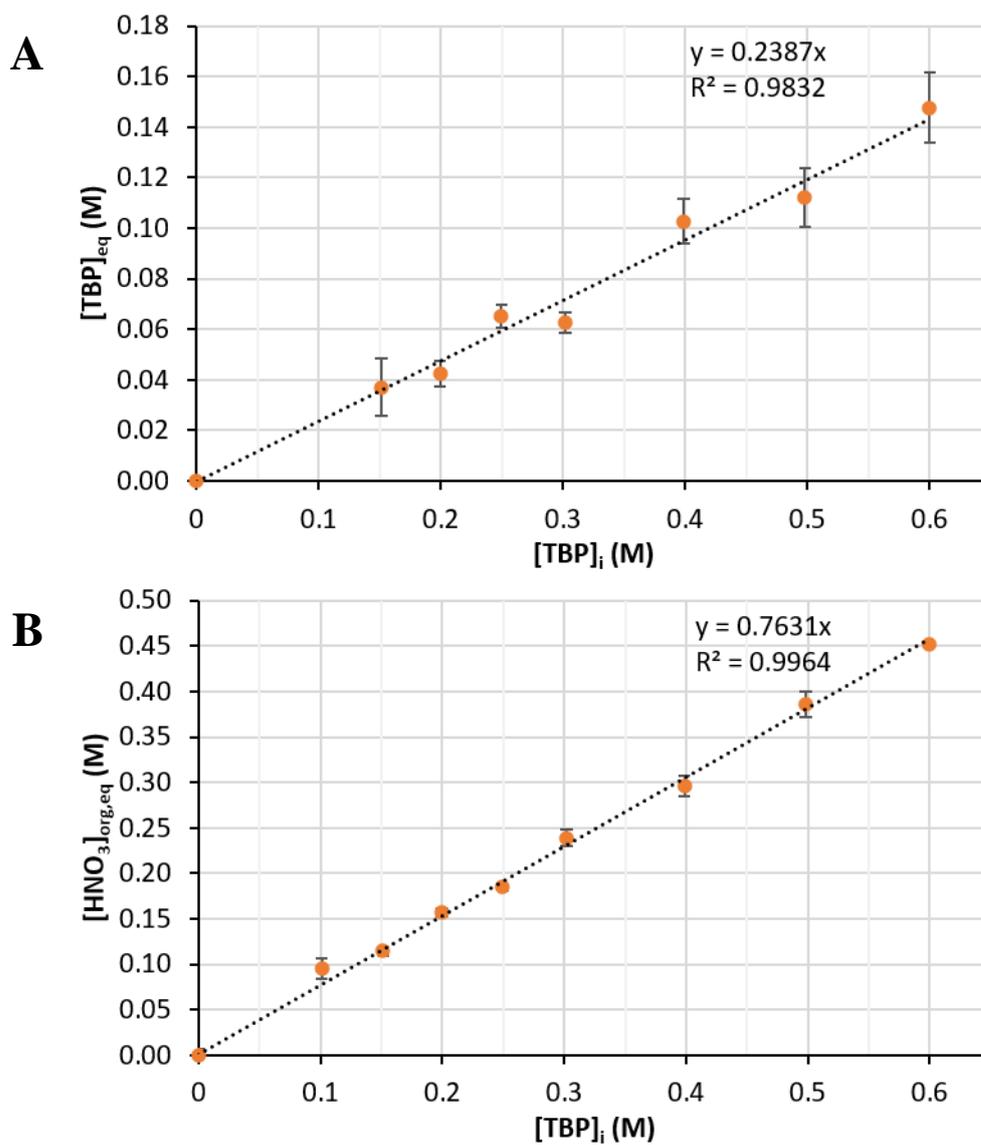
Figure B.2. *A) Free TBP concentration and B) organic acid concentrations with changing initial TBP concentrations after contact with 5.7 M nitric acid.*
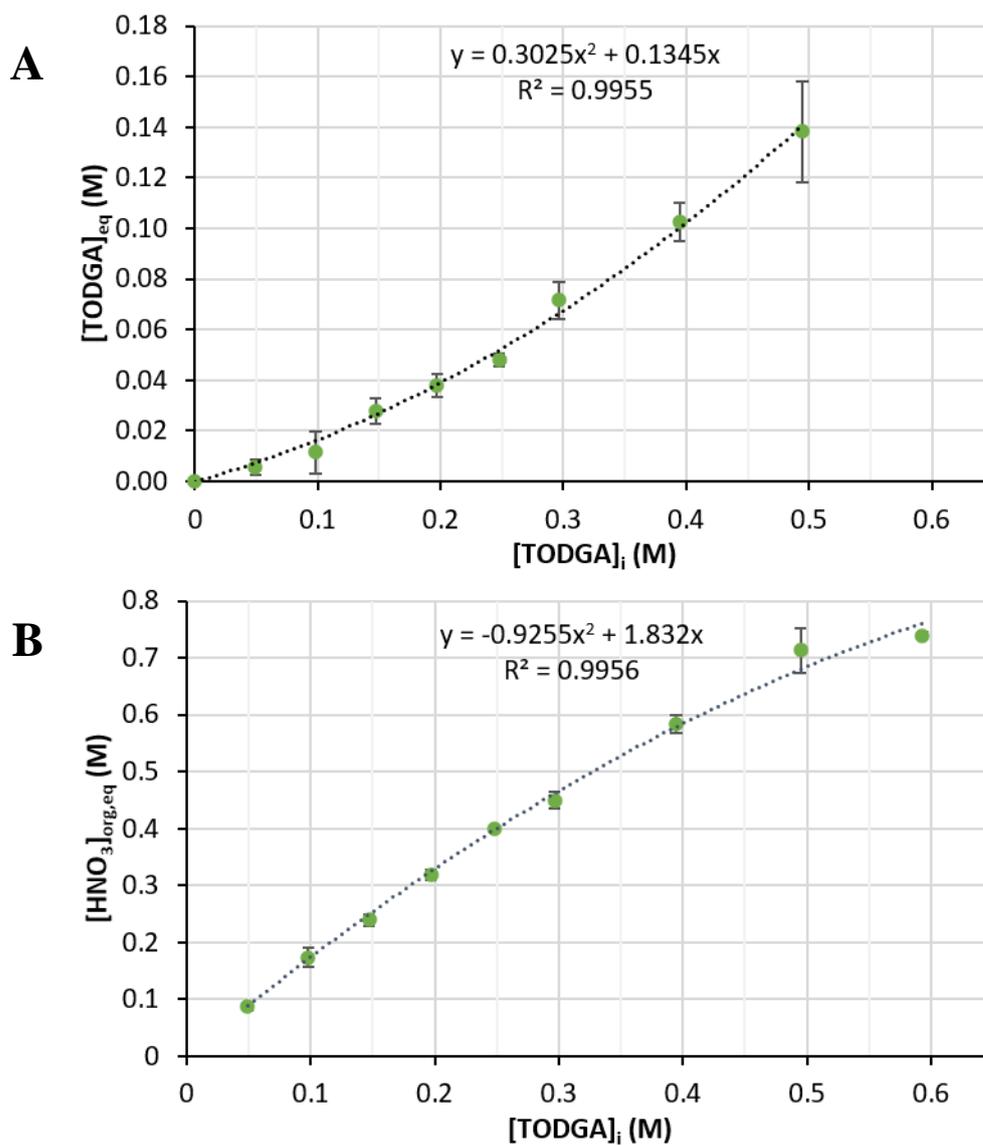
Figure B.3. *A) Free TODGA concentration and B) organic acid concentrations with changing initial TODGA concentrations after contact with 4.7 M nitric acid.*

B.2   Loading Isotherm K_{eq} Determinations
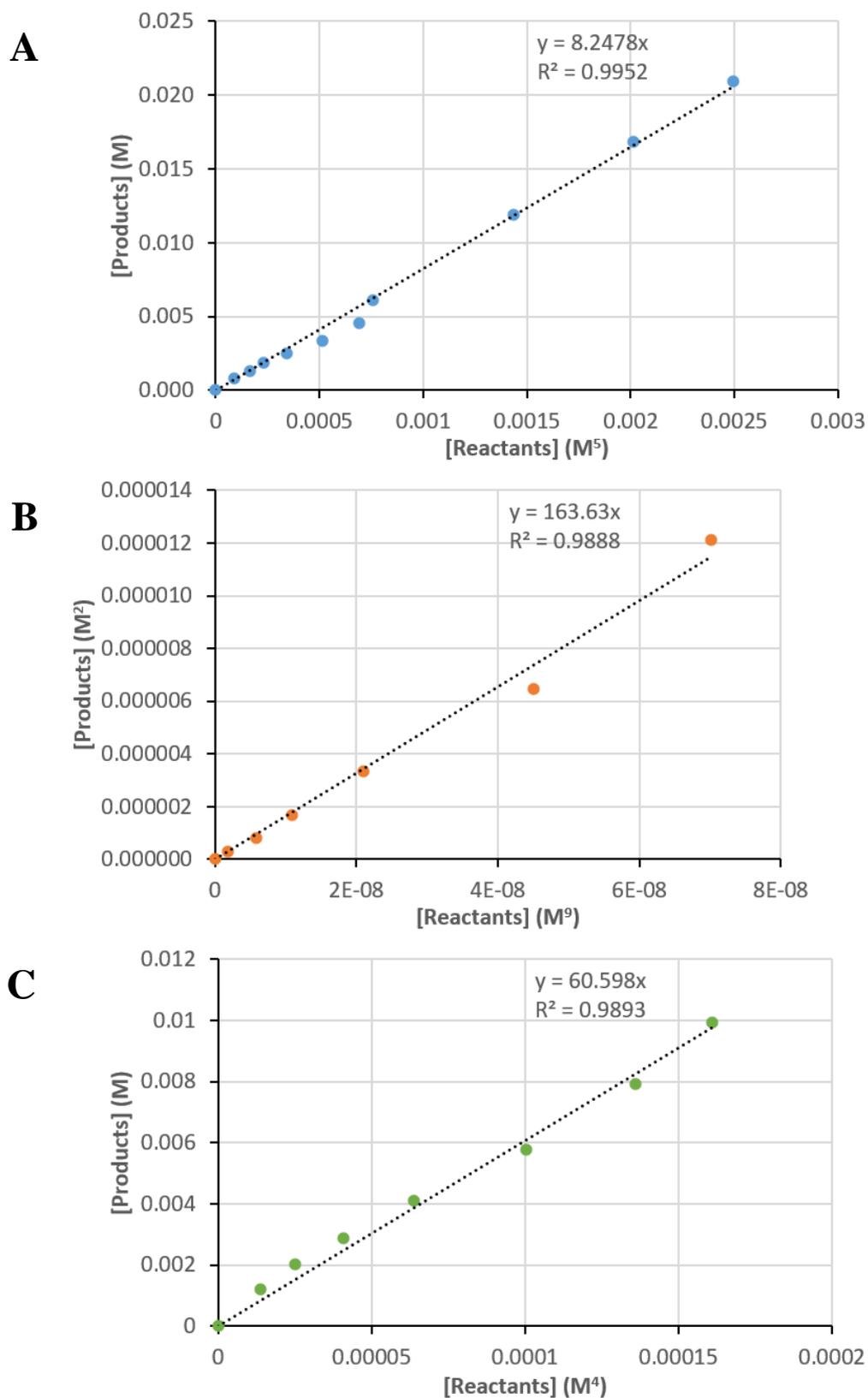
Figure B.4. *K_{eq} determination plots for 0.2 M A) DHOA, B) TBP and C) TODGA based on uranium loading isotherm data collected at 21±2°C.*

B.3   DHOA-TOPO Solvent Extraction Data

The solvent extraction tests in this section were conducted with a different organic diluent (*n*-dodecane with 10wt% 1-decanol as a phase modifier) because tri-*n*-octyl phosphine oxide (TOPO) was found be insoluble in *n*-dodecane. To that end, *N,N*-dihexyl octanamide (DHOA) was also investigated in this diluent to assess whether the 1-decanol phase modifier had any effect on uranium(VI) extraction.
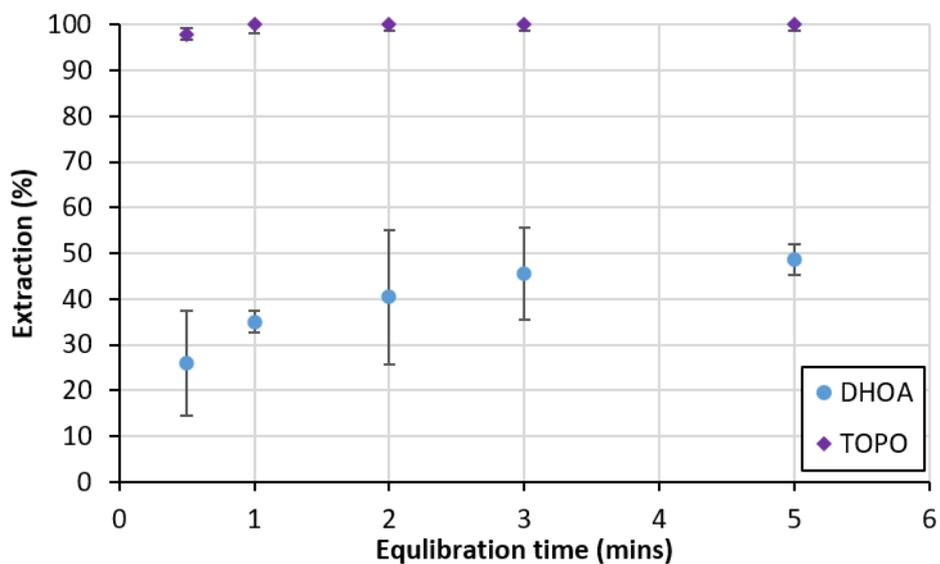
Figure B.5. *Extraction percentage of uranium from 5.7 M nitric acid into 0.2 M ligand in n-dodecane with 10wt% 1-decanol against vial shaking time at 21±2°C. Initial [uranium] = 235±2 ppm.*
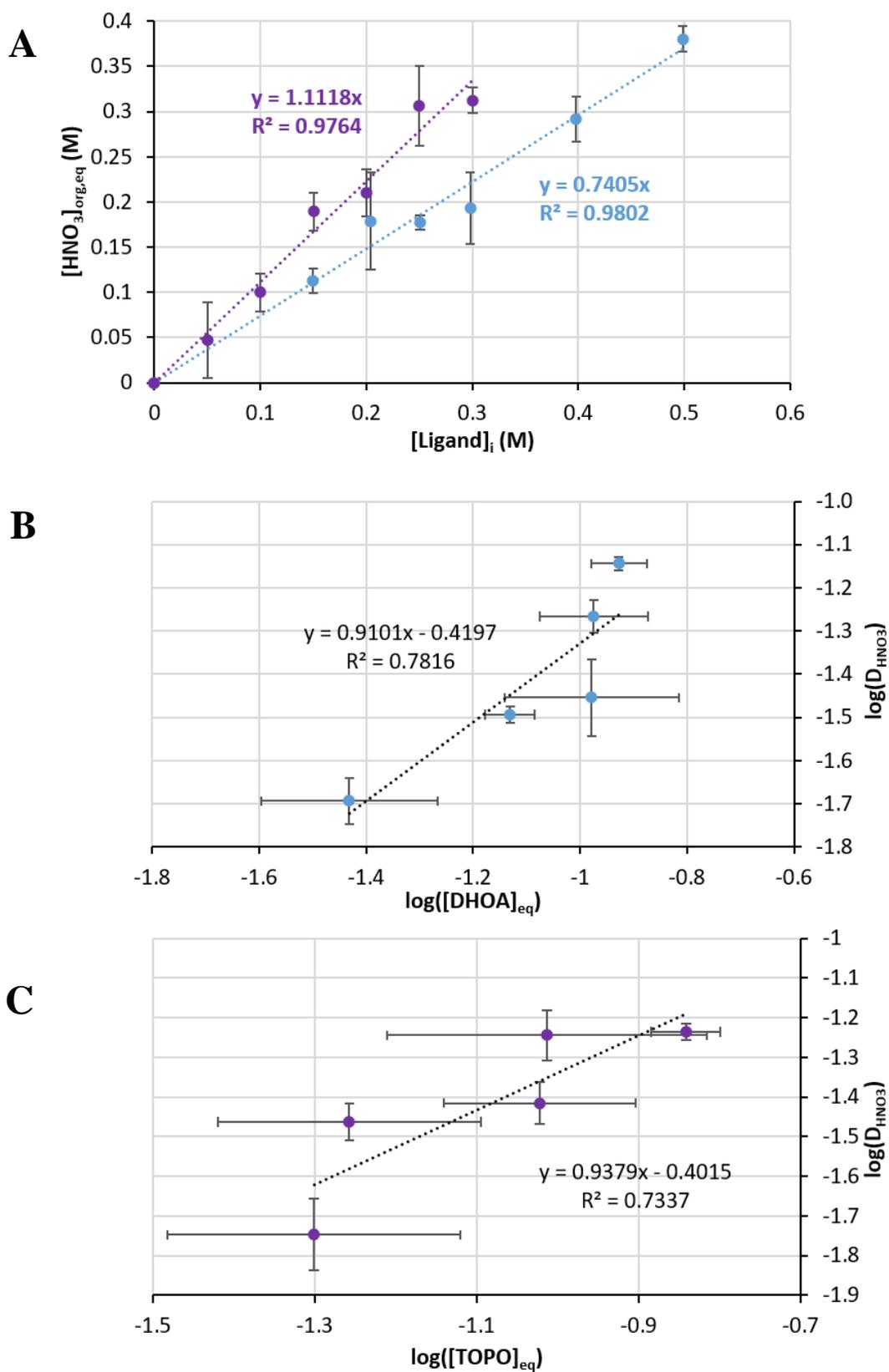
**Figure B.6.** *A) Nitric acid extraction isotherms for DHOA and TOPO in n-dodecane with 10wt% 1-decanol from 5.7 M nitric acid at 21±2°C. B) and C) show the slope analyses for DHOA and TOPO respectively.*
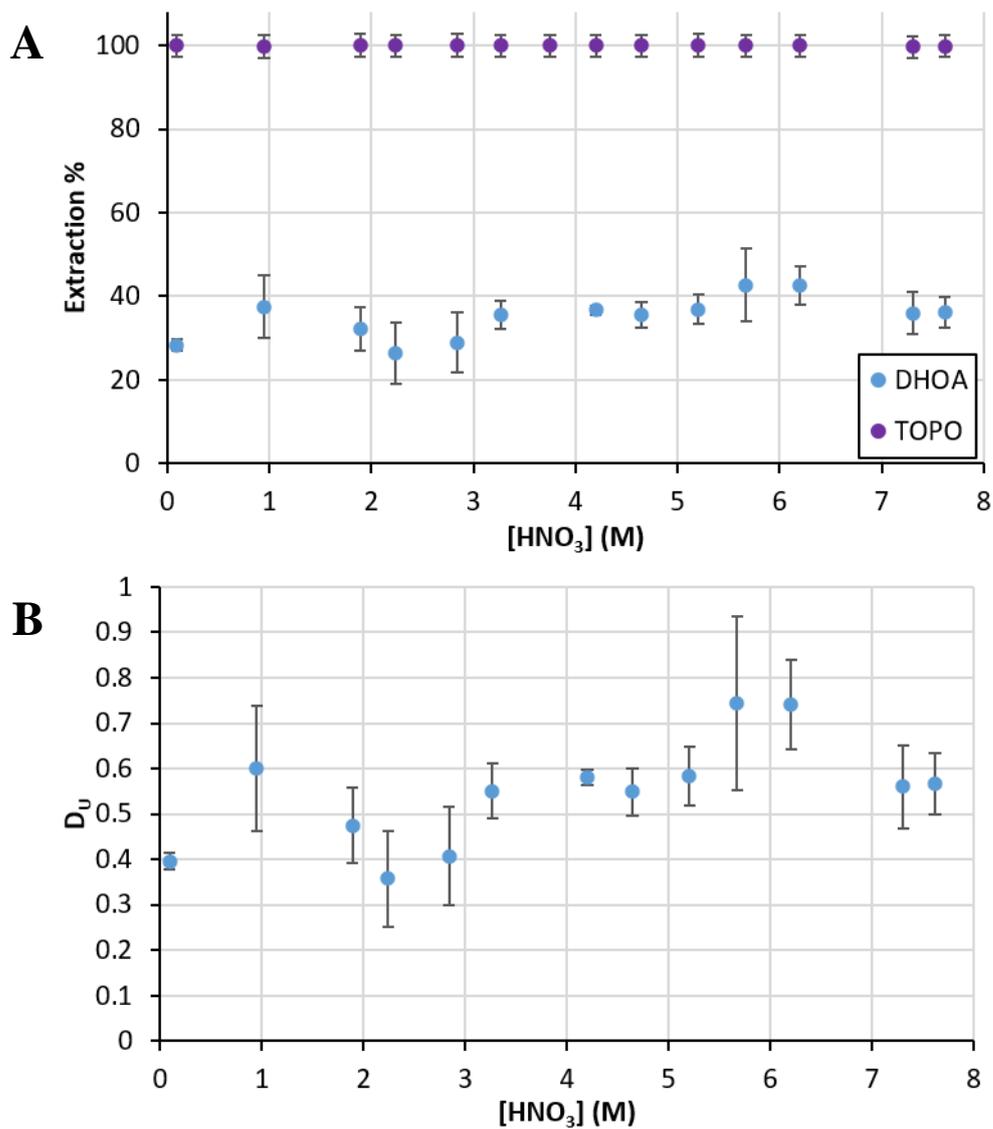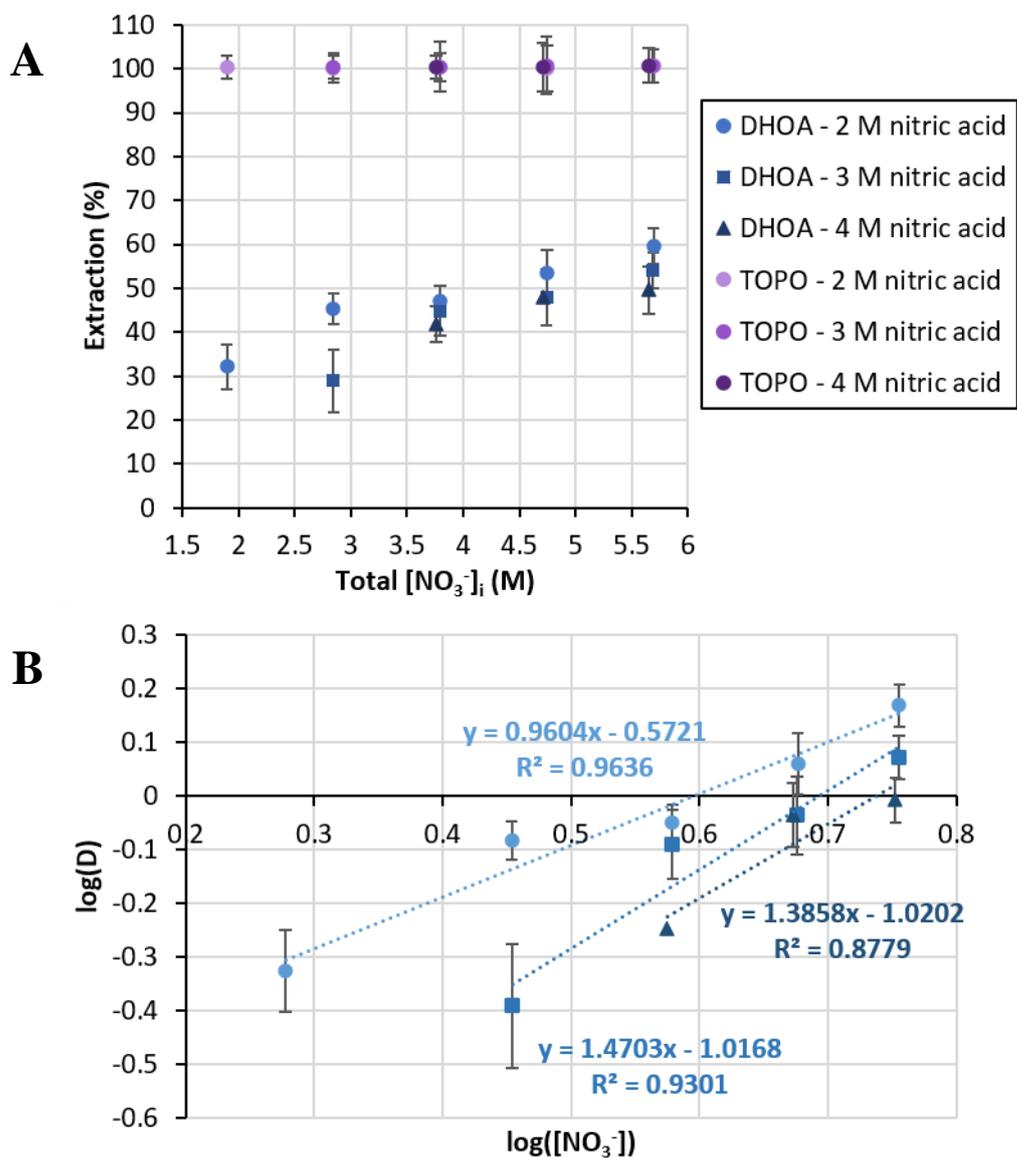
Figure B.7. *pH profiles of uranyl nitrate extraction by 0.2 M DHOA and TOPO in n-dodecane with 10wt% 1-decanol at 21±2°C. Initial [uranium] for DHOA and TOPO tests are 499±4 and 536±10 ppm respectively.*
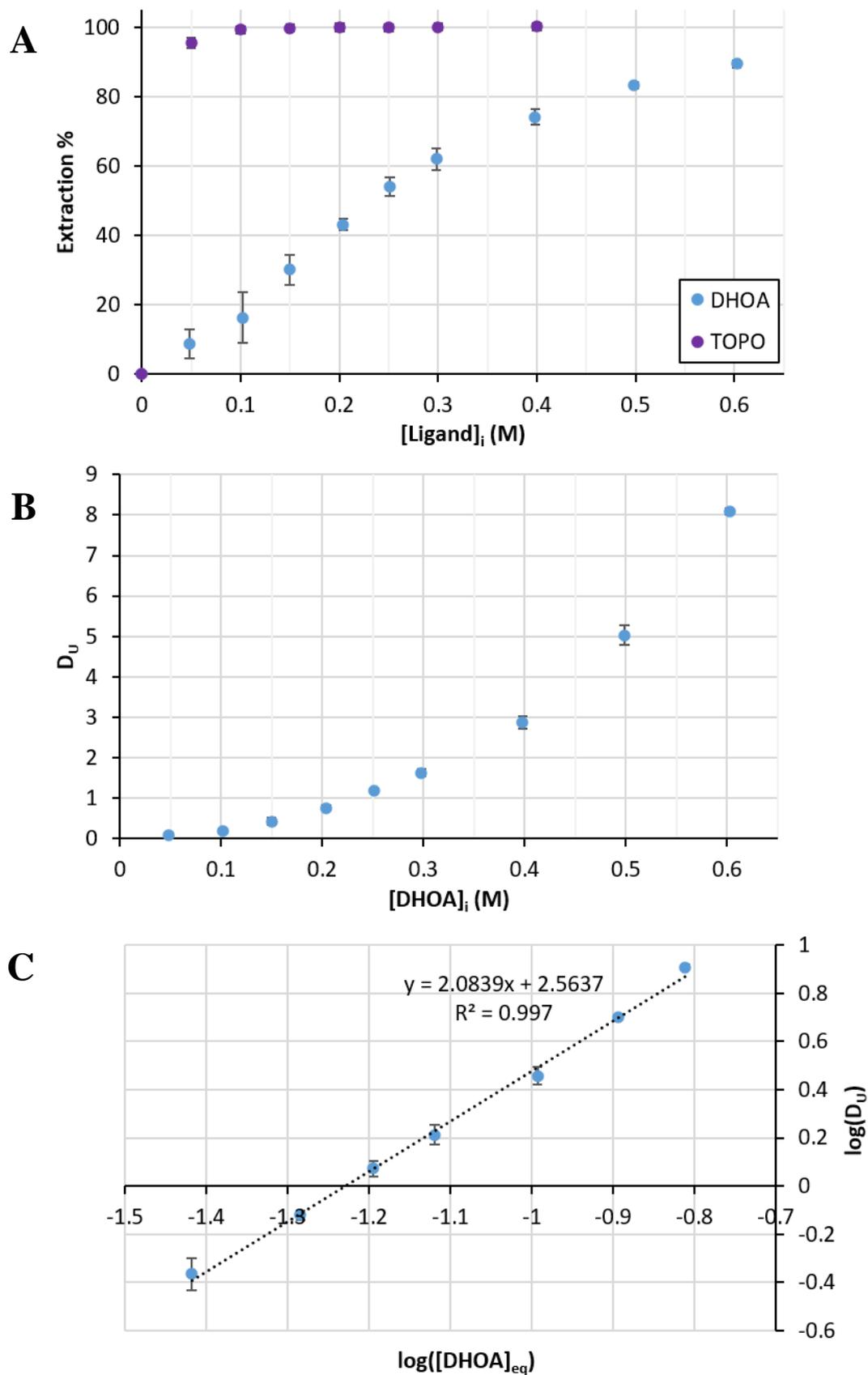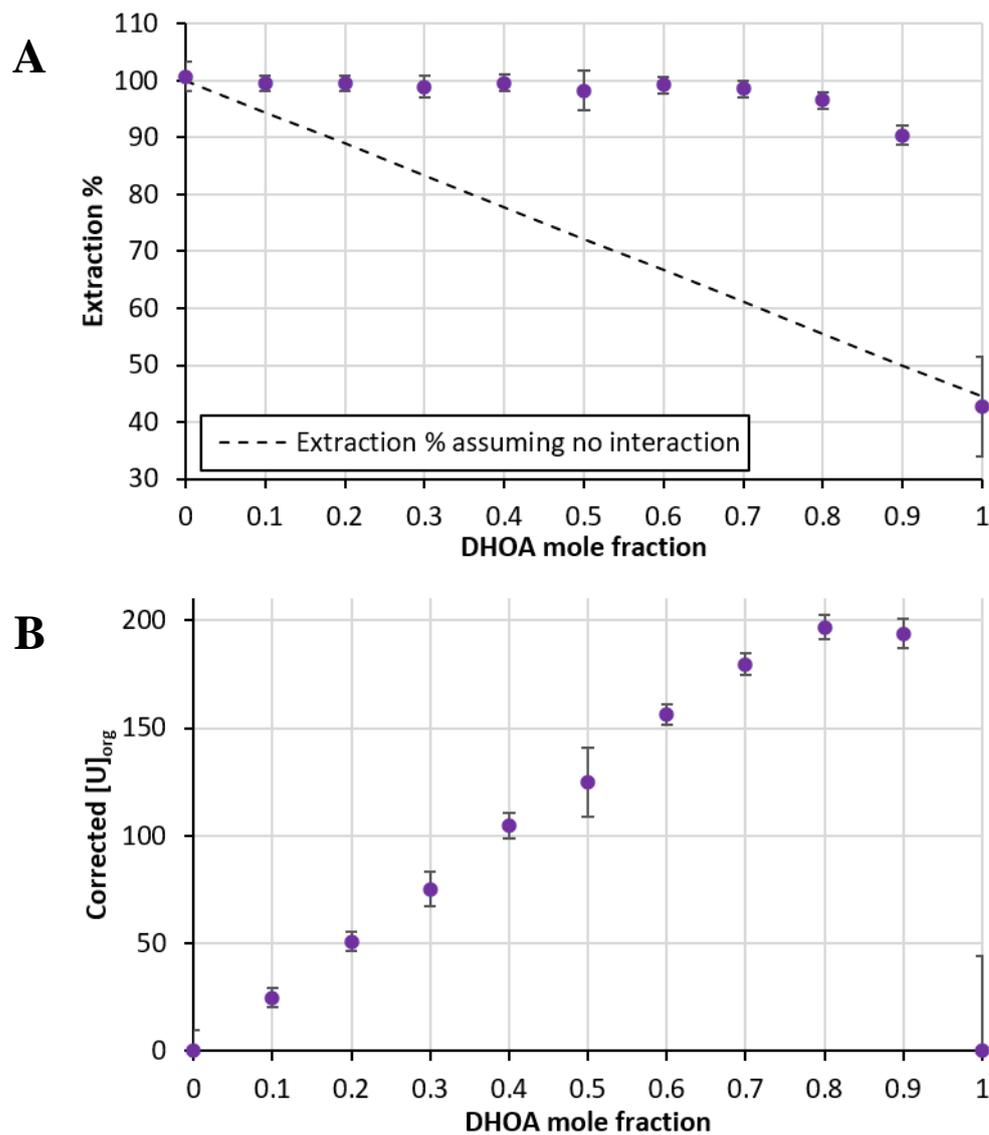
Figure B.8. *Ligand isotherms of uranyl nitrate A) extraction and B) distribution coefficient by DHOA and TOPO in n-dodecane with 10wt% 1-decanol from 5.7 M HNO₃ at 21±2°C. Initial [uranium] for DHOA and TOPO tests are 529±4 ppm. C) shows slope analysis plot for DHOA.*
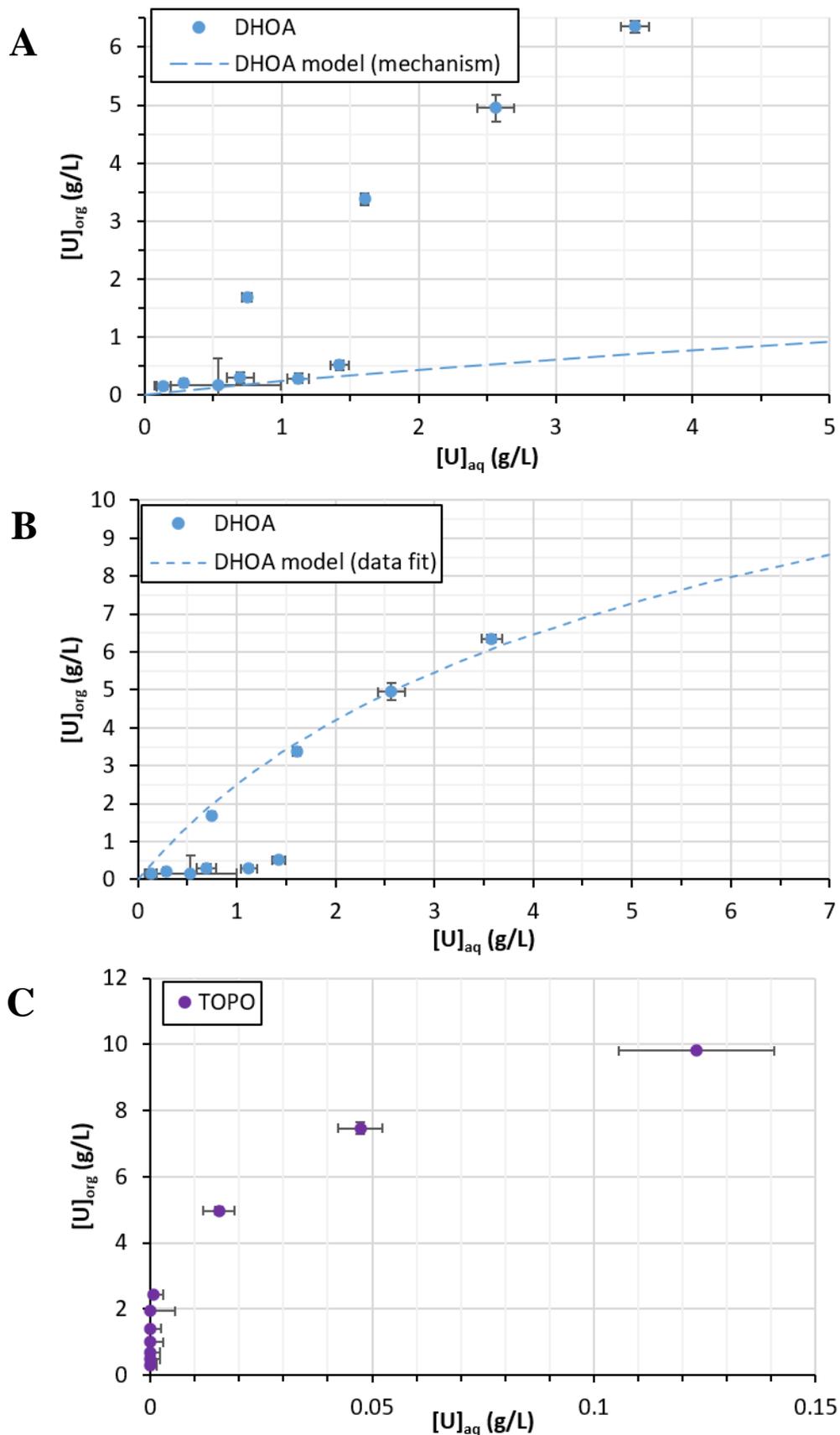
Figure B.9. *Uranyl nitrate loading isotherms with 0.2 M DHOA and TOPO in n-dodecane with 10wt% 1-decanol from 5.7 M HNO₃ at 21±2°C. A) depicts DHOA loading with models based on the extraction mechanism, B) shows DHOA loading with modified model fit, and C) shows TOPO loading.*

Figure B.10. *A) Uranyl nitrate extraction with varying nitrate concentrations in different nitric acid concentrations with 0.2 M DHOA and TOPO in n-dodecane with 10wt% 1-decanol at 21±2°C. Initial [uranium] for DHOA and TOPO tests are 596±16 and 551±10 ppm respectively. B) shows the slope analysis plots for the DHOA systems.*

Figure B.11. *DHOA-TOPO Job plots at 5.7 M nitric acid at 21±2°C. Initial [uranium] = 479±5 ppm. A) depicts the distribution Job plot. B) depicts the organic [uranium] Job plot.*